

COOPERATIVE CONTROL OF NONLINEAR MULTI-AGENT
SYSTEMS

LEI LIU

A DISSERTATION SUBMITTED TO THE FACULTY OF GRADUATE
STUDIES
IN PARTIAL FULFILMENT OF THE REQUIREMENTS
FOR THE DEGREE OF

DOCTOR OF PHILOSOPHY

GRADUATE PROGRAM IN EARTH AND SPACE SCIENCE
YORK UNIVERSITY
TORONTO, ONTARIO
JUNE 2016

©LEI LIU, 2016

Abstract

Multi-agent systems have attracted great interest due to their potential applications in a variety of areas. In this dissertation, a nonlinear consensus algorithm is developed for networked Euler-Lagrange multi-agent systems. The proposed consensus algorithm guarantees that all agents can reach a common state in the workspace. Meanwhile, the external disturbances and structural uncertainties are fundamentally considered in the controller design. The robustness of the proposed consensus algorithm is then demonstrated in the stability analysis. Furthermore, experiments are conducted to validate the effectiveness of the proposed consensus algorithm.

Next, a distributed leader-follower formation tracking controller is developed for networked nonlinear multi-agent systems. The dynamics of each agent are modeled by Euler-Lagrange equations, and all agents are guaranteed to track a desired time-varying trajectory in the presence of noise. The fault diagnosis strategy of the nonlinear multi-agent system is also investigated with the help of differential

geometry tools. The effectiveness of the proposed controller is verified through simulations.

To further extend the application area of the multi-agent technique, a distributed robust controller is then developed for networked Lipschitz nonlinear multi-agent systems. With the appearance of system uncertainties and external disturbances, a sampled-data feedback control protocol is carried out through the Lyapunov functional approach. The effectiveness of the proposed controller is verified by numerical simulations. Other than the robustness and sampled-data information exchange, this dissertation is also concerned with the event-triggered consensus problem for the Lipschitz nonlinear multi-agent systems. Furthermore, the sufficient condition for the stochastic stabilization of the networked control system is proposed based on the Lyapunov functional method. Finally, simulation is conducted to demonstrate the effectiveness of the proposed control algorithm.

In this dissertation, the cooperative control of networked Euler-Lagrange systems and networked Lipschitz systems is investigated essentially with the assistance of nonlinear control theory and diverse controller design techniques. The main objective of this work is to propose realizable control algorithms for nonlinear multi-agent systems.

This thesis is dedicated to my family

Acknowledgements

I would like to express my deepest gratitude to my supervisor Prof. Jinjun Shan for his consistent support, encouragement and being an outstanding mentor and friend throughout the past six years. I benefited enormously from many stimulating conversations with him about various research topics. The inspiring environment Prof. Shan created, allowed me to grow both personally and professionally. I would also like to thank Prof. Michael Daly and Prof. Jianguo Wang, for serving on my advisory committee. In our yearly meetings, Prof. Daly and Prof. Wang provided many constructive comments that greatly improved the quality of this dissertation.

I would also like to thank Prof. Hugh H.T. Liu for allowing me to use the 3-DOF helicopter platform at the University of Toronto, Institute for Aerospace Studies (UTIAS). Thanks also to Dr. Chen Gao, Dr. Mingfeng Zhang and Mr. Zhongjie Lin for their generous help during the experimental operation at UTIAS. I am also grateful to Prof. Christopher J. Damaren at UTIAS, for many inspiring discussions on passivity theory.

My thanks also go to my many labmates: Ryan Orszulik, Xiaogang Wang, Ampere Kui, Yuan Ren, Yanfang Liu, Liu Yang, Likun Liu, Jifeng Guo, Xiaobu Xue, Inseon Kim, Qian Sun, Shawn Walker, Chongyang Lyu, Dongming Li, Haibin Shang, Nicholas Bijmens, Michael Voutsogiannakis and Marc Savoie for their companionship and many enlightening conversations. Particularly, I would like to express my thanks to Ryan for many insightful discussions on research and advice on academic writing.

Finally, I would like to express my warmest gratitude to my parents. This dissertation would not have been possible without their consistent support and unconditional love.

Table of Contents

Abstract	ii
Dedication	iv
Acknowledgements	v
Table of Contents	vii
List of Tables	xi
List of Figures	xii
1 Introduction	1
1.1 Mathematical model of the single agent	7
1.2 Malfunction of multi-agent systems	11
1.3 Communication structure	15
1.4 Network-induced challenges	18

1.4.1	Sampled-data communication	18
1.4.2	Topology switching	21
1.4.3	Event-triggered signal update	22
1.5	Research Objectives and Organization	23
1.6	Major Contributions	28
2	Preliminaries	29
2.1	Notations	29
2.2	Algebraic graph theory	30
2.3	Perturbed systems	33
2.4	Nonlinear realization theory	35
3	Distributed Consensus for Networked Nonlinear Systems	38
3.1	Problem statement	40
3.2	Distributed consensus algorithm development	41
3.2.1	Stability analysis with perturbation term	44
3.2.2	Stability analysis with structural uncertainty	53
3.3	Experimental results	57
4	Synchronization of Networked Nonlinear Multi-agent Systems with Fault Diagnosis	66
4.1	Problem formulation	70

4.2	Controller design with fault diagnosis	72
4.2.1	Distributed formation control with system noise	73
4.2.2	Fault diagnosis	83
4.3	Simulations	91
5	Sampled-data Synchronization Control of Networked Nonlinear Systems	127
5.1	Problem formulation	130
5.2	Distributed sampled-data controller design	131
5.3	Simulations	145
6	Event-triggered Sampled-data Leader-follower Consensus of Networked Nonlinear Systems with Stochastic Switching Topology	150
6.1	Problem formulation	152
6.2	Stability analysis	157
6.3	Simulations	166
7	Conclusions and Future Work	175
7.1	Conclusions	175
7.2	Future Work	178
	Appendix A Relevant Theorems	182

Appendix B Selected Publications	185
Bibliography	186

List of Tables

3.1	Parameters of helicopter system	61
4.1	Parameters of helicopter system	92
6.1	Parameters of the networked system	170

List of Figures

1.1	Group behaviors of social animals	2
1.2	Terrestrial Planet Finder [1]	3
1.3	Networked multi-agent systems	5
1.4	Centralized structure: a central controller exists in the networked system	15
1.5	Decentralized structure: there is no central controller and agents share the information locally	16
2.1	Communication topology	32
3.1	Feedback system	55
3.2	3-DOF helicopter system at UTIAS	58
3.3	Communication topology	61
3.4	Experimental results of Leaderless consensus	63
3.5	Experimental results of Leader-follower consensus	64

4.1	Fault diagnosis configuration	91
4.2	Fault diagnosis strategy	92
4.3	Fault recovery strategy	93
4.4	Communication topology	94
4.5	Topology switching with faulty helicopter 1	95
4.6	Topology switching with faulty helicopter 2	96
4.7	Topology switching with faulty helicopter 1 and 3	97
4.8	Topology switching with faulty helicopter 4	98
4.9	Desired trajectory	98
4.10	Noise	99
4.11	Tracking errors of six helicopters	99
4.12	Residuals of six helicopters	100
4.13	Health indicators of six helicopters	101
4.14	Tracking errors with faulty helicopter 1 (actuator fault)	102
4.15	Tracking errors with faulty helicopter 1 (sensor fault)	102
4.16	Tracking errors of six helicopters	103
4.17	Health indicators of six helicopters	104
4.18	Residual signals with faulty helicopter 1 (actuator fault)	105
4.19	Tracking errors of six helicopters	106
4.20	Health indicators of six helicopters	107

4.21	Residual signals with faulty helicopter 2 (actuator fault)	108
4.22	Tracking errors of six helicopters	109
4.23	Health indicators of six helicopters	110
4.24	Residual signals with faulty helicopter 1 and 3 (actuator fault) . . .	111
4.25	Tracking errors of six helicopters	112
4.26	Health indicators of six helicopters	113
4.27	Residual signals with faulty helicopter 4 (actuator fault)	114
4.28	Tracking errors of six helicopters	115
4.29	Health indicators of six helicopters	116
4.30	Residual signals with faulty helicopter 1 (sensor fault)	117
4.31	Tracking errors of six helicopters	118
4.32	Health indicators of six helicopters	119
4.33	Residual signals with faulty helicopter 2 (sensor fault)	120
4.34	Tracking errors of six helicopters	121
4.35	Health indicators of six helicopters	122
4.36	Residual signals with faulty helicopter 1 and 3 (sensor fault)	123
4.37	Tracking errors of six helicopters	124
4.38	Health indicators of six helicopters	125
4.39	Residual signals with faulty helicopter 4 (sensor fault)	126
5.1	Communication topology	147

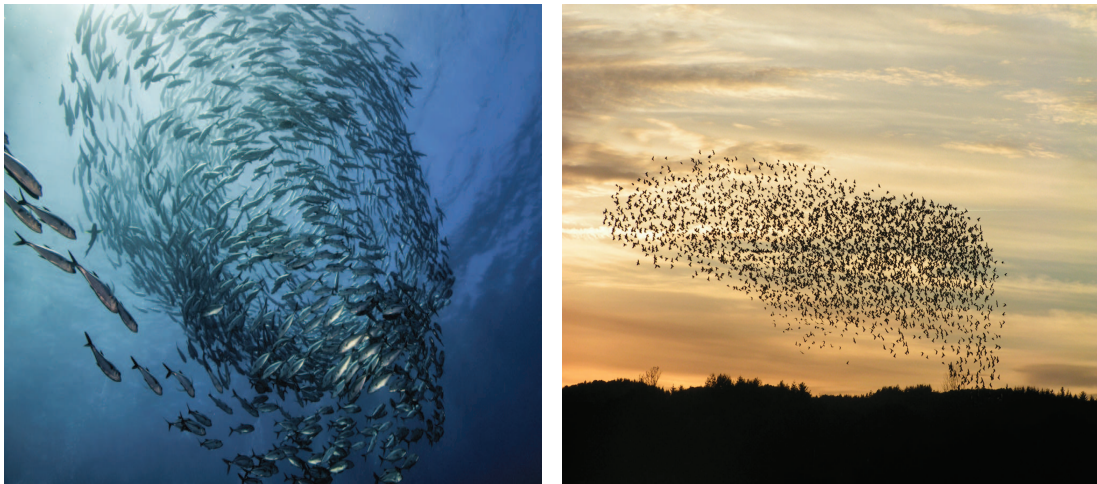
5.2	Trajectory of the leader Chua's circuits system	147
5.3	Trajectory of the follower Chua's circuits system	148
5.4	Synchronization errors	148
5.5	Estimation errors	149
5.6	\mathcal{L}_2 bounded disturbance	149
6.1	Desired trajectory	172
6.2	Communication topologies	172
6.3	Tracking errors	173
6.4	Control input of agent 1	174
6.5	Stochastic switching of the two topologies	174

1 Introduction

Cooperative control of multi-agent or multi-vehicle systems has attracted a broad interest in the last decade [2–8]. Having multiple autonomous agents working cooperatively to achieve a common agreement is typically referred to as cooperative control of multi-agent systems. In many applications, networking multiple agents can offer various benefits, such as greater efficiency and lower cost. The networked multi-agent systems can be potentially applied in diverse areas, i.e. monitoring forest fires, tracking wildlife, spacecraft formation flying, distributed computing and intelligent transportation systems.

The investigation of cooperative control is essentially motivated by the following factors: 1. the group behaviors of social animals. The grouping phenomenon can be widely observed among social animals, i.e. ant swarming, fish schooling and birds flocking [9]. Grouping behaviors can effectively reduce their chance of being caught by the predators because of the enlarged detection area. The underlying principle of the group behaviors of social animals is fundamentally studied in [10].

Along with the “boid model” [10], the behaviors of these social animal groups can be abstracted by three rules: collision avoidance, velocity matching and flock centering. Following these three rules, simulations of group behaviors like schooling or flocking can be implemented in computer animation. In [11], the flocking for multi-agent dynamical systems was further formalized. 2. More complicated prac-



(a) Fish schooling [12]

(b) Birds flocking [13]

Fig. 1.1 Group behaviors of social animals

tical missions. For example, the formation flying technique of multiple spacecraft will possibly enable more planned and proposed space missions [14], i.e. Orion [15], EO-1 [16], Terrestrial Planet Finder (TPF) (cancelled by NASA) [17]. TPF would facilitate a telescope [18] in space instead of on earth. This large, complicated telescope will be imitated by multiple smaller ones. Since a large and variable baseline would enormously increase the resolution of the telescope, formation-flying architec-



Fig. 1.2 Terrestrial Planet Finder [1]

tural baseline will bring out a variety of benefits. These small telescopes are fixed on multiple spacecraft which are implementing precisely formation flying during the mission. As a result, a formation-flying TPF operating with a 1 km baseline in astrophysics imaging mode can achieve resolutions of about 2 milli-arcsecond (mas) [18]. Another example is the formation flying of multiple autonomous unmanned helicopters. The total energy consumption can be effectively reduced if the triangular formation is adopted by the group of multiple autonomous unmanned helicopters.

Most of these practical missions can be typically formulated as multi-agent cooperative control problems, in which achieving a common group objective is the ultimate goal. For example, the group objective will be a common position in the rendezvous mission of multiple mobile robots, and the common group objective for

the attitude synchronization of spacecraft will be the same final attitude angles. Reaching this common group objective is usually referred to as the achievement of consensus or synchronization. In multi-agent cooperative control problems, consensus and synchronization are slightly different in terms of the focus of the specific problem [19]. Consensus is usually adopted when the main focus of the problem is the network connecting linear dynamical agents, while synchronization is typically utilized when the nonlinear dynamical system is essentially involved. Although these differences are pointed out in previous work [19], it is worth noting that the concepts of consensus and synchronization are usually so similar that they can be used interchangeably in many cases [20]. To further improve the readability of this dissertation, “consensus” will be adopted wherever either “consensus” or “synchronization” can be used.

Networking multiple dynamical systems poses significant challenges on both local and global levels. As shown in Figure 1.3, to achieve the consensus, the following challenges must be overcome:

- (i) Mathematical model of the single agent

Linear dynamical agents have been assumed in most of the previous work, however, almost all the practical agents are governed by nonlinear dynamics. Coupling multiple nonlinear dynamical agents will result in a more complicated nonlinear system, which poses further obstacles preventing the use of

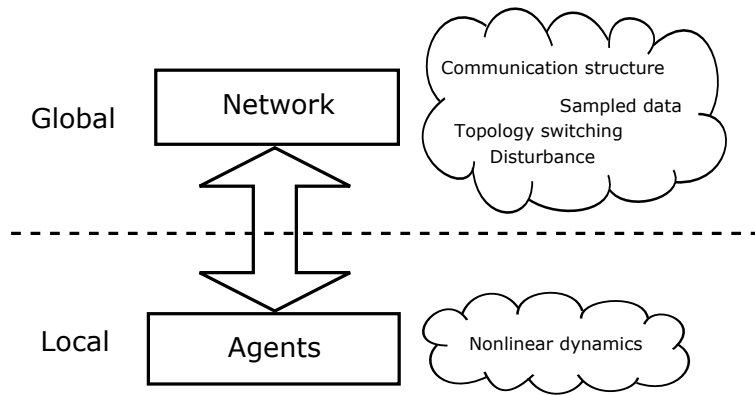


Fig. 1.3 Networked multi-agent systems

classical control techniques. Therefore, extending the linear consensus algorithm to networked nonlinear agents is urgently required to bridge the gap between the theoretical analysis and the practical application.

(ii) Malfunction of multi-agent systems

Safety is always important in applications. Unlike in centralized control systems, there is no central controller in distributed control protocols of multi-agent systems. This implies that no central processor can indicate the faulty agent and the information transmitted by the malfunctioning agent will be continuously accepted by other healthy agents. In this scenario, the group mission could possibly be crashed by any one of the networked agents. Therefore, the capability of detecting certain malfunctions becomes a huge challenge due to the decentralized communication structure. Hence, a fault diagnosis

and recovery strategy for multi-agent systems will be developed in this work.

(iii) Communication structure

To enhance the efficiency of the information exchange among the multiple agents, the communication structure should be appropriately selected in practice. A centralized communication structure is usually adopted because of its stable performance. However, with the growing number of the networked agents, the communication efficiency will be largely reduced. Meanwhile, the increased computational burden may even crash the central computer. Thus, both centralized and decentralized communication structure will be reviewed below and the decentralized communication structure will be adopted in this work.

(iv) Network-induced problems

Networking multiple agents will result in many new problems. For example, the structure of the networked systems might be intermittently changed because of the random interaction switching. Also, the stability of the networked multi-agent systems might be destroyed by the underlying sampled-data information exchange. Meanwhile, the disturbance existing in any vertex of the network can be broadcast to other agents and will have a negative influence on the entire group. These network-induced problems will be thoroughly

investigated in this dissertation.

There are still a lot of challenges existing in multi-agent systems. Among them, the above mentioned problems are the most urgent challenges. For example, since the controller design of the multi-agent systems is definitely based on the dynamical model of individual agent, the development of the control algorithm will be infeasible if the dynamical model of individual agent is not realistic. Also, it is impossible to skip any network-induced problem if the multiple agents are expected to be coupled by the network, otherwise a tiny problem in multi-agent systems might be propagated by the network-induced problem.

1.1 Mathematical model of the single agent

In control community, the behavior of each agent is usually described using its mathematical model. As reviewed above, a linear model was mostly investigated in previous work, where single agent dynamics can be expressed as

$$\dot{\mathbf{x}}_i(t) = \mathbf{u}_i(t) \tag{1.1}$$

where the state vector of agent i is $\mathbf{x}_i(t) \in \mathbb{R}^n$ and the control input is $\mathbf{u}_i(t) \in \mathbb{R}^n$.

A continuous-time consensus algorithm for networked linear agents in Eq. (1.1) can be expressed as [21]

$$\mathbf{u}_i(t) = - \sum_{j \in \mathcal{N}_i(t)} a_{ij}(t) (\mathbf{x}_i(t) - \mathbf{x}_j(t)) \tag{1.2}$$

where $\mathcal{N}_i(t)$ is a set containing the agents whose information is available to agent i , and $a_{ij}(t)$ represents the weighting factor. The networked linear agents in Eq. (1.1) is said to achieve the consensus if $\|\mathbf{x}_i(t) - \mathbf{x}_j(t)\| \rightarrow 0$ as $t \rightarrow \infty$, $\forall i \neq j$ [3].

In addition to the first-order integrator model, the second-order integrator model is also broadly investigated [22, 23]. The second-order integrator model is [24]

$$\begin{cases} \dot{\mathbf{x}}_i(t) = \mathbf{v}_i(t) \\ \dot{\mathbf{v}}_i(t) = \mathbf{u}_i(t) \end{cases} \quad (1.3)$$

where $\mathbf{x}_i(t), \mathbf{v}_i(t) \in \mathbb{R}^n$ are the state vectors and $\mathbf{u}_i(t) \in \mathbb{R}^n$ is the control input. Then consensus algorithm for networked linear agents in Eq. (1.3) is [21]

$$\mathbf{u}_i(t) = - \sum_{j \in \mathcal{N}_i(t)} a_{ij}(t) [(\mathbf{x}_i(t) - \mathbf{x}_j(t)) + \alpha(t) (\mathbf{v}_i(t) - \mathbf{v}_j(t))] \quad (1.4)$$

Although the cooperative control problems have been fairly well solved for networked linear agents, the nonlinear extension is still urgently requested because almost all the mechanical/electrical systems are nonlinear. Therefore, the cooperative control for networked nonlinear systems has attracted more attention recently [25, 26]. For example, the leader-follower consensus problem for second-order nonlinear multi-agent systems was investigated in [27] with a specific type of nonlinearity. In their work, the stability analysis was conducted on the basis of LaSalle's invariance principle. Furthermore, by taking advantage of M-matrix method and the property of nonnegative matrices, the second-order nonlinear multi-agent systems were also investigated in [28], and it was conclusively proven that the

leader-follower consensus can be reached more easily with higher pinning feedback gains. Among these networked nonlinear multi-agent systems, the networked Euler-Lagrange systems are especially important due to their broad applications [29, 30].

Euler-Lagrange system usually refers to a large class of mechanical systems whose dynamics can be described using Lagrange's equations. Lagrange's equations are shown as follows [31]

$$\frac{d}{dt} \frac{\partial L}{\partial \dot{q}_i} - \frac{\partial L}{\partial q_i} = p_i \quad i = 1, \dots, m$$

where the Lagrangian L is defined as the difference between the kinetic and potential energy of the system, q_i is the i th element of the generalized coordinates vector $q \in \mathbb{R}^m$ and p_i is the external force exerting on the i th generalized coordinate. Typically, the Lagrange's equations can be derived based on the energy properties of the specific mechanical system, and its vector form is more commonly utilized. The vector form of Lagrange's equations is

$$\frac{d}{dt} \frac{\partial L}{\partial \dot{\mathbf{q}}} - \frac{\partial L}{\partial \mathbf{q}} = \mathbf{p}$$

where $\mathbf{p} = [p_1, \dots, p_m]^T$. Once the kinetic energy and the potential energy of a mechanical system are specified, the dynamics of the mechanical system can be generally formulated as

$$\mathbf{M}\ddot{\mathbf{x}} + \mathbf{C}\dot{\mathbf{x}} + \mathbf{g} = \mathbf{u}$$

where matrices \mathbf{M} , \mathbf{C} and vector \mathbf{g} can be explicitly derived using the Lagrange's

equations. Vectors \mathbf{x} and \mathbf{u} are the generalized coordinates and generalized input, respectively.

Consensus algorithms for Euler-Lagrange agents are especially attractive because they have been widely used to model a number of mechanical systems such as autonomous vehicles, rigid manipulators and flexible payloads. Therefore, an algorithm that can solve the consensus problem for Euler-Lagrange systems will be useful for a large number of practical consensus seeking problems. In [29], a model-independent consensus algorithm for networked Euler-Lagrange agents, which can realize distributed leaderless consensus, is presented with convergence analysis conducted using Matrosov's theorem. Consensus will be achieved as long as the undirected communication topology is connected. Distributed containment control is studied in [32] for Euler-Lagrange systems and the parametric uncertainties are also considered. Furthermore, the leaderless consensus algorithm is studied using a directed graph. In [32], a distributed consensus problem is studied with the combination of classical adaptive consensus. Time-delays and the switching topology are both considered in the controller design. The authors constructed an elaborate Lyapunov function which proved the stability of their controller. Parametric uncertainties are considered in [33], where the distributed containment control and leaderless synchronization are achieved in the presence of constant parameter uncertainties. Similarly, Ref. [34] solves the consensus control problem for Euler-Lagrange

systems in the appearance of unknown parameters and time-varying delay.

Except for the Euler-Lagrange systems, the networked Lipschitz nonlinear systems [35–38] have also been investigated due to the generality of the Lipschitz system. The Lipschitz system can represent not only mechanical systems but also electrical systems, while the Euler-Lagrange system is mostly adopted to describe the dynamics of a mechanical system. The Lipschitz nonlinear system is usually referred to as a dynamical system in which the nonlinear term in the dynamics equation satisfies the Lipschitz condition, namely, the nonlinear mapping $\mathbf{f} : \mathbb{R}^n \times \mathbb{R} \rightarrow \mathbb{R}^n$ satisfies

$$\|\mathbf{f}(x, t) - \mathbf{f}(y, t)\| \leq L \|\mathbf{x} - \mathbf{y}\|$$

Many nonlinearities satisfy the Lipschitz condition in practice. For example, the sinusoidal terms in robotic dynamics are all globally Lipschitz [39, 40]. Moreover, even terms like x^2 can also be regarded as Lipschitz if the operating range of x is bounded [41].

1.2 Malfunction of multi-agent systems

One of the most representative applications of consensus algorithm is the realization of large-scale wireless sensor networks. A wireless sensor network, with multiple small and cheap sensors, can cover a vastly larger area than a single, expensive and complicated sensing device. The actualization of large-scale wireless sensor

networks will hugely benefit weather measurement and forecasting, pollution or forest fire monitoring, measurements of electromagnetic pollution and so on. With the growth of the network scale, the sensing area is rapidly enlarged. Simultaneously, the number of sensing devices are increased, which not only complicates the hardware system, but also makes the computational complexity greater. Accordingly, the increasing scale of wireless sensor network may add the risk of hardware and software bugs, which may prevent the networked sensors converging to the desired estimation value. Consequently, the problem of fault-tolerant algorithm in multi-agent systems emerges. Since all the agents are coupled via network and no centralized controller can monitor the entire system, it is highly possible that the team objective will be crashed if one agent stops functioning normally. Unlike the centralized faulty system, the nonfunctional agent in a distributed system is probably unobservable by the agents out of its neighborhood. Hence, the fault detection and isolation (FDI) problem is more challenging in multi-agent systems. To deal with the faulty agents in distributed multi-agent systems, Ref. [42] developed a distributed function calculation method with a broadcast model. Each agent updates its state periodically as a weighted linear combination of its own state and the neighbors'. Since the weights of a consensus algorithm are determined by the network structure, its fault-tolerant capability to a specific malicious behavior is decided by the communication topology. Consequently, Ref. [42] concluded that all

of the nodes can converge to the same value asymptotically if the network topology satisfies certain conditions. A useful tool for FDI is the so-called “motion probes.” With the help of motion probes, Ref. [43] discussed a way of detecting a faulty agent with single integrator dynamics. The basic idea in that paper is to take advantage of the natural properties of group motions, such as the preservation of centroid of the network or weighted average of the initial states, to achieve the fault detection. In addition to their work, Ref. [44] further investigated active fault diagnosis and identification. The work in [44] was also an application of the motion probe method developed in [43]. Along with the function recovery method for linear consensus network, Ref. [44] proposed a formal classification for agent faults. If the agent does not update its state information according to the predetermined iteration strategy, this kind of fault is called “stuck.” An agent with stuck will drift away from the expected destination, but it is still visible to its neighbors with respect to the communication topology. Ref. [44] proposed an effective identification method dealing with stuck, in which the state of a faulty agent will be compared with its neighbors’ states. If all the states are equal, then it is fault-free. Otherwise, a faulty agent is detected. A further complicated situation, multiple stuck faults, is also discussed by the authors. The group will converge to a convex hull generated by the stuck agents [45]. Similarly, the presence of this kind of fault can be detected by examining its state and its neighbors’ states as well. In sum, any disagreement enduring a

sufficiently long time between static agents will expose the stuck agents. Another kind of fault, called divergence fault, happens when a sensor recurrently sends out incorrect signals. These signals could be increasing or decreasing constantly in their values. By inspecting the sustained increments or decrements, this kind of fault can be detected based on model identification. Unlike the classification in [44], two kinds of misbehaving agents are categorized mathematically in [46]: non-colluding (or faulty) and Byzantine (malicious) agent. As for the non-colluding agents, their malfunctions are purely caused by random faults. If the intriguing messages are disseminated by an agent with the purpose of destroying the group mission, this agent is denoted as the Byzantine agent. Other than the fault detection strategies based on an ideal model, the influence caused by unknown input is investigated by [47]. A bank of unknown input observers are recruited for FDI in a network with linear time invariant (LTI) systems. The existence of this kind of unknown input observers are proven for the networks of interconnected second-order LTI systems. Ref. [47] takes the investigation further on the distributed feasibility of unknown input observer according to the system structure. Meanwhile, with the removal method of faulty agents carried out, applications to power networks and robotic formations are presented as illustrative examples. To mitigate the computational work load for each agent, Ref. [48] conducts a real-time distributed fault detection strategy. The information redundancy of each agent is realized by in-

specting its neighbors, i.e. only local information is needed. The robustness is also considered in the proposed fault isolation procedure. It is revealed that the group performance is guaranteed in the presence of model uncertainties and disturbances.

1.3 Communication structure

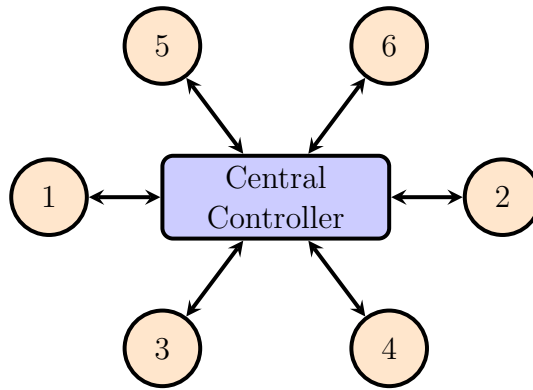


Fig. 1.4 Centralized structure: a central controller exists in the networked system

In control community, one of two approaches is usually implemented to solve the synchronization problem. The first is centralized control, which extends classical control theory based on the assumption that a central controller exists. The multi-agent system is treated as a multiple-input multiple-output (MIMO) system and the central controller can maneuver all the agents in the system [49]. The other approach is that of distributed control in which each agent can only detect its neighbors' information according to the communication topology. In the dis-

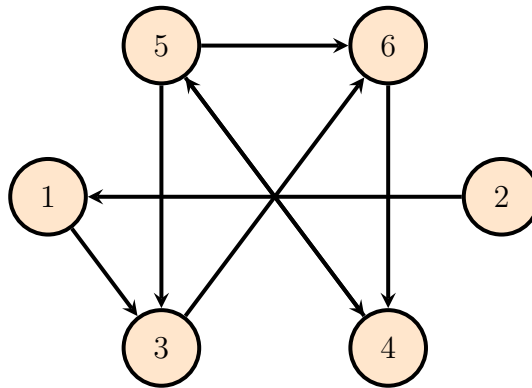


Fig. 1.5 Decentralized structure: there is no central controller and agents share the information locally

tributed control approach, the networked agents share information locally according to the communication topology, and the desired trajectory vector of each agent will be derived individually based on the local information. Obviously, the rich availability of mathematical tools in classical control theory extensively enables the development of the cooperative controller in centralized direction. However, a fully connected network is presumed in the centralized control of multi-agent systems along with a central processor, which will fundamentally disable the feasibility of the centralized control scheme when a large number of agents are involved in the group. This is because, with the growing number of agents, the computational and communication workload in the centralized strategy will be increased consistently, and will eventually exceed the the capability of the central processor. Compared to the centralized control strategy, the decentralized approach can be character-

ized by its effectiveness involving a large number of agents because no centralized controller is expected in the decentralized approach. Thus, strong computational capability is not demanded in the distributed consensus seeking algorithm. During the design of consensus law, the specific characteristics of a single agent are usually disregarded and only dynamics are extracted mathematically. Then, the group behaviors will be described by the coupled agent dynamics. Owing to the coupling relationship, the structure of the communication network plays a crucial role naturally and can be represented by graph Laplacian. Due to the mathematical essentiality of the graph Laplacian, it rapidly became an important tool for the description of communication topology [50]. With the assistance of graph theory, distributed consensus schemes have been systematically developed for agents with linear dynamics [6]. The distributed consensus problem was first studied in [51] from the perspective of control. After this, several important papers were published successively in the control community. In [52], the authors studied a n -agent model coupled via time-dependent communication links. This model can be applied in various research topics, such as synchronization, swarming and distributed decision making, among others. Ref. [53] provides a theoretical explanation for the model proposed in [54], while Ref. [4] provides a theoretical framework for the robust analysis of multi-agent systems. The method of analysis is developed based on algebraic graph theory and Nyquist criterion. The formation stability of the agents

can be decided by the eigenvalues of the graph Laplacian matrix via the analysis method. The consensus seeking method with the consideration of time-delays and switching topologies was studied in [5].

1.4 Network-induced challenges

1.4.1 Sampled-data communication

In multi-agent systems, the agents are coupled by the wireless network; they are not physically connected to each other and the information is transmitted through a digital network intermittently. Therefore, the sampled-data information becomes a challenging problem for local controllers equipped on each agent due to the discontinuous information transmission. With the appearance of sampled-data information exchange, the leader-follower consensus problem was investigated in [55]. In their work, the M-matrix theory is applied to derive the sufficient conditions for system stability, while the velocity and acceleration of the leader are unavailable for the controller. Furthermore, the stable sampling period can be indicated based on their results. The sampled-data information was considered in [56] for double-integrator multi-agent systems. Both undirected and directed interactions were studied in their work. The zero final velocity and constant final velocity consensus were achieved based on the discrete-time dynamics model. In [57], the consensus

seeking problem was also considered for second-order multi-agent systems. Unlike in [56], both synchronous and asynchronous sampling measurements were investigated with the consideration of sampled-data information exchange. With the appearance of nonlinear dynamics, the sampled-data problem was studied in [58] along a discrete-time approach and the Euler approximate method was adopted to derive the discrete-time models. Then, a discrete-time output feedback controller was proposed in their work based on the Euler approximate models. Other than discretization of the continuous-time dynamical model, a reversed approach is also proven to be effective for the sampled-data control problem. In the reversed approach, the sampled-data problem is not investigated based on the discrete-time dynamical model. Instead, the discrete-time problem (sampled-data controller design) is transformed into a continuous-time problem assuming that the discrete-time control signal is caused by time-varying delays [59] in a continuous-time system. This reversed approach was adopted in [60] to derive a robust sampled-data controller, and a sufficient linear matrix inequalities (LMIs) condition was proposed on the basis of descriptor approach to time-delay systems. In their work, the piecewise-linear delay function played a key role for the connection between the sampling system and the continuous-time system. To further bridge the gap between the piecewise continuous state space and the smooth vector field, Ref. [61] conducted an improvement on the discontinuous Lyapunov functional method, based on which a sufficient

condition with less conservativeness is presented for sampled-data systems. Moreover, Ref. [62] refined the previous work and developed a unified method for a sampled-data control problem via the time-delay approach. Furthermore, the exponential convergence is guaranteed and the convergent rate is directly represented by a parameter in the discontinuous Lyapunov functional. On the basis of the well-developed sampled-data control theory in linear system, researchers have begun paying attention to the consensus seeking problem for nonlinear systems sharing the sampled-data information. With the presence of the Lipschitz nonlinearity, Ref. [63] proposed a consensus seeking protocol for networked nonlinear systems and the time-delay technique is applied to deal with the sampled-data information. Coupled by a strongly connected network in [63], the consensus can be achieved by a set of nonlinear agents. Furthermore, their results were extended to the communication structure with a directed spanning tree. Other than the sampled-data information and nonlinear dynamics, system perturbation (uncertainty or noise) is another significant challenge for the consensus achievement. The mismatched parametric uncertainties were considered in [64], and an adaptive consensus tracking algorithm was investigated for a group of nonlinear agents. The measurement noises were considered in [65], and a sampled-data consensus tracking algorithm was developed based on the delay decomposition technique. In their work, the necessary and sufficient conditions for mean square bounded consensus tracking was

proposed with the assistance of the augmented matrix method and probability limit theory.

1.4.2 Topology switching

The time-varying topology in consensus problem was widely investigated [5,66] because it is comparatively more generic. In the appearance of the switching communication interaction, the leader-follower consensus with uncertain Euler-Lagrange systems was studied in [67], and the convergence of the error systems was guaranteed by their distributed adaptive controller. Moreover, the communication topology in their work is not necessarily connected all the time. Ref. [68] conducted the research on Markovian switching topology for second-order multi-agent systems, and a necessary and sufficient condition for consensus achievement was presented in their work. Markovian switching topology was also considered in [69], where the leader-follower consensus problem was investigated with the consideration of non-linear dynamics and communication delay. Furthermore, Ref. [70] discussed the leader-follower consensus with switching topology for a general linear agent, and the convergence of the closed-loop control system was proven along the Riccati-inequality-based approach. With the consideration of the switching topology, the leader-follower consensus control was investigated on the basis of the discrete-time multi-agent systems in [71]. Both fixed and switching topologies were considered

in [22] with a globally reachable leader. In their work, the finite-time convergent leader-follower consensus problem was studied and the second-order consensus was successfully reached. To further extend the leader-follower consensus algorithm to second-order nonlinear multi-agent systems with both fixed and time-varying communication topologies, Ref. [72] presented the sufficient conditions for consensus achievement along the Lyapunov approach. A class of nonlinear dynamics was dealt with in their work, and the leader-follower consensus was achieved with local intermittent information.

1.4.3 Event-triggered signal update

Coupling multiple agents can also increase the workload of each agent because both local and global information must be dealt with on time. To reduce the computational burden for each single agent, event-triggered control strategy was investigated [73–78]. In event-triggered control protocol, the control output is not implemented consistently or periodically. Instead, it is carried out once the event-triggered conditions are violated. Namely, the control output is updated intermittently according to the event-triggered conditions. Therefore, the workload of each agent can be immensely reduced through the event-triggered strategy. The event-triggered consensus problem for first-order multi-agent systems was investigated in [79] and the event-triggered conditions were proposed for both centralized and

distributed situations. Moreover, the self-triggered multi-agent control protocol was proposed to relax the trigger condition. The event-triggered control algorithm was extended to the second-order multi-agent systems in [23]. Particularly, the Lipschitz nonlinearity was considered in their work because the nonlinear dynamics is almost unavoidable in practice. The leader-follower consensus problem for Lipschitz nonlinear multi-agent systems was also considered in [80], where the jointly connected topology was assumed for the coupling relationship.

1.5 Research Objectives and Organization

The main research objective of this dissertation is to develop the consensus algorithms for networked nonlinear systems with the occurrence of disturbances, uncertainties and possible system malfunctions. In addition to the nonlinear extension of the agent dynamics, the network-induced problems, including sampled-data communication and topology switching, will be investigated systematically.

Chapter 2 briefly explains the algebraic graph theory, perturbation theory and nonlinear realization theory that will be utilized in the following chapters. In order to mathematically describe the communication structure, the terminologies and basic principles in algebraic graph theory are used in the controller design. For example, the coupling relationship of the agent position vector is described using Laplacian matrix, and this coupled vector is usually considered as an important

indicator for the consensus achievement. In the practical applications, disturbances and uncertainties are mostly unavoidable, which in turn implies that the dynamical equation of the control system will be perturbed by some time-varying parameters. Hence, the stability of the perturbed multi-agent systems is investigated with the assistance of perturbation theory in this work. In any applications of multi-agent systems, safety is always a compelling requirement. Therefore, the fault diagnosis technique is discussed in this dissertation. To enable the detection of the possible fault, observability of the possible fault is the precondition. Thus, the observability of the possible fault will be investigated using the nonlinear realization theory.

Then, a consensus algorithm for networked Euler-Lagrange systems is investigated in Chapter 3 with experimental verification. The mathematical description of the networked Euler-Lagrange systems and the main work in Chapter 3 are presented in Section 3.1. In Section 3.2, the nonlinear consensus algorithm is investigated with the consideration of disturbance and uncertainty. With the appearance of bounded disturbances and time-varying uncertainties, the consensus seeking algorithm is designed in Section 3.2 and the stability of the networked system is analyzed based on the perturbation theory. The robustness against structural uncertainty is analyzed through a passivity approach in Section 3.2.2. Section 3.3 presents the experimental tests using four Quanser's 3-DOF helicopters.

Next, Chapter 4 is concerned with a distributed leader-follower formation track-

ing problem with the appearance of an additive noise. In Section 4.1, the distributed leader-follower formation tracking problem is formulated for networked Euler-Lagrange systems. Section 4.2 presents the basic assumptions and stability analysis. Particularly, the mathematical expression of the bounded noise is presented. Bounded noise is very common in controller design because of its generality. However, most of them assumed that the noise was bounded by a known constant. Unlike the previous work, the bounded noise in this work is bounded by an unknown time-varying boundary instead of a constant. A passivity-based control technique is adopted in Section 4.2.1. Moreover, the distributed leader-follower controller is proposed and the system stability is analyzed using the tools in non-smooth analysis. On top of the distributed leader-follower controller, an observer-based fault diagnosis strategy is presented in Section 4.2.2. In Section 4.3, simulations are conducted using six networked 3-DOF helicopters.

Different from the Euler-Lagrange system, the Lipschitz system can be used to represent not only mechanical system but also electrical system. Namely, the Lipschitz system is more generic compared to the Euler-Lagrange system. Therefore, a distributed \mathcal{H}_∞ consensus seeking problem is studied for networked Lipschitz nonlinear systems in Chapter 5. Other than the nonlinear dynamics, sampled-data information exchange is also considered in Chapter 5. In Section 5.1, the consensus seeking problem of networked Lipschitz systems is formulated based on the

sampled-data communication. The sampled-data controller design is presented in Section 5.2. Unlike the previous work, the output-feedback controller is investigated in this work. Meantime, a state observer is proposed to estimate the state information. In the controller development, sampled-data communication poses a huge challenge for the stability analysis because both discrete-time and continuous-time states are existing in the sampled-data multi-agent systems. To overcome this challenge, the convergence of the observer and controller is proven via a Lyapunov functional approach, in which the sampled-data dynamics are equivalently described by a time-delay differential equation. Furthermore, an optimization algorithm is developed to derive the controller and observer gains iteratively. Moreover, the external disturbance is also considered in the controller design, and the influence of the disturbance is minimized based on the \mathcal{H}_∞ robust control theory. In Section 5.3, a distributed synchronization of four identical Chua's circuits is conducted with the consideration of sampled-data communication and \mathcal{L}_2 -bounded disturbance.

Then, Chapter 6 presents an event-triggered consensus controller for networked Lipschitz systems. In Section 6.1, the event-triggered consensus problem is formulated with the consideration of stochastic switching communication topology. In the event-triggered consensus problem, the control signal is implemented neither continuously nor periodically. Basically, the control signal is carried out only if an event-triggered condition is violated. Namely, the computational resource is avail-

able for any other work when the event-triggered condition is satisfied. Therefore, the event-triggered consensus controller will effectively reduce the computational burden for each agent. With the help of the Lyapunov functional method, an event-triggered consensus controller and its event-triggered condition are proposed in Section 6.1. Section 6.2 presents the stability analysis of the networked Lipschitz systems coupled by the proposed event-triggered consensus controller. In this work, the event-triggered condition is verified periodically according to the communication period. Therefore, both the sampled-data communication and the event-triggered condition are taken into account in the stability analysis. Furthermore, a random parameter is contained in the Lyapunov functional because of the inclusion of the stochastic switching communication topology. The switching of the random parameter and the communication topology is mathematically described by a finite Markov jump process. Except for the stability analysis, an LMI-based optimization algorithm is also proposed to enable the iterative derivation of controller gains. In Section 6.3, four identical Chua's circuits are coupled by a stochastic structure-switching network in the simulation. The event-triggered consensus is achieved successfully, which further demonstrates the effectiveness of the proposed event-triggered consensus controller.

Finally, Chapter 7 concludes this dissertation with some future research directions.

1.6 Major Contributions

The major contributions of this dissertation are:

- (i) Design of a realizable nonlinear consensus algorithm for networked Euler-Lagrange systems with the consideration of bounded disturbance and structural uncertainty.
- (ii) Robustness analysis for networked Euler-Lagrange systems, in which the influence of the bounded disturbance and the structural uncertainty is investigated from the point of view of a passive system.
- (iii) Incorporating a passivity-based term in the distributed leader-follower formation tracking controller, which enables the robustness against a boundary-unknown noise.
- (iv) Design of an observer-based fault diagnosis strategy for networked Euler-Lagrange systems, and discussion of the observability of possible faults for networked Euler-Lagrange systems using differential geometry tools.
- (v) Development of an \mathcal{H}_∞ robust synchronization controller for networked Lipschitz nonlinear systems with sampled-data communication.
- (vi) Design of an event-triggered consensus controller for networked Lipschitz nonlinear systems with sampled-data communication and switching topologies.

2 Preliminaries

This chapter introduces the algebraic graph theory, perturbation theory and nonlinear realization theory. The main objective of this chapter is to pave the way for the theoretical analysis in the following chapters. Therefore, the explanation in this chapter is not a self-contained treatment of these theoretical tools. Instead, only the topics closely related to our controller design are presented.

2.1 Notations

The notation utilized in this work is fairly standard. The n -dimensional Euclidean space is denoted by \mathbb{R}^n . The dual space of \mathbb{R}^n is defined by $(\mathbb{R}^n)^*$ and the element in $(\mathbb{R}^n)^*$ is denoted as $\mathbf{a}^* \in (\mathbb{R}^n)^*$. The superscript “ T ” represents matrix transpose, and a symmetric matrix \mathbf{M} is denoted as a positive definite matrix by $\mathbf{M} > 0$. In symmetric matrix, “ \star ” is used to indicate the entry implied by the symmetry. Unless explicitly explained, \mathbf{I} and $\mathbf{0}$ are referred to as identity matrix and zero matrix with appropriate dimensions. The inner product of vectors $\mathbf{a}, \mathbf{b} \in \mathbb{R}^n$

is denoted as $\langle \mathbf{a}, \mathbf{b} \rangle$. The Kronecker product of matrices $\mathbf{A} \in \mathbb{R}^{n \times m}$ and $\mathbf{B} \in \mathbb{R}^{j \times k}$ is defined as follows

$$\mathbf{A} \otimes \mathbf{B} = \begin{bmatrix} a_{11}\mathbf{B} & a_{12}\mathbf{B} & \dots & a_{1m}\mathbf{B} \\ a_{21}\mathbf{B} & a_{22}\mathbf{B} & \dots & a_{2m}\mathbf{B} \\ \vdots & \vdots & \ddots & \vdots \\ a_{n1}\mathbf{B} & a_{n2}\mathbf{B} & \dots & a_{nm}\mathbf{B} \end{bmatrix}$$

Definition 2.1. *The networked multiple agents achieve the consensus if*

$$\lim_{t \rightarrow \infty} \|\mathbf{x}_i(t) - \mathbf{x}_j(t)\| = 0, \quad \forall p_i, p_j \in \mathcal{V}(k)$$

where $\mathbf{x}_i \in \mathbb{R}^n$ is the state of agent p_i .

Definition 2.2. [81] *A continuous function $\alpha : [0, a) \rightarrow [0, \infty)$ is said to belong to class \mathcal{K} if it is strictly increasing and $\alpha(0) = 0$. It is said to belong to class \mathcal{K}_∞ if $a = \infty$ and $\alpha(r) \rightarrow \infty$ as $r \rightarrow \infty$.*

Definition 2.3. [81] *A continuous function $\beta : [0, a) \times [0, \infty) \rightarrow [0, \infty)$ is said to belong to class \mathcal{KL} if, for each fixed s , the mapping $\beta : (r, s)$ belongs to class \mathcal{K} with respect to r and, for each fixed r , the mapping $\beta : (r, s)$ is decreasing with respect to s and $\beta : (r, s) \rightarrow 0$ as $s \rightarrow \infty$.*

2.2 Algebraic graph theory

A weighted directed graph (digraph) \mathcal{G} is used to describe the communication relationship between the n agents [5]. The vertex set of graph \mathcal{G} is defined as

$\mathcal{V}(k) \subset \mathbb{R}^n$. Each vertex point is labeled by $p_i \in \mathcal{V}(k)$ for $i = 1, 2, \dots, k$. The edge set is denoted as $\mathcal{E}_{\mathcal{G}}(\mathcal{V}(k)) \subset \mathcal{V}(k) \times \mathcal{V}(k)$. The adjacency element e_{ij} belongs to the edge set $\mathcal{E}_{\mathcal{G}}(\mathcal{V}(k))$ as long as the information of p_j can be detected by p_i , $e_{ij} = 1 \quad \forall i \neq j$, e_{ii} is assumed to be zero for all $p_i \in \mathcal{V}(k)$. The information received by vertex p_i from the vertex p_j is referred to as in-direction information flow, with the requirement that the vertex p_i can detect the vertex p_j . If there always exists a path from vertex p_i to vertex $p_j \in \mathcal{V}(k) \setminus \{p_i\}$, the vertex p_i is defined as a center of the graph \mathcal{G} [82]. The weighted adjacency matrix is constructed as $\mathbf{A} = [e_{ij}]$, $\mathcal{N}_{\mathcal{G}}(p_i) = \{p_j \in \mathcal{V}(k) : (p_i, p_j) \in \mathcal{E}_{\mathcal{G}}(\mathcal{V}(k))\}$ is the neighbor map of agent p_i . The in-degree and out-degree are defined as $deg_{in}(p_i) = \sum_{p_j \in \mathcal{N}_{\mathcal{G}}(p_i)} e_{ji}$ and $deg_{out}(p_i) = \sum_{p_j \in \mathcal{N}_{\mathcal{G}}(p_i)} e_{ij}$. The degree matrix of \mathcal{G} is a diagonal matrix $\mathbf{\Gamma}$ with element $\mathbf{\Gamma}_{ij}$, where $\mathbf{\Gamma}_{ij} = 0 \quad \forall i \neq j$ and $\mathbf{\Gamma}_{ii} = deg_{out}(p_i)$. The graph Laplacian of \mathcal{G} is denoted as

$$\mathcal{L}(\mathcal{G}) = \mathbf{\Gamma} - \mathbf{A}$$

For example, in Figure 2.1, the arrow from agent 1 to agent 5 indicates that agent 1 has access to the information of agent 5, namely, the state information of agent 5 is available to agent 1 and $e_{15} \in \mathcal{E}_{\mathcal{G}}(\mathcal{V}(6))$. The weighted adjacency matrix

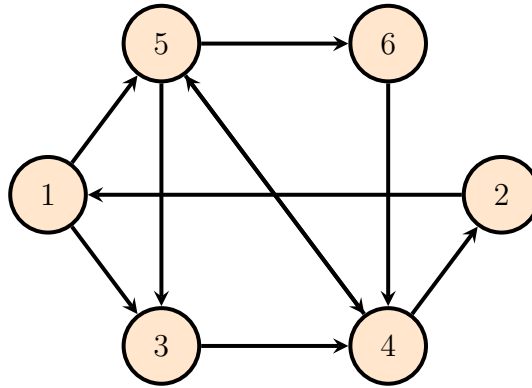


Fig. 2.1 Communication topology

is

$$\mathbf{A} = \begin{bmatrix} 0 & 0 & 1 & 0 & 1 & 0 \\ 1 & 0 & 0 & 0 & 0 & 0 \\ 0 & 0 & 0 & 1 & 0 & 0 \\ 0 & 1 & 0 & 0 & 1 & 0 \\ 0 & 0 & 1 & 1 & 0 & 1 \\ 0 & 0 & 0 & 1 & 0 & 0 \end{bmatrix}$$

and the degree matrix is

$$\mathbf{\Gamma} = \begin{bmatrix} 2 & 0 & 0 & 0 & 0 & 0 \\ 0 & 1 & 0 & 0 & 0 & 0 \\ 0 & 0 & 1 & 0 & 0 & 0 \\ 0 & 0 & 0 & 2 & 0 & 0 \\ 0 & 0 & 0 & 0 & 3 & 0 \\ 0 & 0 & 0 & 0 & 0 & 1 \end{bmatrix}$$

Consequently, the Laplacian of the graph in Figure 2.1 is

$$\mathcal{L}(\mathcal{G}) = \begin{bmatrix} 2 & 0 & -1 & 0 & -1 & 0 \\ -1 & 1 & 0 & 0 & 0 & 0 \\ 0 & 0 & 1 & -1 & 0 & 0 \\ 0 & -1 & 0 & 2 & -1 & 0 \\ 0 & 0 & -1 & -1 & 3 & -1 \\ 0 & 0 & 0 & -1 & 0 & 1 \end{bmatrix}$$

For a Laplacian matrix, $\mathbf{1}_n$ is always a right eigenvector associated with the zero

eigenvalue, i.e. $\mathcal{L}(\mathcal{G}) \mathbf{1}_n = \mathbf{0}$, where $\mathbf{1}_n$ is a n -dimensional vector with 1 as each element.

2.3 Perturbed systems

The dynamics of a system can be theoretically described using a nonlinear dynamical equation as follows

$$\dot{\mathbf{x}} = f(t, \mathbf{x}) \tag{2.1}$$

where $\mathbf{f} : [0, \infty) \times \mathbf{D} \rightarrow \mathbb{R}^n$ is piecewise continuous in t and locally Lipschitz in \mathbf{x} on $[0, \infty) \times \mathbf{D}$, and $\mathbf{x} \in \mathbf{D} \subset \mathbb{R}^n$, where \mathbf{D} contains the origin $\mathbf{x} = 0$. However, perturbation is mostly unavoidable in practice due to modeling errors and other unmodeled effects. Hence, Eq. (2.1) is usually revised with the appearance of a perturbation term $\mathbf{g}(t, \mathbf{x})$ as

$$\dot{\mathbf{x}} = \mathbf{f}(t, \mathbf{x}) + \mathbf{g}(t, \mathbf{x}) \tag{2.2}$$

where $\mathbf{g} : [0, \infty) \times \mathbf{D} \rightarrow \mathbb{R}^n$. In practice, the explicit formulation of the perturbation is usually unknown, while only the upper boundary of the perturbation can be measured, namely, the maximum value of $\|\mathbf{g}(t, \mathbf{x})\|$ is known. In order to analyze the convergence of the perturbed system (2.2), Lemma 2.1 is presented in [81]

Lemma 2.1. *Let $\mathbf{x} = 0$ be an exponentially stable equilibrium point of the nominal system (2.1). Let $V(t, \mathbf{x})$ be a Lyapunov function of the nominal system that*

satisfies the inequalities

$$c_1 \|\mathbf{x}\|^2 \leq V(t, \mathbf{x}) \leq c_2 \|\mathbf{x}\|^2 \quad (2.3)$$

$$\frac{\partial V}{\partial t} + \frac{\partial V}{\partial \mathbf{x}} f(t, \mathbf{x}) \leq -c_3 \|\mathbf{x}\|^2 \quad (2.4)$$

$$\left\| \frac{\partial V}{\partial \mathbf{x}} \right\| \leq c_4 \|\mathbf{x}\| \quad (2.5)$$

in $[0, \infty) \times D$, where $D = \{x \in \mathbb{R}^n \mid \|x\| < r\}$. Suppose the perturbation term $\mathbf{g}(t, \mathbf{x})$ satisfies

$$\|\mathbf{g}(t, \mathbf{x})\| \leq \delta < \frac{c_3}{c_4} \sqrt{\frac{c_1}{c_2}} \theta r \quad (2.6)$$

for all $t \geq 0$, all $\mathbf{x} \in D$, and some positive constant $\theta < 1$. Then, for all $\|\mathbf{x}(t_0)\| < \sqrt{\frac{c_1}{c_2}}$, the solution $\mathbf{x}(t)$ of the perturbed system (2.2) satisfies

$$\|\mathbf{x}(t)\| \leq k \exp[-\gamma(t - t_0)] \|\mathbf{x}(t_0)\|, \forall t_0 \leq t < t_0 + T$$

and

$$\|\mathbf{x}(t)\| \leq b, \quad \forall t \geq t_0 + T$$

for some finite T , where

$$k = \sqrt{\frac{c_2}{c_1}}, \quad \gamma = \frac{(1 - \theta)c_3}{2c_2}, \quad b = \frac{c_4}{c_3} \sqrt{\frac{c_2}{c_1}} \frac{\delta}{\theta}$$

To further deal with the nonvanishing perturbation, the input-to-state stable is defined as follows

Definition 2.4. Consider the following system which is obtained by incorporating a piecewise continuous function $\mathbf{u}(t)$ to Eq. (2.1) [81],

$$\dot{\mathbf{x}} = \mathbf{f}(t, \mathbf{x}) + \mathbf{u}(t) \quad (2.7)$$

where $\mathbf{u}(t)$ is a bounded function of t for all $t \geq 0$. The system (2.7) is said to be input-to-state stable if Eq. (2.1) has a globally uniformly asymptotically stable equilibrium point at the origin $\mathbf{x} = 0$, and there exist a class \mathcal{KL} function β and a class \mathcal{K} function γ such that for any initial state $\mathbf{x}(t_0)$ and any bounded input $\mathbf{u}(t)$, the solution $\mathbf{x}(t)$ exists for all $t \geq t_0$ and satisfies

$$\|\mathbf{x}(t)\| \leq \beta(\|\mathbf{x}(t_0)\|, t - t_0) + \gamma(\sup_{t_0 \leq \tau \leq t} \|\mathbf{u}(\tau)\|)$$

Then, the input-to-state stability can be analyzed using the following lemma

Lemma 2.2. [81] Suppose the right-hand side of Eq. (2.7) is continuously differentiable and globally Lipschitz in (\mathbf{x}, \mathbf{u}) , uniformly in t . If the unperturbed system (2.1) has a globally exponentially stable equilibrium point at the origin $\mathbf{x} = 0$, then the system (2.7) is input-to-state stable.

2.4 Nonlinear realization theory

Nonlinear realization theory will be adopted to investigate the coupling relationship between the specific agent fault and the feasibility of the fault diagnosis

method. It is not expected to systematically explain the nonlinear realization theory in this section. Instead, only the content closely related to our work will be described, and all the theorems in this section will be concisely presented without proof. The detailed nonlinear realization theory can be found in [83].

Suppose n smooth vector fields $\mathbf{f}_1, \mathbf{f}_2, \dots, \mathbf{f}_n$ are defined on open set U , and the vectors span a vector space at any fixed point $\mathbf{x} \in U$. Then, a distribution is identified by the vector fields $\{\mathbf{f}_1, \mathbf{f}_2, \dots, \mathbf{f}_n\}$ as

$$\Delta = \text{span} \{\mathbf{f}_1, \mathbf{f}_2, \dots, \mathbf{f}_n\} \quad (2.8)$$

Particularly, $\Delta(\mathbf{x})$ is denoted as the value of Δ at a point \mathbf{x} . The annihilator of $\Delta(\mathbf{x})$ can be defined

$$\Delta^\perp(\mathbf{x}) = \{\mathbf{a}^* \in (\mathbb{R}^n)^* : \langle \mathbf{a}^*, \mathbf{b} \rangle = 0, \forall \mathbf{b} \in \Delta(\mathbf{x})\}$$

The smallest distribution that contains Δ and is invariant under the vector fields $\{\mathbf{g}_1, \mathbf{g}_2, \dots, \mathbf{g}_n\}$ is denoted by $\langle \mathbf{g}_1, \mathbf{g}_2, \dots, \mathbf{g}_n | \Delta \rangle$.

The Lie product of two vector fields $\mathbf{f}_1 \in \mathbb{U}$ and $\mathbf{f}_2 \in \mathbb{U}$ at each $\mathbf{x} \in \mathbb{U}$ can be defined as follows

$$[\mathbf{f}_1, \mathbf{f}_2](\mathbf{x}) = \frac{\partial \mathbf{f}_2}{\partial \mathbf{x}} \mathbf{f}_1(\mathbf{x}) - \frac{\partial \mathbf{f}_1}{\partial \mathbf{x}} \mathbf{f}_2(\mathbf{x})$$

In order to calculate $\langle \mathbf{g}_1, \mathbf{g}_2, \dots, \mathbf{g}_n | \Delta \rangle$, the following lemma is used (Lemma 1.8.2 in [83])

Lemma 2.3. *Suppose Δ is a distribution and $\zeta_1, \zeta_2, \dots, \zeta_q$ are a set of vector fields, the nondecreasing sequence of distributions Δ_k can be calculated by the iteration in Eq. (2.9), and $\Delta_k \subset \langle \zeta_1, \zeta_2, \dots, \zeta_q | \Delta \rangle, \forall k$.*

$$\begin{aligned} \Delta_0 &= \Delta \\ \Delta_k &= \Delta_{k-1} + \sum_{i=1}^q [\zeta_i, \Delta_{k-1}] \end{aligned} \tag{2.9}$$

If there exists an integer \bar{k} such that $\Delta_{\bar{k}} = \Delta_{\bar{k}+1}$, then

$$\Delta_{\bar{k}} = \langle \zeta_1, \zeta_2, \dots, \zeta_q | \Delta \rangle$$

On the basis of the above presented notations, the input-output relationship for an affine nonlinear system can be presented in the following theorem (Theorem 3.3.2 in [83])

Theorem 2.1. *Consider a nonlinear control system of the following form*

$$\begin{aligned} \dot{\mathbf{x}} &= \mathbf{f}(\mathbf{x}) + \sum_{i=1}^m \mathbf{g}_i(\mathbf{x})u_i \\ y_j &= h_j(\mathbf{x}) \quad 1 \leq j \leq p \end{aligned} \tag{2.10}$$

The output y_j is unaffected by the input u_i if and only if the following condition is satisfied

$$\langle \mathbf{f}, \mathbf{g}_1, \dots, \mathbf{g}_m | \text{span} \{ \mathbf{g}_i \} \rangle \subset (\text{span} \{ dh_j \})^\perp \tag{2.11}$$

3 Distributed Consensus for Networked Nonlinear Systems

There have been many consensus algorithms developed for linear agents [6, 84], while nonlinear agents are more generic in applications. Among them, consensus algorithms for networked Euler-Lagrange agents are particularly attractive because of their broad applications. Furthermore, as an applicable nonlinear consensus algorithm, the controller should not only guarantee the achievement of consensus, but also be robust to the bounded external disturbance. Therefore, in this chapter, the robustness against the external disturbance will be investigated in the sense of input-to-state stability. Specifically, the nominal system and structural uncertainty will be considered together as a feedback control system. Meantime, the external disturbance will be treated as a system input. In this configuration, if the feedback control system is input-to-state stable, then the system stability will not be destroyed by the external disturbance. Otherwise, the negative influence generated by the external disturbance will be amplified by the feedback control

system, which will eventually lead to the system instability. Hence, to effectively solve the consensus seeking and input-to-state robustness problems, a nonlinear robust control strategy is proposed in this chapter for networked Euler-Lagrange systems based on perturbation and passivity theory. The consensus of the nonlinear multi-agent systems is guaranteed in the presence of structural uncertainty and external disturbance.

The remainder of this chapter is organized as follows. Section 3.1 presents the research background on Euler-Lagrange systems and the challenges due to nonlinear dynamics. Section 3.2 develops a nonlinear consensus algorithm for networked Euler-Lagrange systems. The structural uncertainties and external disturbances are considered in the controller design. The closed-loop control system is simplified into cascade systems by the proposed consensus seeking algorithm. Due to the external disturbances, the previous stability criteria for cascade systems cannot be applied directly. Hence, the stability of the perturbed cascade systems is analyzed first and the system is proven to be able to converge to a bounded region under perturbations. Then, the concept of input-to-state consensus is proposed with a strict mathematical definition. Based on the proposed theorems, the consensus seeking algorithm is proven to be robust to bounded perturbations for multiple Euler-Lagrange systems. The state information is coupled via the communication topology, which is depicted using a digraph. Moreover, the influence of the struc-

tural uncertainty is discussed in the presence of external disturbances. The \mathcal{L}_2 stability of the structurally uncertain system is proven based on the passivity theorem. In Section 3.3, experimental results with four 3 degrees of freedom helicopters are presented, and the hardware tests demonstrate the effectiveness of the proposed controller.

3.1 Problem statement

Nonlinear consensus algorithm will be designed for multiple networked Euler-Lagrange systems, also referred to as agents. The n -dimensional Euler-Lagrange dynamical system can be described by

$$\mathbf{M}_i[\mathbf{x}_i(t)]\ddot{\mathbf{x}}_i(t) + \mathbf{C}_i[\mathbf{x}_i(t), \dot{\mathbf{x}}_i(t)]\dot{\mathbf{x}}_i(t) + \mathbf{g}_i[\mathbf{x}_i(t)] = \mathbf{v}_i(t), \quad i \in \{1, 2, \dots, k\} \quad (3.1)$$

where $\mathbf{v}_i(t) \in \mathbb{R}^n$ is the control input, $\mathbf{x}_i(t) \in \mathbb{R}^n$ is the vector of generalized coordinates, $\mathbf{M}_i[\mathbf{x}_i(t)] \in \mathbb{R}^{n \times n}$ is the symmetric positive definite inertia matrix, $\mathbf{C}_i[\mathbf{x}_i(t), \dot{\mathbf{x}}_i(t)]\dot{\mathbf{x}}_i(t) \in \mathbb{R}^n$ is the vector of Coriolis and centrifugal forces, $\mathbf{g}_i[\mathbf{x}_i(t)] \in \mathbb{R}^n$ is the vector of gravitational force.

In this chapter, we will develop a distributed consensus seeking algorithm, by which a group of nonlinear dynamical systems can reach consensus asymptotically in the absence of modeling errors and disturbances. Furthermore, the closed-loop control system is expected to be bounded under the influence of bounded external

disturbances and system uncertainties. Unlike the previous work, the dynamics of each agent in this work will be depicted by a nonlinear ordinary differential equation, i.e. the Euler-Lagrange equation. A group of Euler-Lagrange agents governed by the proposed controller are expected to converge to a common final state. It is assumed that the agents can continuously exchange state information via a wireless network. Therefore their states are coupled by the network, in which the relationships between the nodes are depicted using communication topology, represented by a weighted directed graph. It is assumed that only relative coordinates of the neighbors are available for every agent, hence, global coordinates of the neighbors are not necessary for the purpose of consensus and each agent can only detect the relative state information of its neighbors with respect to the communication topology. The nonlinear dynamics of this system bring a lot of challenges to the consensus seeking algorithm design because it requires a combination of nonlinear control and a consensus seeking strategy.

3.2 Distributed consensus algorithm development

The nonlinear control and consensus seeking are brought together in a nonlinear consensus algorithm. The first problem to be solved in this section is the nonlinear consensus seeking algorithm design.

A relative error vector is defined as

$$\mathbf{e}_i(t) = \int_{t_0}^t \sum_{p_j \in \mathcal{N}_G(p_i)} \left(\mathbf{x}_j(\tau) - \mathbf{x}_i(\tau) \right) d\tau - \mathbf{x}_i(t) \quad (3.2)$$

Here, $\mathbf{x}_j(\tau) - \mathbf{x}_i(\tau)$ is referred to as the relative error term between agent i and j . Since the vector $\mathbf{x}_j(t)$ does not appear solely other than that in the relative error term, the global coordinate of agent j , $\mathbf{x}_j(t)$, with respect to the inertial frame is not necessarily required if the relative error term can be derived directly by the position measuring device.

The nonlinear consensus controller is then designed as follows

$$\mathbf{v}_i = \hat{\mathbf{M}}_i(\mathbf{x}_i)\boldsymbol{\tau}_i + \hat{\mathbf{C}}_i(\mathbf{x}_i, \dot{\mathbf{x}}_i)\dot{\mathbf{x}}_i + \hat{\mathbf{g}}_i(\mathbf{x}_i) \quad (3.3)$$

where $\hat{\mathbf{M}}_i(\mathbf{x}_i)$, $\hat{\mathbf{C}}_i(\mathbf{x}_i, \dot{\mathbf{x}}_i)$ and $\hat{\mathbf{g}}_i(\mathbf{x}_i)$ are the nominal terms of $\mathbf{M}_i(\mathbf{x}_i)$, $\mathbf{C}_i(\mathbf{x}_i, \dot{\mathbf{x}}_i)$ and $\mathbf{g}_i(\mathbf{x}_i)$. Namely, $\hat{\mathbf{M}}_i(\mathbf{x}_i)$, $\hat{\mathbf{C}}_i(\mathbf{x}_i, \dot{\mathbf{x}}_i)$ and $\hat{\mathbf{g}}_i(\mathbf{x}_i)$ represent the ideal values of $\mathbf{M}_i(\mathbf{x}_i)$, $\mathbf{C}_i(\mathbf{x}_i, \dot{\mathbf{x}}_i)$ and $\mathbf{g}_i(\mathbf{x}_i)$, respectively. $\boldsymbol{\tau}_i = \sum_{p_j \in \mathcal{N}_G(p_i)} (\dot{\mathbf{x}}_j - \dot{\mathbf{x}}_i) + \mathbf{K}_d \dot{\mathbf{e}}_i + \mathbf{K}_p \mathbf{e}_i + \mathbf{K}_i \int_{t_0}^t \mathbf{e}_i(\tau) d\tau$, the control gain matrices $\mathbf{K}_p = \text{diag}\{k_p, k_p, \dots, k_p\}$, $\mathbf{K}_i = \text{diag}\{k_i, k_i, \dots, k_i\}$, $\mathbf{K}_d = \text{diag}\{k_d, k_d, \dots, k_d\}$, the control gains k_p , k_i and k_d are positive constants.

Remark 3.1. *Ideally, the nominal terms should be the same as the actual terms if the mathematical model is precisely developed, i.e. $\hat{\mathbf{M}}_i(\mathbf{x}_i) = \mathbf{M}_i(\mathbf{x}_i)$, $\hat{\mathbf{C}}_i(\mathbf{x}_i, \dot{\mathbf{x}}_i) = \mathbf{C}_i(\mathbf{x}_i, \dot{\mathbf{x}}_i)$ and $\hat{\mathbf{g}}_i(\mathbf{x}_i) = \mathbf{g}_i(\mathbf{x}_i)$. However, modeling errors are usually unavoidable due to the measurement errors, limitations of the models and the influence*

of unmodeled effects, etc. If the nominal and actual terms are not identical, their difference will yield the mismatched uncertainty.

Remark 3.2. *Other than the mismatched uncertainties and external disturbances, the structural uncertainty in the closed-loop system is also considered in this work. The mismatched uncertainty is produced by the open-loop model mismatch, while the structural uncertainty is generated by the network-induced perturbations. Namely, the mismatched uncertainty is a function of system states, while the structural uncertainty is a function related to the variables in the closed-loop control system.*

The structural uncertainty that exists in the closed-loop system is defined as follows.

Definition 3.1. *A bounded function $\Delta_i : \mathbb{R}^{3n} \rightarrow \mathbb{R}^{3n}$ is defined as a structural uncertainty of a feedback control system, if Δ_i is generated in the closed-loop system and referred to as a function of the closed-loop error vector.*

To distinguish from the structural uncertainty, the perturbation term produced by the external disturbance and the mismatched uncertainty are defined as follows.

Definition 3.2. *A time-varying function $\omega_i : [0, \infty) \rightarrow \mathbb{R}^n$ is defined as a perturbation term of the system in Eq. (3.1), if it is a bounded input signal resulting from the external disturbance and the mismatched uncertainty.*

According to these definitions, the structural uncertainty and the perturbation term will have dissimilar influences on the control system. Since the structural uncertainty is generated by the closed-loop control system, all states are probably influenced. In contrast, the perturbation term only affects part of the system states directly. Although the influence of the perturbation term may also be propagated by the states' coupling, its influence is distinctly different from that of the structural uncertainty.

Remark 3.3. *In the previous work [32–34, 85, 86], the uncertain constant parameters of the system are usually referred to as system uncertainty. However, the time-varying disturbances and structural uncertainty are much more common. We thus investigate these kinds of time-varying uncertainties, which is one of the most important differences of this work.*

In the following, the stability analysis is carried out with the consideration of the perturbation term and structural uncertainty, respectively.

3.2.1 Stability analysis with perturbation term

In this section, only the perturbation term defined in Definition 3.2 is considered. The twofold analysis of stability and robustness are necessary before applying the proposed controller. First, the following theorem is presented.

Theorem 3.1. *Suppose that the perturbation term $\boldsymbol{\omega}_i$ is bounded by a positive constant ω_m and the nonlinear agents represented by Eq. (3.1) are dominated by controller in Eq. (3.3). If the communication graph contains a center, then it can be guaranteed that the networked nonlinear systems converge to a bounded consensus neighborhood.*

Proof. Substitute the controller in Eq. (3.3) into the Euler-Lagrange dynamical system in Eq. (3.1), the closed-loop control system of agent i is derived in state space as follows

$$\dot{\boldsymbol{\zeta}}_i = \mathbf{A}\boldsymbol{\zeta}_i + \mathbf{D}\boldsymbol{\omega}_i \quad (3.4)$$

where $\boldsymbol{\zeta}_i = [\boldsymbol{\rho}_i^{1T} \quad \boldsymbol{\rho}_i^{2T} \quad \boldsymbol{\rho}_i^{3T}]^T$, $\mathbf{A} = \mathbf{A}_p \otimes \mathbf{I}_n$, $\mathbf{A}_p = \begin{bmatrix} 0 & 1 & 0 \\ 0 & 0 & 1 \\ -k_i & -k_p & -k_d \end{bmatrix}$, $\mathbf{D} = [\mathbf{0} \quad \mathbf{0} \quad \mathbf{I}_n]^T$, $\boldsymbol{\rho}_i^1 = \int_{t_0}^t \mathbf{e}_i dt$, $\boldsymbol{\rho}_i^2 = \mathbf{e}_i$ and $\boldsymbol{\rho}_i^3 = \dot{\mathbf{e}}_i$. Taking the time derivative of Eq. (3.2), it is obtained that

$$\begin{aligned} \dot{\mathbf{e}}_i(t) &= - \sum_{p_j \in \mathcal{N}_{\mathcal{G}}(p_i)} (\mathbf{x}_i(t) - \mathbf{x}_j(t)) - \dot{\mathbf{x}}_i(t) \\ \implies \dot{\mathbf{x}}_i(t) &= - \sum_{p_j \in \mathcal{N}_{\mathcal{G}}(p_i)} (\mathbf{x}_i(t) - \mathbf{x}_j(t)) - \dot{\mathbf{e}}_i(t) \end{aligned}$$

Therefore, Eq. (3.2) can be reorganized as

$$\dot{\boldsymbol{\xi}} = -(\mathcal{L}_k \otimes \mathbf{I}_n)\boldsymbol{\xi} + \boldsymbol{\mathfrak{E}} \quad (3.5)$$

where the lumped generalized coordinates $\boldsymbol{\xi} = [\mathbf{x}_1^T \quad \mathbf{x}_2^T \quad \cdots \quad \mathbf{x}_k^T]^T$, the lumped derivative of error vectors $\boldsymbol{\mathfrak{E}} = -[\dot{\mathbf{e}}_1^T \quad \dot{\mathbf{e}}_2^T \quad \cdots \quad \dot{\mathbf{e}}_k^T]^T$.

Defining the Lyapunov function $V_1 = \zeta_i^T \mathbf{P} \zeta_i$ with a real symmetric positive definite matrix \mathbf{P} , with $\omega_i \equiv 0$ it can be derived that

$$\lambda_{\min}(\mathbf{P}) \|\zeta_i\|^2 \leq V_1 \leq \lambda_{\max}(\mathbf{P}) \|\zeta_i\|^2 \quad (3.6)$$

$$\frac{\partial V_1}{\partial t} + \frac{\partial V_1}{\partial \zeta_i} \mathbf{A} \zeta_i \leq \lambda_{\max}(-\mathbf{Q}) \|\zeta_i\|^2 \quad (3.7)$$

$$\left\| \frac{\partial V_1}{\partial \zeta_i} \right\| \leq 2\lambda_{\max}(\mathbf{P}) \|\zeta_i\| \quad (3.8)$$

where $\lambda_{\max}(\cdot)$ and $\lambda_{\min}(\cdot)$ are the maximum and minimum eigenvalues of matrix. \mathbf{Q} is a symmetric positive definite matrix defined by $\mathbf{A}^T \mathbf{P} + \mathbf{P} \mathbf{A} = -\mathbf{Q}$. Comparing the inequalities (3.6-3.8) with the inequalities (2.3-2.5) in Lemma 2.1, it is obtained that $c_1 = \lambda_{\min}(\mathbf{P})$, $c_2 = \lambda_{\max}(\mathbf{P})$, $c_3 = -\lambda_{\max}(-\mathbf{Q})$ and $c_4 = 2\lambda_{\max}(\mathbf{P})$. Furthermore

$$\begin{aligned} \dot{V}_1 &\leq \lambda_{\max}(-\mathbf{Q}) \|\zeta_i\|^2 + 2\omega_m \lambda_{\max}(\mathbf{P}) \|\zeta_i\| \\ &\leq (1 - \theta) \lambda_{\max}(-\mathbf{Q}) \|\zeta_i\|^2 + \theta \lambda_{\max}(-\mathbf{Q}) \|\zeta_i\|^2 \\ &\quad + 2\omega_m \lambda_{\max}(\mathbf{P}) \|\zeta_i\| \\ &\leq (1 - \theta) \lambda_{\max}(-\mathbf{Q}) \|\zeta_i\|^2, \quad \forall \|\zeta_i\| \geq -\frac{2\omega_m \lambda_{\max}(\mathbf{P})}{\theta \lambda_{\max}(-\mathbf{Q})} \end{aligned}$$

where $0 < \theta < 1$ and $\omega_m = \{x \in \mathbb{R}^+ \cup \{0\} : x = \sup \|\omega_i\|\}$.

Accordingly,

$$\|\zeta_i\| \leq \rho(\omega_i), \quad \forall t \geq t_0 + t_T$$

where $\rho(\omega_i) = -\frac{2\omega_m \lambda_{\max}^2(\mathbf{P})}{\theta \lambda_{\min}(\mathbf{P}) \lambda_{\max}(-\mathbf{Q})}$ and t_T is a finite time.

Since $\|\dot{\mathbf{e}}_i\| \leq \|\zeta_i\|$, the boundary of \mathfrak{E} can be conducted as follows

$$\|\mathfrak{E}\| \leq \sum_{i=1}^k \|\dot{\mathbf{e}}_i\| \leq \sum_{i=1}^k \|\zeta_i\| \leq \sum_{i=1}^k \rho(\omega_i) \quad (3.9)$$

Choose $V_{2l} = \delta_l^2(t)$ as the Lyapunov function for Eq. (3.5), where $\delta_l(t) = \max\{x_{1l}, x_{2l}, \dots, x_{kl}\} - \min\{x_{1l}, x_{2l}, \dots, x_{kl}\}$ and x_{il} is the l th element of \mathbf{x}_i . Without loss of generality, suppose that the agents p_b and p_s have the maximum and minimum values in the l th channel, i.e. $x_{bl} = \max\{x_{1l}, x_{2l}, \dots, x_{kl}\}$ and $x_{sl} = \min\{x_{1l}, x_{2l}, \dots, x_{kl}\}$ for the agents p_b and p_s , then it is obtained when $\|\mathfrak{E}\| = 0$ that

$$\begin{aligned} \dot{V}_{2l} &= 2\delta_l(t)\dot{\delta}_l(t) \\ &= 2\delta_l(t)[\dot{x}_{bl}(t) - \dot{x}_{sl}(t)] \\ &= 2\delta_l(t) \left[\sum_{p_j \in \mathcal{N}_{\mathcal{G}}(p_b)} (x_{jl} - x_{bl}) - \sum_{p_j \in \mathcal{N}_{\mathcal{G}}(p_s)} (x_{jl} - x_{sl}) \right] \end{aligned} \quad (3.10)$$

Due to the definition of x_{bl} and x_{sl} , both $\sum_{p_j \in \mathcal{N}_{\mathcal{G}}(p_b)} (x_{jl} - x_{bl})$ and $-\sum_{p_j \in \mathcal{N}_{\mathcal{G}}(p_s)} (x_{jl} - x_{sl})$ are negative, which implies that $\dot{V}_{2l} < 0 \forall x_{bl} \neq x_{sl}$. With $\|\mathfrak{E}\| \neq 0$, the convergence analysis for Eq. (3.5) can be considered as a special case of the results in [87], based on which the metric term $\delta_l(t)$, $l = 1, 2, \dots$, naturally converges to a bounded consensus area if the communication graph has a center. \square

Remark 3.4. According to Theorem 3.1, the performance of the consensus algorithm can be improved by minimizing the influence of perturbation ω_i (an extreme

case is that the system will achieve consensus when $\omega_i = 0$). The robust \mathcal{H}_∞ controller is utilized for the purpose of optimization in this work. It has been proven in classical robust control theory that an \mathcal{H}_∞ controller can minimize the gain of the system transfer function [88], by which the influence of ω_i is minimized. Consequently, the following theorem is presented.

Theorem 3.2. *Consider the networked nonlinear systems in Eq. (3.1) with bounded perturbation ω_i , and suppose it is governed by the controller in Eq. (3.11), then the networked nonlinear systems in Eq. (3.1) can reach the minimum consensus area.*

$$\mathbf{v}_i = \hat{\mathbf{M}}_i(\mathbf{x}_i)(\tau_i - \mathbf{u}_i) + \hat{\mathbf{C}}_i(\mathbf{x}_i, \dot{\mathbf{x}}_i)\dot{\mathbf{x}}_i + \hat{\mathbf{g}}_i(\mathbf{x}_i) \quad (3.11)$$

where \mathbf{u}_i is the robust \mathcal{H}_∞ output feedback controller, and the value of \mathbf{u}_i can be obtained from

$$\begin{aligned} \dot{\hat{\mathbf{q}}}_i &= \mathbf{A}_K \hat{\mathbf{q}}_i + \mathbf{B}_K \mathbf{y}_i \\ \mathbf{u}_i &= \mathbf{C}_K \hat{\mathbf{q}}_i \end{aligned} \quad (3.12)$$

The parameters \mathbf{A}_K , \mathbf{B}_K and \mathbf{C}_K can be derived using LMI techniques (see Theorem A.2 in the Appendix) [89, 90].

Proof. The system can be reorganized by using the following procedure, the same as that used in the proof of Theorem 3.1. The state-space expression is then derived

as

$$\begin{bmatrix} \dot{\varrho}_i^1 \\ \dot{\varrho}_i^2 \\ \dot{\varrho}_i^3 \end{bmatrix} = \begin{bmatrix} 0 & 1 & 0 \\ 0 & 0 & 1 \\ -k_i & -k_p & -k_d \end{bmatrix} \otimes \mathbf{I}_n \begin{bmatrix} \varrho_i^1 \\ \varrho_i^2 \\ \varrho_i^3 \end{bmatrix} + \begin{bmatrix} 0 \\ 0 \\ \mathbf{I}_n \end{bmatrix} \omega_i + \begin{bmatrix} 0 \\ 0 \\ \mathbf{I}_n \end{bmatrix} \mathbf{u}_i$$

Based on the classical robust control theory [88], the system gain from ω_i to the measured output is minimized if a robust \mathcal{H}_∞ controller exists. In this case, the sub-controller in Eq. (3.12) minimizes the gain of transfer function from ω_i to its measured output. That is why \mathfrak{E} in Eq. (3.9) is minimized. Namely, the networked nonlinear systems can reach the minimum consensus area. \square

The stability of the proposed consensus seeking algorithm has been strictly analyzed in Theorem 3.2. As for robustness, it was first studied in [91] in the sense of input-to-state stability for a linear consensus seeking algorithm. A Kalman consensus scheme was developed and the robustness of their linear consensus algorithm with respect to the noise on the communication channel was analyzed. Ref. [87] investigated the input-to-state stability and integral input-to-state stability for the networked systems with single-integrator agents. With the assistance of \mathcal{L}_∞ and \mathcal{L}_1 norms, the robustness of a linear consensus algorithm was analyzed and the sufficient/necessary connectivity conditions were obtained. In Ref. [81], the input-to-state stability of the nonlinear systems was investigated. Motivated by their work, the input-to-state properties of the proposed controller were further investigated for nonlinear cascade systems with strict mathematical proofs in this work. The robustness of the networked nonlinear systems was analyzed based on the concept of input-to-state consensus.

Lemma 3.1. *Consider ω_i as an input and ζ_i as the state vector, Eq. (3.4) is*

input-to-state stable if $k_p > 0$, $k_d > 0$ and $0 < k_i < k_p k_d$.

Proof. According to Lemma 2.2, the system in Eq. (3.4) is input-to-state stable if $\dot{\boldsymbol{\zeta}}_i = \mathbf{A}\boldsymbol{\zeta}_i$ has an exponentially stable equilibrium point at $\mathbf{x} = \mathbf{0}$. Based on linear control theory, $\mathbf{x} = \mathbf{0}$ is an exponentially stable equilibrium point of $\dot{\boldsymbol{\zeta}}_i = \mathbf{A}\boldsymbol{\zeta}_i$ if \mathbf{A} is a Hurwitz matrix. Let λ_i ($i = 1, 2, 3$) be the eigenvalues of the matrix \mathbf{A}_p , then the eigenvalues of the matrix \mathbf{A} are $\lambda_i \forall i = 1, 2, 3$. According to Theorem A.3, the algebraic multiplicity for each λ_i equals to the dimension of \mathbf{I}_n . Therefore, it is straightforward that the matrix \mathbf{A} is Hurwitz if $k_p > 0$, $k_d > 0$ and $0 < k_i < k_p k_d$. \square

The input-to-state stability is different between the classical nonlinear systems and the networked systems. In the classical nonlinear system, the state vectors of a nonlinear system will eventually converge to zero. However, the state vectors of a networked system will converge to a non-predetermined common value, which is not necessarily zero. This difference makes the following definition crucial.

Definition 3.3. *The system in Eq. (3.5) is said to be input-to-state consensusable if $\boldsymbol{\mathfrak{E}}(t)$ is bounded and there exists a class \mathcal{KL} function p_1 , a class \mathcal{K} function p_2 and a disagreement vector $\boldsymbol{\delta}(t)$ satisfying*

$$\|\boldsymbol{\delta}(t)\| \leq p_1(\|\boldsymbol{\delta}(t_0)\|, t - t_0) + p_2\left(\sup_{t_0 \leq s \leq t} \|\boldsymbol{\mathfrak{E}}(s)\|\right), \quad \forall t \geq t_0 \quad (3.13)$$

where $\delta_l(t) = \max \{x_{1l}, x_{2l}, \dots, x_{kl}\} - \min \{x_{1l}, x_{2l}, \dots, x_{kl}\}$ is the l th element of $\boldsymbol{\delta}(t)$. $\boldsymbol{\delta}(t_0)$ is the initial value of the disagreement vector.

According to Definition 3.3, all the agents would always remain in a neighborhood of each other, and no agent will diverge as long as $\boldsymbol{\epsilon}(t)$ is a bounded signal. Namely, the networked nonlinear systems will be robust to $\boldsymbol{\epsilon}(t)$ if Eq. (3.13) holds.

Lemma 3.2. Consider $\boldsymbol{\epsilon}(t)$ as an input, the system in Eq. (3.5) is input-to-state consensusable if and only if it can reach consensus when $\boldsymbol{\epsilon}(t) = 0$.

Proof. (Sufficiency.) If the system in Eq. (3.5) is input-to-state consensusable, then Eq. (3.13) holds. Since $\sup_{t_0 \leq s \leq t} \|\boldsymbol{\epsilon}(s)\| \equiv 0$ with the assumption $\|\boldsymbol{\epsilon}(t)\| = 0$, it can be derived directly from its definition that

$$\|\boldsymbol{\delta}(t)\| \leq p_1(\|\boldsymbol{\delta}(t_0)\|, t - t_0)$$

Since $p_1(\cdot)$ is a class \mathcal{KL} function, $\|\boldsymbol{\delta}(t)\| = 0$ is a uniformly asymptotically stable equilibrium point. Accordingly, $\mathbf{x}_i(t)$ converges to a common value asymptotically. Namely, the system in Eq. (3.5) reaches consensus when $\boldsymbol{\epsilon}(t) = 0$.

(Necessity.) If the system in Eq. (3.5) can reach consensus when $\boldsymbol{\epsilon}(t) = 0$, the communication graph must contain a center [6]. According to the analysis in [87,91], the following inequality is true for any bounded $\boldsymbol{\epsilon}(t)$ if the communication graph has a center

$$\|\boldsymbol{\delta}(t)\| \leq \bar{p}_1(\|\boldsymbol{\delta}(t_0)\|, t - t_0) + \bar{p}_2 \left(\sup_{t_0 \leq s \leq t} \|\boldsymbol{\epsilon}(s)\| \right), \quad \forall t \geq t_0 \quad (3.14)$$

where $\bar{p}_1(\cdot)$ is a class \mathcal{KL} function and $\bar{p}_2(\cdot)$ is a class \mathcal{K} function [87]. Compare Eq. (3.14) with Eq. (3.13), it is straightforward that the system in Eq. (3.5) is input-to-state consensusable. \square

Based on the concept of input-to-state stability and Lemma 3.2, it can be proven that the systems in Eqs. (3.4, 3.5) are each robust. However, they are coupled into a cascade system together in this work. The robustness of the cascade system has not yet been discussed. To address this, the following theorem is presented.

Theorem 3.3. *Suppose a group of Euler-Lagrange dynamical agents of the form of Eq. (3.1) are coupled via a weighted directed graph $\mathcal{G}(x)$ and they are governed by the controller in Eq. (3.3), the closed-loop systems are robust to any bounded perturbation ω_i if Eq. (3.4) is input-to-state stable and the system in Eq. (3.5) can reach consensus when $\mathbf{e}(t) = 0$.*

Proof. According to Lemma 3.2, the system in Eq. (3.5) is input-to-state consensusable. Therefore, there are two class \mathcal{KL} functions $q_1(\cdot)$, $q_3(\cdot)$ and two class \mathcal{K} functions $q_2(\cdot)$, $q_4(\cdot)$ such that

$$\begin{aligned}\|\zeta_i(t)\| &\leq q_1(\|\zeta_i(t_0)\|, t - t_0) + q_2(\omega_m) \\ \|\delta(t)\| &\leq q_3(\|\delta(t_0)\|, t - t_0) + q_4\left(\sum_{i=1}^k \rho(\omega_i)\right)\end{aligned}$$

Assume $\mathbf{\Gamma} = [\zeta_1^T \quad \zeta_2^T \quad \cdots \quad \zeta_k^T \quad \delta^T]^T$, and since $\|\mathbf{\Gamma}\| \leq \sum_{i=1}^k \|\zeta_i\| + \|\delta\|$, $\|\delta\| \leq \|\mathbf{\Gamma}\|$ and $\left\| \begin{bmatrix} \zeta_1^T & \zeta_2^T & \cdots & \zeta_k^T \end{bmatrix}^T \right\| \leq \|\mathbf{\Gamma}\|$, there is a class \mathcal{KL} function $q(\cdot)$ and a

class \mathcal{K} function $q'(\cdot)$ satisfying

$$\|\mathbf{\Gamma}(t)\| \leq q(\|\mathbf{\Gamma}(t_0)\|, t - t_0) + q'(\omega_m)$$

where $q(a, b) = kq_1(a, b) + q_3(a, b)$, $q'(a) = kq_2(a) + q_4\left(\frac{-2ak\lambda_{max}^2(\mathbf{P})}{\theta\lambda_{min}(\mathbf{P})\lambda_{max}(\mathbf{A}^T\mathbf{P}+\mathbf{P}\mathbf{A})}\right)$.

Consequently, the robustness of the cascade system is proven in the sense of input-to-state stability. \square

3.2.2 Stability analysis with structural uncertainty

In this section, both structural uncertainties and external disturbances are taken into account. It has been shown in the previous section that the proposed control law is robust to a bounded perturbation term. However, this analysis is carried out without structural uncertainty, which widely exists in practice. Moreover, the influence caused by the bounded perturbation may be propagated by the structural uncertainty; hence, a control law that is robust to the structural uncertainty is desired. The main objective is to prove that the closed-loop dynamical system is passive from the perturbation term to the output under some types of structural uncertainties. Since it is impossible for a control law to be robust to all kinds of structural uncertainties, the constraints on the structural uncertainty should also be analyzed.

To consider the structural uncertainty, Eq. (3.4) is revised to the following form

$$\dot{\zeta}_i = \mathbf{A}\zeta_i + \Delta_i(\zeta_i) + \mathbf{D}\omega_i \quad (3.15)$$

where $\Delta_i(\zeta_i)$ is the lumped term of structural uncertainty and satisfies $\|\Delta_i(\zeta_i)\| \leq \|\Theta_i(\zeta_i)\|$ with $\|\Theta_i(\zeta_i)\|$ being the boundary function of the structural uncertainty.

Lemma 3.3. *Suppose that the structural uncertainty $\|\Delta_i(\zeta_i)\| \leq \|\Theta_i(\zeta_i)\| < \lambda_{\min}(-\mathbf{A})\|\zeta_i\|$. If the system in Eq. (3.1) is controlled by Eq. (3.3) with the perturbation term ω_i , the following dynamical system is robust strictly passive from ω to \mathbf{y}*

$$\begin{aligned} \dot{\zeta} &= \bar{\mathbf{A}}\zeta + \Delta(\zeta) + \bar{\mathbf{D}}\omega \\ \mathbf{y} &= \bar{\mathbf{D}}^T\zeta \end{aligned} \quad (3.16)$$

where $\zeta = [\zeta_1^T \ \zeta_2^T \ \cdots \ \zeta_k^T]^T \in \mathbb{R}^{3nk}$, $\bar{\mathbf{A}} = \mathbf{I}_k \otimes \mathbf{A} \in \mathbb{R}^{3nk \times 3nk}$, $\bar{\mathbf{D}} = \mathbf{I}_k \otimes \mathbf{D} \in \mathbb{R}^{3nk \times 3nk}$, $\Delta(t) = [\Delta_1^T \ \Delta_2^T \ \cdots \ \Delta_k^T]^T \in \mathbb{R}^{3nk}$, and $\omega = [\omega_1^T \ \omega_2^T \ \cdots \ \omega_k^T]^T \in \mathbb{R}^{3nk}$.

Proof. For the system in Eq. (3.15), a positive definite function $V(\zeta_i)$ is chosen to be $V(\zeta_i) = \frac{1}{2}\zeta_i^T\zeta_i$. So [92]

$$\mathbf{L}_f V(\zeta_i) = \zeta_i^T \mathbf{A} \zeta_i$$

$$\mathbf{L}_g V(\zeta_i) = \zeta_i^T \mathbf{D} = \dot{\mathbf{e}}_i^T$$

$$\mathbf{L}_e V(\zeta_i) = \zeta_i^T$$

According to Eq. (A.3), the following inequality implies the robust strict passivity of Eq. (3.15)

$$\zeta_i^T \mathbf{A} \zeta_i < -\|\zeta_i\| \|\Theta_i(\zeta_i)\| \quad (3.17)$$

Moreover, Eq. (3.17) is true if the following inequality holds

$$\|\Theta_i(\zeta_i)\| < \lambda_{\min}(-\mathbf{A}) \|\zeta_i\| \quad (3.18)$$

According to Theorem A.1, it can be derived that the system in Eq. (3.15) is passive from $\boldsymbol{\omega}_i$ to $\dot{\mathbf{e}}_i$ if the inequality (3.18) is satisfied. Combining $\dot{\zeta}_i = \mathbf{A} \zeta_i + \boldsymbol{\Delta}_i(\zeta_i) + \mathbf{D} \boldsymbol{\omega}_i$ ($i = 1, 2, \dots, k$), Eq. (3.16) is formed. Since all blocks are decoupled, the proof of passivity of Eq. (3.16) from $\boldsymbol{\omega}$ to \mathbf{y} is trivial. \square

Theorem 3.4. *If $\|\Theta_i(\zeta_i)\| < \lambda_{\min}(-\mathbf{A}) \|\zeta_i\|$ ($i = 1, 2, \dots, k$) is true and the system with transfer matrix $s(s\mathbf{I}_{nk} + \mathcal{L}_k \otimes \mathbf{I}_n)^{-1}$ is passive, then the feedback control system shown in Figure 3.1 is \mathcal{L}_2 stable. In Figure 3.1, $\mathbf{G}(\cdot)$ is an operator from $\boldsymbol{\omega} + \boldsymbol{\xi}$ to $\dot{\mathbf{e}}$ and $\mathbf{C}(s) := s(s\mathbf{I}_{kn} + \mathcal{L}_k \otimes \mathbf{I}_n)^{-1}$.*

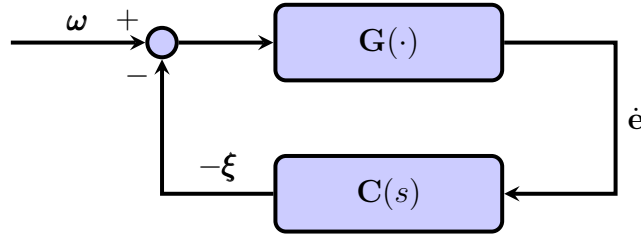


Fig. 3.1 Feedback system

Remark 3.5. *The feedback system shown in Figure 3.1 is re-shaped from the closed-loop system consisting of Eq. (3.3) and Eq. (3.1). Therefore, it only reveals the relationship between the perturbation term and the system output.*

Proof. On the basis of Lemma 3.3, the operator $\mathbf{G}(\cdot)$ is robust strictly passive [92] if $\|\Theta_i(\zeta_i)\| < \lambda_{\min}(-\mathbf{A}) \|\zeta_i\|$ ($i = 1, 2, \dots, k$). According to the passivity theorem [93], the feedback system shown in Figure 3.1 is \mathcal{L}_2 stable if $\mathbf{C}(s)$ is passive and $\mathbf{G}(\cdot)$ is strictly passive. \square

Therefore, the proposed control algorithm is robust to the bounded perturbation term with the consideration of structural uncertainty. Theorem 3.4 further provides an approach for the determination of the boundary of the structural uncertainty.

Remark 3.6. *In the previous works [32–34, 85, 86], the system uncertainties are categorized by their sources. They are investigated contemporaneously in the robustness analysis. Most of the previous works only discuss the robustness with one specific kind of uncertainty. However, system uncertainties are diverse in practice and the presence of only one kind of uncertainty seldom occurs. Therefore, by correlating the bounded perturbation and structural uncertainty, the current results provide a more detailed scope for the robustness analysis. Also, the relationship between the communication topology and \mathcal{L}_2 stability is derived. These achievements are different from the previous work and meaningful in both theoretical and practical*

applications.

3.3 Experimental results

To verify the effectiveness of the proposed consensus algorithm, experiments are conducted using four Quanser’s 3-DOF helicopters facilitated at the Flight Systems & Control (FSC) Laboratory of University of Toronto Institute for Aerospace Studies (UTIAS). Figure 3.2 shows a photo of the 3-DOF helicopter platform [94] and the definition of its parameters [95].

The motion along the elevation axis is described as [96]

$$J_e \ddot{\alpha} = K_f l_a \cos(\beta) V_s - m g l_a \sin(\alpha + \alpha_0)$$

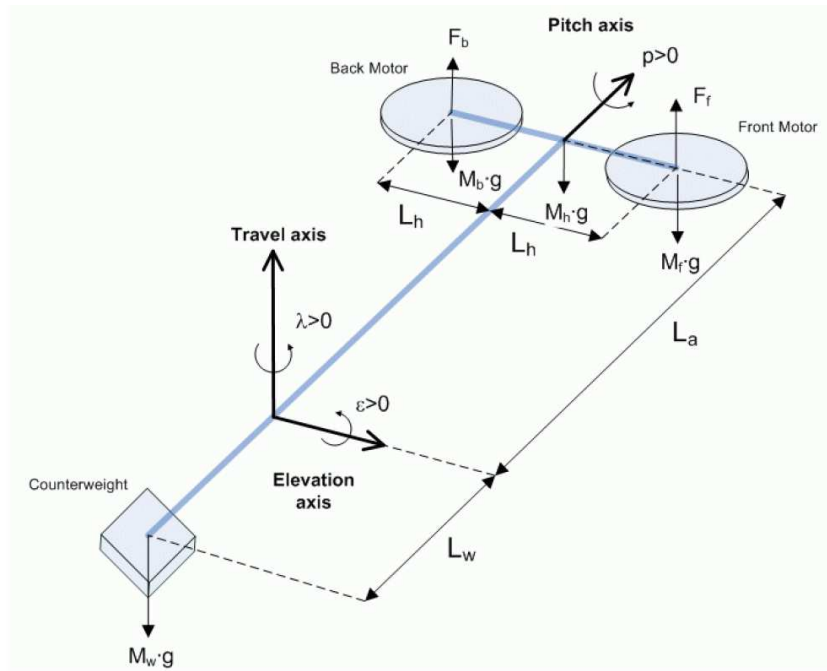
where α is the elevation angle with initial value α_0 , $\beta \in \{x \in \mathbb{R} : -\frac{\pi}{2} \leq x \leq \frac{\pi}{2}\}$ is the pitch angle, J_e is the moment of inertia of the system about the elevation axis, K_f is the force constant of the motor/propeller combination, l_a is the distance from the pivot point to the helicopter body, V_s is the sum of voltages applied to the front and back motors, m is the effective mass about the elevation axis and g is the gravitational constant.

The pitch axis is governed by the difference in the forces created by the front and back propellers

$$J_p \ddot{\beta} = K_f l_h V_d$$



(a)



(b)

Fig. 3.2 3-DOF helicopter system at UTIAS

where J_p is the moment of inertia of the system about the pitch axis, l_h is the distance from the pitch axis to either motor and V_d is the difference between the voltages applied to the front and back motors.

The dynamics of the single helicopter system can be described by the following equation [96]

$$\begin{bmatrix} \frac{J_e}{K_f l_a \cos(\beta)} & 0 \\ 0 & \frac{J_p}{K_f l_h} \end{bmatrix} \begin{bmatrix} \ddot{\alpha} \\ \ddot{\beta} \end{bmatrix} + \begin{bmatrix} \frac{mg \sin(\alpha + \alpha_0)}{K_f \cos(\beta)} \\ 0 \end{bmatrix} = \begin{bmatrix} V_s \\ V_d \end{bmatrix} \quad (3.19)$$

In Section 3.1, it is assumed that $\mathbf{v}_i(t) \in \mathbb{R}^n$ and $\mathbf{x}_i(t) \in \mathbb{R}^n$. This means that the proposed consensus algorithms are only effective for fully actuated dynamical systems. However, the 3-DOF helicopter is an under-actuated mechanical system. To resolve this problem, the motion along the travel direction is not controlled. This is why the state along the traveling direction is not included in Eq. (3.19). This simplification will not influence the experiment because the consensus seeking is tested in the direction of elevation, which is not coupled with the travel axis motion.

Two sets of tests are carried out, i.e. leaderless consensus and leader-follower consensus. In the leaderless consensus, four helicopters will start at the same elevation angle ($\alpha = -27.5^\circ$). In the first 10 sec, they will proceed to different elevation angles and stay there for 10 sec. At 20 sec, the consensus controller is switched on. With this controller, the four helicopters will converge to the same attitude angle asymptotically, and consensus is realized. Since the presented consensus algorithm

is input-to-state stable, the system is robust to the bounded external disturbances. Hence, the external disturbances will be included in the second experiment by touching the helicopters. As for the leader-follower consensus experiment, one of the helicopters is chosen as the leader and the other three will be followers. During the experiment, the leader tracks a pre-determined trajectory. All the helicopters have the same consensus seeking strategy. They only take advantage of the local information from their neighbors. That is why the global information is not necessary. Each helicopter only needs its neighbors' relative error information, which means that the coordinates with respect to the inertial frame are not necessary. Each helicopter has the same consensus seeking strategy but their duties are different because they are at different vertices of the communication topology. The leader's out-degree is zero, but the followers' are not. Namely, the duty of a helicopter is decided by its position in the communication topology, not by its controller structure or controller parameters.

Two communication topologies are implemented in the experiments, as shown in Figure 3.3. Topology 1 is used in the leaderless consensus since no agent in this topology has an out-degree of zero. In Topology 2, helicopter 1 serves as the leader. It can be seen by comparing Topology 2 with Topology 1 that helicopter 1 cannot detect helicopter 2 via the communication topology, i.e. there is no in-direction information flow to agent 1. In this situation, the out-degree of helicopter 1 is zero.

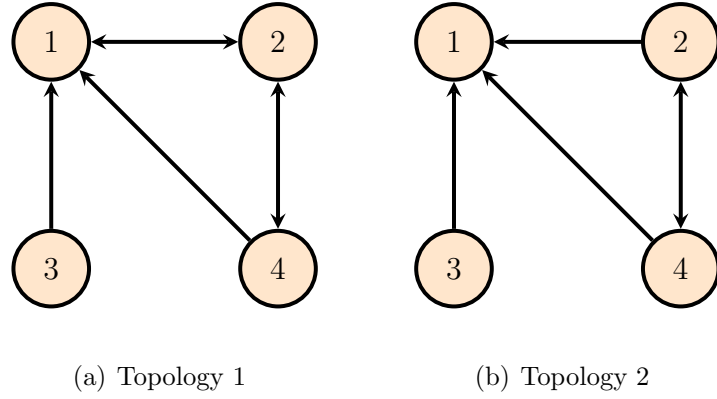


Fig. 3.3 Communication topology

The values of system parameters and control gains are shown in Table 3.1.

Table 3.1 Parameters of helicopter system

Parameter	Value
Moment of inertia about elevation axis, J_e	1.03 (kg · m ²)
Moment of inertia about pitch axis, J_p	0.0455 (kg · m ²)
Transfer coefficient, K_f	0.625 (N/V)
Distance from propeller center to elevation axis, l_a	0.648 (m)
Distance from propeller center to pitch axis, l_h	0.178 (m)
K_p	10 (N/V)
K_i	11 (N/V)
K_d	11 (N/V)

For the experiments, the value of the feedback gain is derived based on Lemma 3.1. The parameter matrices of the output feedback \mathcal{H}_∞ controller are derived using the Linear Matrix Inequalities (LMI) Control Toolbox in MATLAB. The generated

matrices are

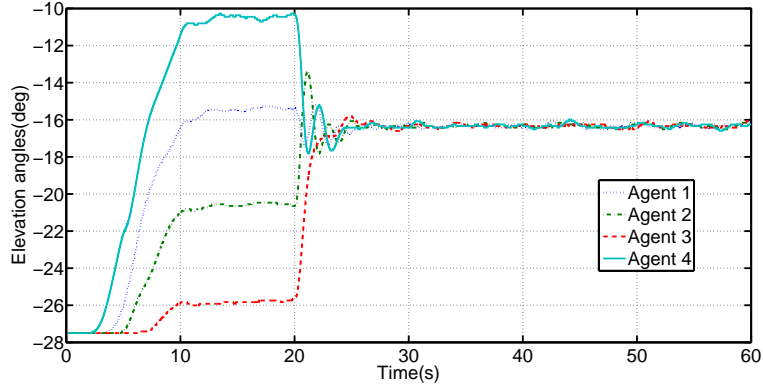
$$\mathbf{A}_K = \begin{bmatrix} -2.6859 & 0.0000 & 0.0000 & 1.9388 & 0.0000 & -1.3119 \\ 0.0000 & -2.6859 & -1.9388 & 0.0000 & -1.3119 & 0.0000 \\ 0.0000 & 3.9909 & -21.7238 & -0.0000 & -33.6963 & 0.0000 \\ -3.9909 & 0.0000 & 0.0000 & -21.7238 & 0.0000 & 33.6963 \\ 0.0000 & 1.4109 & -11.0742 & 0.0000 & -32.1967 & 0.0000 \\ 1.4109 & 0.0000 & 0.0000 & 11.0742 & 0.0000 & -32.1967 \end{bmatrix}$$

$$\mathbf{B}_K = \begin{bmatrix} 0.0000 & -1.7642 & 0.0000 & 1.2795 & 0.0000 & -0.0833 \\ 1.7642 & 0.0000 & -1.2795 & 0.0000 & 0.0833 & 0.0000 \\ -1.1431 & 0.0000 & -0.5160 & 0.0000 & 2.4193 & 0.0000 \\ 0.0000 & -1.1431 & 0.0000 & -0.5160 & 0.0000 & 2.4193 \\ 5.2439 & 0.0000 & 5.3147 & 0.0000 & 1.2372 & 0.0000 \\ 0.0000 & -5.2439 & 0.0000 & -5.3147 & 0.0000 & -1.2372 \end{bmatrix}$$

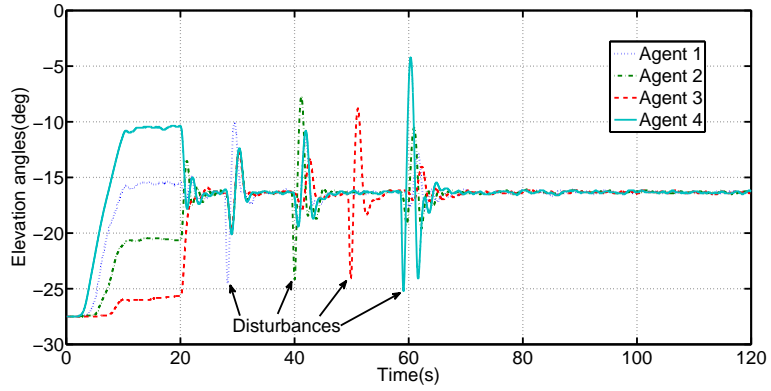
$$\mathbf{C}_K = \begin{bmatrix} 0.0000 & 6.5882 & -2.3729 & 0.0000 & -11.8531 & 0.0000 \\ -6.5882 & 0.0000 & 0.0000 & -2.3729 & 0.0000 & 11.8531 \end{bmatrix}$$

Figure 3.4 shows the experimental results of the leaderless consensus. At the beginning, all four helicopters have the same elevation angle of -27.5° . Then, these helicopters are all driven to different elevation angles and maintained these positions. At $t = 20$ sec, the control strategy is switched to consensus seeking. It can be seen from Figure 3.4(a) that the four helicopters converge to a common angle quickly.

In Figure 3.4(b), several peaks can be observed after $t = 20$ sec due to the external disturbances generated by touching the helicopters. However, the proposed consensus algorithm has the ability to reject the external disturbances and the helicopters can still achieve consensus, even when disturbances occur. Particularly, the disturbance transmission can also be exhibited in Figure 3.4(b). At $t = 40$ sec,



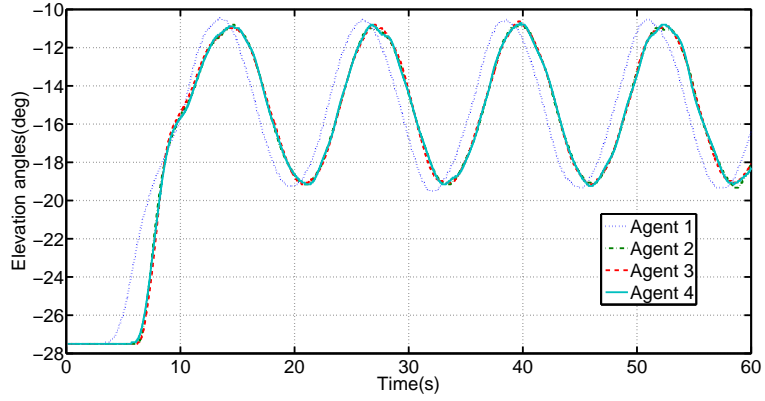
(a) Consensus



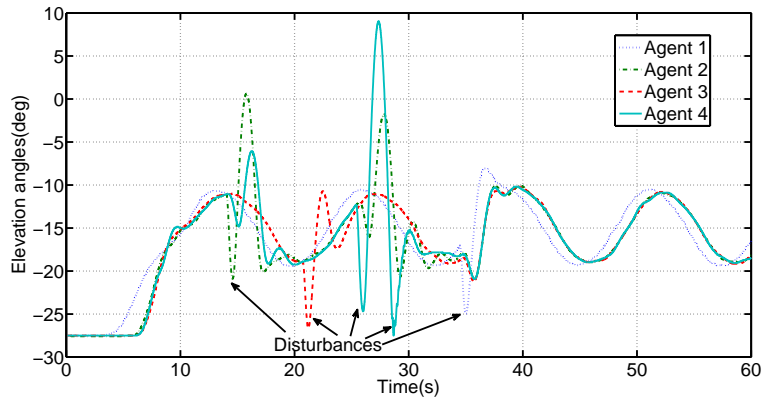
(b) Consensus with disturbance

Fig. 3.4 Experimental results of Leaderless consensus

the elevation angles of helicopter 3 and 4 are disturbed when only helicopter 2 is touched. Namely, the disturbance exerted on helicopter 2 has been transmitted to its neighbors due to the coupling relationship. Apparently, the consensus is also guaranteed even when the disturbance has been transmitted to the neighboring agents, which further demonstrates the robustness of the proposed controller.



(a) Consensus



(b) Consensus with disturbance

Fig. 3.5 Experimental results of Leader-follower consensus

The experimental results of leader-follower consensus are shown in Figure 3.5. The sinusoidal trajectory of the leader helicopter is pre-determined as shown in Figure 3.5(a). All the followers can track the same trajectory, with a small delay that can be observed between the leader and the followers. This situation is expected since all the followers would remain in their own states until the relative errors

are detected. As before, disturbances are included in the leader-follower consensus seeking process, as seen in Figure 3.5(b). It is clear that the four helicopters can maintain consensus even with the external disturbances. Experimental videos can be found at <http://www.yorku.ca/jjshan/Experiments.html>.

It is observed from the experiments that if one helicopter is disturbed, all its neighbors can be negatively influenced due to the coupling relationship. Similarly, if one helicopter has a malfunction, the malfunction will probably also be transmitted to its neighbors. Therefore, the fault diagnosis strategy of the networked Euler-Lagrange systems will be discussed in the next chapter.

Remark 3.7. *In the theoretical analysis, the consensus can be achieved if the parameters of controller satisfy certain bounded conditions. However, the values of these parameters should be repeatedly adjusted in the experiment. For example, the input-to-state stability of the system in Eq. (3.4) can be guaranteed if the values of k_p , k_d and k_i belong to the set $\mathcal{F} = \{k_p, k_d, k_i : k_p > 0, k_d > 0 \text{ and } 0 < k_i < k_p k_d\}$. In the numerical simulations, any value that satisfies this condition could guarantee the input-to-state stability of the system in Eq. (3.4) because the unmodeled perturbations are not included in the simulations; however, inappropriate selection of the parameters in \mathcal{F} might result in the slow convergence or other unexpected results in the experiment. Therefore, to ensure the achievement of the consensus, the adjustment of the parameters is usually necessary in the practical applications.*

4 Synchronization of Networked Nonlinear Multi-agent Systems with Fault Diagnosis

As a specific type of coordination for multiple networked agents, the synchronized formation tracking of multi-agent systems has been broadly investigated through a centralized approach. Ref. [97] is a representative work of position synchronization, in which a centralized protocol for position synchronization of multiple axes was presented using the cross-coupling technique. The inclusion of an adaptive control strategy further enhanced the robustness of their controller. The experimental validation of their synchronization control scheme can be found in [98]. A further investigation on synchronous tracking control appeared in [96], where multiple 3-DOF helicopters were utilized in the experimental tests. To enable the motion synchronization, a generalized synchronization error strategy was developed along with the feedforward dynamic term and a PD feedback term. The asymptotical convergence was globally performed by the networked helicopters. With the advancement of multi-agent techniques, more and more attention has been paid to

the decentralized approach with networked nonlinear agents [99, 100]. With the appearance of a Lipschitz-type nonlinear dynamics, the linear decentralized control algorithm can be extended to the networked Lipschitz nonlinear systems [101]. In [102], a leader-follower consensus protocol was studied for networked systems in the presence of Lipschitz nonlinear dynamics, and the synchronization can be achieved using their distributed consensus algorithm with jointly connected topology. The decentralized control strategies were further investigated for networked nonlinear systems with Lipschitz-type nonlinear dynamics and semi-Lipschitz nonlinear dynamics in [103] and [104] respectively. The exponential synchronization of genetic oscillators was discussed in [105], and the nonlinear dynamics in their work were assumed to be either monotonic increasing or monotonic decreasing functions. The nonlinear dynamics investigated in [106] occurs randomly in the dynamical systems, where the consensus criteria were derived on the basis of stochastic analysis. To further extend the decentralized control strategy to nonlinear systems, a distributed leader-follower formation tracking scheme was developed for networked Euler-Lagrange systems in this work. The Euler-Lagrange model is widely adopted to describe a large class of mechanical systems. Consequently, the research on synchronous formation tracking of multiple agents with Euler-Lagrange dynamics is especially useful due to its potential applications. Some recent work on decentralized control of Euler-Lagrange systems can be found in [107, 108] where the lead-

erless consensus seeking strategies were developed. In this work, a leader-follower synchronization problem is studied. It is assumed that some agents have access to the desired trajectory, while the others can only share their information with their neighbors. An agent is defined as a leader if it can obtain the desired trajectory; otherwise it is a follower. The synchronization is guaranteed by all leaders, while the followers keep the formation with respect to the communication topology containing a spanning tree. Because of the distributed information sharing among followers, the usefulness of the proposed controller is scarcely influenced by the growth of the number of followers. Hence, a synchronization problem with a large number of followers can be effectively solved by the proposed protocol. Meanwhile, the synchronous tracking is extensively enhanced by the undirected coupling structure of the leaders. Moreover, the proposed controller will be able to benefit many networked Euler-Lagrange systems, such as unmanned aerial vehicles (UAVs), robots and aircraft, etc., if uncertainties are taken into account appropriately. Therefore, system uncertainties and external disturbances are considered in terms of a bounded noise. Unlike the common solution on the bounded noise, the boundary of the noise is unavailable to the proposed controller in this chapter. To cope with the influence rendered by the noise, a discontinuous control scheme is incorporated into the synchronization protocol. Accordingly, the networked Euler-Lagrange systems are guaranteed to solve the formation tracking problem through

a distributed approach if no fault happens to any agent in the system.

Since all agents are coupled via network and no central controller monitors the entire system, it is highly possible that the team objective will be crashed when an agent stops proper functioning. In this work, an active fault detection strategy is discussed for networked nonlinear systems. The super-twisting sliding mode observer is adopted to generate the residual signals which act as the indicators of specific faults. With the assistance of tools in differential geometry, it is revealed that either sensor fault or actuator fault has direct influence on the residual output. Furthermore, the divergence of the residual signal on account of the actuator/sensor fault is proven in terms of single channel. Consequently, the proposed residual can be used as an effective alarm signal for the recovery algorithm, which is further demonstrated in the simulations.

The remainder of this chapter is organized as follows. In Section 4.1, the main problem to be solved in this chapter is formulated mathematically. Each agent is modeled using the Euler-Lagrange equation due to its broad applications. Section 4.2 presents the controller design and fault diagnosis strategy. With assumptions on system noise and communication topology, a nonlinear trajectory tracking scheme is proposed through a distributed approach. The stability analysis is carried out based on the theory of Filippov's solution. It is further proven that all leaders in the system can track the trajectory synchronously in the presence of noise. Without the

global knowledge of the desired trajectory, the followers can still reach consensus in a distributed manner if the communication topology contains a spanning tree. Moreover, the nonlinear multi-agent systems are enhanced to be fault tolerant by the proposed active fault diagnosis strategy. In Section 4.3, the 3-DOF helicopter system is adopted as an agent model, and six helicopters will perform the distributed trajectory tracking in the simulations. Meanwhile, the simulations are implemented with actuator and sensor faults, respectively. Both leader and follower faults are simulated to demonstrate the effectiveness of the active fault diagnosis strategy.

4.1 Problem formulation

As reviewed above, the synchronization of multiple Euler-Lagrange systems is not a new topic. However, most of the previous works have been carried out in a centralized approach. The synchronization in decentralized approach for multiple Euler-Lagrange systems was proposed in [29], where a model-independent consensus algorithm was proposed to realize the distributed leaderless consensus. The author did the convergence analysis using Matrosov's theorem, and the consensus was reached with an undirected communication topology. In addition, the distributed containment control for Euler-Lagrange systems was investigated in [30]. The parametric uncertainties were also taken into account to enhance the robustness of their controller. Furthermore, the leaderless consensus algorithm was stud-

ied with a directed graph. In our work, the distributed synchronization of multiple Euler-Lagrange systems is investigated without the global knowledge of the desired trajectory.

A network of p Euler-Lagrange dynamical systems operates in the workspace \mathbb{R}^n . The system can be modeled by

$$\mathbf{M}_i[\mathbf{x}_i(t)]\ddot{\mathbf{x}}_i(t) + \mathbf{C}_i[\mathbf{x}_i(t), \dot{\mathbf{x}}_i(t)]\dot{\mathbf{x}}_i(t) + \mathbf{g}_i[\mathbf{x}_i(t)] = \mathbf{u}_i(t) + \mathbf{f}_i(t) \quad (4.1)$$

where $i \in \{1, 2, \dots, p\}$, $\mathbf{u}_i(t) \in \mathbb{R}^n$ is the control input, $\mathbf{x}_i(t) \in \mathbb{R}^n$ is the vector of generalized coordinates, $\mathbf{M}_i[\mathbf{x}_i(t)] \in \mathbb{R}^{n \times n}$ is the moments of inertia matrix, $\mathbf{C}_i[\mathbf{x}_i(t), \dot{\mathbf{x}}_i(t)]\dot{\mathbf{x}}_i(t) \in \mathbb{R}^n$ is the vector of Coriolis and centrifugal forces, $\mathbf{g}_i[\mathbf{x}_i(t)] \in \mathbb{R}^n$ is the vector of gravitational force. The Euler-Lagrange equation has the following properties:

(a) Symmetric positive definite: the moment of inertia matrix $\mathbf{M}_i[\mathbf{x}_i(t)]$ is symmetric positive definite in the entire workspace.

(b) Skew symmetry: let $\dot{\mathbf{M}}_i[\mathbf{x}_i(t)]$ and $\mathbf{C}_i[\mathbf{x}_i(t), \dot{\mathbf{x}}_i(t)]$ be the matrices defined in Eq. (4.1), then the matrix $\dot{\mathbf{M}}_i[\mathbf{x}_i(t)] - 2\mathbf{C}_i[\mathbf{x}_i(t), \dot{\mathbf{x}}_i(t)]$ is skew symmetric.

The first objective in this chapter is to design a feedback controller, by which all agents can track a predetermined trajectory asymptotically. Only some of the agents (leaders) know the desired trajectory; others (followers) have no direct information about the desired trajectory. In addition to the asymptotical trajectory tracking, the leaders are able to perform the trajectory tracking synchronously by

sharing the neighbors' information with other neighbors. The generalized coordinates are broadcast to the followers locally with respect to the communication topology. Meanwhile, uncertainties are considered including parameter uncertainties, structure uncertainties, mismatched model and disturbances.

Since the formation tracking mission is carried out in the sense of distributed approach, any fault that may be tolerated by a centralized control system could cause catastrophic failures due to the propagation of a single fault through the network. With the growth of the network complexity, this risk is progressively generated. Therefore, the second objective of this work is to develop the fault diagnosis and task recovery techniques for the networked nonlinear systems.

4.2 Controller design with fault diagnosis

Before presenting the controller design, a few assumptions are put forward.

Assumption 4.1. *The disturbances of the dynamical system (4.1) are bounded by the following inequality*

$$\|\mathbf{f}_i(t)\| \leq \mu_{i1} + \mu_{i2} \|\mathbf{x}_i(t)\| + \mu_{i3} \|\dot{\mathbf{x}}_i(t)\| \quad a.e. \quad (4.2)$$

where μ_{i1} , μ_{i2} and μ_{i3} are unknown constants and *a.e.* denotes almost everywhere.

Remark 4.1. *The disturbances are characterized by the parameters μ_{i1} , μ_{i2} and μ_{i3} . However, they are unknown for the control system. Namely, μ_{i1} , μ_{i2} and μ_{i3}*

are specified in the stability analysis but never available for the controller.

Assumption 4.2. *The communication topology is described by a directed graph (digraph) in the networked system and the digraph contains a spanning tree with a leader as the root. Furthermore, all the leaders communicate with each other via an undirected subgraph.*

Assumption 4.3. *Both the actuator fault and sensor fault are considered in this chapter. However, it is assumed that only one type of fault occurs at any time.*

Due to the occurrence of system uncertainties and external disturbances, the switched control strategy is adopted and the discontinuous control signal will thus be generated by the proposed controller. With the concept of Filippov's solution in nonsmooth analysis, the stability analysis is presented with the help of Filippov set-valued map $K[f]$. It is defined as: $K[f](\mathbf{x}, t) = \bigcap_{\delta > 0} \bigcap_{\mu(N)=0} \overline{co} \{f(B(\mathbf{x}, \delta) \setminus N, t)\}$ [109], where $f : \mathbb{R}^n \times \mathbb{R} \rightarrow \mathbb{R}^m$, $\mu(\cdot)$ represents the Lebesgue measure and n does not necessarily equal to m .

4.2.1 Distributed formation control with system noise

Defining $\mathbf{x}_d(t) \in \mathbb{R}^n$ as the desired generalized coordinates which satisfies $\mathbf{x}_d(t)$, $\dot{\mathbf{x}}_d(t)$, $\ddot{\mathbf{x}}_d(t) \in \mathcal{L}_\infty$. Without loss of generality, it is assumed that some of the agents belong to $\mathcal{L} \triangleq \{v_i : i = 1, \dots, k \text{ and } k \leq p\}$ and have knowledge of the desired

trajectory, while others belong to $\mathcal{X} \setminus \mathfrak{L}$ and do not have knowledge of the desired trajectory. Therefore, the tracking error of agent $v_i \in \mathfrak{L}$ is

$$\mathbf{e}_i(t) = \mathbf{x}_d(t) - \mathbf{x}_i(t) \quad (4.3)$$

with the coupling tracking error

$$\begin{aligned} \mathbf{e}_i^*(t) = & \mathbf{e}_i(t) \\ & + b_i \int_0^t \sum_{v_j \in \mathfrak{N}(v_i)} \left\{ \sum_{v_j \in \mathfrak{N}(v_i)} [\mathbf{e}_i(\tau) - \mathbf{e}_j(\tau)] - \sum_{v_k \in \mathfrak{N}(v_j)} [\mathbf{e}_j(\tau) - \mathbf{e}_k(\tau)] \right\} d\tau \end{aligned} \quad (4.4)$$

where $b_i > 0$, $\mathfrak{N}(v_i) = \mathcal{N}_{\mathcal{G}}(v_i) \cap \mathfrak{L}$. Observed from Eq. (4.4), the coupling tracking error consists of two parts, trajectory tracking error and synchronization error. With the convergence of $\mathbf{e}_i(t)$, the agents belonging to \mathfrak{L} can converge to the desired trajectory. Meanwhile, $\int_0^t \sum_{v_j \in \mathfrak{N}(v_i)} \left\{ \sum_{v_j \in \mathfrak{N}(v_i)} [\mathbf{e}_i(\tau) - \mathbf{e}_j(\tau)] - \sum_{v_k \in \mathfrak{N}(v_j)} [\mathbf{e}_j(\tau) - \mathbf{e}_k(\tau)] \right\} d\tau$ represents the synchronization error relative to the group motion of the agents belonging to \mathfrak{L} . Since an enhanced synchronization is conducted for the agents belonging to \mathfrak{L} , the information of $v_j \in \mathfrak{N}(v_i)$ and $v_k \in \mathfrak{N}(v_j)$ is demanded by v_i . As for the agents belonging to $\mathcal{X} \setminus \mathfrak{L}$, they have the following tracking error

$$\mathbf{e}_i(t) = \mathbf{x}_{di}^{\emptyset}(t) - \mathbf{x}_i(t) \quad (4.5)$$

where

$$\dot{\mathbf{x}}_{di}^{\emptyset}(t) = \frac{1}{\rho_i} \sum_{v_j \in \mathcal{N}_{\mathcal{G}}(v_i)} \{ \dot{\mathbf{x}}_j(t) - \varepsilon_i [\mathbf{x}_i(t) - \mathbf{x}_j(t)] \} \quad (4.6)$$

and ρ_i is the in-degree of vertex v_i and ε_i is a positive constant.

With these definitions, the stack vector of the system tracking error can be expressed as

$$\mathbf{e}^*(t) = \mathbf{e}(t) + \mathbf{B}\mathcal{L}_p \otimes \mathbf{I}_n \int_0^t \mathcal{L}_p \otimes \mathbf{I}_n \mathbf{e}(\tau) d\tau \quad (4.7)$$

where $\mathbf{e}(t) = \bar{\mathbf{x}}(t) - \mathbf{x}(t)$, $\mathbf{B} \triangleq \text{diag} \{ b_1 \ b_2 \ \cdots \ b_{p_i} \ 0 \ \dots \ 0 \} \otimes \mathbf{I}_n$, $\mathcal{L}_p = \begin{bmatrix} \mathcal{L}_{p_i} & \mathbf{0} \\ \mathbf{0} & \mathbf{0} \end{bmatrix}$ is a p dimensional matrix, \mathcal{L}_{p_i} is the Laplacian matrix corresponding to the undirected subgraph of leaders with $p_i = |\mathcal{L}|$ and

$$\begin{aligned} \bar{\mathbf{x}}(t) &= \left[\underbrace{\mathbf{x}_d^T(t) \ \dots \ \mathbf{x}_d^T(t)}_{p_i} \ \mathbf{x}_{d1}^{\otimes T}(t) \ \dots \ \mathbf{x}_{d(p-p_i)}^{\otimes T}(t) \right]^T \\ \mathbf{x}(t) &= \left[\mathbf{x}_1^T(t) \ \mathbf{x}_2^T(t) \ \dots \ \mathbf{x}_p^T(t) \right]^T \end{aligned}$$

A coupling error is further defined as

$$\mathbf{c}(t) = \dot{\mathbf{e}}^*(t) + \Lambda \mathbf{e}^*(t) \quad (4.8)$$

where $\Lambda \triangleq \text{diag} \{ \lambda_1 \ \lambda_2 \ \cdots \ \lambda_p \} \otimes \mathbf{I}_n$ with $\lambda_i > 0$.

A sliding mode controller is proposed to deal with the trajectory tracking considering the system uncertainties and disturbances in the Filippov sense [110]. The entire state space \mathbb{R}^{pn} is split into two parts by a hypersurface. Since the hypersurface Σ can be defined by a scalar indicator (or event) function [111] $h : \mathbb{R}^{pn} \rightarrow \mathbb{R}$, the hypersurface in this work can be expressed implicitly as

$$\mathbf{e}^T(t) \mathbf{e}(t) = 0 \quad (4.9)$$

The basic idea in this work is that Eqs. (4.5, 4.6) form a linear consensus seeking dynamics if $\mathbf{e}_i = 0$ [6]. Therefore, the nonlinear consensus seeking problem is transformed into a linear problem if the nonlinear dynamics can be forced into the hypersurface described in Eq. (4.9). As for the agents belonging to \mathfrak{L} , they can merely work on the synchronization due to the knowledge of the desired trajectory. The nonlinear control law is thus designed as

$$\begin{aligned} \mathbf{u}_i(t) = & k_1 \mathbf{c}_i(t) + k_2 \sum_{v_j \in \mathfrak{N}(v_i)} \left\{ \sum_{v_j \in \mathfrak{N}(v_i)} [\mathbf{e}_i(t) - \mathbf{e}_j(t)] - \sum_{v_k \in \mathfrak{N}(v_j)} [\mathbf{e}_j(t) - \mathbf{e}_k(t)] \right\} \\ & + \mathbf{M}_i[\mathbf{x}_i(t)] \dot{\Phi}_i(t) + \mathbf{C}_i[\mathbf{x}_i(t), \dot{\mathbf{x}}_i(t)] \Phi_i(t) + \mathbf{g}_i[\mathbf{x}_i(t)] \\ & + \begin{bmatrix} 1 \\ \|\mathbf{x}_i(t)\| \\ \|\dot{\mathbf{x}}_i(t)\| \end{bmatrix}^T \hat{\boldsymbol{\mu}}_i(t) \text{sgn}(\mathbf{c}_i(t)) \end{aligned} \quad (4.10)$$

with the update law

$$\dot{\hat{\boldsymbol{\mu}}}_i(t) = \begin{bmatrix} 1 \\ \|\mathbf{x}_i(t)\| \\ \|\dot{\mathbf{x}}_i(t)\| \end{bmatrix} \text{sgn}(\mathbf{c}_i(t))^T \mathbf{c}_i(t) \quad (4.11)$$

where $k_2 > 0 \forall v_i \in \mathfrak{L}$ otherwise $k_2 = 0$ and

$$\begin{aligned} \Phi_i(t) = & \dot{\mathbf{x}}_i(t) + b_i \sum_{v_j \in \mathfrak{N}(v_i)} \left\{ \sum_{v_j \in \mathfrak{N}(v_i)} [\mathbf{e}_i(t) - \mathbf{e}_j(t)] - \sum_{v_k \in \mathfrak{N}(v_j)} [\mathbf{e}_j(t) - \mathbf{e}_k(t)] \right\} \\ & + \lambda_i \mathbf{e}_i^*(t) \end{aligned}$$

$$\text{sgn}(\mathbf{c}_i(t)) \triangleq \begin{bmatrix} \text{sgn}(c_{i1}(t)) & \text{sgn}(c_{i2}(t)) & \cdots & \text{sgn}(c_{in}(t)) \end{bmatrix}^T$$

In Eq. (4.10), the terms $k_1 \mathbf{c}_i(t) + k_2 \sum_{v_j \in \mathfrak{N}(v_i)} \left\{ \sum_{v_j \in \mathfrak{N}(v_i)} [\mathbf{e}_i(t) - \mathbf{e}_j(t)] - \sum_{v_k \in \mathfrak{N}(v_j)} [\mathbf{e}_j(t) - \mathbf{e}_k(t)] \right\} + \mathbf{M}_i[\mathbf{x}_i(t)] \dot{\Phi}_i(t) + \mathbf{C}_i[\mathbf{x}_i(t), \dot{\mathbf{x}}_i(t)] \Phi_i(t) + \mathbf{g}_i[\mathbf{x}_i(t)]$ will ensure the

convergence of the coupling error vector in Eq. (4.8), and the robustness against disturbance will be guaranteed by the term $\begin{bmatrix} 1 \\ \|\mathbf{x}_i(t)\| \\ \|\dot{\mathbf{x}}_i(t)\| \end{bmatrix}^T \hat{\boldsymbol{\mu}}_i(t) \text{sgn}(\mathbf{c}_i(t))$.

Theorem 4.1. *Suppose that the system uncertainties and external disturbances satisfy Assumption 4.1, and the system communication topology fulfills Assumption 4.2, then the proposed nonlinear controller in Eq. (4.10) solves the synchronized formation control problem in a distributed manner.*

Remark 4.2. *Substituting the control law in Eq. (4.10) into Eq. (4.1), the closed-loop system is described by a set of differential equations with discontinuous right hand side. That is why the classical qualitative criteria for stability analysis cannot be adopted here. The stability is studied in the sense of Filippov solution [110] due to the assumption of discontinuous vector field in the control law. With the assistance of nonsmooth analysis, the convergence criteria in discontinuous system is developed in [112]. Two theorems in [112] are utilized in the following proof.*

Remark 4.3. *On the basis of Assumption 4.2 and the coupling tracking error defined in Eq. (4.7), the information sharing among the leaders is more complex than that among the followers. A tradeoff with respect to the communication cost and the synchronous quality occurs among the leaders when the control algorithm is applied. Namely, the communication cost is usually expected to be decreased in practice, but the low communication cost will result in a lower synchronous quality.*

Hence, the complexity of the network should be appropriately designed, according to the limitations in specific practical applications, to achieve the balance between the communication cost and the synchronous quality.

Proof. The Lyapunov function is defined as follows

$$\begin{aligned} \mathbf{V} = & \frac{1}{2}\mathbf{c}^T\mathbf{M}\mathbf{c} + \frac{1}{2}k_2[\mathcal{L}_p \otimes \mathbf{I}_n\mathbf{e}]^T \mathcal{L}_p \otimes \mathbf{I}_n\mathbf{e} + \frac{1}{2}\tilde{\boldsymbol{\mu}}^T\tilde{\boldsymbol{\mu}} \\ & + \frac{1}{2}\left[\mathcal{L}_p \otimes \mathbf{I}_n \int_0^t \mathcal{L}_p \otimes \mathbf{I}_n\mathbf{e}d\tau\right]^T k_2\mathbf{B}\Lambda \left[\mathcal{L}_p \otimes \mathbf{I}_n \int_0^t \mathcal{L}_p \otimes \mathbf{I}_n\mathbf{e}d\tau\right] \end{aligned} \quad (4.12)$$

where $\mathbf{M} \triangleq \text{diag}\{\mathbf{M}_1 \ \mathbf{M}_2 \ \cdots \ \mathbf{M}_p\}$, the vector of estimation parameters is $\hat{\boldsymbol{\mu}} = [\hat{\boldsymbol{\mu}}_1^T \ \hat{\boldsymbol{\mu}}_2^T \ \cdots \ \hat{\boldsymbol{\mu}}_p^T]^T$, the nominal vector of the estimation parameters is $\boldsymbol{\mu} = [\boldsymbol{\mu}_1^T \ \boldsymbol{\mu}_2^T \ \cdots \ \boldsymbol{\mu}_p^T]^T$, $\boldsymbol{\mu}_i = [\mu_{i1} \ \mu_{i2} \ \mu_{i3}]^T$, their error vector is $\tilde{\boldsymbol{\mu}} = \hat{\boldsymbol{\mu}} - \boldsymbol{\mu}$, and $\mu_i = \sum_{j=1}^p \mu_{ji} \ \forall i = 1, 2, 3$. For simplicity, the domain of \mathbf{c} , \mathbf{e} and $\tilde{\boldsymbol{\mu}}$ is ignored in the equations.

According to the Property 6 in [113], it is derived from Eq. (4.12) that

$$\begin{aligned} \partial V = & K[\nabla V] \begin{pmatrix} t \\ \mathbf{c} \\ \mathbf{e} \\ \int_0^t \mathbf{e}d\tau \\ \tilde{\boldsymbol{\mu}} \end{pmatrix} \\ = & \begin{bmatrix} \frac{1}{2}\mathbf{c}^T\dot{\mathbf{M}} \\ \mathbf{c}^T\dot{\mathbf{M}} \\ k_2[\mathcal{L}_p \otimes \mathbf{I}_n\mathbf{e}]^T \mathcal{L}_p \otimes \mathbf{I}_n \\ \left[\mathcal{L}_p \otimes \mathbf{I}_n \int_0^t \mathcal{L}_p \otimes \mathbf{I}_n\mathbf{e}d\tau\right]^T k_2\mathbf{B}\Lambda \mathcal{L}_p \otimes \mathbf{I}_n \mathcal{L}_p \otimes \mathbf{I}_n \\ \tilde{\boldsymbol{\mu}}^T \end{bmatrix} \end{aligned} \quad (4.13)$$

According to Eq. (4.8)

$$\mathbf{M}\dot{\mathbf{c}} = \mathbf{M}(\ddot{\mathbf{e}} + \mathbf{B}\mathcal{L}_p \otimes \mathbf{I}_n \mathcal{L}_p \otimes \mathbf{I}_n \dot{\mathbf{e}} + \Lambda \dot{\mathbf{e}}^*) = \mathbf{M}\dot{\boldsymbol{\Phi}} - \mathbf{M}\ddot{\mathbf{x}} \quad (4.14)$$

Based on Theorem A.5 in Appendix and Eq. (4.14), it is obtained that

$$\begin{aligned}
\tilde{V} &= \mathbf{c}^T \mathbf{M} (\ddot{\mathbf{x}} + \mathbf{B} \mathcal{L}_p \otimes \mathbf{I}_n \mathcal{L}_p \otimes \mathbf{I}_n \dot{\mathbf{e}} + \Lambda \dot{\mathbf{e}}^*) - \mathbf{c}^T \mathbf{M} \ddot{\mathbf{x}} \\
&\quad + \frac{1}{2} \mathbf{c}^T \dot{\mathbf{M}} \mathbf{c} + k_2 (\mathcal{L}_p \otimes \mathbf{I}_n \mathbf{e})^T \mathcal{L}_p \otimes \mathbf{I}_n \dot{\mathbf{e}} \\
&\quad + \left(\mathcal{L}_p \otimes \mathbf{I}_n \int_0^t \mathcal{L}_p \otimes \mathbf{I}_n \mathbf{e} d\tau \right)^T k_2 \mathbf{B} \Lambda \mathcal{L}_p \otimes \mathbf{I}_n \mathcal{L}_p \otimes \mathbf{I}_n \mathbf{e} + \tilde{\boldsymbol{\mu}}^T K [\tilde{\boldsymbol{\mu}}] \\
&= \mathbf{c}^T \mathbf{M} (\ddot{\mathbf{x}} + \mathbf{B} \mathcal{L}_p \otimes \mathbf{I}_n \mathcal{L}_p \otimes \mathbf{I}_n \dot{\mathbf{e}} + \Lambda \dot{\mathbf{e}}^*) - \mathbf{c}^T (K[\mathbf{u}] + \mathbf{f} - \mathbf{C} \dot{\mathbf{x}} - \mathbf{g}) \\
&\quad + \frac{1}{2} \mathbf{c}^T \dot{\mathbf{M}} \mathbf{c} + k_2 (\mathcal{L}_p \otimes \mathbf{I}_n \mathbf{e})^T \mathcal{L}_p \otimes \mathbf{I}_n \dot{\mathbf{e}} \\
&\quad + \left(\mathcal{L}_p \otimes \mathbf{I}_n \int_0^t \mathcal{L}_p \otimes \mathbf{I}_n \mathbf{e} d\tau \right)^T k_2 \mathbf{B} \Lambda \mathcal{L}_p \otimes \mathbf{I}_n \mathcal{L}_p \otimes \mathbf{I}_n \mathbf{e} + \tilde{\boldsymbol{\mu}}^T K [\dot{\boldsymbol{\mu}}] \\
&= -\mathbf{c}^T (k_1 \mathbf{c} + k_2 \mathcal{L}_p \otimes \mathbf{I}_n \mathcal{L}_p \otimes \mathbf{I}_n \mathbf{e} + \mathbf{C} \mathbf{c} + K[\mathbf{u}_\omega] + \mathbf{f}) + \frac{1}{2} \mathbf{c}^T \dot{\mathbf{M}} \mathbf{c} \\
&\quad + k_2 (\mathcal{L}_p \otimes \mathbf{I}_n \mathbf{e})^T \mathcal{L}_p \otimes \mathbf{I}_n \dot{\mathbf{e}} \\
&\quad + \left(\mathcal{L}_p \otimes \mathbf{I}_n \int_0^t \mathcal{L}_p \otimes \mathbf{I}_n \mathbf{e} d\tau \right)^T k_2 \mathbf{B} \Lambda \mathcal{L}_p \otimes \mathbf{I}_n \mathcal{L}_p \otimes \mathbf{I}_n \mathbf{e} + \tilde{\boldsymbol{\mu}}^T K [\dot{\boldsymbol{\mu}}] \\
&= -\mathbf{c}^T k_1 \mathbf{c} - \mathbf{c}^T (K[\mathbf{u}_\omega] + \mathbf{f}) + \mathbf{c}^T \left(\frac{1}{2} \dot{\mathbf{M}} - \mathbf{C} \right) \mathbf{c} \\
&\quad - k_2 \mathbf{c}^T \mathcal{L}_p \otimes \mathbf{I}_n \mathcal{L}_p \otimes \mathbf{I}_n \mathbf{e} + k_2 [\mathcal{L}_p \otimes \mathbf{I}_n \mathbf{e}]^T \mathcal{L}_p \otimes \mathbf{I}_n \dot{\mathbf{e}} \\
&\quad + \left(\mathcal{L}_p \otimes \mathbf{I}_n \int_0^t \mathcal{L}_p \otimes \mathbf{I}_n \mathbf{e} d\tau \right)^T k_2 \mathbf{B} \Lambda \mathcal{L}_p \otimes \mathbf{I}_n \mathcal{L}_p \otimes \mathbf{I}_n \mathbf{e} + \tilde{\boldsymbol{\mu}}^T K [\dot{\boldsymbol{\mu}}] \quad (4.15)
\end{aligned}$$

where

$$\mathbf{u}_\omega = \begin{bmatrix} \text{sgn}(\mathbf{c}_1) \begin{bmatrix} 1 & \|\mathbf{x}_1\| & \|\dot{\mathbf{x}}_1\| \end{bmatrix} \hat{\boldsymbol{\mu}}_1 \\ \text{sgn}(\mathbf{c}_2) \begin{bmatrix} 1 & \|\mathbf{x}_2\| & \|\dot{\mathbf{x}}_2\| \end{bmatrix} \hat{\boldsymbol{\mu}}_2 \\ \vdots \\ \text{sgn}(\mathbf{c}_p) \begin{bmatrix} 1 & \|\mathbf{x}_p\| & \|\dot{\mathbf{x}}_p\| \end{bmatrix} \hat{\boldsymbol{\mu}}_p \end{bmatrix}$$

$\mathbf{c}_i \in \mathbb{R}^n$, $\mathbf{c} = [\mathbf{c}_1^T \quad \mathbf{c}_2^T \quad \dots \quad \mathbf{c}_p^T]^T$ and $\mathbf{C} \triangleq \text{diag} \{ \mathbf{C}_1 \quad \mathbf{C}_2 \quad \dots \quad \mathbf{C}_p \}$.

Due to the skew symmetry property, it is obtained that

$$\mathbf{x}^T \left\{ \dot{\mathbf{M}}_i[\mathbf{x}_i(t)] - 2\mathbf{C}_i[\mathbf{x}_i(t), \dot{\mathbf{x}}_i(t)] \right\} \mathbf{x} = 0 \quad \forall \mathbf{x} \in \mathbb{R}^n \quad (4.16)$$

Further manipulation can yield the skew symmetry property for the stack matrices \mathbf{M} and \mathbf{C}

$$\mathbf{c}^T \left\{ \frac{1}{2} \dot{\mathbf{M}} - \mathbf{C} \right\} \mathbf{c} = 0 \quad \forall \mathbf{c} \in \mathbb{R}^{np} \quad (4.17)$$

Substituting Eq. (4.7) and Eq. (4.8) into $k_2 \mathbf{c}^T \mathcal{L}_p \otimes \mathbf{I}_n \mathcal{L}_p \otimes \mathbf{I}_n \mathbf{e}(t)$ renders

$$\begin{aligned} & k_2 \mathbf{c}^T \mathcal{L}_p \otimes \mathbf{I}_n \mathcal{L}_p \otimes \mathbf{I}_n \mathbf{e}(t) \\ &= k_2 \left(\dot{\mathbf{e}} + \mathbf{B} \mathcal{L}_p \otimes \mathbf{I}_n \mathcal{L}_p \otimes \mathbf{I}_n \mathbf{e} + \Lambda \mathbf{e} + \Lambda \mathbf{B} \mathcal{L}_p \otimes \mathbf{I}_n \int_0^t \mathcal{L}_p \otimes \mathbf{I}_n \mathbf{e} d\tau \right)^T \\ & \quad \times \mathcal{L}_p \otimes \mathbf{I}_n \mathcal{L}_p \otimes \mathbf{I}_n \mathbf{e}(t) \\ &= k_2 \dot{\mathbf{e}}^T \mathcal{L}_p \otimes \mathbf{I}_n \mathcal{L}_p \otimes \mathbf{I}_n \mathbf{e}(t) + k_2 (\mathbf{B} \mathcal{L}_p \otimes \mathbf{I}_n \mathcal{L}_p \otimes \mathbf{I}_n \mathbf{e})^T \mathcal{L}_p \otimes \mathbf{I}_n \mathcal{L}_p \otimes \mathbf{I}_n \mathbf{e}(t) \\ & \quad + k_2 \Lambda \mathbf{e}^T \mathcal{L}_p \otimes \mathbf{I}_n \mathcal{L}_p \otimes \mathbf{I}_n \mathbf{e}(t) + k_2 \left(\Lambda \mathbf{B} \mathcal{L}_p \otimes \mathbf{I}_n \int_0^t \mathcal{L}_p \otimes \mathbf{I}_n \mathbf{e} d\tau \right)^T \\ & \quad \times \mathcal{L}_p \otimes \mathbf{I}_n \mathcal{L}_p \otimes \mathbf{I}_n \mathbf{e}(t) \end{aligned} \quad (4.18)$$

Therefore

$$\begin{aligned} & -k_2 \mathbf{c}^T \mathcal{L}_p \otimes \mathbf{I}_n \mathcal{L}_p \otimes \mathbf{I}_n \mathbf{e}(t) + k_2 (\mathcal{L}_p \otimes \mathbf{I}_n \mathbf{e})^T \mathcal{L}_p \otimes \mathbf{I}_n \dot{\mathbf{e}} \\ & \quad + \left(\mathcal{L}_p \otimes \mathbf{I}_n \int_0^t \mathcal{L}_p \otimes \mathbf{I}_n \mathbf{e} d\tau \right)^T k_2 \mathbf{B} \Lambda \mathcal{L}_p \otimes \mathbf{I}_n \mathcal{L}_p \otimes \mathbf{I}_n \mathbf{e}(t) \\ &= -k_2 (\mathbf{B} \mathcal{L}_p \otimes \mathbf{I}_n \mathcal{L}_p \otimes \mathbf{I}_n \mathbf{e})^T \mathcal{L}_p \otimes \mathbf{I}_n \mathcal{L}_p \otimes \mathbf{I}_n \mathbf{e}(t) \\ & \quad - k_2 \Lambda \mathbf{e}^T \mathcal{L}_p \otimes \mathbf{I}_n \mathcal{L}_p \otimes \mathbf{I}_n \mathbf{e}(t) \leq 0 \end{aligned} \quad (4.19)$$

With this result and Assumption 4.1, $\dot{\tilde{V}}$ is derived as follows

$$\dot{\tilde{V}} \leq -\mathbf{c}^T k_1 \mathbf{c} - \mathbf{c}^T (K[\mathbf{u}_\omega] + \mathbf{f}) + \tilde{\boldsymbol{\mu}}^T K \begin{bmatrix} \dot{\boldsymbol{\mu}} \end{bmatrix} \quad (4.20)$$

To deal with the noise, a passivity-based control law [114] is adopted in this work. The noise boundary in this work is different from that in [114]. As stated in Assumption 4.1, the noise boundary is also influenced by the derivative of the generalized coordinates of the dynamical system. This is especially the case if the friction disturbance is considered.

Substituting the update law in Eq. (4.11) into Eq. (4.20) yields

$$\begin{aligned} \dot{\tilde{V}} &\leq -\mathbf{c}^T k_1 \mathbf{c} - \mathbf{c}^T (K[\mathbf{u}_\omega] + \mathbf{f}) + [\hat{\boldsymbol{\mu}} - \boldsymbol{\mu}]^T K \begin{bmatrix} \dot{\boldsymbol{\mu}} \end{bmatrix} \\ &\leq -\mathbf{c}^T k_1 \mathbf{c} - \mathbf{c}^T K[\mathbf{u}_\omega] - \mathbf{c}^T \mathbf{f} + \sum_{i=1}^p \hat{\boldsymbol{\mu}}_i^T \begin{bmatrix} 1 \\ \|\mathbf{x}_i\| \\ \|\dot{\mathbf{x}}_i\| \end{bmatrix} \text{SGN}(\mathbf{c}_i)^T \mathbf{c}_i \\ &\quad - \sum_{i=1}^p \boldsymbol{\mu}_i^T \begin{bmatrix} 1 \\ \|\mathbf{x}_i\| \\ \|\dot{\mathbf{x}}_i\| \end{bmatrix} \text{SGN}(\mathbf{c}_i)^T \mathbf{c}_i \\ &\leq -\mathbf{c}^T k_1 \mathbf{c} - \mathbf{c}^T \mathbf{f} - \sum_{i=1}^p \boldsymbol{\mu}_i^T \begin{bmatrix} 1 \\ \|\mathbf{x}_i\| \\ \|\dot{\mathbf{x}}_i\| \end{bmatrix} \text{SGN}(\mathbf{c}_i)^T \mathbf{c}_i \end{aligned} \quad (4.21)$$

where $\text{SGN}(\mathbf{c}) = \begin{cases} \{1\} & \text{if } x > 0 \\ [-1, 1] & \text{if } x = 0 \\ \{-1\} & \text{if } x < 0 \end{cases}$ is the set-valued sign function as defined in [113]. Since $\mu_i = \sum_{j=1}^p \mu_{ji} \forall i = 1, 2, 3$, the last two terms in Eq. (4.21) are non-positive and it is thus obtained

$$\dot{\tilde{V}} \leq -\mathbf{c}^T k_1 \mathbf{c} \quad (4.22)$$

According to the set-valued LaSalle theorem [112], it can be concluded that $\mathbf{e}_i \rightarrow 0 \forall v_i \in \mathcal{X}$ and $\mathbf{e}_i \rightarrow \mathbf{e}_j \forall v_i, v_j \in \mathcal{L}$ as $t \rightarrow \infty$. Therefore, the consensus seeking protocol depicted by Eq. (4.6) achieves consensus in a distributed manner as long as the state vector is forced in the supersurface $\mathbf{e}(t)^T \mathbf{e}(t) = 0$. Hence, the synchronized formation tracking problem is solved by the proposed distributed nonlinear control law in Eq. (4.10) if the communication topology contains a spanning tree with a leader as the root. \square

Remark 4.4. *As mentioned in Remark 4.3, the synchronization studied in this work is different from that in previous papers. This difference is explicitly explained in the above paragraph. The proposed control algorithm can guarantee not only the consensus of positions, but also the consensus of the error vectors $\mathbf{e}_i \forall v_i \in \mathcal{L}$ as the time evolves. Namely, with the achievement of the synchronization of the relative errors, the formation of the leaders is further guaranteed while the trajectory tracking is being conducted.*

Remark 4.5. *The asymptotical convergence is validated by the stability analysis. However, two kinds of convergence, tracking convergence and synchronous convergence, are included in the proposed control algorithm. It can be observed from the stability proof that the convergence rate of synchronization is directly determined by the network strength which is represented by the parameter b_i . The relationship exhibited in Eq. (4.4) implies that the performance of the synchronization is explicitly*

determined by the network strength. If b_i is set to zero, then the network coupling disappeared. In this extreme situation, there is no synchronization conducted because the only error dynamics in Eq. (4.4) will be the tracking error with respect to the desired trajectory. In contrast, the trajectory tracking will be slowed down with an extremely strong network connection. Therefore, the value of b_i should be selected appropriately in the applications regarding the balance between the trajectory tracking and the synchronization.

4.2.2 Fault diagnosis

The active fault diagnosis problem in multi-agent systems is investigated in this part. In the previous work on multi-agent fault diagnosis, the agent model is usually assumed to be single/double integrator. However, most mechanical systems cannot be represented by a single/double integrator model. The generalization of the fault diagnosis strategy to a nonlinear system is compelled by many practically emerging applications in multi-agent networks.

The possible faults are modeled as shown in Eqs. (4.23, 4.24)

$$\mathbf{M}_i[\mathbf{x}_i(t)]\ddot{\mathbf{x}}_i(t) + \mathbf{C}_i[\mathbf{x}_i(t), \dot{\mathbf{x}}_i(t)]\dot{\mathbf{x}}_i(t) + \mathbf{g}_i[\mathbf{x}_i(t)] = \mathbf{u}_i(t) + \boldsymbol{\xi}_i(t) \quad (4.23)$$

$$\mathbf{y}_i(t) = \mathbf{x}_i(t) + \boldsymbol{\zeta}_i(t) \quad (4.24)$$

where $\boldsymbol{\xi}_i(t)$ denotes the actuator fault, $\mathbf{y}_i(t)$ is the detected state information with

$\zeta_i(t)$ defined as the sensor fault. The observer-based fault detection method is utilized to generate the residual signal for the purpose of fault diagnosis.

The observer-based fault detection method is widely investigated due to its effectiveness and flexibility. The basic idea of this method is to generate a set of signals by comparing the measured with the estimated outputs. The faults in the systems are indicated by these signals, referred to as the residuals. The observer-based fault detection and isolation method is well developed in linear system [115, 116]. However, it is restricted by the diversity of nonlinear systems. In this work, an observer-based fault detection method for networked nonlinear systems is discussed. The super-twisting based sliding mode observer is utilized due to its effectiveness for a large class of nonlinear systems. Equipped with the sliding mode observer design techniques [117–119], the nonlinear observer of Eq. (4.1) for channel j has the following form [120]

$$\begin{aligned}
\dot{\hat{y}}_{i1}^j(t) &= \hat{y}_{i2}^j(t) - k_3 \sqrt{|\hat{y}_{i1}^j(t) - y_i^j(t)|} \operatorname{sgn}(\hat{y}_{i1}^j(t) - y_i^j(t)) \\
\dot{\hat{y}}_{i2}^j(t) &= -k_4 \operatorname{sgn}(\hat{y}_{i1}^j(t) - y_i^j(t)) + \tilde{\mathbf{m}}_i^j[\mathbf{y}_i(t)] \mathbf{u}_i^j(t) - \tilde{\mathbf{c}}_i^j[\mathbf{y}_i(t), \dot{\mathbf{y}}_i(t)] \dot{\mathbf{y}}_i(t) \\
&\quad - \tilde{\mathbf{m}}_i^j[\mathbf{y}_i(t)] \mathbf{g}_i[\mathbf{y}_i(t)] \\
r_i^j &= q_{i1}^j(t) q_{i1}^j(t)
\end{aligned} \tag{4.25}$$

where $q_{i1}^j(t) = \hat{y}_{i1}^j(t) - y_i^j(t)$, r_i^j is the residual signal, \hat{y}_{i1}^j is the estimation of agent position, \hat{y}_{i2}^j is the estimation of agent velocity, k_3 and k_4 are positive constants.

$\tilde{\mathbf{m}}_i^j[\mathbf{y}_i(t)]$ and $\tilde{\mathbf{c}}_i^j[\mathbf{y}_i(t), \dot{\mathbf{y}}_i(t)]$ are the row vectors corresponding to channel j , and

they are derived following the approach in [120].

In terms of the nonlinear observer in Eq. (4.25), the following error dynamics are yielded by substituting Eq. (4.24) into Eq. (4.25) and subtracting Eq. (4.23) from Eq. (4.25)

$$\begin{aligned} \dot{q}_{i1}^j(t) &= q_{i2}^j(t) - k_3 \sqrt{|q_{i1}^j(t)|} \text{sgn}(q_{i1}^j(t)) \\ \dot{q}_{i2}^j(t) &= -k_4 \text{sgn}(q_{i1}^j(t)) + \rho_i^j(t) + \bar{h}_i^j(\zeta_i, \xi_i) \end{aligned} \quad (4.26)$$

where $q_{i2}^j(t) = \hat{y}_{i2}^j(t) - \hat{y}_i^j(t)$ and $\rho_i^j(t)$ is the mismatched dynamics out of the corresponding channel. It is assumed that $\rho_i^j(t)$ is bounded by an experimentally obtained constant ρ . $\bar{h}_i^j(\zeta_i, \xi_i)$ is the extra term caused by fault vectors and it cannot be explicitly formulated due to the flexibility of the dynamic model. However, a straightforward property of $\bar{h}_i^j(\zeta_i, \xi_i)$ is that it will cease to be zero with either non-zero ζ_i or ξ_i . With possible faults, the error dynamics are organized in vector form as follows

$$\begin{aligned} \dot{\mathbf{q}}_{i1}(t) &= \mathbf{q}_{i2}(t) - k_3 \begin{bmatrix} \sqrt{|q_{i1}^1(t)|} & 0 & 0 & 0 \\ 0 & \sqrt{|q_{i1}^2(t)|} & 0 & 0 \\ 0 & 0 & \ddots & 0 \\ 0 & 0 & 0 & \sqrt{|q_{i1}^n(t)|} \end{bmatrix} \text{sgn}(\mathbf{q}_{i1}(t)) \\ \dot{\mathbf{q}}_{i2}(t) &= -k_4 \text{sgn}(\mathbf{q}_{i1}(t)) + \boldsymbol{\rho}_i(t) + \bar{\mathbf{h}}_i(\zeta_i, \xi_i) \\ \mathbf{r}_i &= \begin{bmatrix} q_{i1}^1(t) & 0 & 0 & 0 \\ 0 & q_{i1}^2(t) & 0 & 0 \\ 0 & 0 & \ddots & 0 \\ 0 & 0 & 0 & q_{i1}^n(t) \end{bmatrix} \mathbf{q}_{i1}(t) \end{aligned} \quad (4.27)$$

where \mathbf{q}_{i1} , \mathbf{q}_{i2} , $\boldsymbol{\rho}_i(t)$ and $\bar{\mathbf{h}}_i(\zeta_i, \xi_i)$ are n -dimensional stack vectors of q_{i1}^j , q_{i2}^j , $\rho_i^j(t)$

and $\bar{h}_i^j(\zeta_i, \xi_i)$, respectively. The expected fault detection algorithm should work in this way: \mathbf{r}_i is a zero vector in the fault-free condition, i.e. $\xi_i = \zeta_i = 0$. When any fault occurs, i.e. either ξ_i or ζ_i ceases to be zero, the residual signal \mathbf{r}_i grows accordingly. Since the fault-free dynamics of Eq. (4.27) is equivalent to that of the fundamental form of the super-twisting algorithm, the robustly global finite-time stability can be guaranteed by Theorem 2 in [119]. Namely, $\mathbf{r}_i = 0$, $\forall \xi_i = \zeta_i = 0$. Meantime, the presence of either actuator fault or sensor fault will lead to a non-zero value for the term $\bar{h}_i(\zeta_i, \xi_i)$. By intuition, this would influence the stability of Eq. (4.27). However, the super-twisting structure brought a challenge for the strictly mathematical analysis. Therefore, two parts of work should be carried out in this section. First, a convincing analysis should be proposed to indicate that the residual signal \mathbf{r}_i will be affected by any change in $\bar{h}_i(\zeta_i, \xi_i)$. Namely, the term $\bar{h}_i(\zeta_i, \xi_i)$ is not decoupled from the output \mathbf{r}_i . Otherwise, any fault signal will not be indicated by the residual signal \mathbf{r}_i if the super-twisting structure decouples $\bar{h}_i(\zeta_i, \xi_i)$ from \mathbf{r}_i . After the coupling relationship is demonstrated, the divergent condition should be derived regarding a non-zero $\bar{h}_i(\zeta_i, \xi_i)$. Motivated by previous work [121–123], the influence of the term $\bar{h}_i(\zeta_i, \xi_i)$ will be studied using the differential geometry tools developed in the nonlinear realization theory [83].

Theorem 4.2. *Suppose that the actuator fault or sensor fault occurs as stated in Assumption 4.3, then the residual signal \mathbf{r}_i is affected by the term $\bar{h}_i(\zeta_i, \xi_i)$ appeared*

in Eq. (4.27), i.e. the super-twisting structure will never decouple the $\mathbf{h}_i(\zeta_i, \xi_i)$ from \mathbf{r}_i .

Proof. With the presence of either actuator fault or sensor fault, the error dynamics in Eq. (4.27) can be reorganized into the affine nonlinear dynamics form

$$\dot{\mathbf{q}}_i(t) = \mathbf{f}_{A_i}(\mathbf{q}_i(t)) + \mathbf{F}_{B_i}\boldsymbol{\chi}_i \quad (4.28)$$

$$\mathbf{r}_i = \mathbf{f}_{C_i}(\mathbf{q}_i(t)) = \begin{bmatrix} (q_{i1}^1(t))^2 \\ (q_{i1}^2(t))^2 \\ \vdots \\ (q_{i1}^n(t))^2 \end{bmatrix} \quad (4.29)$$

where $\mathbf{F}_{B_i} = \begin{bmatrix} 0 \\ 1 \end{bmatrix} \otimes \mathbf{I}_n$, $\mathbf{q}_i(t) = [\mathbf{q}_{i1}(t) \quad \mathbf{q}_{i2}(t)]^T$, $\boldsymbol{\chi}_i = \boldsymbol{\rho}_i(t) + \mathbf{h}_i(\zeta_i, \xi_i)$ and

$$\mathbf{f}_{A_i}(\mathbf{q}_i(t)) = \begin{bmatrix} q_{i2}^1(t) - k_3 \sqrt{|q_{i1}^1(t)|} \text{sgn}(q_{i1}^1(t)) \\ q_{i2}^2(t) - k_3 \sqrt{|q_{i1}^2(t)|} \text{sgn}(q_{i1}^2(t)) \\ \vdots \\ q_{i2}^n(t) - k_3 \sqrt{|q_{i1}^n(t)|} \text{sgn}(q_{i1}^n(t)) \\ -k_4 \text{sgn}(q_{i1}^1(t)) \\ -k_4 \text{sgn}(q_{i1}^2(t)) \\ \vdots \\ -k_4 \text{sgn}(q_{i1}^n(t)) \end{bmatrix}.$$

Based on the affine nonlinear dynamics in Eqs. (4.28, 4.29), it is derived that

$$\text{span} \{d\mathbf{f}_{C_i}\mathbf{q}_i(t)\} = \text{span} \left\{ \begin{bmatrix} 2q_{i1}^1(t) \\ \mathbf{0}_{2n-1} \end{bmatrix}, \begin{bmatrix} 0 \\ 2q_{i1}^2(t) \\ \mathbf{0}_{2n-2} \end{bmatrix}, \dots, \begin{bmatrix} \mathbf{0}_{n-1} \\ 2q_{i1}^n(t) \\ \mathbf{0}_n \end{bmatrix} \right\} \quad (4.30)$$

where $\mathbf{0}_n$ denotes an n -dimensional zero vector.

Define $\Pi_0 = \text{span}\{\mathbf{b}_i\}$, where \mathbf{b}_i ($i = 1, 2, \dots, n$) is the column vector of the vector field \mathbf{F}_{B_i} . Then, $\Pi_j := \Pi_{j-1} + [\mathbf{f}_{A_i}, \Pi_{j-1}] + \sum_{i=1}^n [\mathbf{b}_i, \Pi_{j-1}]$ and the symbol $[\mathbf{b}_i, \Pi_{j-1}]$ represents the Lie bracket of two vector fields. Due to the fact that

the condition $\Pi_j \subset \langle \mathbf{f}_{A_i}, \mathbf{b}_1, \dots, \mathbf{b}_n | \text{span}\{\mathbf{b}_i\} \rangle$ is always true, the smallest invariant distribution $\langle \mathbf{f}_{A_i}, \mathbf{b}_1, \dots, \mathbf{b}_n | \text{span}\{\mathbf{b}_i\} \rangle$ does not belong to the annihilator of $\text{span}\{d\mathbf{f}_{C_i} \mathbf{q}_i(t)\}$ if $\Pi_j \not\subset \text{span}\{d\mathbf{f}_{C_i} \mathbf{q}_i(t)\}^\perp$, $\exists \Pi_j \subset \langle \mathbf{f}_{A_i}, \mathbf{b}_1, \dots, \mathbf{b}_n | \text{span}\{\mathbf{b}_i\} \rangle$. To this end, the following distribution is derived

$$\Pi_1 = \Pi_0 + [\mathbf{f}_{A_i}, \Pi_0] + \sum_{i=1}^n [\mathbf{b}_i, \Pi_0] \quad (4.31)$$

Due to the bilinear property of the Lie bracket of vector fields, it can be further yielded that

$$\begin{aligned} \Pi_1 &= \text{span}\{\mathbf{b}_i\} + \sum_{j=1}^n [\mathbf{f}_{A_i}, \mathbf{b}_j] + \sum_{i=1}^n \sum_{j=1}^n [\mathbf{b}_i, \mathbf{b}_j] \\ &= \text{span}\{\mathbf{b}_i\} + \text{span}\{\mathbf{v}_{2n}^1, \mathbf{v}_{2n}^2, \dots, \mathbf{v}_{2n}^n\} \\ &= \text{span}\{\mathbf{v}_{2n}^i\} \quad \forall i = 1, 2, \dots, 2n \end{aligned} \quad (4.32)$$

where \mathbf{v}_{2n}^i denotes a $2n$ -dimensional vector whose i -th element is 1, and all the other elements are 0. Apparently, $\Pi_1 \not\subset \text{span}\{d\mathbf{f}_{C_i} \mathbf{q}_i(t)\}^\perp$, which demonstrates that \mathbf{r}_i must be affected by $\boldsymbol{\chi}_i$ according to Theorem 2.1. Namely, the super-twisting structure will never decouple $\tilde{\mathbf{h}}_i(\boldsymbol{\zeta}_i, \boldsymbol{\xi}_i)$ from \mathbf{r}_i . \square

In addition, the signal \mathbf{r}_i should also be divergent (or at least change distinctly in the amplitude) once a fault occurs. However, only coupling condition is proposed in the above work. Hence, the following theorem is presented to illustrate the divergent condition in the presence of actuator/sensor fault.

Theorem 4.3. *Suppose that the actuator fault and sensor fault are modeled in Eq. (4.23) and satisfy Assumption 4.3. The signal \mathbf{r}_i in the observer-based fault detection algorithm (4.27) is divergent if $\bar{h}_i^j(\boldsymbol{\zeta}_i, \boldsymbol{\xi}_i) > \rho + k_4 + \varepsilon$ or $\bar{h}_i^j(\boldsymbol{\zeta}_i, \boldsymbol{\xi}_i) < -k_4 - \rho - \varepsilon$, where ε is a positive constant.*

Proof. If $\bar{h}_i^j(\boldsymbol{\zeta}_i, \boldsymbol{\xi}_i) > k_4 + \rho + \varepsilon$, regarded as channel j , represents the j th element of vector $\bar{\mathbf{h}}_i(\boldsymbol{\zeta}_i, \boldsymbol{\xi}_i)$, the error term $q_{i2}^j(t)$ can be derived as follows

$$\begin{aligned}
q_{i2}^j(t) &= q_{i2}^j(t_0) + \int_{t_0}^t -k_4 \text{sgn}(q_{i1}^j(\tau)) + \rho_i^j(\tau) + \bar{h}_i^j(\boldsymbol{\zeta}_i, \boldsymbol{\xi}_i) dt \\
&> \int_{t_0}^t -k_4 \text{sgn}(q_{i1}^j(\tau)) + k_4 + \varepsilon dt \\
&= k_4 \int_{t_0}^t [1 - \text{sgn}(q_{i1}^j(\tau))] dt + \int_{t_0}^t \varepsilon dt
\end{aligned} \tag{4.33}$$

The inequality (4.33) implies that $q_{i2}^j(t)$ is monotonically increasing since $1 - \text{sgn}(q_{i1}^j(t)) \geq 0$ and $\varepsilon > 0$. According to Eq. (4.26), it is obtained that

$$\dot{q}_{i1}^j(t) > k_4 \int_{t_0}^t [1 - \text{sgn}(q_{i1}^j(\tau))] dt + \int_{t_0}^t \varepsilon dt - k_3 \sqrt{|q_{i1}^j(t)|} \text{sgn}(q_{i1}^j(t))$$

It is straightforward that $\dot{q}_{i1}^j(t) > 0 \forall q_{i1}^j(t) \leq 0$, namely, $q_{i1}^j(t)$ is monotonically increasing if $q_{i1}^j(t) \leq 0$. Assuming that $q_{i1}^j(t)$ is convergent for any $t \in \mathbb{R}^+$, then there must be a positive constant \bar{q} so that $q_{i1}^j(t) < \bar{q} < \infty \forall t \in \mathbb{R}^+$ when $q_{i1}^j(t)$ is positive. This assumption in turn implies that

$$\dot{q}_{i1}^j(t) > k_4 \int_{t_0}^t [1 - \text{sgn}(q_{i1}^j(\tau))] dt + \int_{t_0}^t \varepsilon dt - k_3 \sqrt{\bar{q}}$$

Thus, there must exist a positive constant \bar{t} satisfying $\bar{t} = t_0 + k_3\sqrt{\bar{q}}/\varepsilon$, and it is always true that $\dot{q}_{i1}^j(t) > 0 \forall t > \bar{t}$. As a result, $q_{i1}^j(t)$ is unbounded since $q_{i1}^j(t) > 0$ and $\dot{q}_{i1}^j(t) > 0$ are both true. That is why the convergence assumption is incorrect, namely, $q_{i1}^j(t)$ is divergent if $h_i^j(\zeta_i, \xi_i) > \rho + k_4 + \varepsilon$, which further implies that the signal \mathbf{r}_i is divergent if $h_i^j(\zeta_i, \xi_i) > \rho + k_4 + \varepsilon$. In the case of $h_i^j(\zeta_i, \xi_i) < -k_4 - \rho - \varepsilon$, the proof is similar and thus ignored here. \square

The vector \mathbf{r}_i can be selected as the residual signal regarding the conclusion in Theorem 4.3. Based on the residual generation algorithm constructed above, a technical scope of fault detection and function recovery strategy is explained in Figure 4.1. The residual signal r_i^j generated by Eq. (4.25) is considered as an alarm. A fault can be identified if the amplitude of r_i^j is greater than a predetermined threshold. Detailed fault detection process is explained in Figure. 4.2. Furthermore, the faulty agent will be discarded by the recovery algorithm as explained in Figure. 4.3. Since the network contains a spanning tree, all the neighbors of the faulty agent can be acknowledged. Therefore, the group mission will not be demolished by the faulty agent.

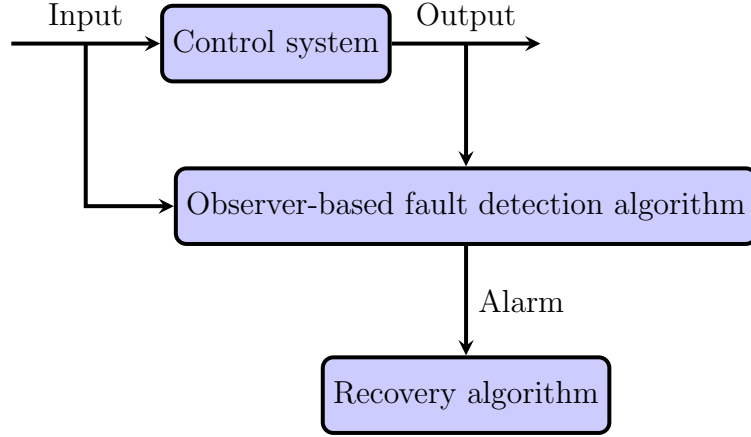


Fig. 4.1 Fault diagnosis configuration

4.3 Simulations

The proposed distributed formation control law is applied to six 3-DOF helicopters. Three of them have access to the desired trajectory while the others can only receive their neighbors' information. The dynamical model of 3-DOF helicopter in [96] is adopted as

$$\begin{bmatrix} \frac{J_e}{K_f l_a \cos(\beta)} & 0 \\ 0 & \frac{J_p}{K_f l_h} \end{bmatrix} \begin{bmatrix} \ddot{\alpha} \\ \ddot{\beta} \end{bmatrix} + \begin{bmatrix} \frac{mg \sin(\alpha + \alpha_0)}{K_f \cos(\beta)} \\ 0 \end{bmatrix} = \begin{bmatrix} V_s \\ V_d \end{bmatrix} \quad (4.34)$$

where J_e and J_p are the moments of inertia about the elevation and pitch axis, correspondingly, α and β are elevation and pitch angle, respectively, V_s is the sum of voltages applied to the front and back motors, and V_d is the difference between the voltages. The system parameters are shown in Table 4.1, and the communication topology is shown in Figure 4.4.

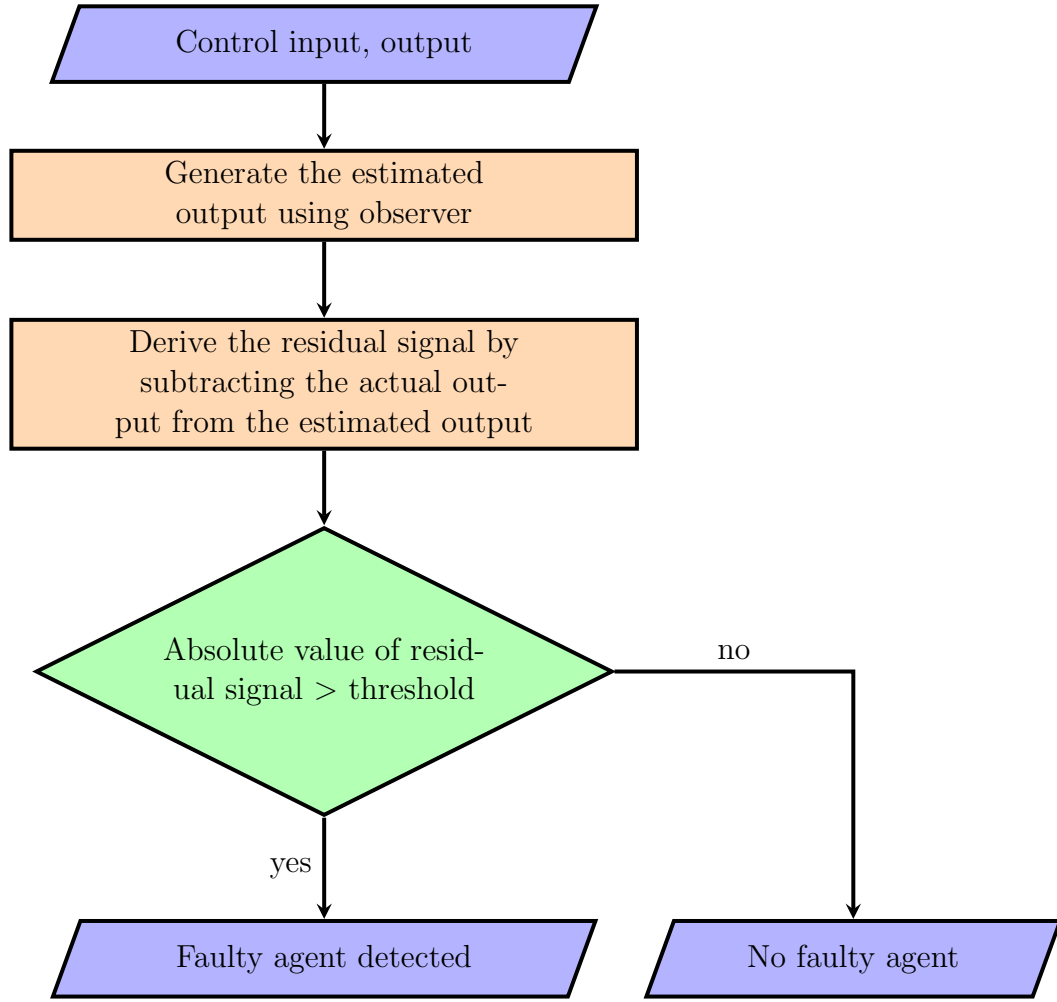


Fig. 4.2 Fault diagnosis strategy

Table 4.1 Parameters of helicopter system

Parameter	Value
Moment of inertia about elevation axis, J_e	1.044 (kg · m ²)
Moment of inertia about pitch axis, J_p	0.0455 (kg · m ²)
Transfer coefficient, K_f	0.625 (N/V)
Distance from propeller center to elevation axis, l_a	0.648 (m)
Distance from propeller center to pitch axis, l_h	0.178 (m)

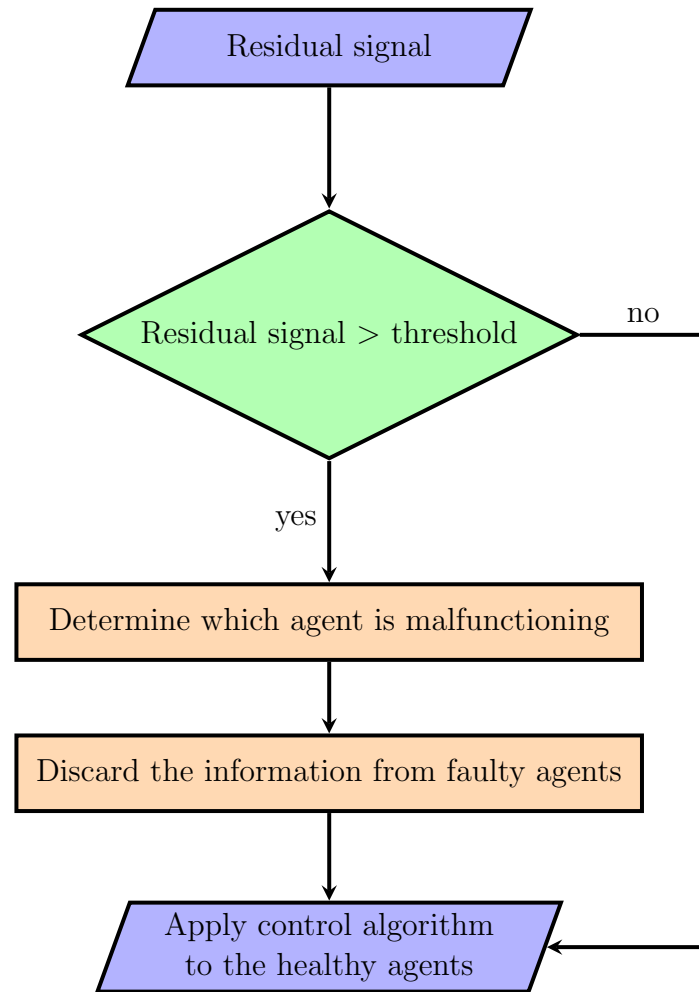


Fig. 4.3 Fault recovery strategy

The desired trajectory about elevation is shown in Figure 4.9, and the noise is generated using the formula in Eq. (4.35)

$$f_i = 0.1 + 0.2|\alpha_i| + 0.3|\dot{\alpha}_i| + W(t) \quad (4.35)$$

where $W(t)$ is the white noise whose variance is 0.1. Figure 4.10 shows the noise

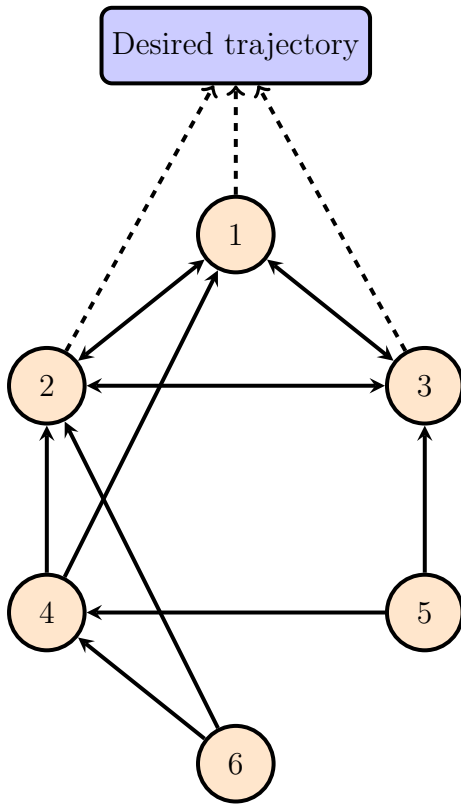


Fig. 4.4 Communication topology

in the simulations, and the tracking errors of the six helicopters are displayed in Figure 4.11.

Since all helicopters are functioning properly, none of the residual signals is divergent as shown in Figure 4.12 and none of the health indicators reports alarm. Here, the health indicator can only be one or zero. It is equal to one in normal condition, but becomes to be zero if malfunctioning is detected. It is observed in Figure 4.13 that the value of all the health indicators is one, which implies that no

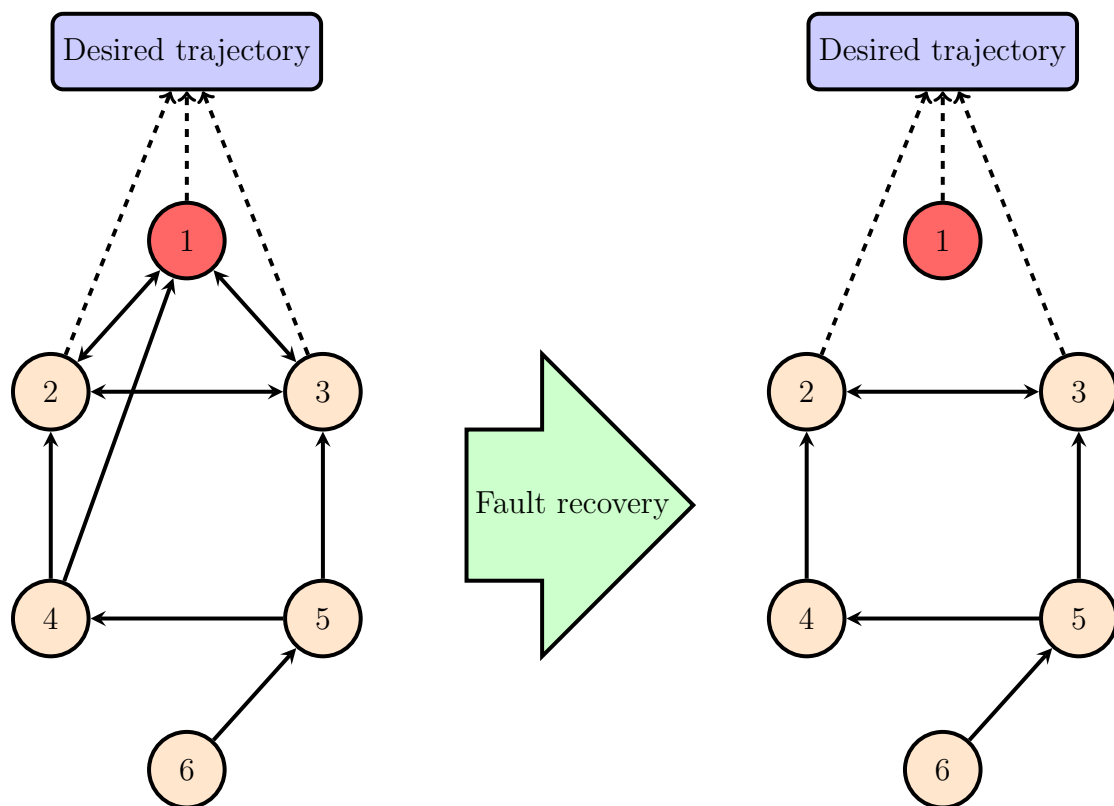


Fig. 4.5 Topology switching with faulty helicopter 1

malfunction is detected.

Since the fault diagnosis strategy is discussed in this work, the system is also simulated in the presence of faulty agents. There are many kinds of faults in practice [124–126]. Without loss of generality, the ineffectiveness of actuator and sensor is considered in this work. Figure 4.14 shows the tracking errors of six helicopters if both motors of helicopter 1 stop working. It is revealed in the simulation that all the helicopters fail to track the desired trajectory. This is because helicopter 2

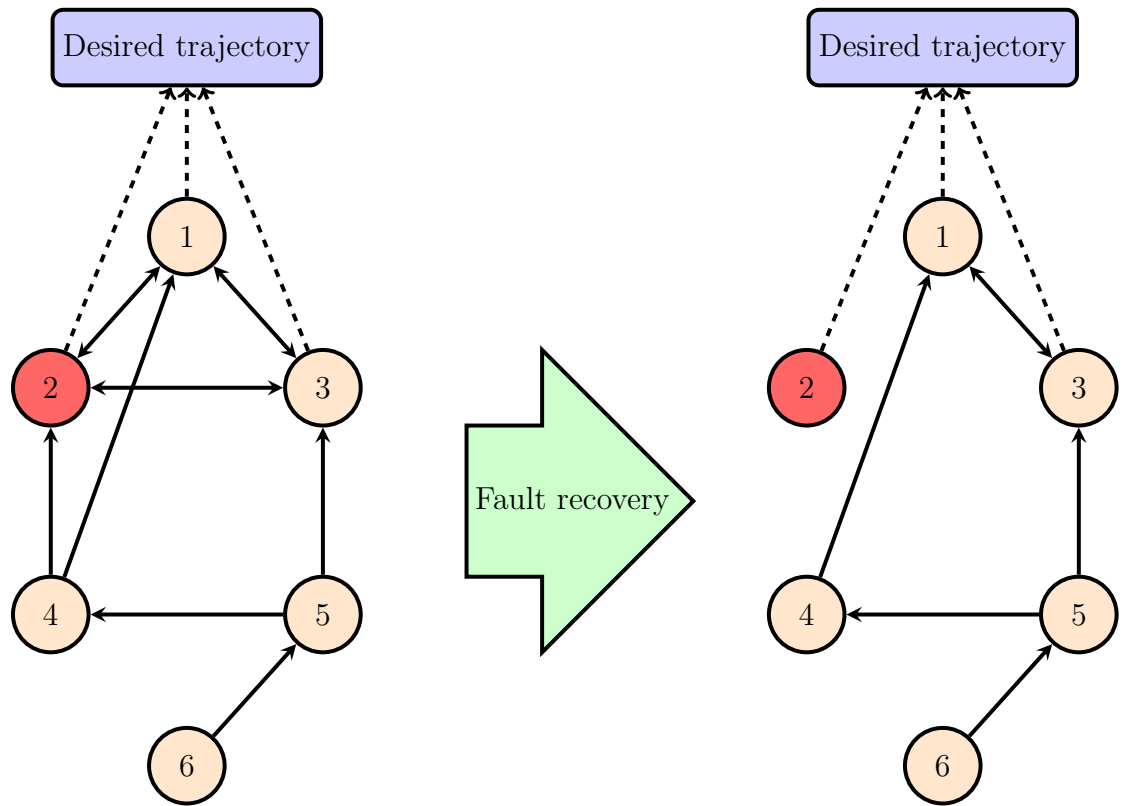


Fig. 4.6 Topology switching with faulty helicopter 2

and 3 need to keep synchronization with helicopter 1. Helicopters 4, 5 and 6 do not have the knowledge of the desired trajectory, and they can only keep consensus with the leaders. Similarly, the failure of tracking of six helicopters is exhibited in Figure 4.15. Since an incorrect feedback signal was provided by the faulty sensor, helicopter 1 is out of control. Accordingly, other helicopters are negatively affected by the faulty signal of helicopter 1 and the formation tracking mission completely failed because of one malfunctioning helicopter.

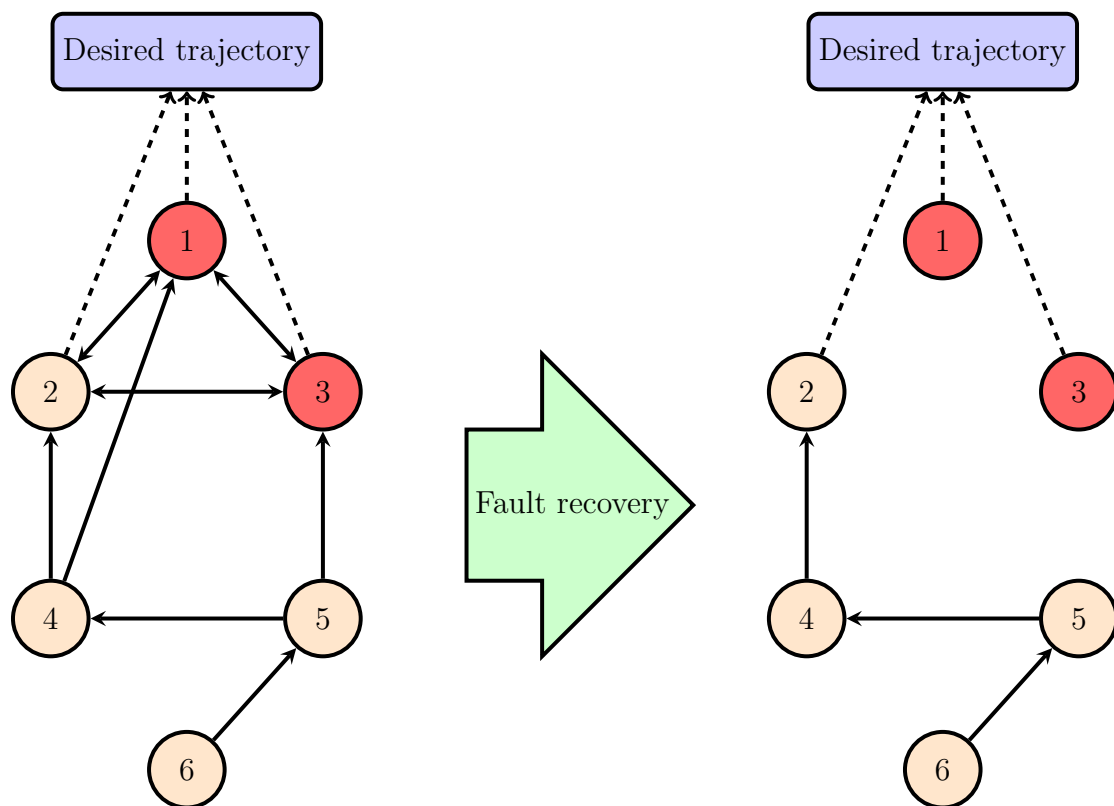


Fig. 4.7 Topology switching with faulty helicopter 1 and 3

To enable the capability of the active fault tolerant in the networked systems, the fault diagnosis strategy discussed in Section 4.2.2 is incorporated. In the presence of a residual generator, the fault of helicopter 1 is detected by a properly selected threshold value. In the simulation, the threshold value is chosen to be 0.02. It means that the fault alarm will be broadcast if the absolute value of the residual signal is greater than 0.02. The tracking errors of agent 1 and others are shown in Figure 4.16. Obviously, the malfunctioning of the faulty helicopter is

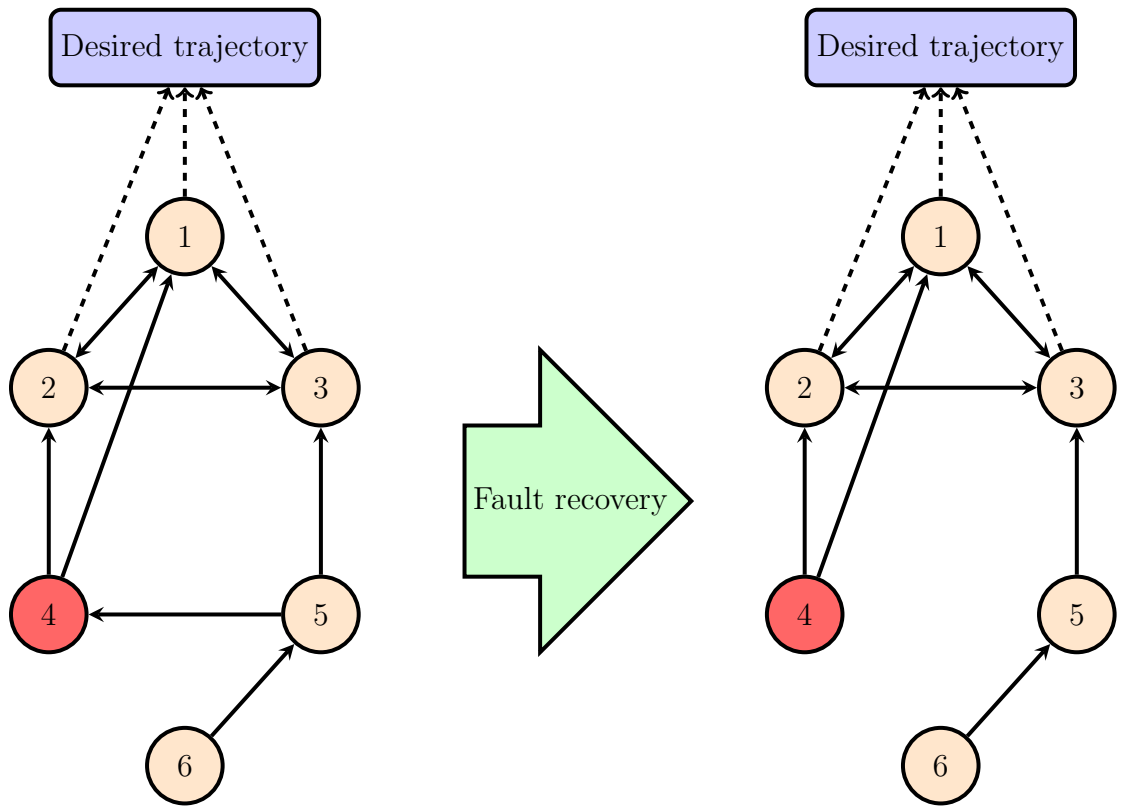


Fig. 4.8 Topology switching with faulty helicopter 4

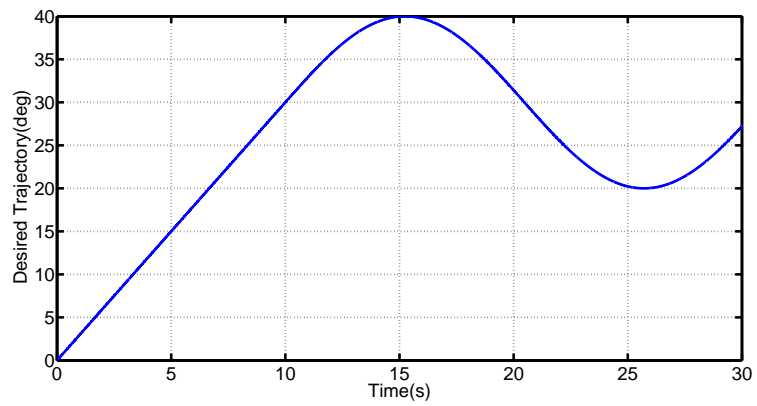


Fig. 4.9 Desired trajectory

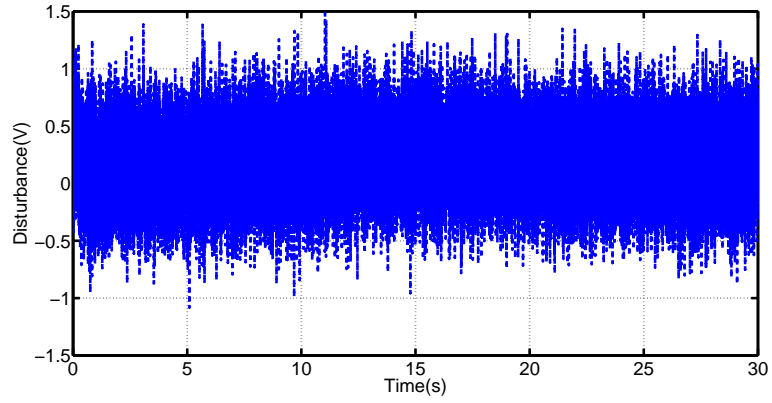


Fig. 4.10 Noise

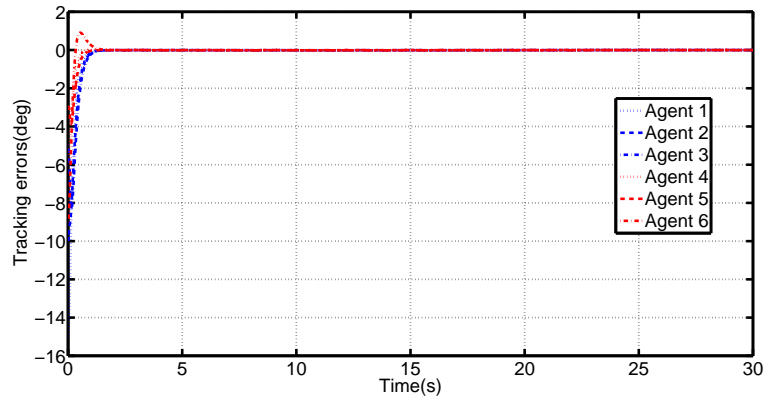


Fig. 4.11 Tracking errors of six helicopters

observed in Figure 4.16(a). The remaining helicopters actively ignore the faulty signal from the faulty helicopter and achieve synchronization. Figure 4.5 shows the topology switching based on the proposed fault diagnosis strategy. Meanwhile, the effectiveness of the fault recovery strategy is shown in Figure 4.17, where the health indicator precisely reports the occurrence of the fault of helicopter 1. The

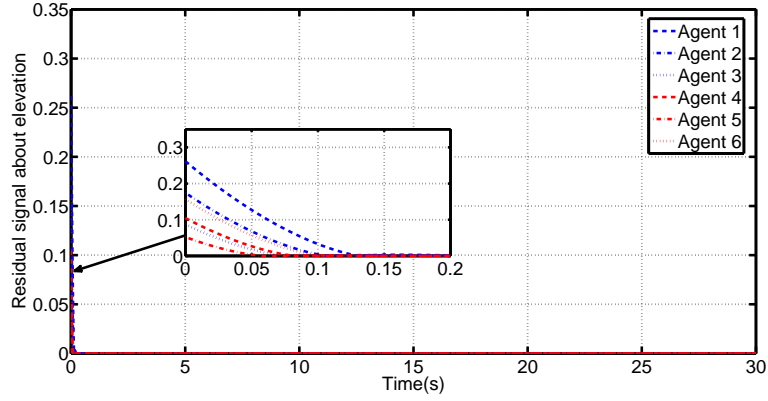


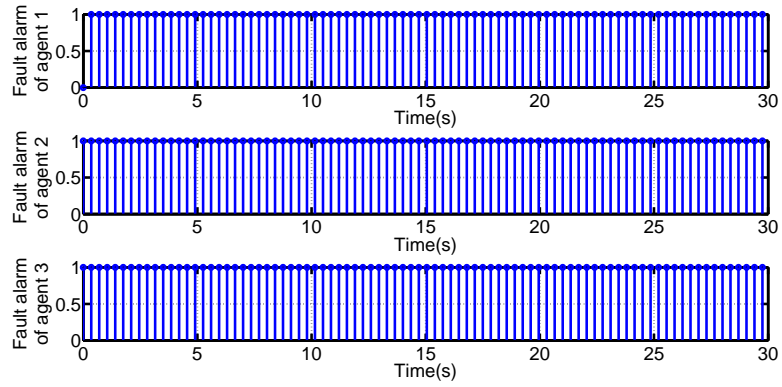
Fig. 4.12 Residuals of six helicopters

corresponding residual signal is shown in Figure 4.18.

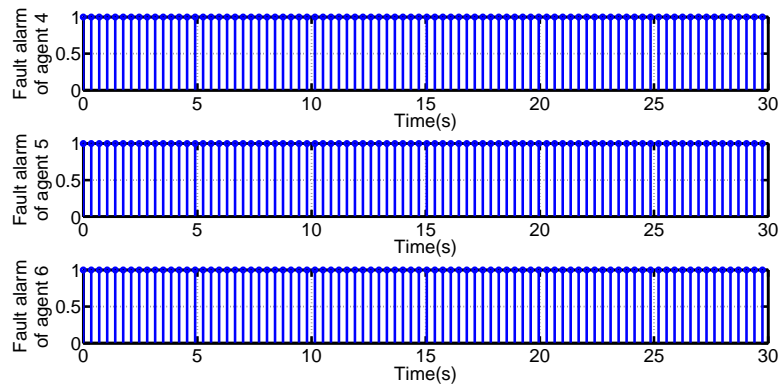
Similarly, if an actuator fault occurs at agent 2, the tracking errors, health indicators and residuals are shown in Figure 4.19, Figure 4.20 and Figure 4.21, respectively. Also, similar fault recovery strategy is exhibited in Figure 4.6.

Only one faulty agent is considered in the above simulations, but multiple faulty agents are also possible in practice. Therefore, two faulty agents are considered in the following demonstration. Agent 1 and 3 are both suffering from actuator fault, and the fault recovery strategy is shown in Figure 4.7

Correspondingly, the tracking errors, health indicators and residuals are shown in Figure 4.22, Figure 4.23 and Figure 4.24. It is observed that the tracking errors of the healthy helicopters converge to zero successfully, namely, healthy agents are not influenced by the faulty agent. Meanwhile, the agent fault has been indi-



(a) Health indicators of helicopter 1, 2 and 3



(b) Health indicators of helicopter 4, 5 and 6

Fig. 4.13 Health indicators of six helicopters

cated precisely in Figure 4.23, which further demonstrates the effectiveness of the observer-based fault diagnosis strategy.

To further verify the effectiveness of the proposed fault diagnosis strategy when follower malfunctioning happens, the follower fault condition is also simulated with faulty agent 4. The tracking errors, health indicators and residuals are shown in

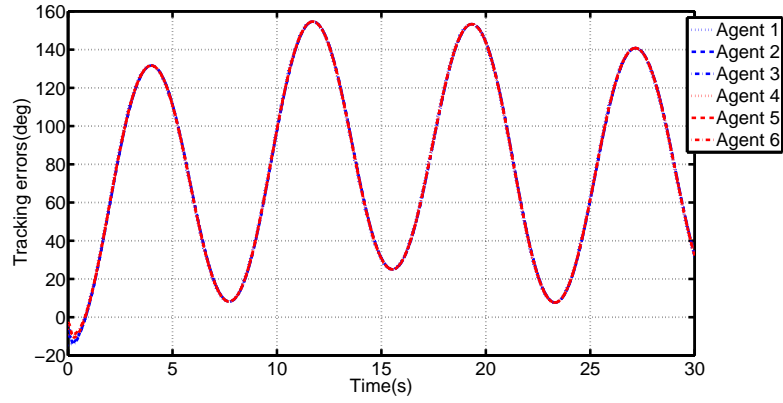


Fig. 4.14 Tracking errors with faulty helicopter 1 (actuator fault)

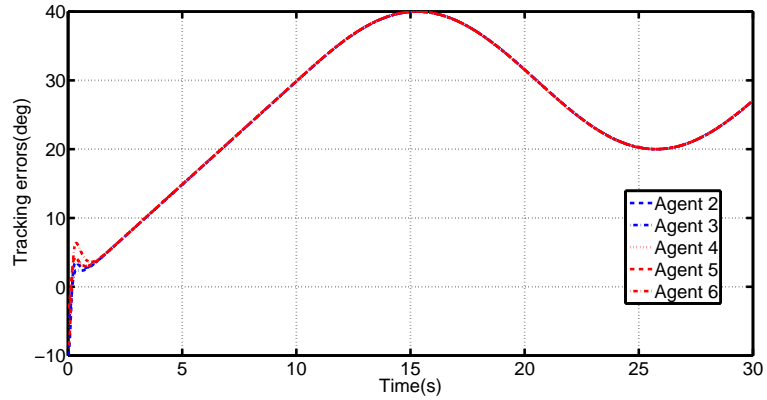
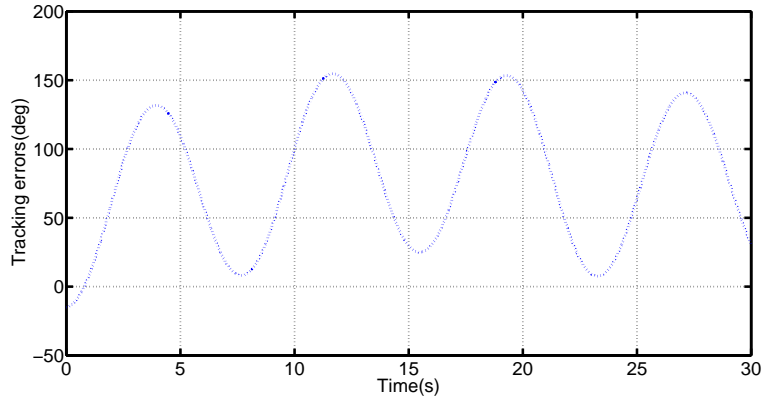


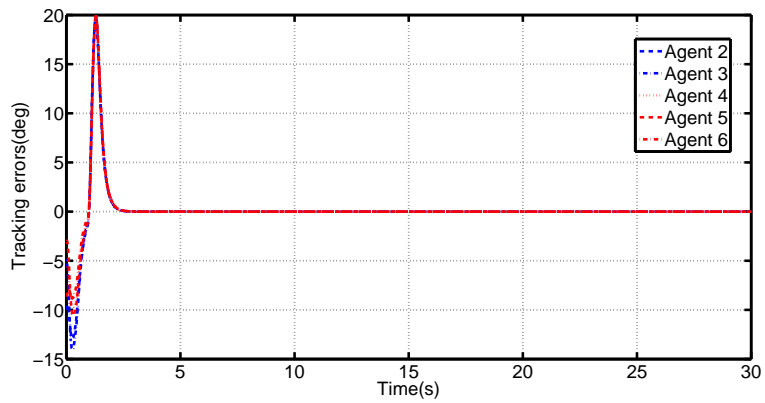
Fig. 4.15 Tracking errors with faulty helicopter 1 (sensor fault)

Figure 4.25, Figure 4.26 and Figure 4.27. Accordingly, the fault recovery strategy is presented in Figure 4.8.

In the above simulations, actuator fault has been considered with both faulty leaders and follower conditions. Other than actuator fault, sensor fault is another type of common fault. In order to further demonstrate the capability of the pro-



(a) Tracking error of helicopter 1

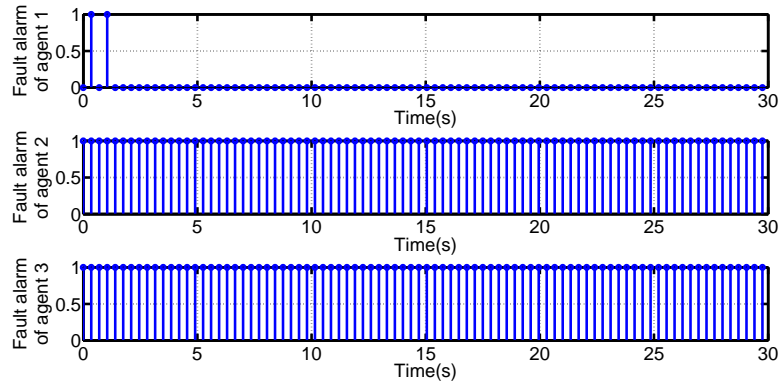


(b) Tracking errors of healthy helicopters

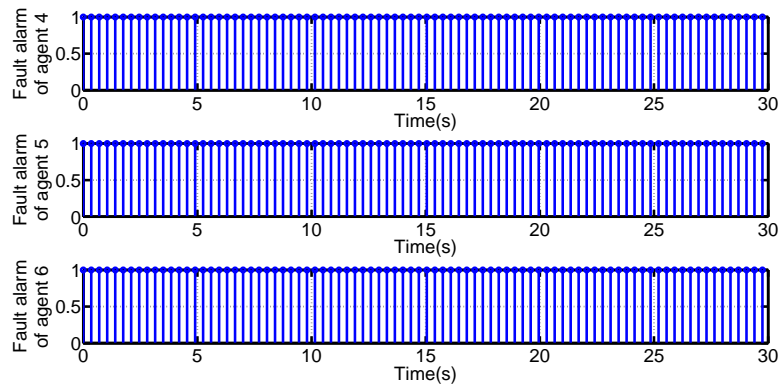
Fig. 4.16 Tracking errors of six helicopters

posed fault diagnosis strategy, the sensor fault will be considered in the following simulations. It is assumed that sensor fault occurs at agent 1, then the tracking errors, health indicators and residuals are shown in Figure 4.28, Figure 4.29 and Figure 4.30.

If agent 2 has the sensor fault, the tracking errors, health indicators and residuals



(a) Health indicators of helicopter 1, 2 and 3



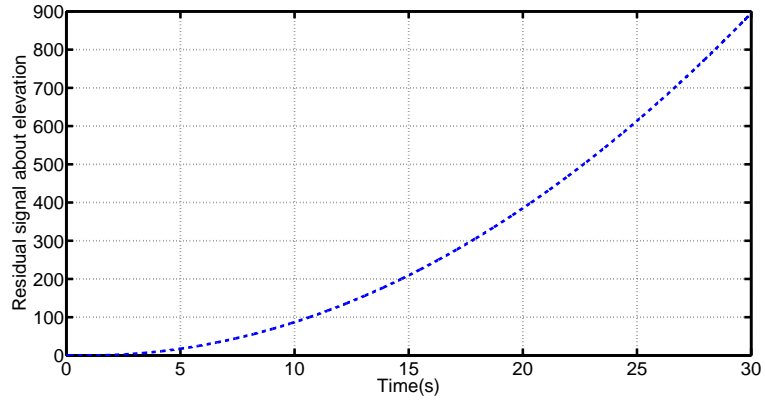
(b) Health indicators of helicopter 4, 5 and 6

Fig. 4.17 Health indicators of six helicopters

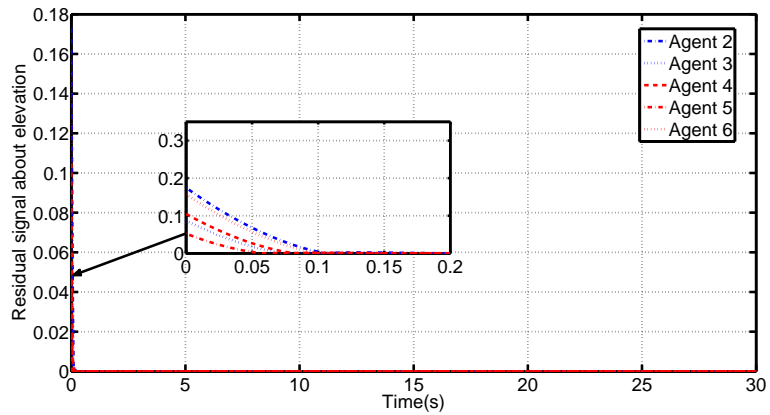
are shown in Figure 4.31, Figure 4.32 and Figure 4.33.

Similarly, if both agent 1 and 3 encounter sensor fault, the tracking errors, health indicators and residuals are shown in Figure 4.34, Figure 4.35 and Figure 4.36.

Also, the faulty follower condition is considered with faulty agent 4, and the tracking errors, health indicators and residuals are shown in Figure 4.37, Figure 4.38



(a) Residual signal of helicopter 1

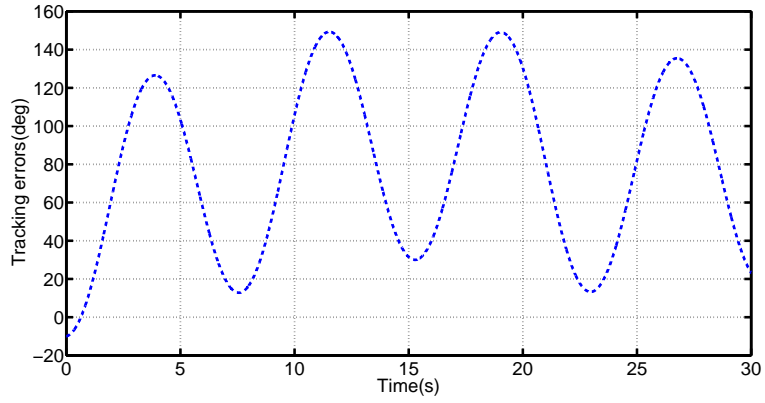


(b) Residual signals of helicopter 2, 3, 4, 5 and 6

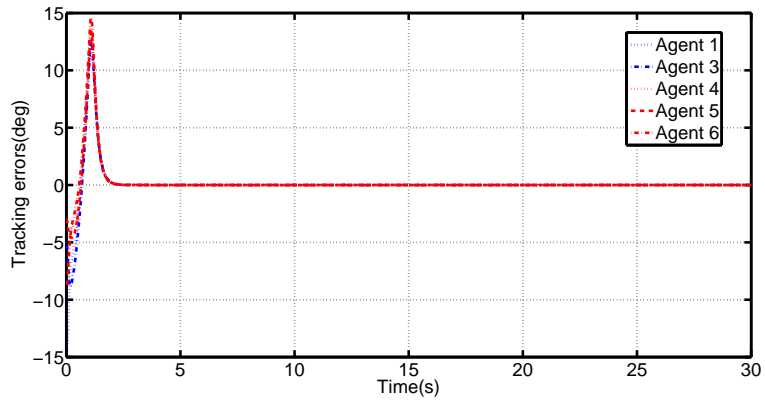
Fig. 4.18 Residual signals with faulty helicopter 1 (actuator fault)

and Figure 4.39.

Apparently, in all the simulations with sensor fault, the fault detection strategy successfully indicated all the faulty agents. Meanwhile, all the formation tracking missions are achieved based on the proposed fault recovery strategy, which further demonstrates the effectiveness of the proposed fault diagnosis strategy.



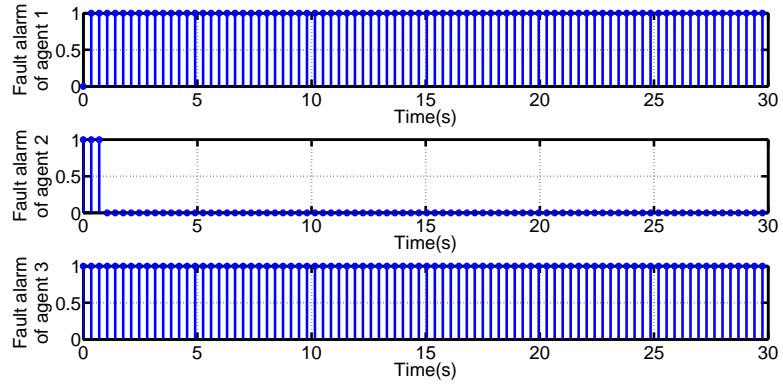
(a) Tracking error of helicopter 2



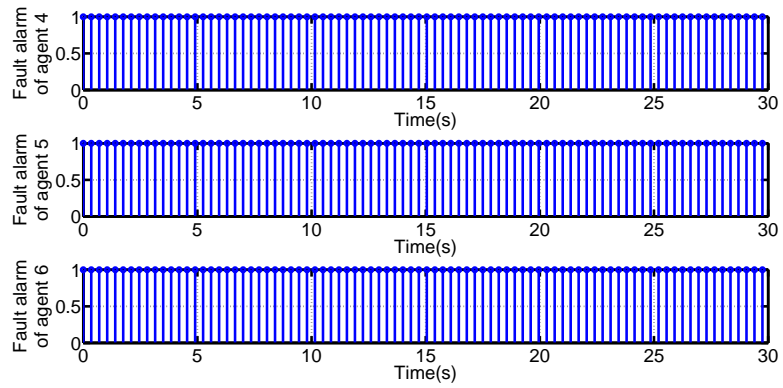
(b) Tracking errors of healthy helicopters

Fig. 4.19 Tracking errors of six helicopters

In this chapter, both the robust synchronization and fault diagnosis problems are solved for networked Euler-Lagrange systems. To further generalize the cooperative control algorithm for networked nonlinear systems, the consensus seeking algorithm for networked Lipschitz systems will be investigated in the next chapter.

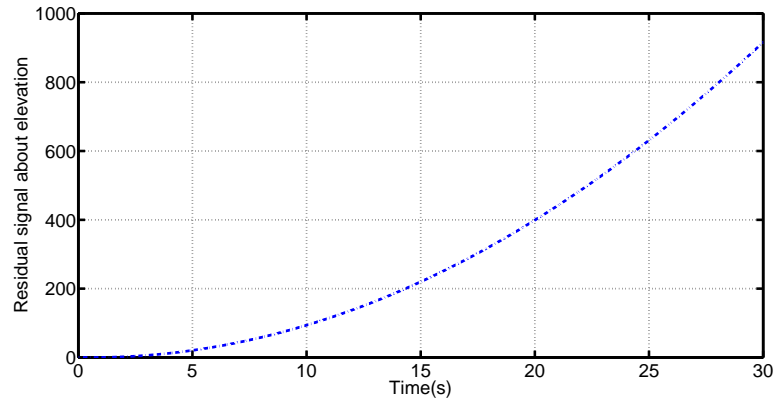


(a) Health indicators of helicopter 1, 2 and 3

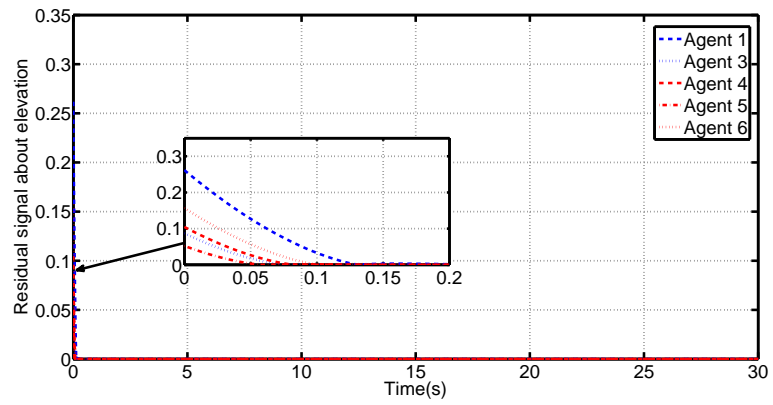


(b) Health indicator of helicopter 4, 5 and 6

Fig. 4.20 Health indicators of six helicopters

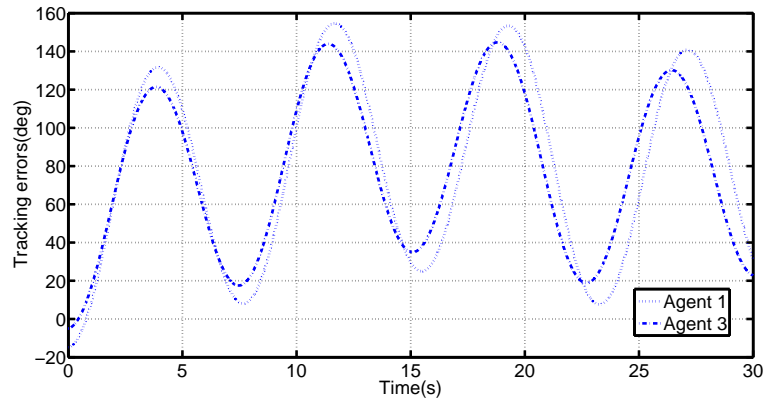


(a) Residual signal of helicopter 2

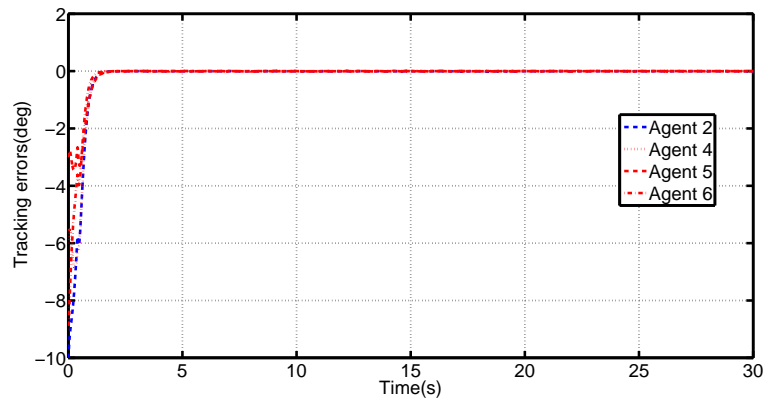


(b) Residual signals of helicopter 1, 3, 4, 5 and 6

Fig. 4.21 Residual signals with faulty helicopter 2 (actuator fault)

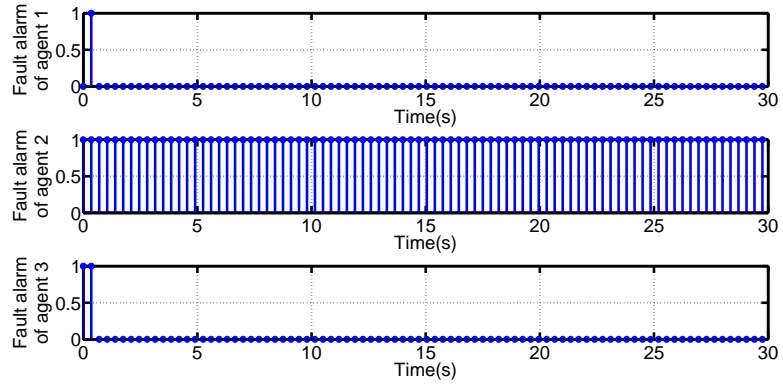


(a) Tracking errors of helicopter 1 and 3

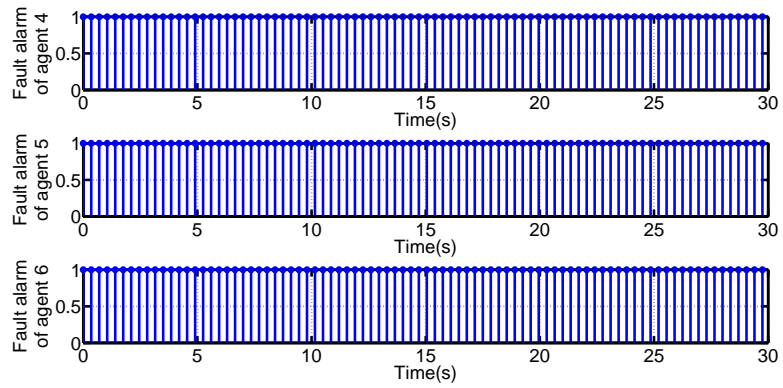


(b) Tracking errors of healthy helicopters

Fig. 4.22 Tracking errors of six helicopters

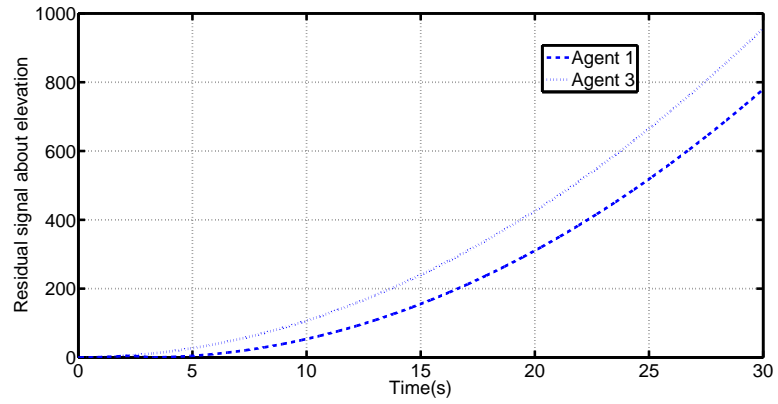


(a) Health indicators of helicopter 1, 2 and 3

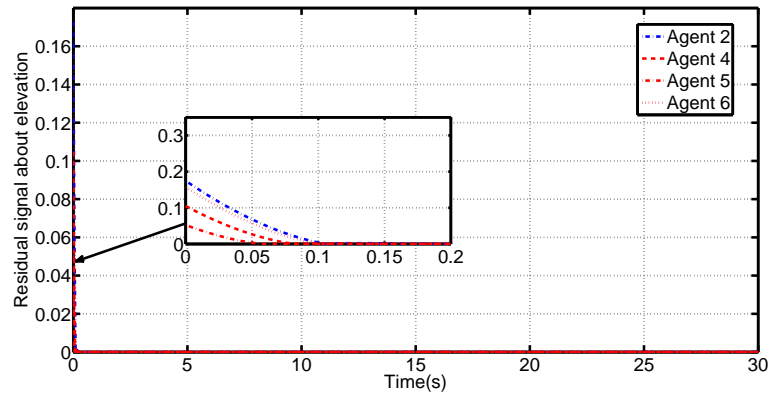


(b) Health indicators of helicopter 4, 5 and 6

Fig. 4.23 Health indicators of six helicopters

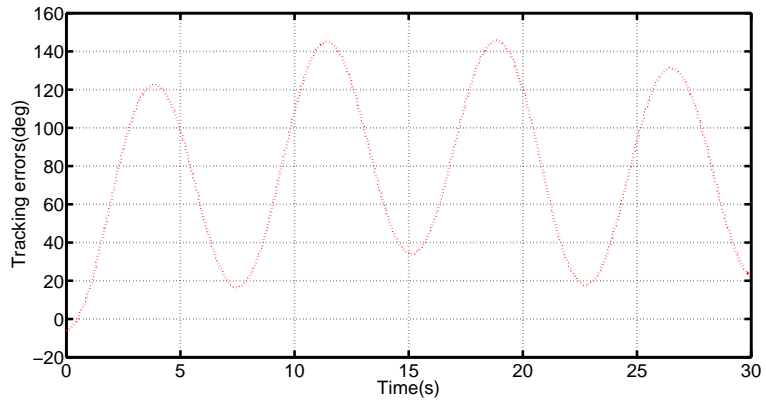


(a) Residual signals of helicopter 1 and 3

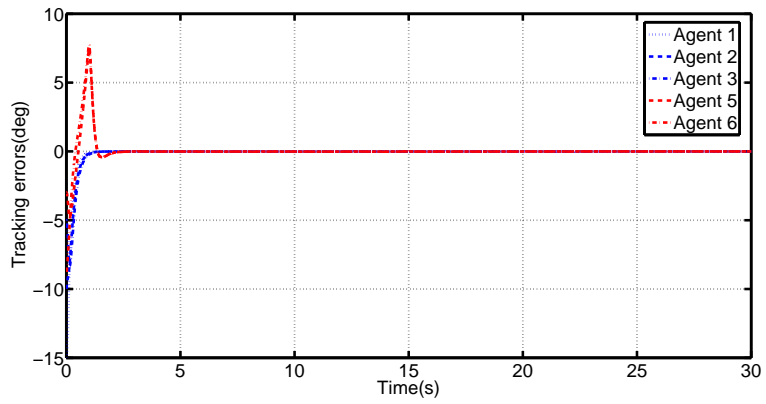


(b) Residual signals of helicopter 2, 4, 5 and 6

Fig. 4.24 Residual signals with faulty helicopter 1 and 3 (actuator fault)

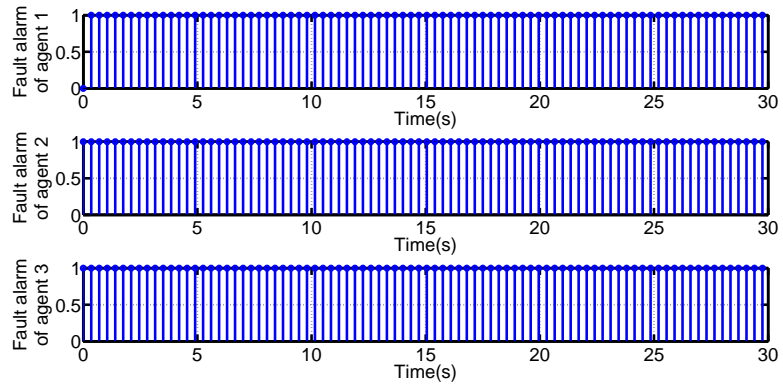


(a) Tracking error of helicopter 4

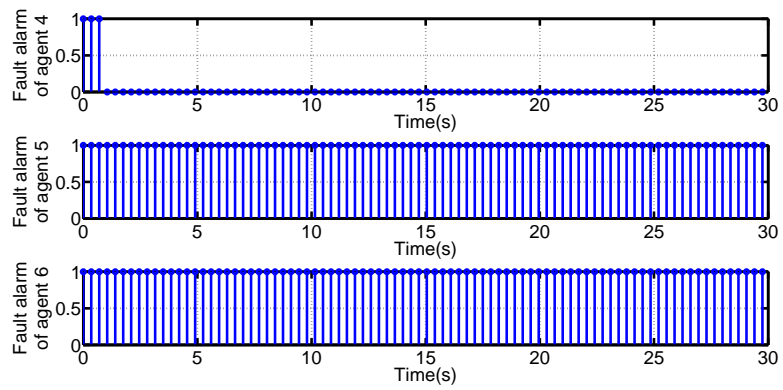


(b) Tracking errors of healthy helicopters

Fig. 4.25 Tracking errors of six helicopters

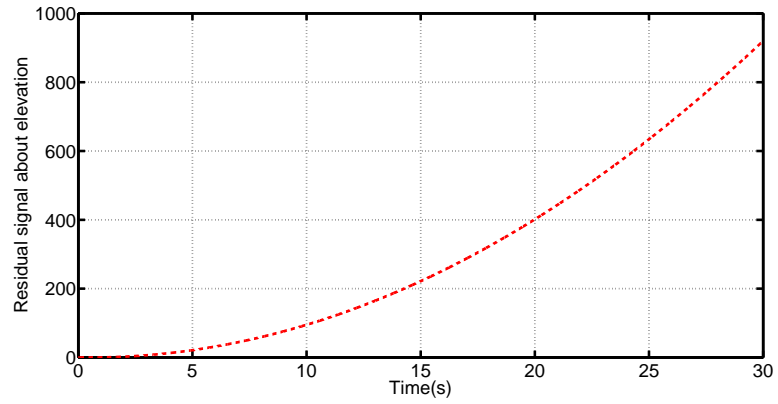


(a) Health indicators of helicopter 1, 2 and 3

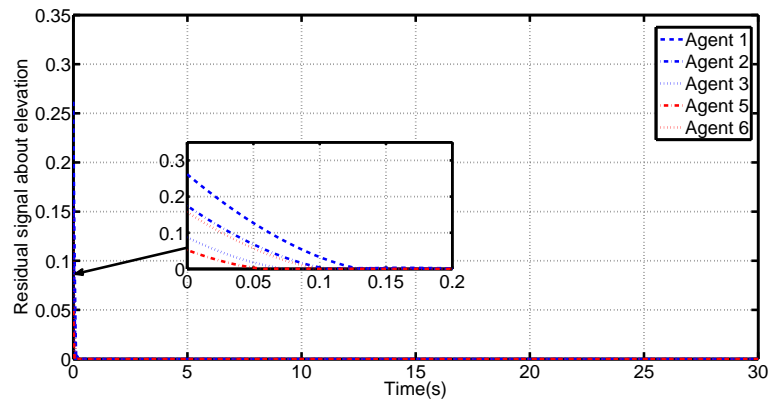


(b) Health indicators of helicopter 4, 5 and 6

Fig. 4.26 Health indicators of six helicopters

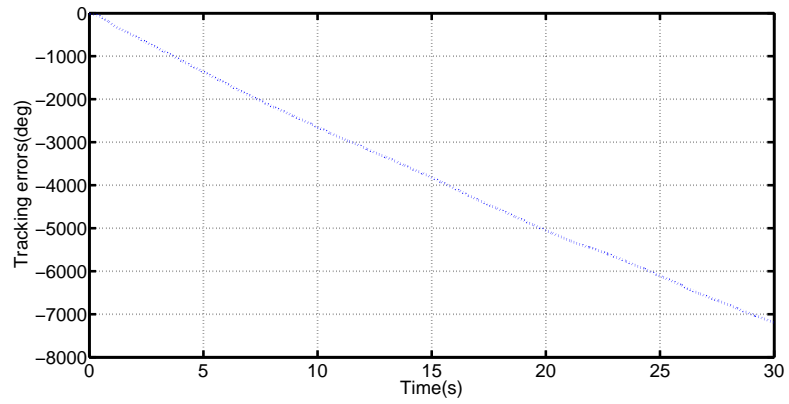


(a) Residual signal of helicopter 4

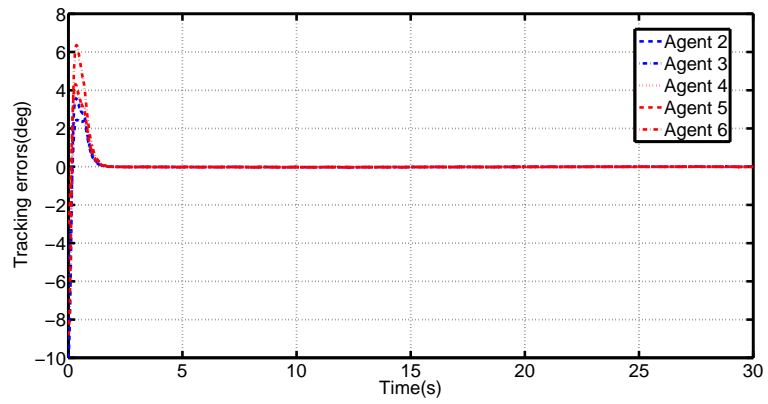


(b) Residual signals of helicopter 1, 2, 3, 5 and 6

Fig. 4.27 Residual signals with faulty helicopter 4 (actuator fault)

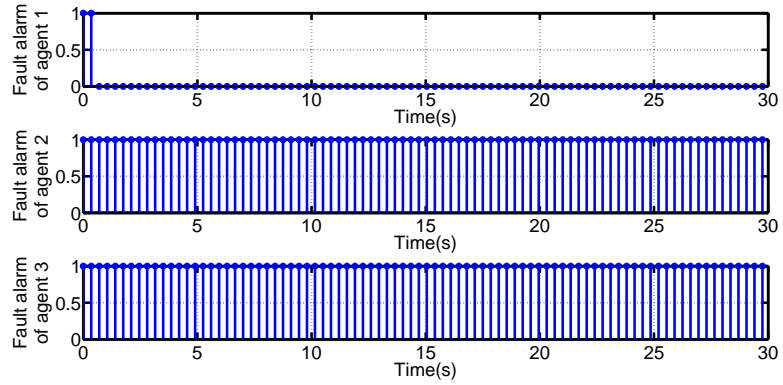


(a) Tracking error of helicopter 1

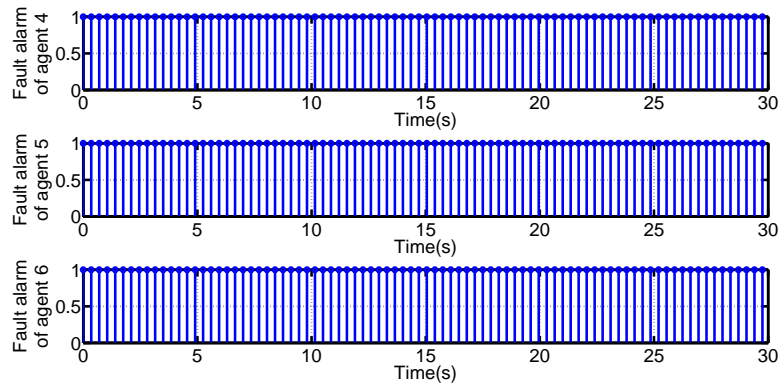


(b) Tracking errors of healthy helicopters

Fig. 4.28 Tracking errors of six helicopters

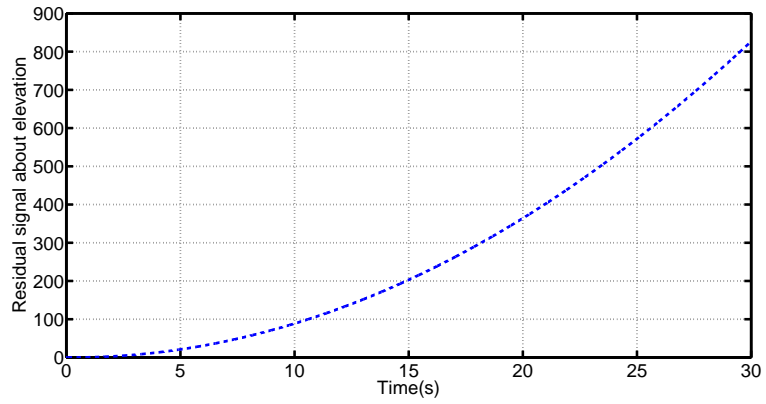


(a) Health indicators of helicopter 1, 2 and 3

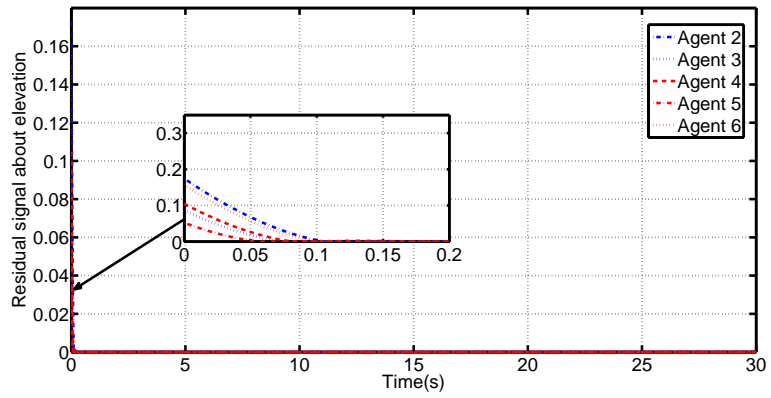


(b) Health indicators of helicopter 4, 5 and 6

Fig. 4.29 Health indicators of six helicopters

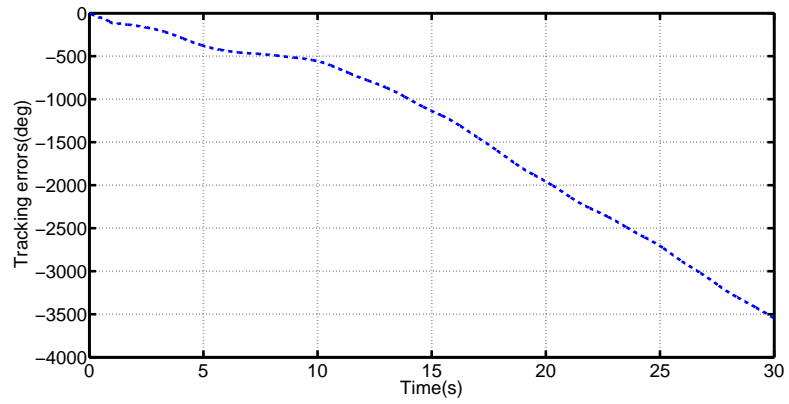


(a) Residual signal of helicopter 1

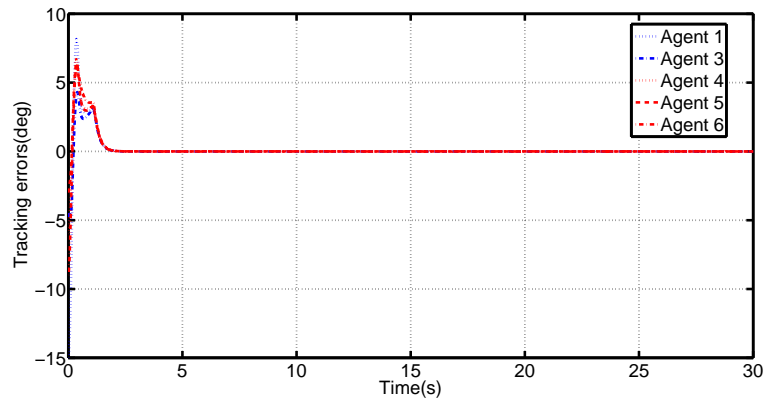


(b) Residual signals of helicopter 2, 3, 4, 5 and 6

Fig. 4.30 Residual signals with faulty helicopter 1 (sensor fault)

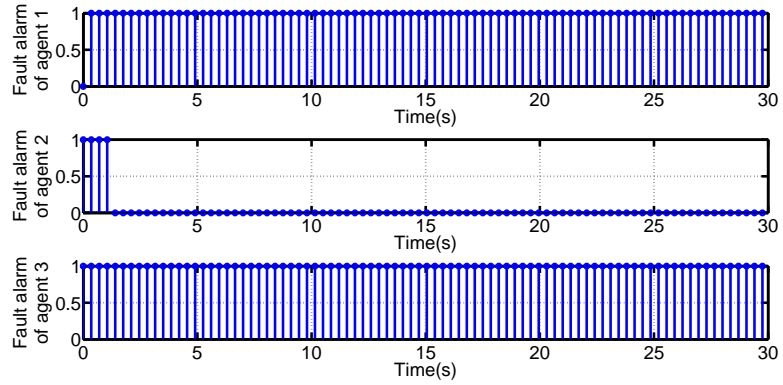


(a) Tracking error of helicopter 2

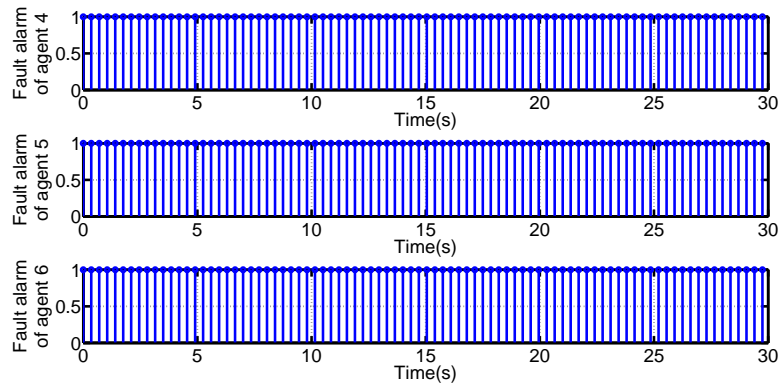


(b) Tracking errors of healthy helicopters

Fig. 4.31 Tracking errors of six helicopters

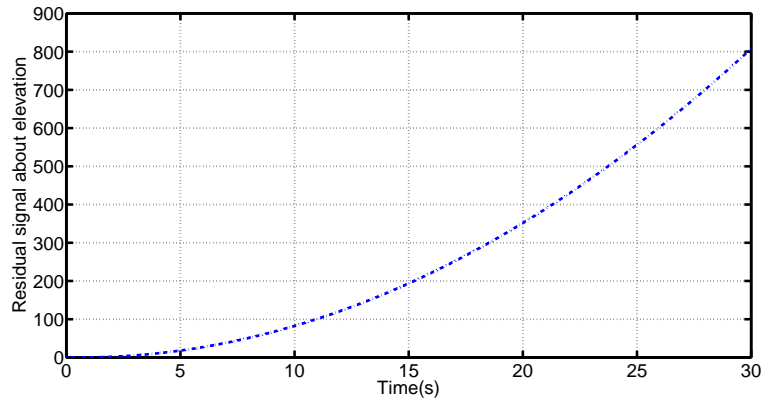


(a) Health indicators of helicopter 1, 2 and 3

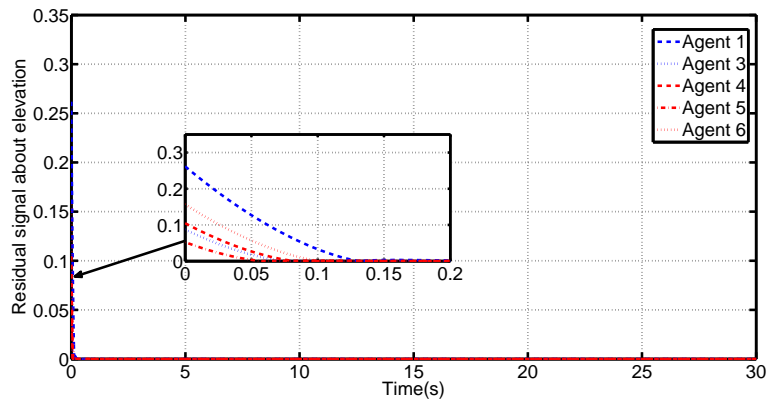


(b) Health indicators of helicopter 4, 5 and 6

Fig. 4.32 Health indicators of six helicopters

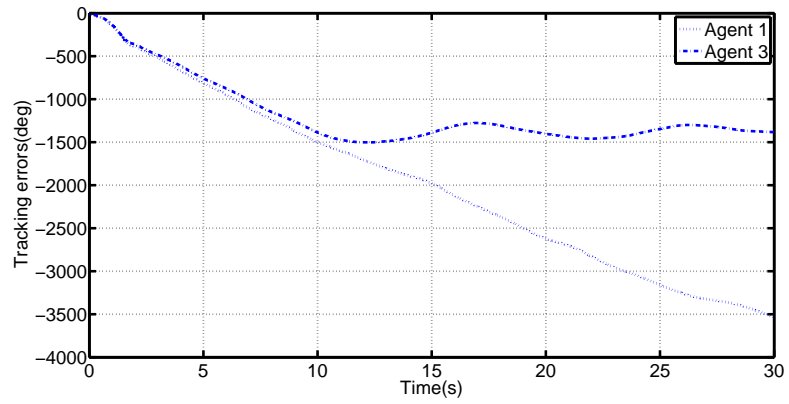


(a) Residual signal of helicopter 2

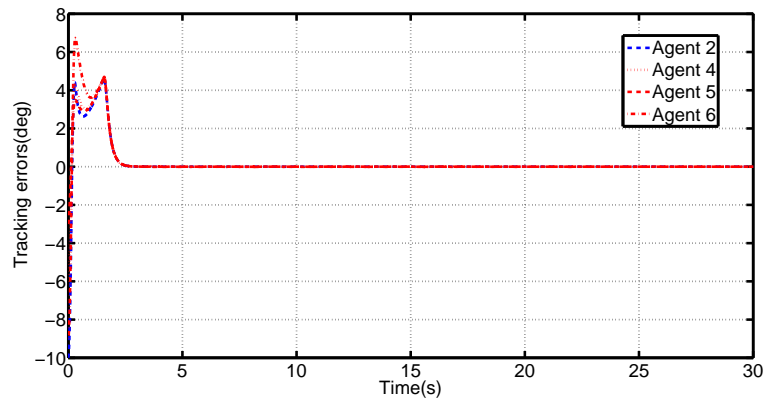


(b) Residual signals of helicopter 1, 3, 4, 5 and 6

Fig. 4.33 Residual signals with faulty helicopter 2 (sensor fault)

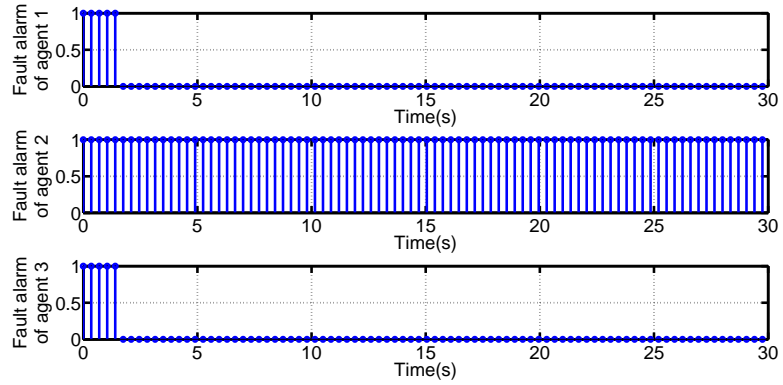


(a) Tracking errors of helicopter 1 and 3

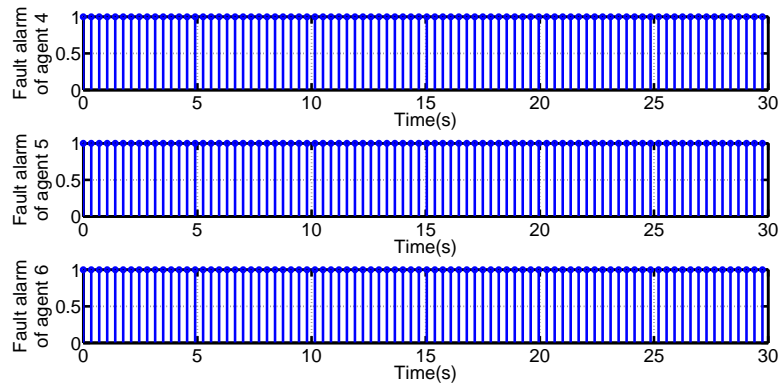


(b) Tracking errors of healthy helicopters

Fig. 4.34 Tracking errors of six helicopters

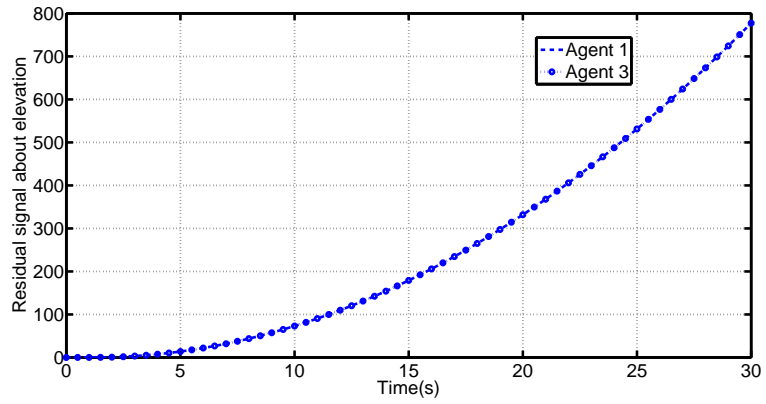


(a) Health indicators of helicopter 1, 2 and 3

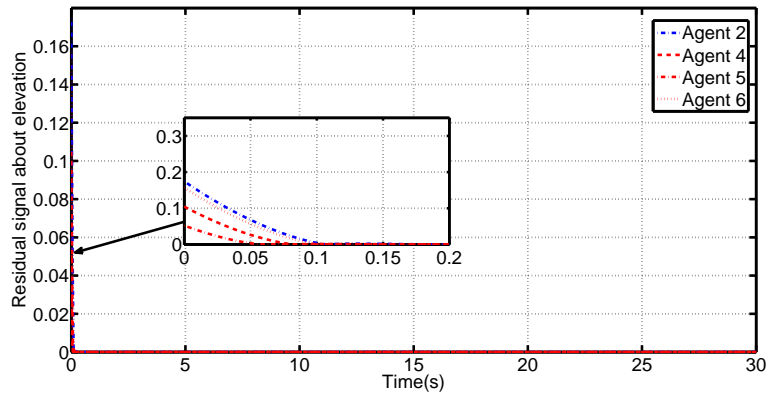


(b) Health indicators of helicopter 4, 5 and 6

Fig. 4.35 Health indicators of six helicopters

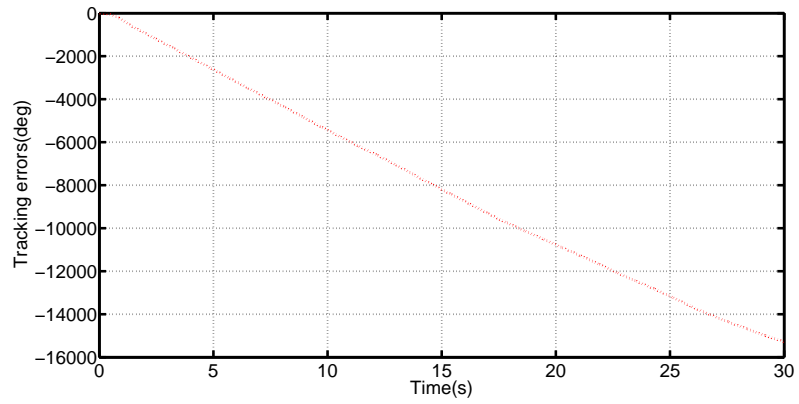


(a) Residual signals of helicopter 1 and 3

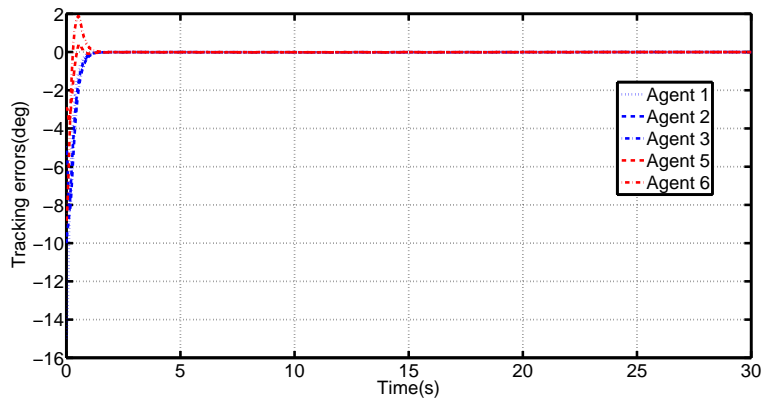


(b) Residual signals of helicopter 2, 4, 5 and 6

Fig. 4.36 Residual signals with faulty helicopter 1 and 3 (sensor fault)

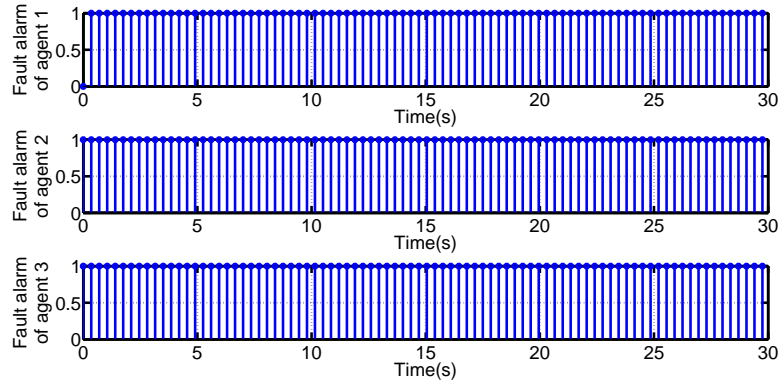


(a) Tracking errors of helicopter 4

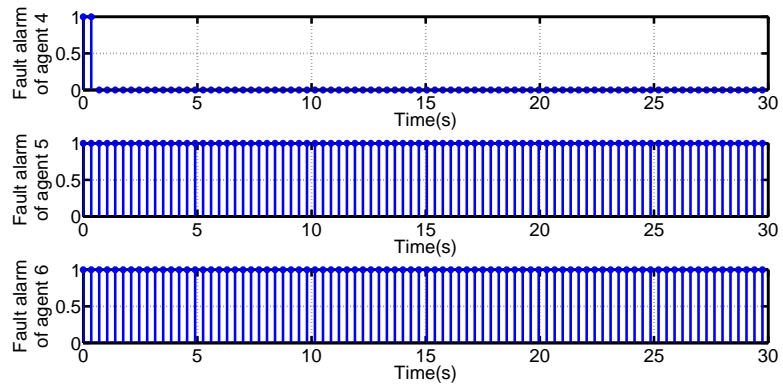


(b) Tracking errors of healthy helicopters

Fig. 4.37 Tracking errors of six helicopters

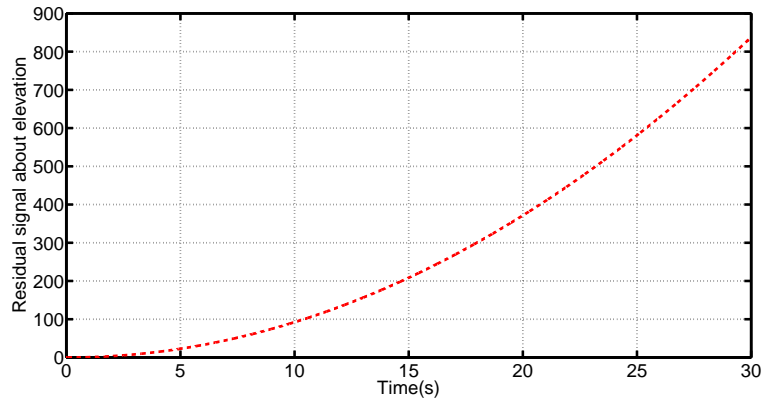


(a) Health indicators of helicopter 1, 2 and 3

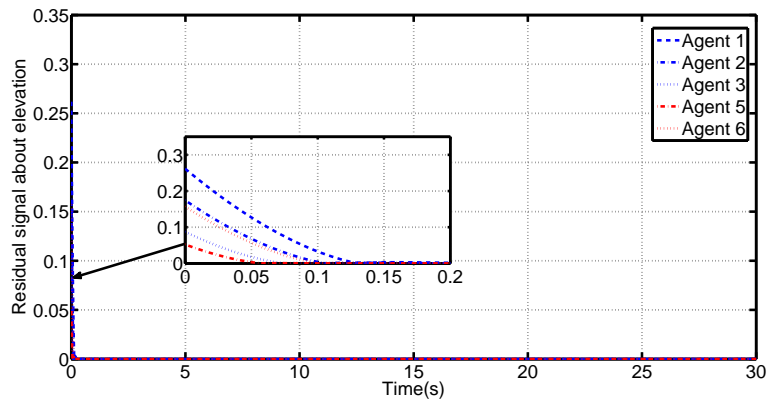


(b) Health indicators of helicopter 4, 5 and 6

Fig. 4.38 Health indicators of six helicopters



(a) Residual signal of helicopter 4



(b) Residual signals of helicopter 1, 2, 3, 5 and 6

Fig. 4.39 Residual signals with faulty helicopter 4 (sensor fault)

5 Sampled-data Synchronization Control of Networked Nonlinear Systems

In order to bridge the gap between the theoretical sampled-data controller and its application, it is quite necessary to extend the sampled-data control algorithm from linear systems to their nonlinear counterparts. Almost all the mechanical/electrical systems are fundamentally nonlinear and the linear dynamics is a rudimentary simplification. Thus, the nonlinear extension of the linear sampled-data controller naturally plays an important part in practical applications, and the Lipschitz nonlinear dynamical system will be investigated in this work. Moreover, compared to the state feedback controller in previous work, output feedback controller is more widely applicable because the system states are not directly measurable for most dynamical systems [127]. Hence, the availability of state information should not be presumed for a relatively general nonlinear system. Therefore, an observer-based output feedback controller will be presented in this chapter. Furthermore, system uncertainty is usually unavoidable in the dynamical model of

mechanical/electrical system due to various unmodeled effects. It is thus crucial to enhance the robustness of the proposed control algorithm. Consequently, an \mathcal{H}_∞ robust controller is investigated in this work to strengthen the robustness of the entire control system. Basically, compared to the previous work, this chapter presents a more generic control strategy for multi-agent systems in terms of dynamics model and controller structure. Unlike in [56, 57], the dynamics model in this work is described using Lipschitz nonlinearity and the state information is not available for the controller. As for the structure of the controller, it is more flexible to adopt the output feedback structure rather than state feedback [26, 29, 56, 96, 97, 128] and state feedback structure can be considered as a special case in output feedback structure. Meanwhile, the state observer offers a larger area of application of the proposed controller because, in certain circumstances, more state information can be estimated by the observer for further utilization.

In this chapter, the synchronization problem for a set of networked nonlinear agents is resolved with the consideration of modeling errors, system uncertainties and external disturbances. The nonlinearity of the agent dynamics is characterized by a Lipschitz nonlinear term. Since the modeling error is fairly unavoidable in practice, the multiplicative uncertainty and additive disturbance caused by potential modeling errors are essentially considered in the error dynamics and stability analysis. Motivated by the previous work [59–61, 129, 130], the stability analysis is

conducted using the time-delay technique in the appearance of discontinuous states (sampled-data measurements), and the sufficient conditions for system stability are systematically developed along the Lyapunov functional approach. Moreover, a controller and observer gain deriving method is presented on the basis of sufficient conditions. Furthermore, an iterative optimization algorithm is developed based on the proposed controller and observer gain deriving method.

The remainder of this chapter is organized as follows. In Section 5.1, the essential problem to be resolved is systematically formulated. Section 5.2 presents the controller design and stability analysis. Based on the assumptions, a feedback controller is developed with the consideration of system uncertainty and external disturbance. The Lyapunov functional approach is applied to deal with the sampled-data measurement. Meanwhile, the sufficient conditions for the stability of the networked systems are derived extensively. Moreover, a controller design method is proposed on the basis of the sufficient conditions. An iterative convex optimization algorithm is further developed to derive the feasible solutions for the controller and observer gains. In Section 5.3, four identical Chua's circuits are adopted in the simulations. With the appearance of an \mathcal{L}_2 bounded disturbance, the state synchronization is achieved when the followers are governed by the proposed controller in a distributed manner. The convergences of synchronization error and estimation error further demonstrate the effectiveness of the proposed control

algorithm.

5.1 Problem formulation

As explained above, many nonlinearities, i.e. sinusoidal or bounded x^2 terms, can be represented by the Lipschitz nonlinearity. Therefore, the Lipschitz nonlinearity is more generic compared to the Euler-Lagrange nonlinearity. Hence, the consensus seeking problem for networked Lipschitz nonlinear agents is considered in this chapter. There are k nonlinear agents operated in n -dimensional state space, and each agent is modeled by

$$\dot{\mathbf{x}}_i(t) = \mathbf{A}\mathbf{x}_i(t) + \mathbf{B}\mathbf{f}(\mathbf{x}_i, t) + \mathbf{u}_i(t_s) \quad (5.1)$$

$$\mathbf{y}_i(t) = \mathbf{C}\mathbf{x}_i(t) \quad (5.2)$$

where $\mathbf{x}_i(t) \in \mathbb{R}^n$ is the state vector of the i th agent, $\mathbf{y}_i(t) \in \mathbb{R}^w$ is the output and $\mathbf{u}_i(t_s) \in \mathbb{R}^v$ is the input, $1 \leq i \leq k$. Since only sampled-data output feedback is available for the controller, the control input $\mathbf{u}_i(t_s)$ can be updated only at discrete time instants t_s satisfying

$$0 \leq t_0 < t_1 < \cdots < t_s < \cdots$$

and $t_{s+1} - t_s \leq h$. Agent structures are characterized by the parameters $\mathbf{A} \in \mathbb{R}^{n \times n}$, $\mathbf{B} \in \mathbb{R}^{n \times n}$ and $\mathbf{C} \in \mathbb{R}^{w \times n}$. The nonlinear function $\mathbf{f} : \mathbb{R}^n \times [0, +\infty) \rightarrow \mathbb{R}^n$ satisfies

the Lipschitz condition, i.e.

$$\|\mathbf{f}(\mathbf{a}, t) - \mathbf{f}(\mathbf{b}, t)\| \leq \gamma \|\mathbf{a} - \mathbf{b}\| \quad \forall \mathbf{a}, \mathbf{b} \in \mathbb{R}^n \quad (5.3)$$

and $\gamma > 0$ is the Lipschitz constant.

The main objective of this chapter is to design a feedback controller for the networked systems, in which the dynamics of each agent are identical and expressed in Eqs. (5.1, 5.2). One of the agents is considered as a leader, while others are followers. It is assumed that each agent transmits information discretely through the underlying digital network. Other than the discontinuous information transmission, the agents can only share information locally, which implies that the leading agent's information is not available for all agents. Moreover, only output information can be shared through the network, and the inherent state information of the networked systems is not available for any agent. Since the modeling error, system uncertainty and external disturbance are considered, the proposed controller must be robust to both multiplicative and additive uncertainty and the influence caused by the additive uncertainty is expected to be minimized.

5.2 Distributed sampled-data controller design

Assumption 5.1. *The states of each agent are observable from the output.*

Assumption 5.2. *The communication topology is depicted by a digraph that con-*

tains a spanning tree. Furthermore, the leader is topologically located at the root of the spanning tree.

Since not all the states are available for the controller $\mathbf{u}_i(t_s)$, an observer-based feedback control algorithm is developed on the basis of Assumption 5.1 as follows

$$\mathbf{u}_i(t_s) = \mathbf{K}_i \left\{ \sum_{v_j \in \mathcal{N}_{\mathcal{G}}(v_i)} [\hat{\mathbf{x}}_i(t_s) - \hat{\mathbf{x}}_j(t_s)] + \mathbf{p}_i [\hat{\mathbf{x}}_i(t_s) - \mathbf{x}_0(t_s)] \right\} \quad (5.4)$$

and the observer is designed as

$$\dot{\hat{\mathbf{x}}}_i(t) = \mathbf{A}\hat{\mathbf{x}}_i(t) + \mathbf{B}\mathbf{f}(\hat{\mathbf{x}}_i, t) + \mathbf{u}_i(t_s) + \mathbf{H}_i [\mathbf{y}_i(t_s) - \hat{\mathbf{y}}_i(t_s)] \quad (5.5)$$

$$\hat{\mathbf{y}}_i(t) = \mathbf{C}\hat{\mathbf{x}}_i(t) \quad (5.6)$$

where \mathbf{p}_i equals to one if the leader's information is available to agent i , otherwise $\mathbf{p}_i = 0$, $\mathbf{K}_i \in \mathbb{R}^{n \times n}$ is the control gain, $\mathbf{H}_i \in \mathbb{R}^{n \times w}$ is the observer gain and $\hat{\mathbf{x}}_i(t)$ is the estimated state vector.

Defining the observer error vector $\tilde{\mathbf{x}}_i(t)$ and position error vector $\bar{\mathbf{x}}_i(t)$ as follows

$$\tilde{\mathbf{x}}_i(t) = \mathbf{x}_i(t) - \hat{\mathbf{x}}_i(t)$$

$$\bar{\mathbf{x}}_i(t) = \mathbf{x}_i(t) - \mathbf{x}_0(t)$$

then, substituting Eq. (5.4) into Eq. (5.1), it is obtained that

$$\begin{aligned} \dot{\mathbf{x}}_i(t) &= \mathbf{A}\mathbf{x}_i(t) + \mathbf{B}\mathbf{f}(\mathbf{x}_i, t) \\ &+ \mathbf{K}_i \left\{ \sum_{v_j \in \mathcal{N}_{\mathcal{G}}(v_i)} [\hat{\mathbf{x}}_i(t_s) - \hat{\mathbf{x}}_j(t_s)] + \mathbf{p}_i [\hat{\mathbf{x}}_i(t_s) - \mathbf{x}_0(t_s)] \right\} \end{aligned} \quad (5.7)$$

Subtracting Eq. (5.5) from Eq. (5.7), it is derived that

$$\dot{\tilde{\mathbf{x}}}_i(t) = \mathbf{A}\tilde{\mathbf{x}}_i(t) + \mathbf{B}[\mathbf{f}(\mathbf{x}_i, t) - \mathbf{f}(\hat{\mathbf{x}}_i, t)] - \mathbf{H}_i\mathbf{C}_i\tilde{\mathbf{x}}_i(t_s) \quad (5.8)$$

the following error dynamics can be derived by subtracting the leader dynamics from Eq. (5.1)

$$\begin{aligned} \dot{\tilde{\mathbf{x}}}_i(t) = & \mathbf{A}\tilde{\mathbf{x}}_i(t) + \mathbf{B}[\mathbf{f}(\mathbf{x}_i(t), t) - \mathbf{f}(\mathbf{x}_0(t), t)] \\ & + \mathbf{K}_i \left\{ \sum_{v_j \in \mathcal{N}_G(v_i)} [\hat{\mathbf{x}}_i(t_s) - \hat{\mathbf{x}}_j(t_s)] + \mathbf{p}_i [\hat{\mathbf{x}}_i(t_s) - \mathbf{x}_0(t_s)] \right\} \end{aligned} \quad (5.9)$$

Remark 5.1. *Ideally, the stability analysis should be conducted essentially based on Eqs. (5.9, 5.8). However, system uncertainty is mostly unavoidable in practice. Therefore, the expression of Eqs. (5.9, 5.8) should be revised with the consideration of mismatched modeling uncertainty. Due to the diversity of unmodeled effects, the mismatched uncertainty can be roughly modeled through various approaches [81, 88]. In this work, they are equivalently modeled as a common effect of both additive and multiplicative uncertainties. Moreover, external disturbance also exists in practical applications. Therefore, the external disturbances are also considered as a portion of the additive uncertainty that is bounded by the \mathcal{L}_2 norm. Namely, both \mathcal{L}_2 -bounded additive and 2-norm bounded multiplicative uncertainties are taken into account in this work.*

Combining the dynamics of k agents, a compact form of the error dynamics

with both additive and multiplicative uncertainties can be organized as

$$\begin{aligned}\dot{\tilde{\mathbf{x}}}(t) &= (\mathbf{I} + \boldsymbol{\Delta}_1) (\mathbf{I}_k \otimes \mathbf{A}) \tilde{\mathbf{x}}(t) + (\mathbf{I}_k \otimes \mathbf{B}) (\mathbf{I} + \boldsymbol{\Delta}_2) [\mathbf{f}(\mathbf{x}(t), t) - \mathbf{f}(\tilde{\mathbf{x}}(t), t)] \\ &\quad - \mathbf{H} [\mathbf{I}_k \otimes \mathbf{C}] \tilde{\mathbf{x}}(t_s) + \mathbf{E}_1 \boldsymbol{\omega}_1\end{aligned}\tag{5.10}$$

$$\begin{aligned}\dot{\bar{\mathbf{x}}}(t) &= (\mathbf{I} + \boldsymbol{\Delta}_3) (\mathbf{I}_k \otimes \mathbf{A}) \bar{\mathbf{x}}(t) + (\mathbf{I}_k \otimes \mathbf{B}) (\mathbf{I} + \boldsymbol{\Delta}_4) [\mathbf{f}(\mathbf{x}(t), t) - \mathbf{f}(\mathbf{x}_0(t), t)] \\ &\quad + \mathbf{K} [(\boldsymbol{\mathcal{L}} + \boldsymbol{\mathcal{D}}) \otimes \mathbf{I}_n] [\bar{\mathbf{x}}(t_s) - \tilde{\mathbf{x}}(t_s)] + \mathbf{E}_2 \boldsymbol{\omega}_2\end{aligned}\tag{5.11}$$

where $\boldsymbol{\Delta}_i, \forall i = 1, \dots, 4$ are the norm-bounded uncertainties, i.e. $\|\boldsymbol{\Delta}_i\| \leq \varepsilon_i$, and $\varepsilon_i \in \mathbb{R}^+$. $\mathbf{H} = \text{diag}\{\mathbf{H}_1, \mathbf{H}_2, \dots, \mathbf{H}_k\}$, $\mathbf{K} = \text{diag}\{\mathbf{K}_1, \mathbf{K}_2, \dots, \mathbf{K}_k\}$, $\boldsymbol{\mathcal{D}} = \text{diag}\{\mathbf{p}_1, \mathbf{p}_2, \dots, \mathbf{p}_k\}$, $\boldsymbol{\omega}_1, \boldsymbol{\omega}_2$ are \mathcal{L}_2 bounded disturbances, and the distribution of the additive uncertainty is specified by \mathbf{E}_1 and \mathbf{E}_2 .

Due to the inequality (5.3), there is

$$[\mathbf{f}(\mathbf{x}_i, t) - \mathbf{f}(\mathbf{x}_0, t)]^T [\mathbf{f}(\mathbf{x}_i, t) - \mathbf{f}(\mathbf{x}_0, t)] - \gamma^2 [\mathbf{x}_i(t) - \mathbf{x}_0(t)]^T [\mathbf{x}_i(t) - \mathbf{x}_0(t)] \leq 0\tag{5.12}$$

where $\gamma > 0$ is the Lipschitz constant.

The following lemma will be used in the stability proof.

Lemma 5.1. [131] *Let \mathcal{Y} be a symmetric matrix and \mathcal{A}, \mathcal{B} be matrices with compatible dimensions and \mathcal{F} satisfying $\mathcal{F}^T \mathcal{F} \leq \mathbf{I}$. Then, $\mathcal{Y} + \mathcal{A} \mathcal{F} \mathcal{B} + \mathcal{B}^T \mathcal{F}^T \mathcal{A}^T < 0$ holds if and only if there exists a scalar $\varepsilon > 0$ such that $\mathcal{Y} + \varepsilon \mathcal{A} \mathcal{A}^T + \varepsilon^{-1} \mathcal{B}^T \mathcal{B} < 0$.*

Theorem 5.1. *Suppose that the communication relationship of the networked non-linear agents in Eqs. (5.1, 5.2) satisfies Assumption 5.2, then the proposed sampled-*

data feedback controller in Eq. (5.4) can guarantee that the vectors of the error dynamics in Eqs. (5.10, 5.11) will converge to zero asymptotically if there exist symmetric matrices $\mathbf{Q}_i > 0$, positive constants $\alpha, \varepsilon_i, i = 1, 2, \dots, 6$, and matrices $\mathbf{N}_1, \mathbf{N}_2 \in \mathbb{R}^{4kn \times kn}$ such that

$$\begin{bmatrix} \boldsymbol{\varphi}_1 & h\boldsymbol{\psi}_1^T & h\boldsymbol{\psi}_2^T & \mathbf{M}_1 \\ \star & -h\mathbf{Q}_2^{-1} & \mathbf{0} & \mathbf{M}_2 \\ \star & \star & -h\mathbf{Q}_5^{-1} & \mathbf{M}_3 \\ \star & \star & \star & \mathbf{M}_4 \end{bmatrix} < 0 \quad (5.13)$$

and

$$\begin{bmatrix} \boldsymbol{\varphi}_1 & h\Pi_1^T \mathbf{N}_1 & h\Pi_2^T \mathbf{N}_2 & \mathbf{M}_5 \\ \star & -h\mathbf{Q}_2 & \mathbf{0} & \mathbf{0} \\ \star & \star & -h\mathbf{Q}_5 & \mathbf{0} \\ \star & \star & \star & \mathbf{M}_6 \end{bmatrix} < 0 \quad (5.14)$$

where

$$\begin{aligned} \boldsymbol{\varphi}_1 &= 2\Pi_1^T \mathbf{N}_1 \boldsymbol{\mathfrak{J}}_1 - 2\Pi_1^T \mathbf{N}_1 \boldsymbol{\mathfrak{J}}_2 + 2\Pi_2^T \mathbf{N}_2 \boldsymbol{\mathfrak{J}}_5 - 2\Pi_2^T \mathbf{N}_2 \boldsymbol{\mathfrak{J}}_6 + \beta\gamma^2 \boldsymbol{\mathfrak{J}}_1^T \boldsymbol{\mathfrak{J}}_1 - \beta \boldsymbol{\mathfrak{J}}_3^T \boldsymbol{\mathfrak{J}}_3 \\ &+ \beta\gamma^2 \boldsymbol{\mathfrak{J}}_5^T \boldsymbol{\mathfrak{J}}_5 - \beta \boldsymbol{\mathfrak{J}}_7^T \boldsymbol{\mathfrak{J}}_7 + \boldsymbol{\mathfrak{J}}_5^T (\mathbf{I}_k \otimes \mathbf{C})^T (\mathbf{I}_k \otimes \mathbf{C}) \boldsymbol{\mathfrak{J}}_5 - \alpha \boldsymbol{\mathfrak{J}}_4^T \boldsymbol{\mathfrak{J}}_4 - \alpha \boldsymbol{\mathfrak{J}}_8^T \boldsymbol{\mathfrak{J}}_8 \\ &+ 2\boldsymbol{\mathfrak{J}}_1^T \mathbf{Q}_1 \boldsymbol{\psi}_1 - \boldsymbol{\mathfrak{J}}_2^T \mathbf{Q}_3 \boldsymbol{\mathfrak{J}}_2 + 2\boldsymbol{\mathfrak{J}}_5^T \mathbf{Q}_4 \boldsymbol{\psi}_2 - \boldsymbol{\mathfrak{J}}_6^T \mathbf{Q}_6 \boldsymbol{\mathfrak{J}}_6 \end{aligned}$$

$$\boldsymbol{\mathfrak{J}}_1 = \text{diag} \{ \mathbf{I}_{kn}, \mathbf{0}_{kn}, \mathbf{0}_{kn}, \mathbf{0}_{kn}, \mathbf{0}_{kn}, \mathbf{0}_{kn}, \mathbf{0}_{kn}, \mathbf{0}_{kn} \}$$

$$\boldsymbol{\mathfrak{J}}_2 = \text{diag} \{ \mathbf{0}_{kn}, \mathbf{I}_{kn}, \mathbf{0}_{kn}, \mathbf{0}_{kn}, \mathbf{0}_{kn}, \mathbf{0}_{kn}, \mathbf{0}_{kn}, \mathbf{0}_{kn} \}$$

\vdots

$$\boldsymbol{\mathfrak{J}}_j = \text{diag} \left\{ \underbrace{\mathbf{0}_{kn}, \dots, \mathbf{0}_{kn}}_{j-1}, \mathbf{I}_{kn}, \underbrace{\mathbf{0}_{kn}, \dots, \mathbf{0}_{kn}}_{8-j} \right\}$$

\vdots

$$\boldsymbol{\mathfrak{J}}_8 = \text{diag} \{ \mathbf{0}_{kn}, \mathbf{0}_{kn}, \mathbf{0}_{kn}, \mathbf{0}_{kn}, \mathbf{0}_{kn}, \mathbf{0}_{kn}, \mathbf{0}_{kn}, \mathbf{I}_{kn} \}$$

$$\mathbf{\Pi}_1 = [\mathbf{I}_{4kn} \quad \mathbf{0}_{4kn}]$$

$$\mathbf{\Pi}_2 = [\mathbf{0}_{4kn} \quad \mathbf{I}_{4kn}]$$

$$\mathbf{M}_1 =$$

$$[\mathbf{0} \quad \sqrt{\delta_1} \boldsymbol{\psi}_{32}^T \quad \mathbf{0} \quad \sqrt{\delta_2} \boldsymbol{\psi}_{42}^T \quad \sqrt{\delta_1} \mathfrak{J}_1^T \mathbf{Q}_1 \boldsymbol{\psi}_{31} \quad \sqrt{\delta_1} \boldsymbol{\psi}_{32}^T \quad \sqrt{\delta_2} \mathfrak{J}_5^T \mathbf{Q}_4 \boldsymbol{\psi}_{41} \quad \sqrt{\delta_2} \boldsymbol{\psi}_{42}^T]$$

$$\mathbf{M}_2 = [\sqrt{\delta_1} h \boldsymbol{\psi}_{31} \quad \mathbf{0}]$$

$$\mathbf{M}_3 = [\mathbf{0} \quad \mathbf{0} \quad \sqrt{\delta_2} h \boldsymbol{\psi}_{41} \quad \mathbf{0} \quad \mathbf{0} \quad \mathbf{0} \quad \mathbf{0} \quad \mathbf{0}]$$

$$\mathbf{M}_4 = \text{diag} \{ -\varepsilon_1 \mathbf{I}, -\varepsilon_1^{-1} \mathbf{I}, -\varepsilon_2 \mathbf{I}, -\varepsilon_2^{-1} \mathbf{I}, -\varepsilon_3 \mathbf{I}, -\varepsilon_3^{-1} \mathbf{I}, -\varepsilon_4 \mathbf{I}, -\varepsilon_4^{-1} \mathbf{I} \}$$

$$\mathbf{M}_5 = [\sqrt{\delta_1} \mathfrak{J}_1^T \mathbf{Q}_1 \boldsymbol{\psi}_{31} \quad \sqrt{\delta_1} \boldsymbol{\psi}_{32}^T \quad \sqrt{\delta_2} \mathfrak{J}_5^T \mathbf{Q}_4 \boldsymbol{\psi}_{41} \quad \sqrt{\delta_2} \boldsymbol{\psi}_{42}^T]$$

$$\mathbf{M}_6 = \text{diag} \{ -\varepsilon_5 \mathbf{I}, -\varepsilon_5^{-1} \mathbf{I}, -\varepsilon_6 \mathbf{I}, -\varepsilon_6^{-1} \mathbf{I} \}$$

$$\boldsymbol{\psi}_1 = [\mathbf{I}_k \otimes \mathbf{A} \quad -\mathbf{H} (\mathbf{I}_k \otimes \mathbf{C}) \quad \mathbf{I}_k \otimes \mathbf{B} \quad \mathbf{E}_1 \quad \mathbf{0} \quad \mathbf{0} \quad \mathbf{0} \quad \mathbf{0}]$$

$$\boldsymbol{\psi}_2 = [\mathbf{0} \quad -\mathbf{K} [(\boldsymbol{\mathcal{L}} + \boldsymbol{\mathcal{D}}) \otimes \mathbf{I}_n] \quad \mathbf{0} \quad \mathbf{0} \quad \mathbf{I}_k \otimes \mathbf{A} \quad \mathbf{K} [(\boldsymbol{\mathcal{L}} + \boldsymbol{\mathcal{D}}) \otimes \mathbf{I}_n] \quad \mathbf{I}_k \otimes \mathbf{B} \quad \mathbf{E}_2]$$

$$\boldsymbol{\psi}_{31} = [\mathbf{I}_{kn} \quad \mathbf{I}_k \otimes \mathbf{B}] \quad \boldsymbol{\psi}_{41} = [\mathbf{I}_{kn} \quad \mathbf{I}_k \otimes \mathbf{B}]$$

$$\boldsymbol{\psi}_{32} = \begin{bmatrix} (\mathbf{I}_k \otimes \mathbf{A}) \mathfrak{J}_1 \\ \mathfrak{J}_3 \end{bmatrix} \quad \boldsymbol{\psi}_{42} = \begin{bmatrix} (\mathbf{I}_k \otimes \mathbf{A}) \mathfrak{J}_5 \\ \mathfrak{J}_7 \end{bmatrix}$$

$$\begin{bmatrix} \Delta_1 & \mathbf{0} \\ \mathbf{0} & \Delta_2 \end{bmatrix}^T \begin{bmatrix} \Delta_1 & \mathbf{0} \\ \mathbf{0} & \Delta_2 \end{bmatrix} \leq \delta_1^2 \quad \begin{bmatrix} \Delta_3 & \mathbf{0} \\ \mathbf{0} & \Delta_4 \end{bmatrix}^T \begin{bmatrix} \Delta_3 & \mathbf{0} \\ \mathbf{0} & \Delta_4 \end{bmatrix} \leq \delta_2^2$$

Proof. Defining the following Lyapunov functional:

$$\begin{aligned} V = & \tilde{\mathbf{x}}^T(t) \mathbf{Q}_1 \tilde{\mathbf{x}}(t) + [h - d(t)] \int_{t-d(t)}^t \dot{\tilde{\mathbf{x}}}^T(\tau) \mathbf{Q}_2 \dot{\tilde{\mathbf{x}}}(\tau) d\tau \\ & + [h - d(t)] \tilde{\mathbf{x}}^T(t_s) \mathbf{Q}_3 \tilde{\mathbf{x}}(t_s) + \bar{\mathbf{x}}^T(t) \mathbf{Q}_4 \bar{\mathbf{x}}(t) \\ & + [h - d(t)] \int_{t-d(t)}^t \dot{\bar{\mathbf{x}}}^T(\tau) \mathbf{Q}_5 \dot{\bar{\mathbf{x}}}(\tau) d\tau + [h - d(t)] \bar{\mathbf{x}}^T(t_s) \mathbf{Q}_6 \bar{\mathbf{x}}(t_s) \end{aligned} \quad (5.15)$$

and

$$\begin{aligned}
\dot{V} = & 2\tilde{\mathbf{x}}^T(t)\mathbf{Q}_1\dot{\tilde{\mathbf{x}}}(t) + [h - d(t)]\dot{\tilde{\mathbf{x}}}^T(t)\mathbf{Q}_2\dot{\tilde{\mathbf{x}}}(t) - \int_{t-d(t)}^t \dot{\tilde{\mathbf{x}}}^T(\tau)\mathbf{Q}_2\dot{\tilde{\mathbf{x}}}(\tau)d\tau \\
& - \tilde{\mathbf{x}}^T(t_s)\mathbf{Q}_3\tilde{\mathbf{x}}(t_s) + 2\bar{\mathbf{x}}^T(t)\mathbf{Q}_4\dot{\bar{\mathbf{x}}}(t) + [h - d(t)]\dot{\bar{\mathbf{x}}}^T(t)\mathbf{Q}_5\dot{\bar{\mathbf{x}}}(t) \\
& - \int_{t-d(t)}^t \dot{\bar{\mathbf{x}}}^T(\tau)\mathbf{Q}_5\dot{\bar{\mathbf{x}}}(\tau)d\tau - \bar{\mathbf{x}}^T(t_s)\mathbf{Q}_6\bar{\mathbf{x}}(t_s)
\end{aligned} \tag{5.16}$$

Incorporating the free weight matrices $\mathbf{N}_1, \mathbf{N}_2$, the following equations can be derived using the Newton-Leibniz formula

$$2\xi_1^T\mathbf{N}_1\tilde{\mathbf{x}}(t) - 2\xi_1^T\mathbf{N}_1\tilde{\mathbf{x}}(t_s) - \int_{t_s}^t 2\xi_1^T\mathbf{N}_1\dot{\tilde{\mathbf{x}}}(\tau)d\tau = 0 \tag{5.17}$$

$$2\xi_2^T\mathbf{N}_2\bar{\mathbf{x}}(t) - 2\xi_2^T\mathbf{N}_2\bar{\mathbf{x}}(t_s) - \int_{t_s}^t 2\xi_2^T\mathbf{N}_2\dot{\bar{\mathbf{x}}}(\tau)d\tau = 0 \tag{5.18}$$

where $\xi_1 = [\tilde{\mathbf{x}}^T(t) \quad \tilde{\mathbf{x}}^T(t_s) \quad [\mathbf{f}(\mathbf{x}, t) - \mathbf{f}(\hat{\mathbf{x}}, t)]^T \quad \boldsymbol{\omega}_1^T]^T$ and

$\xi_2 = [\bar{\mathbf{x}}^T(t) \quad \bar{\mathbf{x}}^T(t_s) \quad [\mathbf{f}(\mathbf{x}, t) - \mathbf{f}(\mathbf{x}_0, t)]^T \quad \boldsymbol{\omega}_2^T]^T$. Specifically, the values of weight matrices $\mathbf{N}_1, \mathbf{N}_2$ are not explicitly constrained by the system dynamics or communication structure, and the inclusion of them will render more flexibility for the entire control system.

Substituting Eq. (5.17) and Eq. (5.18) into Eq. (5.16), the following formula can be derived

$$\begin{aligned}
& \dot{V} + \bar{\mathbf{y}}^T\bar{\mathbf{y}} - \alpha\boldsymbol{\omega}^T\boldsymbol{\omega} \\
\leq & 2\tilde{\mathbf{x}}^T(t)\mathbf{Q}_1\dot{\tilde{\mathbf{x}}}(t) + [h - d(t)]\dot{\tilde{\mathbf{x}}}^T(t)\mathbf{Q}_2\dot{\tilde{\mathbf{x}}}(t) + 2\xi_1^T\mathbf{N}_1\tilde{\mathbf{x}}(t) - 2\xi_1^T\mathbf{N}_1\tilde{\mathbf{x}}(t_s) \\
& - \tilde{\mathbf{x}}^T(t_s)\mathbf{Q}_3\tilde{\mathbf{x}}(t_s) + 2\bar{\mathbf{x}}^T(t)\mathbf{Q}_4\dot{\bar{\mathbf{x}}}(t) + [h - d(t)]\dot{\bar{\mathbf{x}}}^T(t)\mathbf{Q}_5\dot{\bar{\mathbf{x}}}(t) - \bar{\mathbf{x}}^T(t_s)\mathbf{Q}_6\bar{\mathbf{x}}(t_s)
\end{aligned}$$

$$\begin{aligned}
& +2\xi_2^T \mathbf{N}_2 \bar{\mathbf{x}}(t) - 2\xi_2^T \mathbf{N}_2 \bar{\mathbf{x}}(t_s) + \mathfrak{J}_5^T (\mathbf{I}_k \otimes \mathbf{C})^T (\mathbf{I}_k \otimes \mathbf{C}) \mathfrak{J}_5 - \alpha \boldsymbol{\omega}^T \boldsymbol{\omega} \\
& +d(t) \xi_1^T \mathbf{N}_1 \mathbf{Q}_2^{-1} \mathbf{N}_1^T \xi_1 + d(t) \xi_2^T \mathbf{N}_2 \mathbf{Q}_5^{-1} \mathbf{N}_2^T \xi_2 \\
& +\beta \gamma^2 \tilde{\mathbf{x}}^T \tilde{\mathbf{x}} - \beta [\mathbf{f}(\mathbf{x}(t), t) - \mathbf{f}(\hat{\mathbf{x}}(t), t)]^T [\mathbf{f}(\mathbf{x}(t), t) - \mathbf{f}(\hat{\mathbf{x}}(t), t)] \\
& +\beta \gamma^2 \bar{\mathbf{x}}^T \bar{\mathbf{x}} - \beta [\mathbf{f}(\mathbf{x}(t), t) - \mathbf{f}(\mathbf{x}_0(t), t)]^T [\mathbf{f}(\mathbf{x}(t), t) - \mathbf{f}(\bar{\mathbf{x}}_0(t), t)] \\
& - \int_{t-d(t)}^t [\mathbf{N}_1^T \xi_1 + \mathbf{Q}_2 \dot{\tilde{\mathbf{x}}}(\tau)]^T \mathbf{Q}_2^{-1} [\mathbf{N}_1^T \xi_1 + \mathbf{Q}_2 \dot{\tilde{\mathbf{x}}}(\tau)] d\tau \\
& - \int_{t-d(t)}^t [\mathbf{N}_2^T \xi_2 + \mathbf{Q}_5 \dot{\tilde{\mathbf{x}}}(\tau)]^T \mathbf{Q}_5^{-1} [\mathbf{N}_2^T \xi_2 + \mathbf{Q}_5 \dot{\tilde{\mathbf{x}}}(\tau)] d\tau \\
= & 2\tilde{\mathbf{x}}^T(t) \mathbf{Q}_1 (\boldsymbol{\psi}_1 + \boldsymbol{\psi}_{31} \Delta_a \boldsymbol{\psi}_{32}) \boldsymbol{\xi} + 2\bar{\mathbf{x}}^T(t) \mathbf{Q}_4 (\boldsymbol{\psi}_2 + \boldsymbol{\psi}_{41} \Delta_a \boldsymbol{\psi}_{42}) \boldsymbol{\xi} \\
& + [h - d(t)] (\boldsymbol{\psi}_1 \boldsymbol{\xi} + \boldsymbol{\psi}_{31} \Delta_a \boldsymbol{\psi}_{32} \boldsymbol{\xi})^T \mathbf{Q}_2 (\boldsymbol{\psi}_1 + \boldsymbol{\psi}_{31} \Delta_a \boldsymbol{\psi}_{32}) \boldsymbol{\xi} \\
& + 2\xi_1^T \mathbf{N}_1 \tilde{\mathbf{x}}(t) - 2\xi_1^T \mathbf{N}_1 \tilde{\mathbf{x}}(t_s) - \tilde{\mathbf{x}}^T(t_s) \mathbf{Q}_3 \tilde{\mathbf{x}}(t_s) \\
& + [h - d(t)] (\boldsymbol{\psi}_2 \boldsymbol{\xi} + \boldsymbol{\psi}_{41} \Delta_a \boldsymbol{\psi}_{42} \boldsymbol{\xi})^T \mathbf{Q}_5 (\boldsymbol{\psi}_2 + \boldsymbol{\psi}_{41} \Delta_a \boldsymbol{\psi}_{42}) \boldsymbol{\xi} - \bar{\mathbf{x}}^T(t_s) \mathbf{Q}_6 \bar{\mathbf{x}}(t_s) \\
& + 2\xi_2^T \mathbf{N}_2 \bar{\mathbf{x}}(t) - 2\xi_2^T \mathbf{N}_2 \bar{\mathbf{x}}(t_s) + \mathfrak{J}_5^T (\mathbf{I}_k \otimes \mathbf{C})^T (\mathbf{I}_k \otimes \mathbf{C}) \mathfrak{J}_5 - \alpha \boldsymbol{\omega}^T \boldsymbol{\omega} \\
& +d(t) \xi_1^T \mathbf{N}_1 \mathbf{Q}_2^{-1} \mathbf{N}_1^T \xi_1 + d(t) \xi_2^T \mathbf{N}_2 \mathbf{Q}_5^{-1} \mathbf{N}_2^T \xi_2 \\
& +\beta \gamma^2 \tilde{\mathbf{x}}^T \tilde{\mathbf{x}} - \beta [\mathbf{f}(\mathbf{x}(t), t) - \mathbf{f}(\hat{\mathbf{x}}(t), t)]^T [\mathbf{f}(\mathbf{x}(t), t) - \mathbf{f}(\hat{\mathbf{x}}(t), t)] \\
& +\beta \gamma^2 \bar{\mathbf{x}}^T \bar{\mathbf{x}} - \beta [\mathbf{f}(\mathbf{x}(t), t) - \mathbf{f}(\mathbf{x}_0(t), t)]^T [\mathbf{f}(\mathbf{x}(t), t) - \mathbf{f}(\bar{\mathbf{x}}_0(t), t)] \\
& - \int_{t-d(t)}^t [\mathbf{N}_1^T \xi_1 + \mathbf{Q}_2 \dot{\tilde{\mathbf{x}}}(\tau)]^T \mathbf{Q}_2^{-1} [\mathbf{N}_1^T \xi_1 + \mathbf{Q}_2 \dot{\tilde{\mathbf{x}}}(\tau)] d\tau \\
& - \int_{t-d(t)}^t [\mathbf{N}_2^T \xi_2 + \mathbf{Q}_5 \dot{\tilde{\mathbf{x}}}(\tau)]^T \mathbf{Q}_5^{-1} [\mathbf{N}_2^T \xi_2 + \mathbf{Q}_5 \dot{\tilde{\mathbf{x}}}(\tau)] d\tau \tag{5.19}
\end{aligned}$$

where β is an arbitrary positive constant, and

$$\begin{aligned}\bar{\mathbf{y}} &= (\mathbf{I}_k \otimes \mathbf{C}) \bar{\mathbf{x}} \\ \boldsymbol{\varphi}_\Delta &= 2\mathfrak{J}_1^T \mathbf{Q}_1 \boldsymbol{\psi}_{31} \Delta_a \boldsymbol{\psi}_{32} + 2\mathfrak{J}_5^T \mathbf{Q}_4 \boldsymbol{\psi}_{41} \Delta_b \boldsymbol{\psi}_{42} \\ \Delta_a &= \begin{bmatrix} \Delta_1 & \mathbf{0} \\ \mathbf{0} & \Delta_2 \end{bmatrix}, \Delta_b = \begin{bmatrix} \Delta_3 & \mathbf{0} \\ \mathbf{0} & \Delta_4 \end{bmatrix} \\ \boldsymbol{\xi} &= \begin{bmatrix} \boldsymbol{\xi}_1 \\ \boldsymbol{\xi}_2 \end{bmatrix}, \boldsymbol{\omega} = \begin{bmatrix} \boldsymbol{\omega}_1 \\ \boldsymbol{\omega}_2 \end{bmatrix}\end{aligned}$$

It is noticed that Eq. (5.19) is a linear function of $d(t)$, thus inequality (5.20) is equivalent to inequalities (5.21) and (5.22)

$$\dot{V} + \bar{\mathbf{y}}^T \bar{\mathbf{y}} - \alpha \boldsymbol{\omega}^T \boldsymbol{\omega} < 0 \quad (5.20)$$

$$\begin{bmatrix} \boldsymbol{\varphi}_1 & h\boldsymbol{\psi}_1^T & h\boldsymbol{\psi}_2^T \\ \star & -h\mathbf{Q}_2^{-1} & \mathbf{0} \\ \star & \star & -h\mathbf{Q}_5^{-1} \end{bmatrix} + \begin{bmatrix} \boldsymbol{\varphi}_\Delta & h\boldsymbol{\psi}_{32}^T \Delta_a^T \boldsymbol{\psi}_{31}^T & h\boldsymbol{\psi}_{42}^T \Delta_b^T \boldsymbol{\psi}_{41}^T \\ \star & \mathbf{0} & \mathbf{0} \\ \star & \star & \mathbf{0} \end{bmatrix} < 0 \quad (5.21)$$

$$\begin{bmatrix} \boldsymbol{\varphi}_1 & h\boldsymbol{\Pi}_1^T \mathbf{N}_1 & h\boldsymbol{\Pi}_2^T \mathbf{N}_2 \\ \star & -h\mathbf{Q}_2 & \mathbf{0} \\ \star & \star & -h\mathbf{Q}_5 \end{bmatrix} + \begin{bmatrix} \boldsymbol{\varphi}_\Delta & \mathbf{0} & \mathbf{0} \\ \star & \mathbf{0} & \mathbf{0} \\ \star & \star & \mathbf{0} \end{bmatrix} < 0 \quad (5.22)$$

Utilizing the Schur complement [88, 132] and Lemma 5.1, inequality (5.13) can be derived from inequality (5.21) when $d(t) = 0$. Similarly, if $d(t) = h$, inequality (5.14) can be derived on the basis of inequality (5.22). Therefore, inequality (5.20) is true if inequalities (5.13) and (5.14) are satisfied. Furthermore, inequality (5.20) implies that

$$\sqrt{\int_{t_0}^{\infty} \bar{\mathbf{y}}^T(\tau) \bar{\mathbf{y}}(\tau) d\tau} < \sqrt{\alpha} \sqrt{\int_{t_0}^{\infty} \boldsymbol{\omega}^T(\tau) \boldsymbol{\omega}(\tau) d\tau} \quad (5.23)$$

which is derived by integrating both sides of inequality (5.20) and then performing

the following manipulations with zero initial condition

$$\begin{aligned}
V(\infty) - V(t_0) + \int_{t_0}^{\infty} \bar{\mathbf{y}}^T \bar{\mathbf{y}} - \alpha \int_{t_0}^{\infty} \boldsymbol{\omega}^T \boldsymbol{\omega} &< 0 \\
\int_{t_0}^{\infty} \bar{\mathbf{y}}^T \bar{\mathbf{y}} &< \alpha \int_{t_0}^{\infty} \boldsymbol{\omega}^T \boldsymbol{\omega} \\
\sqrt{\int_{t_0}^{\infty} \bar{\mathbf{y}}^T(\tau) \bar{\mathbf{y}}(\tau) d\tau} &< \sqrt{\alpha} \sqrt{\int_{t_0}^{\infty} \boldsymbol{\omega}^T(\tau) \boldsymbol{\omega}(\tau) d\tau}
\end{aligned}$$

According to \mathcal{H}_∞ robust control theory, inequality (5.23) implies that the controller in Eq. (5.4) is robust to \mathcal{L}_2 bounded disturbance $\boldsymbol{\omega}$ and the worst case effect of $\boldsymbol{\omega}$ is minimized when α achieves the minimum feasible value. \square

Inequalities (5.13, 5.14) are the sufficient conditions for the synchronization of systems in Eqs. (5.1, 5.2) under the controller in Eq. (5.4). Namely, if the candidates \mathbf{K}_i and \mathbf{H}_i are available, the inequalities in Theorem 5.1 can be utilized as the criteria for the stability of the closed-loop networked system. However, it is most likely in practice that the parameters of a controller are unavailable, and they are expected to be derived in the first place. Besides, the main purpose of this work is to present a systematic methodology for the derivation of the parameters in controller (5.4). Consequently, the following theorem is further developed.

Theorem 5.2. *Suppose that the communication topology of the networked systems satisfies Assumption 5.2, then the feedback gain \mathbf{K}_i of the controller in Eq. (5.4) and gain \mathbf{H}_i of the observer in Eqs. (5.5, 5.6) have feasible solutions if there exist symmetric matrices $\mathbf{R}_m > 0$, $\mathbf{Q}_r > 0$, positive constants α , ε_r , $r = 1, 2, \dots, 6$, and*

matrices $\mathbf{N}_m \in \mathbb{R}^{4kn \times kn}$ such that

$$\begin{bmatrix} \varphi_1 & h\bar{\psi}_1^T & h\bar{\psi}_2^T & \mathbf{M}_1 \\ \star & -h\mathbf{R}_1 & \mathbf{0} & \mathbf{M}_2 \\ \star & \star & -h\mathbf{R}_2 & \mathbf{M}_3 \\ \star & \star & \star & \mathbf{M}_4 \end{bmatrix} < 0 \quad (5.24)$$

$$\begin{bmatrix} \varphi_1 & h\Pi_1^T \mathbf{N}_1 & h\Pi_2^T \mathbf{N}_2 & \mathbf{M}_5 \\ \star & -h\mathbf{Q}_2 & \mathbf{0} & \mathbf{0} \\ \star & \star & -h\mathbf{Q}_5 & \mathbf{0} \\ \star & \star & \star & \mathbf{M}_6 \end{bmatrix} < 0 \quad (5.25)$$

$$\begin{bmatrix} -\tilde{\mathbf{Q}}_2 & \tilde{\mathbf{Q}}_1 \\ \star & -\tilde{\mathbf{R}}_1 \end{bmatrix} < 0 \quad (5.26)$$

$$\begin{bmatrix} -\tilde{\mathbf{Q}}_5 & \tilde{\mathbf{Q}}_4 \\ \star & -\tilde{\mathbf{R}}_2 \end{bmatrix} < 0 \quad (5.27)$$

where

$$\mathbf{M}_1 =$$

$$\begin{bmatrix} \mathbf{0} & \sqrt{\delta_1} \boldsymbol{\psi}_{32}^T & \mathbf{0} & \sqrt{\delta_2} \boldsymbol{\psi}_{42}^T & \sqrt{\delta_1} \boldsymbol{\mathcal{J}}_1^T \bar{\boldsymbol{\psi}}_{31} & \sqrt{\delta_1} \boldsymbol{\psi}_{32}^T & \sqrt{\delta_2} \boldsymbol{\mathcal{J}}_5^T \bar{\boldsymbol{\psi}}_{41} & \sqrt{\delta_2} \boldsymbol{\psi}_{42}^T \end{bmatrix}$$

$$\mathbf{M}_2 = \begin{bmatrix} \sqrt{\delta_1} h \bar{\boldsymbol{\psi}}_{31} & \mathbf{0} \end{bmatrix}$$

$$\mathbf{M}_3 = \begin{bmatrix} \mathbf{0} & \mathbf{0} & \sqrt{\delta_2} h \bar{\boldsymbol{\psi}}_{41} & \mathbf{0} & \mathbf{0} & \mathbf{0} & \mathbf{0} & \mathbf{0} \end{bmatrix}$$

$$\mathbf{M}_4 = \text{diag}\{-\varepsilon_1 \mathbf{I}, -\tilde{\varepsilon}_1 \mathbf{I}, -\varepsilon_2 \mathbf{I}, -\tilde{\varepsilon}_2 \mathbf{I}, -\varepsilon_3 \mathbf{I}, -\tilde{\varepsilon}_3 \mathbf{I}, -\varepsilon_4 \mathbf{I}, -\tilde{\varepsilon}_4 \mathbf{I}\}$$

$$\mathbf{M}_5 = \begin{bmatrix} \sqrt{\delta_1} \boldsymbol{\mathcal{J}}_1^T \bar{\boldsymbol{\psi}}_{31} & \sqrt{\delta_1} \boldsymbol{\psi}_{32}^T & \sqrt{\delta_2} \boldsymbol{\mathcal{J}}_5^T \bar{\boldsymbol{\psi}}_{41} & \sqrt{\delta_2} \boldsymbol{\psi}_{42}^T \end{bmatrix}$$

$$\mathbf{M}_6 = \text{diag}\{-\varepsilon_5 \mathbf{I}, -\tilde{\varepsilon}_5 \mathbf{I}, -\varepsilon_6 \mathbf{I}, -\tilde{\varepsilon}_6 \mathbf{I}\}$$

$$\bar{\boldsymbol{\psi}}_1 = \begin{bmatrix} \mathbf{Q}_1 (\mathbf{I}_k \otimes \mathbf{A}) & -\bar{\mathbf{H}} (\mathbf{I}_k \otimes \mathbf{C}) & \mathbf{Q}_1 (\mathbf{I}_k \otimes \mathbf{B}) & \mathbf{Q}_1 \mathbf{E}_1 & \mathbf{0} & \mathbf{0} & \mathbf{0} & \mathbf{0} \end{bmatrix}$$

$$\bar{\boldsymbol{\psi}}_2 = \begin{bmatrix} \mathbf{0} & -\bar{\mathbf{K}} [(\boldsymbol{\mathcal{L}} + \boldsymbol{\mathcal{D}}) \otimes \mathbf{I}_n] & \mathbf{0} & \mathbf{0} & \mathbf{Q}_4 (\mathbf{I}_k \otimes \mathbf{A}) & \bar{\mathbf{K}} [(\boldsymbol{\mathcal{L}} + \boldsymbol{\mathcal{D}}) \otimes \mathbf{I}_n] \end{bmatrix}$$

$$\begin{bmatrix} \mathbf{Q}_4 (\mathbf{I}_k \otimes \mathbf{B}) & \mathbf{Q}_4 \mathbf{E}_2 \end{bmatrix}$$

$$\bar{\mathbf{K}} = \mathbf{Q}_4 \mathbf{K}, \bar{\boldsymbol{\psi}}_{31} = \mathbf{Q}_1 \boldsymbol{\psi}_{31}, \mathbf{K} = \text{diag} \{ \mathbf{K}_1, \mathbf{K}_2, \dots, \mathbf{K}_k \}$$

$$\bar{\mathbf{H}} = \mathbf{Q}_1 \mathbf{H}, \bar{\boldsymbol{\psi}}_{41} = \mathbf{Q}_4 \boldsymbol{\psi}_{41}, \mathbf{H} = \text{diag} \{ \mathbf{H}_1, \mathbf{H}_2, \dots, \mathbf{H}_k \}$$

$$\tilde{\mathbf{Q}}_l = \mathbf{Q}_l^{-1}, \tilde{\mathbf{R}}_m = \mathbf{R}_m^{-1}, \tilde{\varepsilon}_r = \varepsilon_r^{-1}$$

$$l = 1, 2, 4, 5, \text{ and } m = 1, 2.$$

Proof. Let

$$\mathbf{R}_1 \leq \mathbf{Q}_1 \mathbf{Q}_2^{-1} \mathbf{Q}_1 \quad (5.28)$$

$$\mathbf{R}_2 \leq \mathbf{Q}_4 \mathbf{Q}_5^{-1} \mathbf{Q}_4 \quad (5.29)$$

Along with inequalities (5.28, 5.29), inequality (5.24) can be derived by pre- and post-multiplying both sides of inequality (5.13) by $\text{diag} \{ \mathbf{I}_{kn}, \mathbf{Q}_1, \mathbf{Q}_4, \mathbf{I}_{8kn} \}$. Furthermore, inequalities (5.26, 5.27) can be obtained by applying Schur complement to inequalities (5.28, 5.29). \square

It is noticed that a set of symmetric matrices $\tilde{\mathbf{Q}}_l$ is included to linearize the inequality (5.13); however, to search for the feasible solutions of inequalities (5.24 - 5.27), the equations $\tilde{\mathbf{Q}}_l = \mathbf{Q}_l^{-1}$ cannot be resolved linearly. Thus, the following theorem and algorithm are proposed based on the cone complementarity linearization method [133].

Lemma 5.2. *If the system in Eqs. (5.1, 5.2) is controlled by the feedback controller (5.4), then the error vectors in Eqs. (5.10, 5.11) can be guaranteed to converge to*

zero and the worst case effect of ω_1, ω_2 is minimized. The feedback gain \mathbf{K}_i of the controller in Eq. (5.4) and gain \mathbf{H}_i of the observer in Eqs. (5.5, 5.6) can be derived as

$$\mathbf{K} = \tilde{\mathbf{Q}}_4 \bar{\mathbf{K}} \quad (5.30)$$

$$\mathbf{H} = \tilde{\mathbf{Q}}_1 \bar{\mathbf{H}} \quad (5.31)$$

and the parameters $\tilde{\mathbf{Q}}_4, \bar{\mathbf{K}}, \tilde{\mathbf{Q}}_1, \bar{\mathbf{H}}, \alpha$ can be obtained by solving the following optimization problem:

$$\begin{aligned} \min \text{ trace } & \left(\sum_l \tilde{\mathbf{Q}}_l \mathbf{Q}_l + \sum_m \tilde{\mathbf{R}}_m \mathbf{R}_m + \sum_r \tilde{\varepsilon}_r \varepsilon_r \right) + \alpha \\ \text{s.t. Inequalities } & (5.24 - 5.27) \text{ and} \end{aligned}$$

$$\begin{bmatrix} \tilde{\mathbf{Q}}_l & \mathbf{I} \\ \star & \mathbf{Q}_l \end{bmatrix} \geq 0, \quad \begin{bmatrix} \tilde{\mathbf{R}}_m & \mathbf{I} \\ \star & \mathbf{R}_m \end{bmatrix} \geq 0, \quad \begin{bmatrix} \tilde{\varepsilon}_r & 1 \\ \star & \varepsilon_r \end{bmatrix} \geq 0 \quad (5.32)$$

Since the optimization problem proposed in Lemma 5.2 is nonlinear, a linearized version is presented in the following algorithm to explore the feasible solutions.

Algorithm 1:

Step 1 Initialize the feasible set $\left\{ \tilde{\mathbf{Q}}_l^0, \mathbf{Q}_l^0, \tilde{\mathbf{R}}_m^0, \mathbf{R}_m^0, \varepsilon_r^0, \tilde{\varepsilon}_r^0 \right\}$ satisfying the constraints in Lemma 5.2.

Step 2 Solve the following convex optimization problem:

$$\min \text{ trace } \left[\sum_l \left(\tilde{\mathbf{Q}}_l^j \mathbf{Q}_l + \tilde{\mathbf{Q}}_l \mathbf{Q}_l^j \right) + \sum_m \left(\tilde{\mathbf{R}}_m^j \mathbf{R}_m + \tilde{\mathbf{R}}_m \mathbf{R}_m^j \right) + \sum_r \left(\tilde{\varepsilon}_r^j \varepsilon_r + \tilde{\varepsilon}_r \varepsilon_r^j \right) \right] + \alpha$$

s.t. Inequalities (5.24-5.27, 5.32)

Step 3 Substitute the feasible set obtained from Step 2 into the inequality (5.13); if it is satisfied, then output the feasible solution and EXIT.

Step 4 If $j > j_{max}$, where j_{max} is the maximum number of iterations, then EXIT.

Step 5 Set $j = j + 1$, and $\{\tilde{\mathbf{Q}}_l^j, \mathbf{Q}_r^j, \tilde{\mathbf{R}}_m^j, \mathbf{R}_m^j, \varepsilon_r^j, \tilde{\varepsilon}_r^j\} = \{\tilde{\mathbf{Q}}_l^f, \mathbf{Q}_r^f, \tilde{\mathbf{R}}_m^f, \mathbf{R}_m^f, \varepsilon_r^f, \tilde{\varepsilon}_r^f\}$, where $\{\tilde{\mathbf{Q}}_l^f, \mathbf{Q}_r^f, \tilde{\mathbf{R}}_m^f, \mathbf{R}_m^f, \varepsilon_r^f, \tilde{\varepsilon}_r^f\}$ is the feasible set from Step 2, then go to Step 2.

Remark 5.2. *It should be noticed that the inequalities stated in Theorem 5.1 are sufficient conditions, which implies that these inequalities are fundamental constraints for the stability of the feedback control system. Further constraints might be included if other performance indices are expected. For example, if one of the control gains is expected to be greater than a specific value, this constraint can be included in addition to the fundamental sufficient conditions.*

Remark 5.3. *Less conservative results are always expected in the LMI-based controller design. For example, less conservative results are derived in Theorem 5.1 by including weight matrices $\mathbf{N}_1, \mathbf{N}_2$ in Eqs. (5.17, 5.18). According to the Lyapunov theory, the LMIs derived in this work are all the sufficient conditions for system stability. Namely, deriving less conservative results is still possible by including more degree of freedom. For instance, if the inequality (5.3) can be replaced by another inequality with more degree of freedom, then the results with less conservativeness can hopefully be derived instead of inequalities (5.13) and (5.14).*

5.3 Simulations

As an example, the proposed distributed controller is applied to four identical Chua's circuits in the simulations. One of them is referred to as the leader ($i = 0$), while others are the followers ($i = 1, 2, 3$). The evolution of a Chua's circuit sensitively depends on the initial values of the state vector [134]. Thus, two identical Chua's circuits with slightly different initial values will evolve along immensely different trajectories. Namely, four Chua's circuits with different initial values will naturally defy synchronization. In this part, the synchronization of four identical Chua's circuits will be accomplished using the proposed control algorithm. The initial states of the four agents are chosen as

$$\mathbf{x}_0(t_0) = \begin{bmatrix} 0.1 \\ 0.5 \\ 0.9 \end{bmatrix}, \mathbf{x}_1(t_0) = \begin{bmatrix} -1 \\ -5 \\ 2 \end{bmatrix}, \mathbf{x}_2(t_0) = \begin{bmatrix} -1.5 \\ 1.5 \\ -5 \end{bmatrix}, \mathbf{x}_3(t_0) = \begin{bmatrix} -0.8 \\ 0.8 \\ -2 \end{bmatrix}$$

and the initial states of all the observers are zero.

The perturbed dynamics of the Chua's Circuit is shown as follows [129]

$$\begin{aligned} \dot{\mathbf{x}}_i(t) &= \mathbf{A}\mathbf{x}_i(t) + \mathbf{B}\mathbf{f}(\mathbf{x}_i(t)) + \mathbf{u}_i(t) + \boldsymbol{\omega}_i \\ y_i(t) &= \mathbf{C}\mathbf{x}_i(t) \end{aligned}$$

where

$$\mathbf{A} = \begin{bmatrix} -am_1 & a & 0 \\ 1 & -1 & 1 \\ 0 & -b & 0 \end{bmatrix} \quad \mathbf{B} = \begin{bmatrix} -a(m_0 - m_1) \\ 0 \\ 0 \end{bmatrix}$$

$$\mathbf{C} = [1 \ 0 \ 0] \quad \mathbf{x}_i(t) = \begin{bmatrix} x_i^1(t) \\ x_i^2(t) \\ x_i^3(t) \end{bmatrix}$$

$$\mathbf{f}(\mathbf{x}_i^1(t)) = \frac{1}{2} (|\mathbf{x}_i^1(t) + c| - |\mathbf{x}_i^1(t) - c|)$$

$$\boldsymbol{\omega}_i = e^{-t/30} \mathbf{W}$$

and $i = 0, 1, 2, 3$, $a = 9$, $b = 14.28$, $c = 1$, $m_0 = \frac{1}{7}$, $m_1 = \frac{2}{7}$, $\mathbf{W} \in \mathbb{R}^3$ is a vector of white noise, $\mathbf{x}_i^1(t)$ is the first element of $\mathbf{x}_i(t)$, and the three elements of $\mathbf{x}_i(t)$ represent voltages across two capacitors and inductor current in chaotic circuit [135].

The control gain K_i and observer gain H_i are chosen as follows

$$K_1 = \begin{bmatrix} -2.9865 & -2.4225 & 0.2864 \\ -0.0741 & -2.4096 & -0.3118 \\ 0.5420 & 4.5975 & -3.7323 \end{bmatrix},$$

$$K_2 = \begin{bmatrix} -1.0145 & -0.9102 & 0.1026 \\ -0.0301 & -0.7060 & -0.1352 \\ 0.2315 & 1.7672 & -1.2829 \end{bmatrix}$$

$$K_3 = \begin{bmatrix} -2.0895 & -3.8703 & 1.1515 \\ -0.2362 & -1.6489 & -0.0126 \\ 1.1466 & 6.8213 & -3.2795 \end{bmatrix}$$

$$H_1 = \begin{bmatrix} 6.1086 \\ 0.4379 \\ -1.1978 \end{bmatrix}, \quad H_2 = \begin{bmatrix} 5.9877 \\ 0.3859 \\ -1.0063 \end{bmatrix}, \quad H_3 = \begin{bmatrix} 5.9873 \\ 0.4161 \\ -1.0328 \end{bmatrix}$$

The communication topology is shown in Figure 5.1, where Agent 1 has access to the leader's output, while other followers are coupled with Agent 1 in a distributed manner. The double scroll attractor of the leader is generated autonomously by

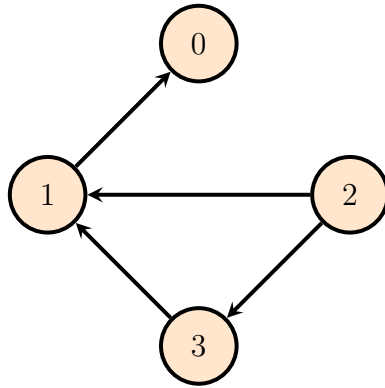


Fig. 5.1 Communication topology

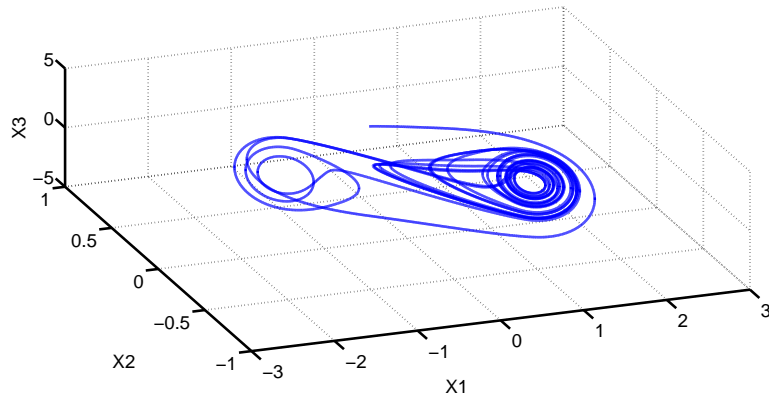


Fig. 5.2 Trajectory of the leader Chua's circuits system

the self-driven dynamics satisfying

$$\dot{\mathbf{x}}_0(t) = \mathbf{A}\mathbf{x}_0(t) + \mathbf{B}\mathbf{f}(\mathbf{x}_0, t) \quad (5.33)$$

The trajectory of Agent 1 (follower) is exhibited in Figure 5.2 and 5.3, respectively. Obvious oscillations can be observed in Figure 5.3, and this phenomenon is caused by the \mathcal{L}_2 bounded disturbances shown in Figure 5.6. Figure 5.4 shows the syn-

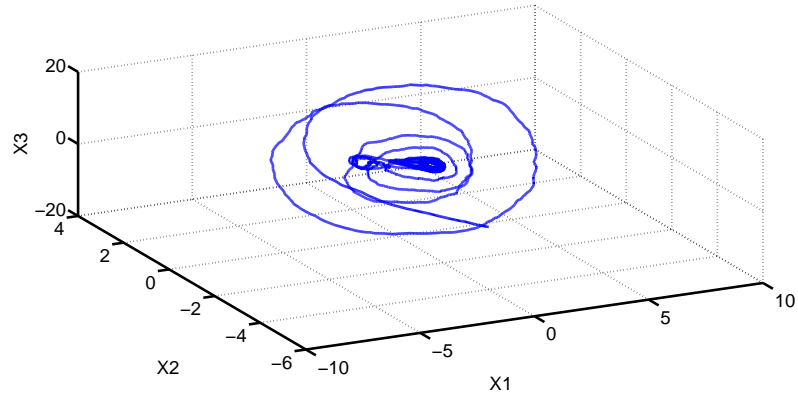


Fig. 5.3 Trajectory of the follower Chua's circuits system

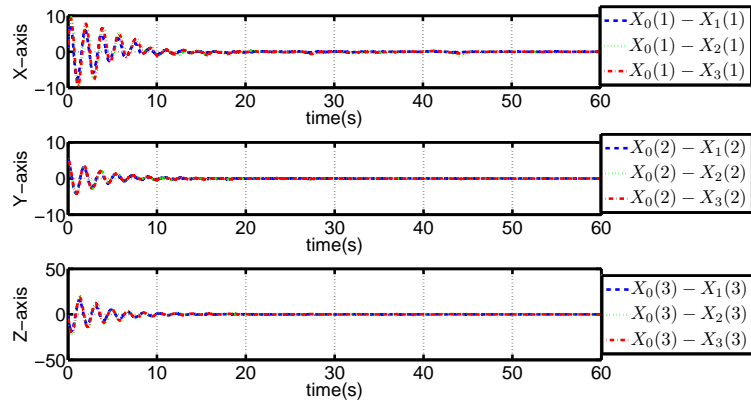


Fig. 5.4 Synchronization errors

chronization errors when the sampling step size is 0.1 sec. The convergences of all estimated errors of the observers are demonstrated in Figure 5.5.

In this chapter, the sampled-data control input is generated based on the periodically updated coupling information. In order to further reduce the computational burden of the local controller, an event-based control algorithm will be presented

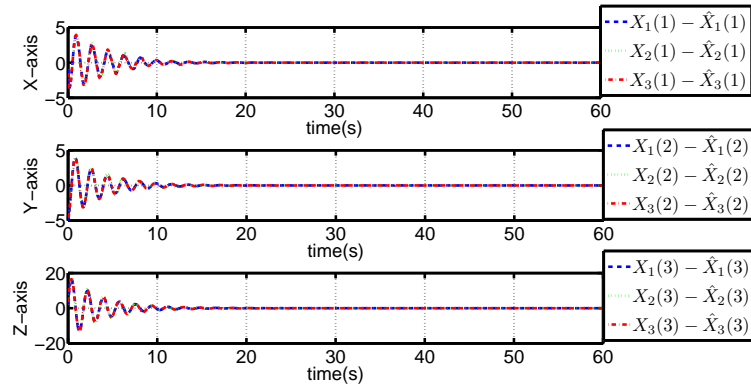


Fig. 5.5 Estimation errors

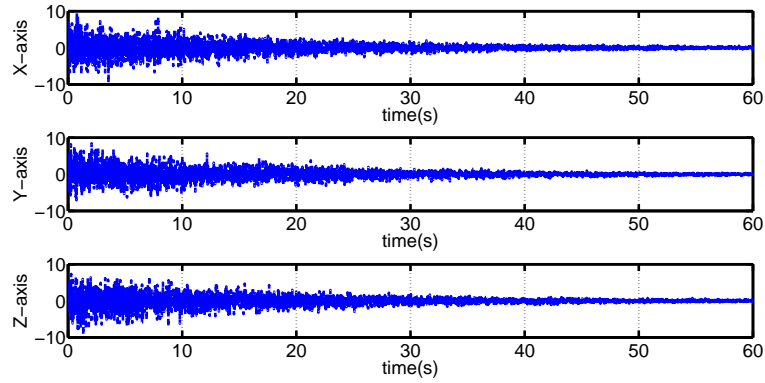


Fig. 5.6 \mathcal{L}_2 bounded disturbance

in the next chapter.

6 Event-triggered Sampled-data Leader-follower Consensus of Networked Nonlinear Systems with Stochastic Switching Topology

Among different types of consensus seeking algorithms, leader-follower consensus is particularly interesting and has received broad attention. In previous research on leader-follower consensus, it is usually assumed that the agents exchange information continuously through the coupling network [3]. However, it is most likely in practice that information sharing can only take place at discrete instants since the bandwidth of the coupling network is limited.

In this chapter, the sampled-data communication is considered along the time-delay equivalent approach. The entire multi-agent system is basically a discrete-time dynamical system because of the sampled-data communication. To better conduct the stability analysis, the time-delay equivalent method [59] is adopted to convert the discrete-time control problem into a continuous-time issue. Obviously,

the sampled-data communication can only reduce the network burden. To further reduce the computational load of each agent, an event-triggered control strategy is integrated and the event-triggered condition is proposed in matrix inequality form. Each agent is only computing the output signal if the event-triggered condition is violated. Namely, the agents' actuators do not have to be updated periodically. Furthermore, the stochastically switched communication topology is considered in this chapter. Since the communication interaction is randomly switched, the finite Markov jump process is recruited to describe the interaction switching of the multi-agent systems.

The remainder of this chapter is organized as follows. In Section 6.1, the non-linear dynamics of the multi-agent systems and the error dynamics are formulated. Meantime, the mathematical description of the interaction relationship between agents is essentially explained using graph theory and Markov jump process. Moreover, an event-triggered condition is proposed to reduce the computational burden of the multi-agent systems. To further clarify the stability of the error dynamics, the stochastic stability is formally defined as well. In Section 6.2, three assumptions are proposed to clearly claim the communication structure. Based on the three assumptions, the controller design and stability analysis are systematically presented with the assistance of Lyapunov functional method. Subsequently, the sufficient condition for the convergence of the error dynamics is derived on the basis of the

stability analysis. Moreover, an iterative convex optimization algorithm is developed to derive the controller gains. Section 6.3 presents the numerical simulation for several Chua's circuits. A distributed leader-follower mission is achieved in the occurrence of stochastically switched interaction. It is shown in the simulation that all tracking errors converge to zero eventually, which demonstrates the effectiveness of the proposed controller.

6.1 Problem formulation

A distributed leader-follower consensus seeking problem is investigated in this work, and k nonlinear agents are included in the multi-agent systems. The dynamics of each nonlinear agent is described as follows

$$\dot{\mathbf{x}}_i(t) = \mathbf{A}\mathbf{x}_i(t) + \mathbf{B}\mathbf{f}(\mathbf{x}_i(t)) + \mathbf{u}_i(t_u) \quad (6.1)$$

where $\mathbf{x}_i(t) \in \mathbb{R}^n$ is the state vector, $\mathbf{u}_i(t_u) \in \mathbb{R}^n$ is the control input, $\mathbf{A} \in \mathbb{R}^{n \times n}$, $\mathbf{B} \in \mathbb{R}^{n \times n}$ are system matrices and nonlinear term $\mathbf{f}(\mathbf{x}_i(t)) \in \mathbb{R}^n$ satisfies the Lipschitz condition, namely, the following inequality is true for any vectors $\mathbf{a} \in \mathbb{R}^n$ and $\mathbf{b} \in \mathbb{R}^n$

$$[\mathbf{f}(\mathbf{a}) - \mathbf{f}(\mathbf{b})]^T [\mathbf{f}(\mathbf{a}) - \mathbf{f}(\mathbf{b})] \leq \alpha^2 (\mathbf{a} - \mathbf{b})^T (\mathbf{a} - \mathbf{b}) \quad (6.2)$$

where $\alpha > 0$ is the Lipschitz constant. The main difference between the model in Eq. (5.1) and the model in Eq. (6.1) is the control input. In the previous chapter,

the input signal is generated periodically and the step size is a predetermined constant. In contrast, the input signal in Eq. (6.1) is generated according to the event-triggered condition. Namely, the step size is time-varying and could be largely different in each step. The desired trajectory is generated by a self-driven nonlinear agent with the following dynamics

$$\dot{\mathbf{x}}_0(t) = \mathbf{A}\mathbf{x}_0(t) + \mathbf{B}\mathbf{f}(\mathbf{x}_0(t)) \quad (6.3)$$

where $\mathbf{x}_0(t) \in \mathbb{R}^n$ is the state vector of the desired trajectory.

The following event-triggered control algorithm is considered

$$\mathbf{u}_i(t_u) = \mathbf{K}_i^{m(t)} \sum_{v_j \in \mathcal{N}_G(v_i)} [\mathbf{x}_i(t_u) - \mathbf{x}_j(t_u)] + \mathbf{K}_i^{m(t)} \mathbf{p}_i [\mathbf{x}_i(t_u) - \mathbf{x}_0(t_u)] \quad (6.4)$$

where $\mathbf{K}_i^{m(t)} \in \mathbb{R}^{n \times n}$, t_u represents the update instant, i.e. $\mathbf{u}_i(t_u)$ only updates its value at discrete-time instants t_u , and $m(t)$ is a finite Markov jump process. The value of $m(t)$ is assigned from a finite set. The transition probability from $m(t) = i$ to $m(t) = j$ is defined as

$$Pr \{m(t + \epsilon) = j | m(t) = i\} = \begin{cases} p_{ij}\epsilon + o(\epsilon) & i \neq j \\ 1 + p_{ii}\epsilon + o(\epsilon) & i = j \end{cases} \quad (6.5)$$

where ϵ is a small positive parameter and $o(\epsilon)/\epsilon \rightarrow 0$. The transition rate p_{ii} and $p_{ij} \geq 0$ satisfy $\sum_{j=1, j \neq i} p_{ij} = -p_{ii}$.

Subtracting the leader's dynamics in Eq. (6.3) from the dynamics of agent i in Eq. (6.1) with the consideration of controller in Eq. (6.4), error dynamics of the

closed-loop control system can be described by the following equation

$$\dot{\mathbf{e}}_i(t) = \mathbf{A}\mathbf{e}_i(t) + \mathbf{B}\mathbf{f}(\mathbf{x}_i(t), \mathbf{x}_0(t)) + \mathbf{u}_i(t_u) \quad (6.6)$$

where $\mathbf{e}_i(t) = \mathbf{x}_i(t) - \mathbf{x}_0(t)$ and $\mathbf{f}(\mathbf{x}_i(t), \mathbf{x}_0(t)) = \mathbf{f}(\mathbf{x}_i(t)) - \mathbf{f}(\mathbf{x}_0(t))$.

Ideally, Eq. (6.6) is the error dynamics of agent i with respect to the desired trajectory. However, imperfect communication network is always unavoidable due to time-varying disturbance and other uncertainties. In order to investigate the robustness against imperfect communication network, the compact form of the error dynamics is formulated in Eq. (6.7) along with the stochastic switching communication topology.

$$\begin{aligned} \dot{\mathbf{e}}(t) = & (\mathbf{I}_k \otimes \mathbf{A}) \mathbf{e}(t) + (\mathbf{I}_k \otimes \mathbf{B}) \bar{\mathbf{f}}(\mathbf{x}(t), \mathbf{x}_0(t)) \\ & + \mathbf{K}^{m(t)} [(\mathcal{L} + \mathfrak{P}) \otimes \mathbf{I}_n + \mathbf{A}_{m(t)}] \mathbf{e}(t_u) \end{aligned} \quad (6.7)$$

where $\bar{\mathbf{f}} : \mathbb{R}^{kn} \times \mathbb{R}^n \rightarrow \mathbb{R}^{kn}$, $\mathbf{e}(t) = [\mathbf{e}_1^T(t) \ \mathbf{e}_2^T(t) \ \dots \ \mathbf{e}_k^T(t)]^T$, $\mathfrak{P} = \text{diag}\{\mathfrak{p}_1, \mathfrak{p}_2, \dots, \mathfrak{p}_k\}$, $\mathbf{K}^{m(t)} = \text{diag}\{\mathbf{K}_1^{m(t)}, \mathbf{K}_2^{m(t)}, \dots, \mathbf{K}_k^{m(t)}\}$ and $\mathbf{A}_{m(t)} \in \mathbb{R}^{n \times n}$ is a function of the finite Markov jump process $m(t)$.

Remark 6.1. *Since the matrix $\mathbf{A}_{m(t)}$ is stochastically switched according to the finite Markov jump process $m(t)$, the communication structure matrix $(\mathcal{L} + \mathfrak{P}) \otimes \mathbf{I}_n + \mathbf{A}_{m(t)}$ is dynamically changing accordingly. Namely, the stochastically switched communication relationship can be thoroughly indicated by $\mathbf{A}_{m(t)}$. Obviously, the*

stochastically switched communication relationship can also be equivalently represented by two stochastically switched matrices $\mathcal{L}^{m(t)}$ and $\mathfrak{P}^{m(t)}$. For the sake of simplicity, the first approach is adopted to represent the stochastically switched communication relationship.

It is commonly assumed in previous work [2, 3] that all the agents exchange information continuously. However, it is most likely in practice that agents can only receive data package discontinuously through limited bandwidth communication network. Therefore, the periodically sampling communication is taken into account in this work. Meanwhile, to further reduce the computational load, an event-triggered manner is investigated for the multi-agent systems as well. In event-triggered control algorithm, the control signal is generated only if the specific event-triggered condition is violated. Obviously, the computational burden is dramatically reduced by the event-triggered controller because the control signal does not have to be generated in each sampling period. Since the communication is still conducted periodically, the event-triggered condition will be verified periodically but the control signal will be calculated only if it is necessary. Motivated by [136], the event-triggered condition is designed as follows

$$\sigma_1 \mathbf{e}_i^T(t_s) \mathbf{P}_i^{m(t)} \mathbf{e}_i(t_s) > \mathbf{r}_i^T(t_s) \mathbf{P}_i^{m(t)} \mathbf{r}_i(t_s) \quad (6.8)$$

where t_s is the periodically sampled time instant, $\mathbf{r}_i(t_s) = \mathbf{e}_i(t_s) - \mathbf{e}_i(t_u)$, $\sigma_1 < 1$ is

a positive constant and $\mathbf{P}_i^{m(t)}$ is the weight matrix.

The desired trajectory is generated by a central workstation. The workstation transmits the trajectory signal intermittently according to the event-triggered condition in Eq. (6.8), and the desired trajectory is sent to the agents in \mathfrak{L}_0 while Eq. (6.8) is violated. Namely, the workstation conducts the signal sampling periodically on $\mathbf{x}_i(t)$ and calculates $\mathbf{r}_i(t_u)$ using $\mathbf{x}_i(t_s)$ to execute the triggering determination on the basis of the event-triggered condition in Eq. (6.8). As for any agent $v_i \in \mathcal{X} \setminus \mathfrak{L}_0$, it has no direct connection with the workstation and they can only exchange information with $v_j \in \mathcal{N}_{\mathcal{G}}(v_i)$.

Unlike the continuous-time dynamical system, the control system in this chapter is a stochastically switched system. Hence, the definition of the stability for Markovian jump system in Eq. (6.7) is presented as follows

Definition 6.1. [137] *Markovian jump system in Eq. (6.7) is stochastically stable if the following condition is satisfied*

$$\lim_{t \rightarrow \infty} E \left\{ \int_0^t \mathbf{e}^T(t) \mathbf{e}(t) dt \right\} < \infty \quad (6.9)$$

Based on the definition of the stability of Markovian jump system in Eq. (6.7), the consensus of the networked control system in Eq. (6.1) can be defined as

Definition 6.2. *The consensus of the networked control system in Eq. (6.1) is considered to be achieved by the control algorithm in Eq. (6.4) if Markovian jump*

system in Eq. (6.7) is ensured to be stochastically stable for any initial condition.

The main objective of this chapter is to develop a control algorithm for the coupled systems in Eq. (6.1). Essentially, the control algorithm is expected to be in the form of Eq. (6.4), and an iterative algorithm will be proposed to numerically derive the feedback gain $\mathbf{K}^{m(t)}$.

6.2 Stability analysis

Assumption 6.1. *The communication interaction can be represented by a digraph containing a spanning tree, and each leader is located at the root of the spanning tree.*

Assumption 6.2. *The desired trajectory information is shared intermittently, and the transmit instants are determined by the event-triggered condition in Eq. (6.8).*

Assumption 6.3. *The communication topology is stochastically switched among finite number of structures, and the switching can be mathematically described by a finite Markov jump process.*

Theorem 6.1. *Suppose that the communication topology of the nonlinear multi-agent systems in Eq. (6.1) and the information sharing satisfy Assumptions 6.1 - 6.3, then the leader-follower consensus of the networked multi-agent systems in Eq. (6.1) can be achieved by the control algorithm presented in Eq. (6.4) if there*

exist symmetric matrices $\mathbf{Q}_r > 0$, $\mathbf{R}_i > 0$, $\mathbf{P} = \text{diag} \left\{ \mathbf{P}_1^{m(t)}, \mathbf{P}_2^{m(t)}, \dots, \mathbf{P}_k^{m(t)} \right\}$ and matrix \mathbf{W} such that

$$\begin{bmatrix} \Phi_1 & h\mathbf{N}^T \\ \star & -h\mathbf{R}_1^{-1} \end{bmatrix} < 0 \quad (6.10)$$

and

$$\begin{bmatrix} \Phi_2 & h\mathbf{W} \\ \star & -h\mathbf{R}_1 \end{bmatrix} < 0 \quad (6.11)$$

where

$$\mathbf{M}_1 = \begin{bmatrix} \mathbf{I} & \mathbf{0} & \mathbf{0} & \mathbf{0} \end{bmatrix}$$

$$\mathbf{M}_2 = \begin{bmatrix} \mathbf{0} & \mathbf{I} & \mathbf{0} & \mathbf{0} \end{bmatrix}$$

$$\mathbf{M}_3 = \begin{bmatrix} \mathbf{0} & \mathbf{0} & \mathbf{I} & \mathbf{0} \end{bmatrix}$$

$$\mathbf{M}_4 = \begin{bmatrix} \mathbf{0} & \mathbf{0} & \mathbf{0} & \mathbf{I} \end{bmatrix}$$

$$\mathbf{N} = \begin{bmatrix} \mathbf{I}_k \otimes \mathbf{A} & \mathbf{K}^{m(t)} [(\mathcal{L} + \mathcal{D}) \otimes \mathbf{I}_n + \mathbf{A}_{m(t)}] & \mathbf{I}_k \otimes \mathbf{B} \\ & -\mathbf{K}^{m(t)} [(\mathcal{L} + \mathcal{D}) \otimes \mathbf{I}_n + \mathbf{A}_{m(t)}] & \end{bmatrix}$$

$$\begin{aligned} \Phi_1 = & \mathbf{M}_1^T \sum_{i=1}^q p_{ri} \mathbf{Q}_i \mathbf{M}_1 + 2\sigma_3 \mathbf{M}_1^T \mathbf{R}_2 \mathbf{N} - \mathbf{M}_1^T \mathbf{R}_2 \mathbf{M}_1 - \mathbf{M}_2^T \mathbf{R}_2 \mathbf{M}_2 + 2\mathbf{M}_1^T \mathbf{R}_2 \mathbf{M}_2 \\ & + 2h\mathbf{M}_1^T \mathbf{R}_2 \mathbf{N} - 2h\mathbf{M}_2^T \mathbf{R}_2 \mathbf{N} + 2\mathbf{W}\mathbf{M}_1 - 2\mathbf{W}\mathbf{M}_2 + \alpha^2 \sigma_2 \mathbf{M}_1^T \mathbf{M}_1 \end{aligned}$$

$$- \sigma_2 \mathbf{M}_3^T \mathbf{M}_3 + \sigma_1 \mathbf{M}_2^T \mathbf{P} \mathbf{M}_2 - \mathbf{M}_4^T \mathbf{P} \mathbf{M}_4$$

$$\begin{aligned} \Phi_2 = & \mathbf{M}_1^T \sum_{i=1}^q p_{ri} \mathbf{Q}_i \mathbf{M}_1 + 2\sigma_3 \mathbf{M}_1^T \mathbf{R}_2 \mathbf{N} - \mathbf{M}_1^T \mathbf{R}_2 \mathbf{M}_1 - \mathbf{M}_2^T \mathbf{R}_2 \mathbf{M}_2 + 2\mathbf{M}_1^T \mathbf{R}_2 \mathbf{M}_2 \\ & + 2\mathbf{W}\mathbf{M}_1 - 2\mathbf{W}\mathbf{M}_2 + \alpha^2 \sigma_2 \mathbf{M}_1^T \mathbf{M}_1 - \sigma_2 \mathbf{M}_3^T \mathbf{M}_3 + \sigma_1 \mathbf{M}_2^T \mathbf{P} \mathbf{M}_2 - \mathbf{M}_4^T \mathbf{P} \mathbf{M}_4 \end{aligned}$$

Remark 6.2. *The time-delay equivalent method is adopted in this work. This*

method was originally developed in [59]. Based on their work, a sufficient condition for sampled-data stabilization of linear systems was proposed in linear matrix inequalities (LMIs) form in [60] along the descriptor approach. To further enhance the theoretical foundation, a discontinuous Lyapunov functional method was presented in [61], based on which the exponential convergence of the sampled-data control system was further investigated in [62] using the discontinuous Lyapunov functional method. The essential part of this method is to recruit an artificial time-delay $d(t)$ so that the sampling time t_s is equivalently converted to $t_s = t - d(t)$ in each sampling period, which implies that the original discontinuous control problem is transformed to a continuous control problem with a time-varying delay.

Proof. Defining the Lyapunov functional

$$\begin{aligned}
V(m(t), r) = & \mathbf{e}^T(t) \mathbf{Q}_r \mathbf{e}(t) + \int_{t-d(t)}^t [h - d(t)] \dot{\mathbf{e}}^T(\tau) \mathbf{R}_1 \dot{\mathbf{e}}(\tau) d\tau \\
& + [h - d(t)] [\mathbf{e}(t) - \mathbf{e}(t_s)]^T \mathbf{R}_2 [\mathbf{e}(t) - \mathbf{e}(t_s)]
\end{aligned} \tag{6.12}$$

The weak infinitesimal operator \mathcal{F} of the stochastic process $\{m(t)\}$ is defined as

$$\mathcal{F}V(m(t)) = \lim_{\epsilon \rightarrow 0^+} \frac{E \{V(m(t + \epsilon))\} - V(m(t))}{\epsilon}$$

Consequently,

$$\begin{aligned}
& \mathcal{F}V(m(t), r) \\
= & \mathbf{e}^T(t) \sum_{i=1}^q p_{ri} \mathbf{Q}_i \mathbf{e}(t) + 2\mathbf{e}^T(t) \mathbf{Q}_r \dot{\mathbf{e}}(t) + [h - d(t)] \dot{\mathbf{e}}^T(t) \mathbf{R}_1 \dot{\mathbf{e}}(t)
\end{aligned}$$

$$\begin{aligned}
& - \int_{t-d(t)}^t \dot{\mathbf{e}}^T(\tau) \mathbf{R}_1 \dot{\mathbf{e}}(\tau) d\tau - [\mathbf{e}(t) - \mathbf{e}(t_s)]^T \mathbf{R}_2 [\mathbf{e}(t) - \mathbf{e}(t_s)] \\
& + 2[h - d(t)] [\mathbf{e}(t) - \mathbf{e}(t_s)]^T \mathbf{R}_2 \dot{\mathbf{e}}(t) \\
= & \mathbf{e}^T(t) \sum_{i=1}^q p_{ri} \mathbf{Q}_i \mathbf{e}(t) + 2\mathbf{e}^T(t) \mathbf{Q}_r \dot{\mathbf{e}}(t) + [h - d(t)] \dot{\mathbf{e}}^T(t) \mathbf{R}_1 \dot{\mathbf{e}}(t) \\
& - \int_{t-d(t)}^t \dot{\mathbf{e}}^T(\tau) \mathbf{R}_1 \dot{\mathbf{e}}(\tau) d\tau - \mathbf{e}^T(t) \mathbf{R}_2 \mathbf{e}(t) - \mathbf{e}^T(t_s) \mathbf{R}_2 \mathbf{e}(t_s) \\
& + 2\mathbf{e}^T(t) \mathbf{R}_2 \mathbf{e}(t_s) + 2[h - d(t)] \mathbf{e}^T(t) \mathbf{R}_2 \dot{\mathbf{e}}(t) \\
& - 2[h - d(t)] \mathbf{e}^T(t_s) \mathbf{R}_2 \dot{\mathbf{e}}(t) \tag{6.13}
\end{aligned}$$

On the basis of the Newton-Leibniz formula, the following equation is obtained with a free weight matrix $\mathbf{W} \in \mathbb{R}^{4kn \times kn}$

$$2\xi^T \mathbf{W} \mathbf{e}(t) - 2\xi^T \mathbf{W} \mathbf{e}(t_s) - 2\xi^T \mathbf{W} \int_{t_s}^t \dot{\mathbf{e}}(\tau) d\tau = 0 \tag{6.14}$$

where $\xi = [\mathbf{e}^T(t) \quad \mathbf{e}^T(t_s) \quad \bar{\mathbf{f}}^T(\mathbf{x}(t), \mathbf{x}_0(t)) \quad \mathbf{r}^T]^T$.

Eq. (6.13) can be further manipulated by considering Eq. (6.14) as follows

$$\begin{aligned}
\mathcal{FV}(m(t), r) & = \mathbf{e}^T(t) \sum_{i=1}^q p_{ri} \mathbf{Q}_i \mathbf{e}(t) + 2\mathbf{e}^T(t) \mathbf{Q}_r \dot{\mathbf{e}}(t) + [h - d(t)] \dot{\mathbf{e}}^T(t) \mathbf{R}_1 \dot{\mathbf{e}}(t) \\
& - \int_{t-d(t)}^t \dot{\mathbf{e}}^T(\tau) \mathbf{R}_1 \dot{\mathbf{e}}(\tau) d\tau - \mathbf{e}^T(t) \mathbf{R}_2 \mathbf{e}(t) - \mathbf{e}^T(t_s) \mathbf{R}_2 \mathbf{e}(t_s) \\
& + 2\mathbf{e}^T(t) \mathbf{R}_2 \mathbf{e}(t_s) + 2[h - d(t)] \mathbf{e}^T(t) \mathbf{R}_2 \dot{\mathbf{e}}(t) \\
& - 2[h - d(t)] \mathbf{e}^T(t_s) \mathbf{R}_2 \dot{\mathbf{e}}(t) \\
& + 2\xi^T \mathbf{W} \mathbf{e}(t) - 2\xi^T \mathbf{W} \mathbf{e}(t_s) - 2\xi^T \mathbf{W} \int_{t_s}^t \dot{\mathbf{e}}(\tau) d\tau \\
= & \mathbf{e}^T(t) \sum_{i=1}^q p_{ri} \mathbf{Q}_i \mathbf{e}(t) + 2\mathbf{e}^T(t) \mathbf{Q}_r \dot{\mathbf{e}}(t) + [h - d(t)] \dot{\mathbf{e}}^T(t) \mathbf{R}_1 \dot{\mathbf{e}}(t)
\end{aligned}$$

$$\begin{aligned}
& -\mathbf{e}^T(t)\mathbf{R}_2\mathbf{e}(t) - \mathbf{e}^T(t_s)\mathbf{R}_2\mathbf{e}(t_s) + 2\xi^T\mathbf{W}\mathbf{e}(t) - 2\xi^T\mathbf{W}\mathbf{e}(t_s) \\
& + 2\mathbf{e}^T(t)\mathbf{R}_2\mathbf{e}(t_s) + 2[h - d(t)]\mathbf{e}^T(t)\mathbf{R}_2\dot{\mathbf{e}}(t) \\
& - 2[h - d(t)]\mathbf{e}^T(t_s)\mathbf{R}_2\dot{\mathbf{e}}(t) + d(t)\xi^T\mathbf{W}\mathbf{R}_1^{-1}\mathbf{W}^T\xi \\
& - \int_{t_s}^t [\mathbf{W}^T\xi + \mathbf{R}_1\dot{\mathbf{e}}(\tau)]^T \mathbf{R}_1^{-1} [\mathbf{W}^T\xi + \mathbf{R}_1\dot{\mathbf{e}}(\tau)] d\tau \quad (6.15)
\end{aligned}$$

Subsequently, the following inequality is equivalent to $\mathcal{FV}(m(t), r) < 0$

$$\begin{aligned}
& \xi^T(t)\mathbf{M}_1^T \sum_{i=1}^q p_{ri}\mathbf{Q}_i\mathbf{M}_1\xi(t) + 2\xi^T(t)\mathbf{M}_1^T\mathbf{Q}_r\mathbf{N}\xi(t) + [h - d(t)]\xi^T(t)\mathbf{N}^T\mathbf{R}_1\mathbf{N}\xi(t) \\
& - \xi^T(t)\mathbf{M}_1^T\mathbf{R}_2\mathbf{M}_1\xi - \xi^T(t)\mathbf{M}_2^T\mathbf{R}_2\mathbf{M}_2\xi + 2\xi^T(t)\mathbf{W}\mathbf{M}_1\xi(t) - 2\xi^T\mathbf{W}\mathbf{M}_2\xi(t) \\
& + 2\xi^T(t)\mathbf{M}_1^T\mathbf{R}_2\mathbf{M}_2\xi(t) + 2[h - d(t)]\xi^T(t)\mathbf{M}_1^T\mathbf{R}_2\mathbf{N}\xi(t) \\
& - 2[h - d(t)]\xi^T(t)\mathbf{M}_2^T\mathbf{R}_2\mathbf{N}\xi(t) + d(t)\xi^T\mathbf{W}\mathbf{R}_1^{-1}\mathbf{W}^T\xi < 0 \quad (6.16)
\end{aligned}$$

Further taking advantage of Eqs. (6.2, 6.8), the following equivalent condition can be obtained

$$\begin{aligned}
& \xi^T(t)\mathbf{M}_1^T \sum_{i=1}^q p_{ri}\mathbf{Q}_i\mathbf{M}_1\xi(t) + 2\xi^T(t)\mathbf{M}_1^T\mathbf{Q}_r\mathbf{N}\xi(t) + [h - d(t)]\xi^T(t)\mathbf{N}^T\mathbf{R}_1\mathbf{N}\xi(t) \\
& - \xi^T(t)\mathbf{M}_1^T\mathbf{R}_2\mathbf{M}_1\xi - \xi^T(t)\mathbf{M}_2^T\mathbf{R}_2\mathbf{M}_2\xi + 2\xi^T(t)\mathbf{W}\mathbf{M}_1\xi(t) - 2\xi^T\mathbf{W}\mathbf{M}_2\xi(t) \\
& + 2\xi^T(t)\mathbf{M}_1^T\mathbf{R}_2\mathbf{M}_2\xi(t) + 2[h - d(t)]\xi^T(t)\mathbf{M}_1^T\mathbf{R}_2\mathbf{N}\xi(t) \\
& + d(t)\xi^T\mathbf{W}\mathbf{R}_1^{-1}\mathbf{W}^T\xi + \alpha^2\sigma_2\xi^T\mathbf{M}_1^T\mathbf{M}_1\xi - \sigma_2\xi^T\mathbf{M}_3^T\mathbf{M}_3\xi + \sigma_1\xi^T\mathbf{M}_2^T\mathbf{P}\mathbf{M}_2\xi \\
& - \xi^T\mathbf{M}_4^T\mathbf{P}\mathbf{M}_4\xi - 2[h - d(t)]\xi^T(t)\mathbf{M}_2^T\mathbf{R}_2\mathbf{N}\xi(t) < 0 \quad (6.17)
\end{aligned}$$

where σ_2 is an arbitrary positive constant.

Since the left hand side of Eq. (6.17) is a linear polynomial of $d(t)$, the following inequalities can be derived by setting $d(t) = 0$ and $d(t) = h$, respectively.

$$\begin{aligned}
& \mathbf{M}_1^T \sum_{i=1}^q p_{ri} \mathbf{Q}_i \mathbf{M}_1 + 2\sigma_3 \mathbf{M}_1^T \mathbf{R}_2 \mathbf{N} + h \mathbf{N}^T \mathbf{R}_1 \mathbf{N} - \mathbf{M}_1^T \mathbf{R}_2 \mathbf{M}_1 \\
& - \mathbf{M}_2^T \mathbf{R}_2 \mathbf{M}_2 + 2\mathbf{M}_1^T \mathbf{R}_2 \mathbf{M}_2 + 2h \mathbf{M}_1^T \mathbf{R}_2 \mathbf{N} - 2h \mathbf{M}_2^T \mathbf{R}_2 \mathbf{N} \\
& + 2\mathbf{W} \mathbf{M}_1 - 2\mathbf{W} \mathbf{M}_2 + \alpha^2 \sigma_2 \mathbf{M}_1^T \mathbf{M}_1 - \sigma_2 \mathbf{M}_3^T \mathbf{M}_3 \\
& + \sigma_1 \mathbf{M}_2^T \mathbf{P} \mathbf{M}_2 - \mathbf{M}_4^T \mathbf{P} \mathbf{M}_4 < 0
\end{aligned} \tag{6.18}$$

and

$$\begin{aligned}
& \mathbf{M}_1^T \sum_{i=1}^q p_{ri} \mathbf{Q}_i \mathbf{M}_1 + 2\sigma_3 \mathbf{M}_1^T \mathbf{R}_2 \mathbf{N} - \mathbf{M}_1^T \mathbf{R}_2 \mathbf{M}_1 \\
& - \mathbf{M}_2^T \mathbf{R}_2 \mathbf{M}_2 + 2\mathbf{M}_1^T \mathbf{R}_2 \mathbf{M}_2 + h \mathbf{W} \mathbf{R}_1^{-1} \mathbf{W}^T \\
& + 2\mathbf{W} \mathbf{M}_1 - 2\mathbf{W} \mathbf{M}_2 + \alpha^2 \sigma_2 \mathbf{M}_1^T \mathbf{M}_1 - \sigma_2 \mathbf{M}_3^T \mathbf{M}_3 \\
& + \sigma_1 \mathbf{M}_2^T \mathbf{P} \mathbf{M}_2 - \mathbf{M}_4^T \mathbf{P} \mathbf{M}_4 < 0
\end{aligned} \tag{6.19}$$

where $\mathbf{R}_2 = \frac{\mathbf{Q}_r}{\sigma_3}$ and σ_3 is an arbitrary nonzero constant.

Along with the Schur complement, Eqs. (6.10) and (6.11) can be derived from Eqs. (6.18) and (6.19) respectively.

Define

$$\begin{aligned}
\tilde{\mathbf{M}}_1 &= \mathbf{M}_1^T \sum_{i=1}^q p_{ri} \mathbf{Q}_i \mathbf{M}_1 + 2\sigma_3 \mathbf{M}_1^T \mathbf{R}_2 \mathbf{N} + h \mathbf{N}^T \mathbf{R}_1 \mathbf{N} - \mathbf{M}_1^T \mathbf{R}_2 \mathbf{M}_1 \\
& - \mathbf{M}_2^T \mathbf{R}_2 \mathbf{M}_2 + 2\mathbf{M}_1^T \mathbf{R}_2 \mathbf{M}_2 + 2h \mathbf{M}_1^T \mathbf{R}_2 \mathbf{N} \\
& - 2h \mathbf{M}_2^T \mathbf{R}_2 \mathbf{N} + 2\mathbf{W} \mathbf{M}_1 - 2\mathbf{W} \mathbf{M}_2 + \alpha^2 \sigma_2 \mathbf{M}_1^T \mathbf{M}_1 - \sigma_2 \mathbf{M}_3^T \mathbf{M}_3
\end{aligned}$$

$$\begin{aligned}
& +\sigma_1\mathbf{M}_2^T\mathbf{P}\mathbf{M}_2 - \mathbf{M}_4^T\mathbf{P}\mathbf{M}_4 \\
\tilde{\mathbf{M}}_2 = & \mathbf{M}_1^T \sum_{i=1}^q p_{ri} \mathbf{Q}_i \mathbf{M}_1 + 2\sigma_3 \mathbf{M}_1^T \mathbf{R}_2 \mathbf{N} - \mathbf{M}_1^T \mathbf{R}_2 \mathbf{M}_1 \\
& -\mathbf{M}_2^T \mathbf{R}_2 \mathbf{M}_2 + 2\mathbf{M}_1^T \mathbf{R}_2 \mathbf{M}_2 + h \mathbf{W} \mathbf{R}_1^{-1} \mathbf{W}^T \\
& +2\mathbf{W}\mathbf{M}_1 - 2\mathbf{W}\mathbf{M}_2 + \alpha^2 \sigma_2 \mathbf{M}_1^T \mathbf{M}_1 - \sigma_2 \mathbf{M}_3^T \mathbf{M}_3 \\
& +\sigma_1\mathbf{M}_2^T\mathbf{P}\mathbf{M}_2 - \mathbf{M}_4^T\mathbf{P}\mathbf{M}_4
\end{aligned}$$

and $\lambda_1 = \min \left\{ \lambda_{\min} \left(\tilde{\mathbf{M}}_1 \right), \lambda_{\min} \left(\tilde{\mathbf{M}}_2 \right) \right\}$. According to Eq. (6.12), it is obtained that

$$\mathcal{F}V(m(t), r) \leq -\lambda_1 \mathbf{e}^T(t) \mathbf{e}(t)$$

On the basis of Dynkin's formula [138], it is also obtained that

$$E[V(m(t), r)] - V(m(t_0), r) \leq -\lambda_1 E \left\{ \int_{t_0}^t \mathbf{e}^T(\tau) \mathbf{e}(\tau) d\tau \right\}$$

and it is further derived that

$$\lambda_1 E \left\{ \int_0^t \mathbf{e}^T(\tau) \mathbf{e}(\tau) d\tau \right\} \leq V(m(t_0), r)$$

Moreover, the following relationship is derived based on Eq. (6.12)

$$E \{V(m(t), r)\} \geq \lambda_2 E \{ \mathbf{e}^T(t) \mathbf{e}(t) \}$$

where $\lambda_2 = \lambda_{\min} \{ \mathbf{Q}_r \}$.

Consequently, following [137], the stochastically stable inequality can be derived

as shown below

$$\lim_{t \rightarrow \infty} E \left\{ \int_0^t \mathbf{e}^T(t) \mathbf{e}(t) dt \right\} \leq \frac{\lambda_2^2}{\lambda_1} < \infty$$

According to Definition 6.1, it is proven that the Markovian jump system in Eq. (6.7) is stochastically stable, which in turn implies that the leader-follower consensus is achieved by the proposed leader-follower consensus algorithm. \square

Theorem 6.2. *Suppose that the communication topology of the nonlinear multi-agent systems in Eq. (6.1) and the information sharing satisfy Assumptions 6.1 - 6.3, then the leader-follower consensus problem of the networked multi-agent systems in Eq. (6.1) is solvable if the following LMIs are feasible*

$$\begin{bmatrix} \Phi_1 & h\tilde{\mathbf{N}}^T \\ \star & -h\mathbf{R}_3 \end{bmatrix} < 0 \quad (6.20)$$

$$\begin{bmatrix} \Phi_2 & h\mathbf{W} \\ \star & -h\mathbf{R}_1 \end{bmatrix} < 0 \quad (6.21)$$

$$\begin{bmatrix} -\tilde{\mathbf{R}}_1 & \tilde{\mathbf{R}}_2 \\ \star & -\tilde{\mathbf{R}}_3 \end{bmatrix} < 0 \quad (6.22)$$

$$\begin{bmatrix} \tilde{\mathbf{R}}_1 & \mathbf{0} & \mathbf{0} \\ \star & \tilde{\mathbf{R}}_2 & \mathbf{0} \\ \star & \star & \tilde{\mathbf{R}}_3 \end{bmatrix} \begin{bmatrix} \mathbf{R}_1 & \mathbf{0} & \mathbf{0} \\ \star & \mathbf{R}_2 & \mathbf{0} \\ \star & \star & \mathbf{R}_3 \end{bmatrix} = \mathbf{I} \quad (6.23)$$

where $\mathbf{K}^{m(t)} = \mathbf{R}_2^{-1}\tilde{\mathbf{K}}^{m(t)}$, and

$$\begin{aligned} \tilde{\mathbf{N}} = & \begin{bmatrix} \mathbf{R}_2 (\mathbf{I}_k \otimes \mathbf{A}) & \tilde{\mathbf{K}}^{m(t)} [(\mathcal{L} + \mathfrak{D}) \otimes \mathbf{I}_n + \mathbf{A}_{m(t)}] & \mathbf{R}_2 (\mathbf{I}_k \otimes \mathbf{B}) \\ & -\tilde{\mathbf{K}}^{m(t)} [(\mathcal{L} + \mathfrak{D}) \otimes \mathbf{I}_n + \mathbf{A}_{m(t)}] \end{bmatrix} \end{aligned}$$

Proof. By pre- and post-multiplying both sides of Eq. (6.10) by $\text{diag}\{\mathbf{I}_{kn}, \mathbf{R}_2\}$, the following inequalities can be obtained

$$\begin{aligned} \begin{bmatrix} \mathbf{I}_{kn} & \mathbf{0} \\ \mathbf{0} & \mathbf{R}_2 \end{bmatrix} \begin{bmatrix} \Phi_1 & h\mathbf{N}^T \\ \star & -h\mathbf{R}_1^{-1} \end{bmatrix} \begin{bmatrix} \mathbf{I}_{kn} & \mathbf{0} \\ \mathbf{0} & \mathbf{R}_2 \end{bmatrix} < 0 \\ \begin{bmatrix} \Phi_1 & h\tilde{\mathbf{N}}^T \\ \star & -h\mathbf{R}_2\mathbf{R}_1^{-1}\mathbf{R}_2 \end{bmatrix} < 0 \end{aligned} \quad (6.24)$$

If

$$\mathbf{R}_3 \leq \mathbf{R}_2 \mathbf{R}_1^{-1} \mathbf{R}_2 \quad (6.25)$$

then the following inequalities are equivalent to Eq. (6.24) based on Schur complement

$$\begin{aligned} \begin{bmatrix} \Phi_1 & h\tilde{\mathbf{N}}^T \\ \star & -h\mathbf{R}_3 \end{bmatrix} &< 0 \\ \begin{bmatrix} -\mathbf{R}_1^{-1} & \mathbf{R}_2^{-1} \\ \star & -\mathbf{R}_3^{-1} \end{bmatrix} &< 0 \end{aligned}$$

Consequently, the LMIs in Eqs. (6.20 - 6.22) and Eq. (6.23) can be derived on the basis of Theorem 6.1. \square

Apparently, the inequalities presented in Theorem 6.2 cannot be solved linearly. Therefore, the cone complementarity linearization method [133] is employed to derive the feedback gain of the proposed controller.

Corollary 6.1. *Suppose that the communication topology of the nonlinear multi-agent systems in Eq. (6.1) and the information sharing satisfy Assumptions 6.1 - 6.3, then the feedback gain $\mathbf{K}_i^{m(t)}$ in Eq. (6.4) and the matrix parameters in Eqs. (6.20 - 6.22) can be derived by solving the following optimization problem*

$$\begin{aligned} \min \text{trace} \left(\sum_{w=1}^3 \tilde{\mathbf{R}}_w \mathbf{R}_w \right) \\ \text{s.t. LMIs in Eqs. (6.20 - 6.22) and} \\ \begin{bmatrix} \tilde{\mathbf{R}}_w & \mathbf{I} \\ \star & \mathbf{R}_w \end{bmatrix} \geq 0 \quad w = 1, 2, 3 \end{aligned} \quad (6.26)$$

Based on the optimization proposed in Corollary 6.1, an iterative algorithm is developed to numerically obtain the feedback gain $\mathbf{K}_i^{m(t)}$ as follows

Algorithm 1:

Step 1 Initialize the maximum number of the iterations i_{max} and the set $\left\{ \tilde{\mathbf{R}}_w^0, \mathbf{R}_w^0, \mathbf{W}^0, \sigma_w^0, \mathbf{P}^0, \mathbf{Q}_i^0, \tilde{\mathbf{N}}^0 \right\}$ that satisfies Eqs. (6.20 - 6.22) and (6.26).

Step 2 Solve the following optimization problem:

$$\begin{aligned} \min \text{ trace } & \sum \left(\tilde{\mathbf{R}}_w^0 \mathbf{R}_w + \tilde{\mathbf{R}}_w \mathbf{R}_w^0 \right) \\ \text{s.t. } & \text{LMIs in Eqs. (6.20 - 6.22) and (6.26)} \end{aligned}$$

Step 3 Substitute the feasible solution derived from Step 2 into Eq. (6.10), if it is satisfied, then output the feasible value of the demanded matrices and EXIT.

Step 4 If $i > i_{max}$, then EXIT. Otherwise, set $i = i + 1$.

Step 5 Update $\left\{ \tilde{\mathbf{R}}_w^j, \mathbf{R}_w^j, \mathbf{W}^j, \sigma_w^j, \mathbf{P}^j, \mathbf{Q}_i^j, \tilde{\mathbf{N}}^j \right\} = \left\{ \tilde{\mathbf{R}}_w^f, \mathbf{R}_w^f, \mathbf{W}^f, \sigma_w^f, \mathbf{P}^f, \mathbf{Q}_i^f, \tilde{\mathbf{N}}^f \right\}$, where $\left\{ \tilde{\mathbf{R}}_w^f, \mathbf{R}_w^f, \mathbf{W}^f, \sigma_w^f, \mathbf{P}^f, \mathbf{Q}_i^f, \tilde{\mathbf{N}}^f \right\}$ is the feasible set derived from Step 2.

Step 6 Go to Step 2.

6.3 Simulations

Four Chua's circuits are utilized in the numerical simulation. In the simulated leader-follower mission, a self-driven Chua's circuit will generate a desired trajectory. At the same time, the desired trajectory is broadcast to agent 1 and 2 ac-

according to the communication topologies in Figure 6.2. Since the desired trajectory is not available to agent 3 and 4, they can only share the trajectory information locally according to the communication topology; thus, they are the followers in the leader-follower mission.

The dynamics of Chua's circuit can be described as follows

$$\dot{\mathbf{x}}_i(t) = \mathbf{A}\mathbf{x}_i(t) + \mathbf{B}\mathbf{f}(\mathbf{x}_i(t)) + \mathbf{u}_i(t)$$

where

$$\mathbf{A} = \begin{bmatrix} -am_1 & a & 0 \\ 1 & -1 & 1 \\ 0 & -b & 0 \end{bmatrix}$$

$$\mathbf{B} = \begin{bmatrix} -a(m_0 - m_1) \\ 0 \\ 0 \end{bmatrix}$$

$$\mathbf{f}(\mathbf{x}_i^1(t)) = \frac{1}{2} (|\mathbf{x}_i^1(t) + c| - |\mathbf{x}_i^1(t) - c|)$$

and $i = 1, 2, 3, 4$, $a = 9$, $b = 14.28$, $c = 1$, $m_0 = \frac{1}{7}$, $m_1 = \frac{2}{7}$ [129].

Since the communication relationship is dynamically changing, two communication topologies are considered in the simulation and they are stochastically switched with the evolution of the simulation. Figures 6.2(a) and 6.2(b) depict these two communication topologies. Accordingly, the stochastic switching matrix $\mathbf{A}_{m(t)}$ corresponding to the two topologies are

$$\mathbf{A}_1 = \mathbf{0}$$

$$\mathbf{A}_2 = \begin{bmatrix} 0 & -1 & 0 & 0 \\ 1 & -1 & 0 & 0 \\ 0 & 0 & 0 & 0 \\ 0 & 0 & 0 & 0 \end{bmatrix}$$

and

$$\mathfrak{P} = \begin{bmatrix} 1 & 0 & 0 & 0 \\ 0 & 1 & 0 & 0 \\ 0 & 0 & 0 & 0 \\ 0 & 0 & 0 & 0 \end{bmatrix}$$

$$\mathcal{L} = \begin{bmatrix} 0 & 0 & 0 & 0 \\ -1 & 1 & 0 & 0 \\ -1 & -1 & 2 & 0 \\ 0 & -1 & 0 & 1 \end{bmatrix}$$

On the basis of the proposed Algorithm 1, the control gains are derived as follows

$$\mathbf{K}_1^1 = \begin{bmatrix} -9.0429 & -1.9674 & 2.5642 \\ -1.0865 & -0.6964 & 0.9170 \\ 1.8661 & 1.2421 & -4.1712 \end{bmatrix}$$

$$\mathbf{K}_2^1 = \begin{bmatrix} -5.0214 & -1.2051 & 1.9471 \\ -0.6351 & -0.3502 & 0.5033 \\ 1.4904 & 0.7295 & -2.4962 \end{bmatrix}$$

$$\mathbf{K}_3^1 = \begin{bmatrix} -2.7293 & -0.5041 & 0.8512 \\ -0.3128 & -0.2145 & 0.2743 \\ 0.6971 & 0.3580 & -1.5550 \end{bmatrix}$$

$$\mathbf{K}_4^1 = \begin{bmatrix} -4.1891 & -0.9237 & 0.9313 \\ -0.5390 & -0.3313 & 0.3395 \\ 0.8084 & 0.5096 & -2.2151 \end{bmatrix}$$

and

$$\begin{aligned}
\mathbf{K}_1^2 &= \begin{bmatrix} -0.6036 & -0.0503 & 0.0143 \\ -0.0433 & -0.2284 & 0.0978 \\ 0.0146 & 0.1039 & -0.3652 \end{bmatrix} \\
\mathbf{K}_2^2 &= \begin{bmatrix} -1.2755 & -0.1100 & 0.0306 \\ -0.0934 & -0.4728 & 0.2101 \\ 0.0316 & 0.2224 & -0.7675 \end{bmatrix} \\
\mathbf{K}_3^2 &= \begin{bmatrix} -0.4295 & -0.0336 & 0.0101 \\ -0.0299 & -0.1644 & 0.0678 \\ 0.0101 & 0.0721 & -0.2591 \end{bmatrix} \\
\mathbf{K}_4^2 &= \begin{bmatrix} -0.6015 & -0.0500 & 0.0143 \\ -0.0431 & -0.2277 & 0.0974 \\ 0.0145 & 0.1035 & -0.3640 \end{bmatrix}
\end{aligned}$$

The weight matrices in event-triggered condition Eq. (6.8) are derived as follows

$$\begin{aligned}
\mathbf{P}_1^1 &= \begin{bmatrix} 27.3842 & 3.5528 & -5.0762 \\ 3.5528 & 18.5185 & -3.5434 \\ -5.0762 & -3.5434 & 25.8452 \end{bmatrix} \\
\mathbf{P}_2^1 &= \begin{bmatrix} 22.0439 & 2.7598 & -4.3137 \\ 2.7598 & 16.1644 & -2.3149 \\ -4.3137 & -2.3149 & 20.7339 \end{bmatrix} \\
\mathbf{P}_3^1 &= \begin{bmatrix} 12.6218 & 0.0041 & -0.6214 \\ 0.0041 & 14.6590 & 0.0203 \\ -0.6214 & 0.0203 & 13.4949 \end{bmatrix} \\
\mathbf{P}_4^1 &= \begin{bmatrix} 16.3012 & 0.3660 & -0.7135 \\ 0.3660 & 16.7023 & -0.2091 \\ -0.7135 & -0.2091 & 16.1869 \end{bmatrix}
\end{aligned}$$

and

$$\mathbf{P}_1^2 = \begin{bmatrix} 12.4384 & -0.0059 & 0.0015 \\ -0.0059 & 12.4944 & 0.0195 \\ 0.0015 & 0.0195 & 12.4740 \end{bmatrix}$$

$$\mathbf{P}_2^2 = \begin{bmatrix} 13.1198 & 0.0434 & -0.0003 \\ 0.0434 & 13.0342 & -0.0766 \\ -0.0003 & -0.0766 & 13.1364 \end{bmatrix}$$

$$\mathbf{P}_3^2 = \begin{bmatrix} 10.7963 & -0.0384 & 0.0053 \\ -0.0384 & 11.0233 & 0.0947 \\ 0.0053 & 0.0947 & 10.9076 \end{bmatrix}$$

$$\mathbf{P}_4^2 = \begin{bmatrix} 12.3957 & -0.0103 & 0.0017 \\ -0.0103 & 12.4643 & 0.0278 \\ 0.0017 & 0.0278 & 12.4327 \end{bmatrix}$$

The initial value of the desired trajectory and the initial positions of the four agents are chosen as

$$\mathbf{x}_{desired}^0 = \begin{bmatrix} 0.1 \\ 0.5 \\ 0.9 \end{bmatrix} \quad \mathbf{x}_1^0 = \begin{bmatrix} -1 \\ -5 \\ 2 \end{bmatrix} \quad \mathbf{x}_2^0 = \begin{bmatrix} 1 \\ -3 \\ 1 \end{bmatrix} \quad \mathbf{x}_3^0 = \begin{bmatrix} -1.5 \\ -2 \\ 2 \end{bmatrix} \quad \mathbf{x}_4^0 = \begin{bmatrix} 1.5 \\ -3 \\ -1 \end{bmatrix}$$

Other parameters used in simulations are shown in Table 6.1

Table 6.1 Parameters of the networked system

Parameter	Value
Sampled period, h	0.01 sec
Lipschitz constant, α	1
σ_1	0.1
σ_2	3
σ_3	5

The desired trajectory of the multi-agent systems is shown in Figure 6.1. It is generated by an input-free Chua's circuit. Applying the controller in Eq. (6.4) to the four agents, the tracking errors, defined as $\mathbf{x}_{desired}(t) - \mathbf{x}_i(t)$, are exhibited in Figures 6.3(a) and 6.3(b). It is clearly observed that all the tracking errors converge

to zero, which firmly demonstrates the effectiveness of the proposed controller. Figure 6.4 shows the control input signals. The solid lines represent the periodically sampled signal, while the event-triggered control input signals are accordingly displayed using those lines other than a solid line. It is clearly shown in the zoom-in window that the update frequency of an event-triggered signal is much lower than the periodically sampled signal. Namely, the event-triggered signal enormously reduces the computational burden of the agents. The switching signal is presented in Figure 6.5, and the value “1” and “-1” indicates the Topology 1 and Topology 2, respectively. It is noticed that only the topology switching between 2.5 sec - 5 sec is shown in Figure 6.5 for better observation. Since the topology is switched according to a Markov jump process, a randomly selected interval is able to display the characteristics of the entire interval.

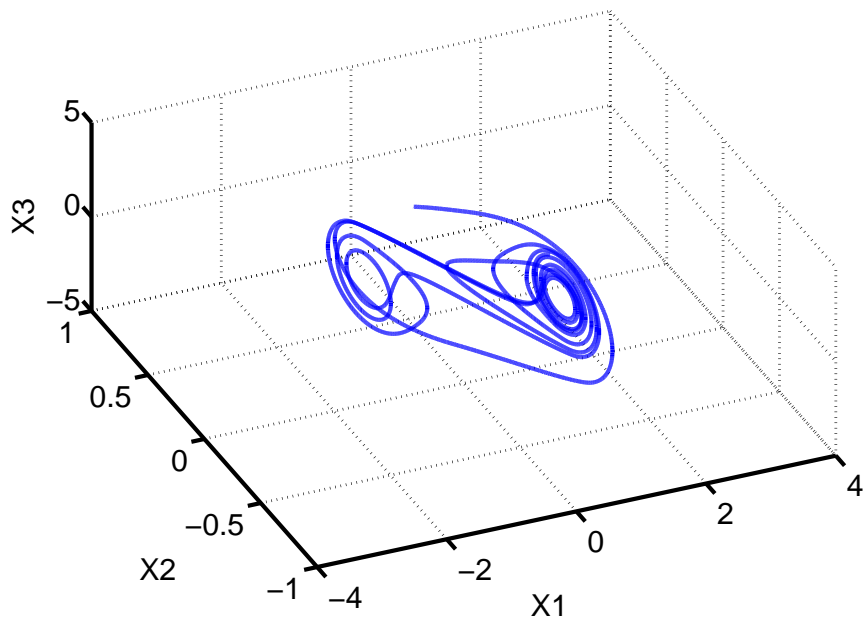
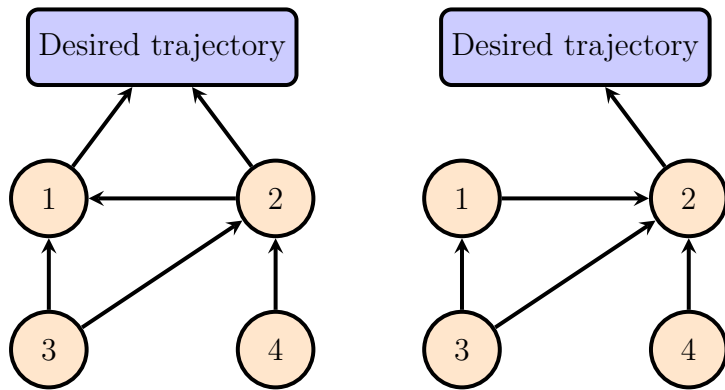
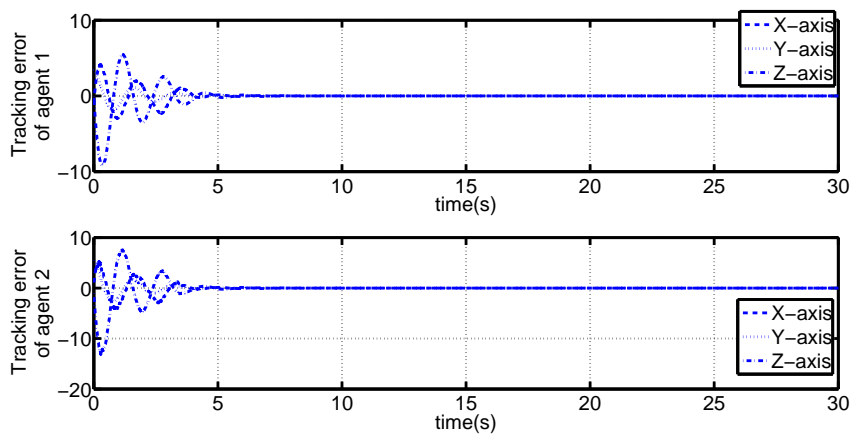


Fig. 6.1 Desired trajectory

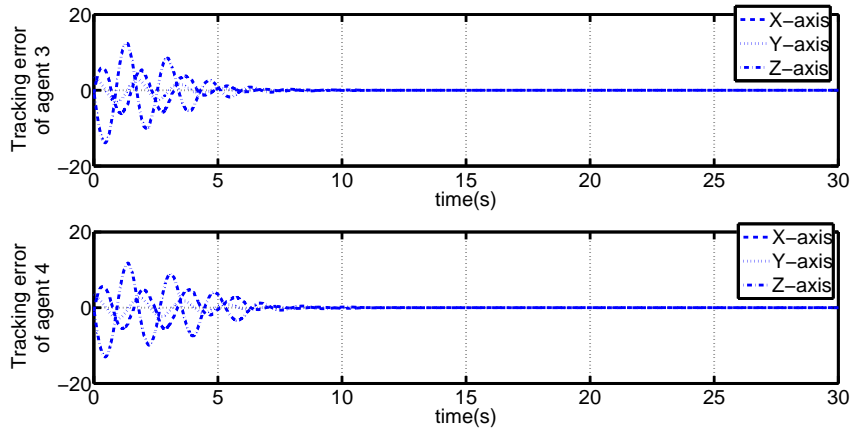


(a) Communication topology 1 (b) Communication topology 2

Fig. 6.2 Communication topologies



(a) Tracking errors of agent 1 and 2



(b) Tracking errors of agent 3 and 4

Fig. 6.3 Tracking errors

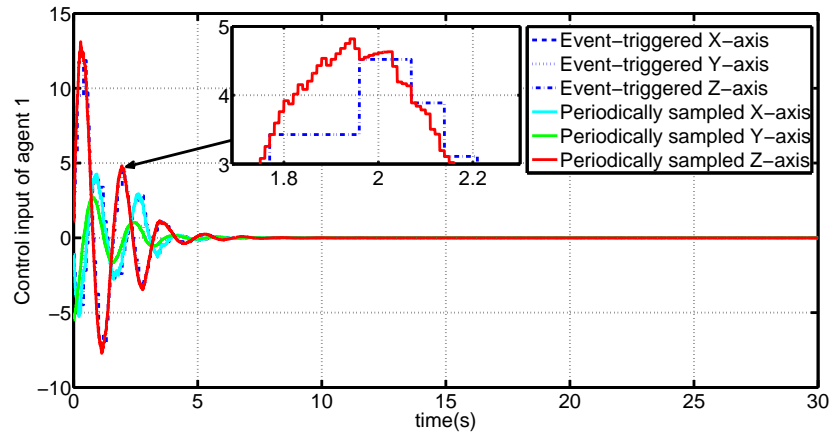


Fig. 6.4 Control input of agent 1

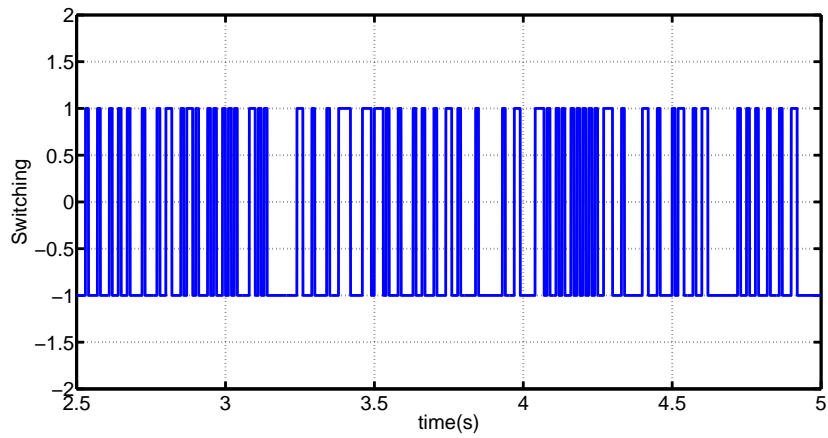


Fig. 6.5 Stochastic switching of the two topologies

7 Conclusions and Future Work

7.1 Conclusions

In this dissertation, the consensus seeking algorithms are essentially developed for networked Euler-Lagrange systems and Lipschitz nonlinear systems, respectively. The nonlinear dynamics of individual agent and the network-induced problems, such as the networked-induced disturbance, sampled-data communication and stochastic topology switching, are systematically discussed for the cooperative control of multi-agent systems.

A consensus seeking algorithm is developed for multiple nonlinear Euler-Lagrange systems. Multiple agents can be steered to a common state in the workspace by the proposed consensus seeking strategy. The effect of structural uncertainties and external disturbances is also taken into account in the control system design. The closed-loop control system is simplified into cascade systems by the proposed controller, and the stability is analyzed based on the perturbed system theory. The concept of input-to-state consensus is defined and used to analyze the robustness of

the developed control algorithm. It is found that the proposed controller is robust to bounded perturbations in the sense of input-to-state stability. An \mathcal{H}_∞ -based optimization algorithm is used to determine the controller parameters in order to improve the consensus achieving performance. The robustness of the proposed controller is further demonstrated under the combination of both external disturbances and structural uncertainty. The leaderless consensus and group trajectory tracking tests are successfully conducted in the hardware experiments, which further demonstrate the effectiveness of the proposed control algorithm in terms of robustness and feasibility.

Next, a distributed formation tracking controller is proposed. The nonlinear dynamics of each agent are modeled as the Euler-Lagrange system. With the proposed control law, all agents can realize formation tracking in the leader-follower manner. Since global knowledge of the desired time-varying trajectory is not presumed, all agents in the workspace reach the formation through a distributed approach. In the presence of system uncertainties and external disturbances, the stability of the proposed control scheme is proven with the assistance of nonsmooth analysis. Remarkably, the boundaries of system uncertainties and external disturbances are not required by the controller. Meanwhile, an active fault diagnosis strategy is successfully developed for the networked nonlinear systems. In the observer-based fault diagnosis scheme, a sliding mode observer is adopted on the basis of the super-

twisting technique. With the assistance of the observer, a residual signal, usually served as an indicator of the possible fault, is generated, and the actuator/sensor faults can be detected if the corresponding residual signal exceeds a certain value. The effectiveness of the proposed controller is verified through simulations. The active fault tolerance is also validated with the presence of actuator/sensor faults.

To further generalize the nonlinear consensus algorithm, an \mathcal{H}_∞ sampled-data consensus algorithm is developed for the networked Lipschitz multi-agent systems. With the consideration of modeling error, system uncertainty and external disturbance, a sampled-data controller is developed and the sufficient conditions for the stability of the controller are thus proposed with the assistance of Lyapunov functional method. The proposed consensus controller can achieve the minimization of the worst case influence of \mathcal{L}_2 bounded disturbance. Meanwhile, the discontinuous issue caused by the sampled-data iteration is essentially resolved along a time-delay compensation approach. Furthermore, an iterative algorithm is developed to automatically derive the feedback and observer gains. The effectiveness of the proposed controller is verified through simulations.

Finally, a leader-follower consensus problem for nonlinear multi-agent systems is solved by an event-triggered consensus controller. In the multi-agent systems, the Markov jump process is adopted to describe the stochastic switching communication relationship. Since the information is locally shared through a digital network,

a time-delay equivalent approach is essentially utilized to solve the discrete-time control problem caused by the discontinuous state feedback. By taking advantage of the Lyapunov functional method, the sufficient condition for system stability is obtained systematically. Moreover, the feedback gain of the proposed controller can be derived by the presented optimization algorithm. Furthermore, the effectiveness of the proposed control algorithm is demonstrated by the numerical simulation.

7.2 Future Work

A lot of problems in cooperative control of multi-agent systems are still unsolved. In this work, the removal of the faulty agent is the most rudimentary approach to realize the function of fault recovery. Apparently, in certain circumstances, the faulty agent is not treated fairly by this kind of fault recovery algorithm. For example, if a healthy agent is indicated as a faulty agent incorrectly by the fault diagnosis algorithm, then the “faulty agent” will be ignored immediately without any attempt at saving the “faulty agent”. Even if an agent is really malfunctioning, it is still possible to save the faulty agent by compensating for the faulty signal. However, in the proposed fault recovery algorithm, the faulty agent is discarded without the consideration of its potential. Therefore, in the future work, the fault recovery algorithm can be improved by taking advantage of the information from the faulty agent. Meanwhile, in the future fault recovery algorithm, the faulty

agent is expected to be kept in the group. Other than the improvement of the fault recovery algorithm, information delay is also an important issue that should be investigated thoroughly in the future.

Delay phenomenon widely exists in multi-agent systems due to the unpredictable uncertainties in the communication network. Since the unexpected delays might result in the instability of the entire system, it has been preliminarily studied in previous works. However, the delay in previous works is usually assumed to be bounded or time-varying. This assumption should be further generalized because delay effect is mostly caused by uncertain factors in the communication network and it is most likely to happen randomly in the multi-agent systems. Consequently, a new consensus seeking protocol for multi-agent systems with the consideration of random communication time delays is expected in the future work. Other than the delay effect, packet loss is another problem induced by the wireless network. During the information transmission, it is very common that several data packets failed to be delivered due to the real-time limitation. In that case, the packet loss becomes an unavoidable problem that may potentially influence the stability of the system. Hence, the failure of data packet delivery is considered in previous works, where the packet delay and loss are both considered, but the packet loss is not explicitly characterized according to the communication process. In application, the packet loss can be caused by issues related to the individual agent, the network,

or a combination of both. Accordingly, the packet loss process should be modeled appropriately in the future work. Based on the packet loss model, the consensus controller is expected to be designed on the basis of stochastic process theory.

Other than the robustness against diverse uncertainties, further improvement of performance is also expected in terms of optimal convergence and intellectual determination. The convergent speed of the multi-agent systems would be enormously influenced by the individual dynamics and network structure. Thus, with the assistance of the advanced optimization techniques, the convergence of the multi-agent systems with nonlinear dynamics should be further optimized when static communication or dynamic communication occurs. Particularly, the network-induced problems, i.e. sampled-data communication, package loss and stochastic communication delay can also be investigated along with the optimization. With the growth of the complexity of the practical missions, intellectual determination is expected in the multi-agent systems both locally and globally. In the local neighborhood, optimal collision avoidance and path planning are always important tasks between the neighbors. The agents are supposed to move to the expected position smoothly with maximum speed and minimum energy consumption. Meanwhile, the group movement also requires intellectual determination. For example, determining the movement direction of the entire group based on video information, or determining which agent should proceed first in a narrow environment.

The intellectual determination can also be combined with fault diagnosis. For instance, how to identify and get rid of a malfunctioning agent with the assistance of video or audio information. Namely, the residual generator could be a smart computer that can identify the faulty agent by observing or listening. Currently, the residual generation largely depends on the measurements of the conventional sensors, based on which a complicated observer will be built in the residual generator. These limitations will instantly disable the detection of a large group of agent faults. However, the incorporation of the intellectual determination might be able to identify these agent faults efficiently. For example, if two agents can observe each other using the video camera, then the faulty behavior of one agent might be “observed” immediately by the other agent without any complicated observer-based algorithm. Similarly, the audio information can also be adopted as an indicator of agent fault if the neighbors are not visually accessible.

A Relevant Theorems

Theorem A.1. (*Robust KYP Lemma*) [92] Consider the following system

$$\begin{aligned}\dot{\mathbf{x}} &= \mathbf{f}(\mathbf{x}) + \Delta\mathbf{f}(\mathbf{x}) + \mathbf{G}(\mathbf{x})\mathbf{u} \\ \mathbf{y} &= \mathbf{h}(\mathbf{x})\end{aligned}\tag{A.1}$$

where $\Delta\mathbf{f}(\mathbf{x})$ denotes the structural uncertainty, which is described by

$$\Delta\mathbf{f}(\mathbf{x}) = \mathbf{E}(\mathbf{x})\boldsymbol{\delta}(\mathbf{x}), \quad \Delta\mathbf{f}(0) = 0\tag{A.2}$$

where $\mathbf{E} : \mathbb{R}^n \rightarrow \mathbb{R}^{n \times m}$ is a known matrix and $\boldsymbol{\delta} : \mathbb{R}^n \rightarrow \mathbb{R}^m$ is unknown. It is assumed that $\boldsymbol{\delta}(\mathbf{x}) \in \{\mathbf{z} : \|\mathbf{z}\| \leq \|\mathbf{n}(\mathbf{x})\|\}$.

The system in Eq. (A.1) is robust strictly passive with a C^1 positive definite function $V(\mathbf{x})$ if

$$\begin{aligned}V(0) &= 0 \\ \mathbf{L}_f V(\mathbf{x}) + \left\| (\mathbf{L}_e V(\mathbf{x}))^T \right\| \|\mathbf{n}(\mathbf{x})\| &< 0, \quad \forall \mathbf{x} \neq 0, \\ \mathbf{L}_g V(\mathbf{x}) &= \mathbf{h}^T(\mathbf{x})\end{aligned}\tag{A.3}$$

Theorem A.2. [139] Consider a proper continuous-time plant $\mathbf{P}(s)$ of order n and its realization is described as

$$\dot{\mathbf{x}} = \mathbf{A}\mathbf{x} + \mathbf{B}_1\boldsymbol{\omega} + \mathbf{B}_2\mathbf{u}$$

$$\mathbf{z} = \mathbf{C}_1\mathbf{x} + \mathbf{D}_{11}\boldsymbol{\omega} + \mathbf{D}_{12}\mathbf{u}$$

$$\mathbf{y} = \mathbf{C}_2\mathbf{x} + \mathbf{D}_{21}\boldsymbol{\omega} + \mathbf{D}_{22}\mathbf{u}$$

Let \mathbf{N}_{12} and \mathbf{N}_{21} denote orthonormal basis of the null spaces of $(\mathbf{B}_2^T, \mathbf{D}_{12}^T)$ and $(\mathbf{C}_2, \mathbf{D}_{21})$ respectively. The suboptimal H_∞ problem of performance γ is solvable if and only if there exist two symmetric matrices $\mathbf{R}, \mathbf{S} \in \mathbb{R}^{n \times n}$ satisfying the following LMIs

$$\begin{aligned} & \begin{bmatrix} \mathbf{N}_{12} & 0 \\ 0 & \mathbf{I} \end{bmatrix}^T \begin{bmatrix} \mathbf{A}\mathbf{R} + \mathbf{R}\mathbf{A}^T & \mathbf{R}\mathbf{C}_1^T & \mathbf{B}_1 \\ \mathbf{C}_1\mathbf{R} & -\gamma\mathbf{I} & \mathbf{D}_{11} \\ \mathbf{B}_1^T & \mathbf{D}_{11}^T & -\gamma\mathbf{I} \end{bmatrix} \begin{bmatrix} \mathbf{N}_{12} & 0 \\ 0 & \mathbf{I} \end{bmatrix} < 0 \\ & \begin{bmatrix} \mathbf{N}_{21} & 0 \\ 0 & \mathbf{I} \end{bmatrix}^T \begin{bmatrix} \mathbf{A}^T\mathbf{S} + \mathbf{S}\mathbf{A} & \mathbf{S}\mathbf{B}_1 & \mathbf{C}_1^T \\ \mathbf{B}_1^T\mathbf{S} & -\gamma\mathbf{I} & \mathbf{D}_{11}^T \\ \mathbf{C}_1 & \mathbf{D}_{11} & -\gamma\mathbf{I} \end{bmatrix} \begin{bmatrix} \mathbf{N}_{21} & 0 \\ 0 & \mathbf{I} \end{bmatrix} < 0 \\ & \begin{bmatrix} \mathbf{R} & \mathbf{I} \\ \mathbf{I} & \mathbf{S} \end{bmatrix} > 0 \end{aligned} \quad (\text{A.4})$$

With the solution of \mathbf{R} and \mathbf{S} in (A.4), the explicit controller formulas can be computed based on the algorithm proposed in Ref. [139].

Theorem A.3. [140] Let $\mathbf{A} \in \mathbb{R}^{n \times n}$ have eigenvalues λ_i , $i \in \underline{n}$, and let $\mathbf{B} \in \mathbb{R}^{m \times m}$ have eigenvalues μ_j , $j \in \underline{m}$. Then the mn eigenvalues of $\mathbf{A} \otimes \mathbf{B}$ are

$$\lambda_1\mu_1, \dots, \lambda_1\mu_m, \lambda_2\mu_1, \dots, \lambda_2\mu_m, \dots, \lambda_n\mu_m.$$

Theorem A.4. [112] Let $x(\cdot)$ be a Filippov solution to $\dot{x} = f(x, t)$ on an interval containing t and $V : \mathbb{R}^n \times \mathbb{R} \rightarrow \mathbb{R}$ be a Lipschitz and in addition, regular function. Then $V(x(t), t)$ is absolutely continuous, $\frac{d}{dt}V(x(t), t)$ exists almost everywhere and

$$\frac{d}{dt}V(x(t), t) \in^{a.e.} \dot{V}(x, t) \quad (\text{A.5})$$

where $\dot{V}(x, t) := \bigcap_{\xi \in \partial V(x(t), t)} \xi^T \begin{pmatrix} K[f](x(t), t) \\ 1 \end{pmatrix}$

Theorem A.5. [112] Let $\dot{x} = f(x, t)$ be essentially locally bounded and $0 \in K[f](0, t)$ in a region $Q \supset \{x \in \mathbb{R}^n \mid \|x\| < r\} \times \{t \mid t_0 \leq t < \infty\}$. Also, let $V : \mathbb{R}^n \times \mathbb{R} \rightarrow \mathbb{R}$ be a regular function satisfying

$$V(0, t) = 0 \quad (\text{A.6})$$

and

$$0 < V_1(\|x\|) \leq V(x, t) \leq V_2(\|x\|) \text{ for } x \neq 0 \quad (\text{A.7})$$

in Q for some $V_1, V_2 \in \text{class } \mathcal{K}$ [81]. Then,

(i) $\dot{V}(x, t) \leq 0$ in Q implies $x(t) \equiv 0$ is a uniformly stable solution.

(ii) If in addition, there exists a class \mathcal{K} functions $\omega(\cdot)$ in Q with the property

$$\dot{V}(x, t) \leq -\omega(t) < 0 \quad (\text{A.8})$$

then the solution $x(t) \equiv 0$ is uniformly asymptotically stable.

B Selected Publications

- [1] **Lei Liu**, Jinjun Shan. “Distributed formation control of networked Euler-Lagrange systems with fault diagnosis,” *Journal of the Franklin Institute*, 352(3), 2015, pp. 952 - 973.
- [2] **Lei Liu**, Jinjun Shan. “Development of a distributed consensus algorithm for multiple EulerLagrange systems,” *IET Control Theory & Application*, 9(2), 2015, pp. 153 - 162.
- [3] **Lei Liu**, Jinjun Shan. “ \mathcal{H}_∞ Robust Synchronization of Nonlinear Multi-agent Systems with Sampled-data Information,” *International Journal of Systems Science*, accepted, DOI:10.1080/00207721.2016.1160457

Bibliography

- [1] “TPF Interferometer,” http://science.nasa.gov/media/medialibrary/2010/03/31/tpf_content.jpg, Accessed: 2016-03-22.
- [2] Olfati-Saber, R., Fax, J. A., and Murray, R. M., “Consensus and Cooperation in Networked Multi-Agent Systems,” *Proceedings of the IEEE*, Vol. 95, No. 1, 2007, pp. 215 – 233.
- [3] Ren, W., “Information consensus in multivehicle cooperative control,” *IEEE Control Systems Magazine*, Vol. 27, No. 2, 2007, pp. 71 – 82.
- [4] Fax, J. and Murray, R., “Information flow and cooperative control of vehicle formations,” *IEEE Transactions on Automatic Control*, Vol. 49, No. 9, 2004, pp. 1465 – 1476.
- [5] Olfati-Saber, R. and Murray, R., “Consensus problems in networks of agents with switching topology and time-delays,” *IEEE Transactions on Automatic Control*, Vol. 49, No. 9, 2004, pp. 1520 – 1533.

- [6] Ren, W. and Beard, R., *Distributed Consensus in Multi-vehicle Cooperative Control*, Springer-Verlag, London, 1st ed., 2008.
- [7] Ren, W. and Cao, Y., *Distributed Coordination of Multi-agent Networks*, Springer-Verlag, London, 1st ed., 2011.
- [8] Li, Z. and Duan, Z., *Cooperative Control of Multi-Agent Systems: A Consensus Region Approach*, CRC Press, 2015.
- [9] Okubo, A., “Dynamical aspects of animal grouping: Swarms, schools, flocks, and herds,” *Advances in Biophysics*, Vol. 22, 1986, pp. 1 – 94.
- [10] Reynolds, C. W., “Flocks, herds and schools: a distributed behavioral model,” *Proceedings of ACM SIGGRAPH Conference*, Anaheim, California, USA, July 27 - 31 1987, pp. 25 – 34.
- [11] Olfati-Saber, R., “Flocking for Multi-Agent Dynamic Systems: Algorithms and Theory,” *IEEE Transactions on Automatic Control*, Vol. 51, No. 3, 2006, pp. 401 – 420.
- [12] “Fish perform schooling behavior,” <https://sites.google.com/site/marineculminatingproject/home/chapter-8-project>, Accessed: 2016-04-07.

- [13] “Birds flocking,” https://upload.wikimedia.org/wikipedia/commons/d/d6/Fugle%2C_%C3%B8rns%C3%B8_073.jpg, Accessed: 2016-04-07.
- [14] Tillerson, M., Inalhan, G., and How, J. P., “Co-ordination and control of distributed spacecraft systems using convex optimization techniques,” *International Journal of Robust and Nonlinear Control*, Vol. 12, No. 2 - 3, 2002, pp. 207 – 242.
- [15] How, J. P., Twigg, R., Weidow, D., Hartman, K., and Bauer, F., “Orion: A low-cost demonstration of formation flying in space using GPS,” *Proceedings of AIAA/AAS Astrodynamics*, Boston, MA, August 10 - 12 1998, pp. 276 – 286.
- [16] Bauer, F., Bristow, J., Folta, D., Hartman, K., Quinn, D., and How, J. P., “Satellite formation flying using an innovative autonomous control system (AutoCon) environment,” *Proceedings of AIAA Guidance, Navigation, and Control Conference*, New Orleans, LA, August 11 - 13 1997, pp. 657 – 666.
- [17] Beichman, C. A., “The Terrestrial Planet Finder: The Search for Life-Bearing Planets Around Other Stars,” *Proceedings of Astronomical Interferometry*, Kona, HI, March 20 - 24 1998, pp. 719 – 723.
- [18] Duren, R. M., “System engineering for spaceborne optical interferometers,” *Proceedings of the IEEE Aerospace Conference*, 2004, pp. 2129 – 2143.

- [19] Wieland, P., Sepulchre, R., and Allgwer, F., “An internal model principle is necessary and sufficient for linear output synchronization,” *Automatica*, Vol. 47, No. 5, 2011, pp. 1068 – 1074.
- [20] Ren, W. and Cao, Y., *Distributed Coordination of Multi-agent Networks: Emergent Problems, Models, and Issues*, Springer-Verlag, London, 2011.
- [21] Ren, W. and Beard, R. W., *Distributed Consensus in Multi-vehicle Cooperative Control: Theory and Applications*, Springer-Verlag, London, 2008.
- [22] Guan, Z.-H., Sun, F.-L., Wang, Y.-W., and Li, T., “Finite-Time Consensus for Leader-Following Second-Order Multi-Agent Networks,” *IEEE Transactions on Circuits and Systems. I, Regular Papers*, Vol. 59, No. 11, 2012, pp. 2646 – 2654.
- [23] Li, H., Liao, X., Huang, T., and Zhu, W., “Event-Triggering Sampling Based Leader-Following Consensus in Second-Order Multi-Agent Systems,” *IEEE Transactions on Automatic Control*, Vol. 60, No. 7, 2015, pp. 1998 – 2003.
- [24] Ren, W., “On consensus algorithms for double-integrator dynamics,” *IEEE Transactions on Automatic Control*, Vol. 53, No. 6, 2008, pp. 1503 – 1509.

- [25] Xu, Y., Tian, Y.-P., and Chen, Y., “Output consensus for multiple non-holonomic systems under directed communication topology,” *International Journal of Systems Science*, Vol. 46, No. 3, 2015, pp. 451 – 463.
- [26] Zhu, Y., Zheng, Y., and Wang, L., “Quantized consensus of multi-agent systems with nonlinear dynamics,” *International Journal of Systems Science*, Vol. 46, No. 11, 2015, pp. 2061 – 2071.
- [27] Song, Q., Cao, J., and Yu, W., “Second-order leader-following consensus of nonlinear multi-agent systems via pinning control,” *Systems & Control Letters*, Vol. 59, 2010, pp. 553 – 562.
- [28] Song, Q., Liu, F., Cao, J., and Yu, W., “M-Matrix Strategies for Pinning-Controlled Leader-Following Consensus in Multiagent Systems With Nonlinear Dynamics,” *IEEE Transactions on Cybernetics*, Vol. 43, No. 6, 2013, pp. 1688 – 1697.
- [29] Ren, W., “Distributed leaderless consensus algorithms for networked Euler-Lagrange systems,” *International Journal of Control*, Vol. 82, No. 11, 2009, pp. 2137 – 2149.
- [30] Mei, J., Ren, W., and Ma, G., “Containment control for multiple euler-lagrange systems with parametric uncertainties in directed networks,” *Pro-*

ceedings of 2011 American Control Conference, San Francisco, California, USA, June 29 - July 1 2011, pp. 2186 – 2191.

- [31] Murray, R. M., Li, Z., and Sastry, S. S., *A mathematical introduction to robotic manipulation*, CRC press, 1994.
- [32] Mei, J., Ren, W., and Ma, G., “Distributed containment control for Lagrangian networks with parametric uncertainties under a directed graph,” *Automatica*, Vol. 48, No. 4, 2012, pp. 653 – 659.
- [33] Mei, J., Ren, W., Chen, J., and Ma, G., “Distributed adaptive coordination for multiple Lagrangian systems under a directed graph without using neighbors velocity information,” *Automatica*, Vol. 49, No. 6, 2013, pp. 1723 – 1731.
- [34] Liu, Y., Min, H., Wang, S., Liu, Z., and Liao, S., “Distributed adaptive consensus for multiple mechanical systems with switching topologies and time-varying delay,” *Systems & Control Letters*, Vol. 64, 2014, pp. 119 – 126.
- [35] Carroll, T. L. and Pecora, L. M., “Synchronizing chaotic circuits,” *IEEE Transactions on Circuits and Systems*, Vol. 38, No. 4, 1991, pp. 453 – 456.

- [36] Kocarev, L. and Parlitz, U., “General approach for chaotic synchronization with applications to communication,” *Physical Review Letters*, Vol. 74, No. 25, 1995, pp. 5028 – 5031.
- [37] Li, K., Zhao, M., and Fu, X., “Projective Synchronization of Driving Response Systems and Its Application to Secure Communication,” *IEEE Transactions on Circuits and Systems*, Vol. 56, No. 10, 2009, pp. 2280 – 2291.
- [38] Suykens, J. A. K., Curran, P. F., and Chua, L. O., “Robust synthesis for masterslave synchronization of Lure Systems,” *IEEE Transactions on Circuits and Systems*, Vol. 46, No. 7, 1995, pp. 841 – 850.
- [39] Zemouche, A. and Boutayeb, M., “On LMI conditions to design observers for Lipschitz nonlinear systems,” *Automatica*, Vol. 49, No. 2, 2013, pp. 585 – 591.
- [40] Ibrir, S., Xie, W. F., and Su, C.-Y., “Observer-based control of discrete-time Lipschitzian non-linear systems: application to one-link flexible joint robot,” *International Journal of Control*, Vol. 78, No. 6, 2005, pp. 385 – 395.
- [41] Rajamani, R., “Observers for Lipschitz Nonlinear Systems,” *IEEE Transactions on Automatic Control*, Vol. 43, No. 3, 1998, pp. 397 – 401.

- [42] Sundaram, S. and Hadjicostis, C. N., “Distributed Function Calculation via Linear Iterative Strategies in the Presence of Malicious Agents,” *IEEE Transactions on Automatic Control*, Vol. 56, No. 7, 2011, pp. 1495 – 1508.
- [43] Franceschelli, M., Egerstedt, M., and Giua, A., “Motion probes for fault detection and recovery in networked control systems,” *Proceedings of the 2008 American Control Conference*, Seattle, Washington, USA, June 11 - 13 2008, pp. 4358 – 4363.
- [44] Franceschelli, M., Giua, A., and Seatzu, C., “Decentralized fault diagnosis for sensor networks,” *Proceedings of the 2009 IEEE International Conference on Automation Science and Engineering*, Bangalore, India, August 22 - 25 2009, pp. 334 – 339.
- [45] Ferrari-Trecate, G., Egerstedt, M., Buffa, A., and Ji, M., “Laplacian Sheep: A Hybrid, Stop-Go Policy for Leader-Based Containment Control,” *Hybrid Systems: Computation and Control*, 2006, pp. 212 – 226.
- [46] Pasqualetti, F., Bicchi, A., and Bullo, F., “Consensus Computation in Unreliable Networks: A System Theoretic Approach,” *IEEE Transactions on Automatic Control*, Vol. 57, No. 1, 2012, pp. 90 – 104.

- [47] Shames, I., Teixeira, A. M., Sandberg, H., and Johansson, K. H., “Distributed fault detection for interconnected second-order systems,” *Automatica*, Vol. 47, No. 12, 2011, pp. 2757 – 2764.
- [48] Guo, M., Dimarogonas, D. V., and Johansson, K. H., “Distributed real-time fault detection and isolation for cooperative multi-agent systems,” *Proceedings of American Control Conference*, 2012, pp. 5270 – 5275.
- [49] Smith, R. S. and Hadaegh, F. Y., “Control of Deep-Space Formation-Flying Spacecraft; Relative Sensing and Switched Information,” *Journal of Guidance, Control, and Dynamics*, Vol. 28, No. 1, 2005, pp. 106 – 114.
- [50] Desai, J. P., Ostrowski, J. P., and Kumar, V., “Modeling and control of formations of nonholonomic mobile robots,” *IEEE Transactions on Robotics*, Vol. 17, No. 6, 2002, pp. 905 – 909.
- [51] Tsitsiklis, J. N., *Problems in decentralized decision making and computation*, Ph.D. thesis, Massachusetts Institute of Technology, Massachusetts, MA, USA, 1984.
- [52] Moreau, L., “Stability of multiagent systems with time-dependent communication links,” *IEEE Transactions on Automatic Control*, Vol. 50, No. 2, 2005, pp. 169 – 182.

- [53] Jadbabaie, A., Lin, J., and Morse, A. S., “Coordination of Groups of Mobile Autonomous Agents Using Nearest Neighbor Rules,” *IEEE Transactions on Automatic Control*, Vol. 48, No. 6, 2003, pp. 988 – 1001.
- [54] Vicsek, T., Czirok, A., Jacob, E. B., Cohen, I., and Schochet, O., “Novel type of phase transitions in a system of self-driven particles,” *Physical Review Letters*, Vol. 75, No. 2, 1995, pp. 1226 – 1229.
- [55] Tang, Z.-J., Huang, T.-Z., Shao, J.-L., and Hu, J.-P., “Leader-following consensus for multi-agent systems via sampled-data control,” *IET Control Theory & Applications*, Vol. 5, No. 14, 2011, pp. 1658 – 1665.
- [56] Cao, Y. and Ren, W., “Multi-vehicle coordination for double-integrator dynamics under fixed undirected/directed interaction in a sampled-data setting,” *International Journal of Robust and Nonlinear Control*, Vol. 20, No. 9, 2010, pp. 987 – 1000.
- [57] Gao, Y. and Wang, L., “Consensus of multiple double-integrator agents with intermittent measurement,” *International Journal of Robust and Nonlinear Control*, Vol. 20, No. 10, 2010, pp. 1140 – 1155.
- [58] Katayama, H., “Design of output feedback consensus controllers for nonlinear sampled-data multi-agent systems of strict-feedback form,” *International Journal of Systems Science*, Vol. 45, No. 9, 2015, pp. 1955 – 1962.

- [59] Mikheev, Y., Sobolev, V., and Fridman, E., “Asymptotic analysis of digital control systems,” *Automation and Remote Control*, Vol. 49, 1988, pp. 1175 – 1180.
- [60] Fridman, E., Seuret, A., and Richard, J.-P., “Robust sampled-data stabilization of linear systems: an input delay approach,” *Automatica*, Vol. 40, No. 8, 2004, pp. 1441 – 1446.
- [61] Naghshtabrizi, P., Hespanha, J. P., and Teel, A. R., “Exponential stability of impulsive systems with application to uncertain sampled-data systems,” *Systems & Control Letters*, Vol. 57, No. 5, 2008, pp. 378 – 385.
- [62] Fridman, E., “A refined input delay approach to sampled-data control,” *Automatica*, Vol. 46, No. 2, 2010, pp. 421 – 427.
- [63] Wen, G., Duan, Z., Yu, W., and Chen, G., “Consensus of multi-agent systems with nonlinear dynamics and sampled-data information: a delayed-input approach,” *International Journal of Robust and Nonlinear Control*, Vol. 23, No. 6, 2013, pp. 602 – 619.
- [64] Zhang, W. and Wang, Z., “Adaptive output consensus tracking of uncertain multi-agent systems,” *International Journal of Systems Science*, Vol. 46, No. 13, 2015, pp. 2367 – 2379.

- [65] Wu, Z., Peng, L., Xie, L., and Wen, J., “Stochastic bounded consensus tracking of second-order multi-agent systems with measurement noises based on sampled-data with general sampling delay,” *International Journal of Systems Science*, Vol. 46, No. 3, 2015, pp. 546 – 561.
- [66] Xi, J., Yang, X., Yu, Z., and Liu, G., “Leaderfollower guaranteed-cost consensusualization for high-order linear swarm systems with switching topologies,” *Journal of The Franklin Institute*, Vol. 352, No. 4, 2015, pp. 1343 – 1363.
- [67] Cai, H. and Huang, J., “Leader-following consensus of multiple uncertain EulerLagrange systems under switching network topology,” *International Journal of General Systems*, Vol. 43, No. 3-4, 2014, pp. 294 – 304.
- [68] Xu, G.-H., Guan, Z.-H., He, D.-X., Chi, M., and Wu, Y.-H., “Distributed tracking control of second-order multi-agent systems with sampled data,” *Journal of The Franklin Institute*, Vol. 351, No. 10, 2014, pp. 4786 – 4801.
- [69] Ding, L. and Guo, G., “Sampled-data leader-following consensus for nonlinear multi-agent systems with Markovian switching topologies and communication delay,” *Journal of The Franklin Institute*, Vol. 352, No. 1, 2015, pp. 369 – 383.

- [70] Ni, W. and Cheng, D., “Leader-following consensus of multi-agent systems under fixed and switching topologies,” *Systems & Control Letters*, Vol. 59, 2010, pp. 209 – 217.
- [71] Mahmoud, M. S. and Khan, G. D., “Leader-following discrete consensus control of multi-agent systems with fixed and switching topologies,” *Journal of The Franklin Institute*, Vol. 352, No. 6, 2015, pp. 2504 – 2525.
- [72] Huang, N., Duan, Z., and Zhao, Y., “Leader-following consensus of second-order non-linear multi-agent systems with directed intermittent communication,” *IET Control Theory & Applications*, Vol. 8, No. 10, 2014, pp. 782 – 795.
- [73] Yin, X. and Yue, D., “Event-triggered tracking control for heterogeneous multi-agent systems with Markov communication delays,” *Journal of the Franklin Institute*, Vol. 350, No. 5, 2013, pp. 1312 – 1334.
- [74] Yin, X., Yue, D., and Hu, S., “Distributed event-triggered control of discrete-time heterogeneous multi-agent systems,” *Journal of the Franklin Institute*, Vol. 350, No. 3, 2013, pp. 651 – 669.
- [75] Zhang, H., Feng, G., Yan, H., and Chen, Q., “Observer-Based Output Feedback Event-Triggered Control for Consensus of Multi-Agent Systems,” *IEEE Transactions on Industrial Electronics*, Vol. 61, No. 9, 2014, pp. 4885 – 4894.

- [76] Chen, X. and Hao, F., “Event-triggered average consensus control for discrete-time multi-agent systems,” *IET Control Theory & Applications*, Vol. 6, No. 16, 2012, pp. 2493 – 2498.
- [77] Guo, G., Ding, L., and Han, Q.-L., “A distributed event-triggered transmission strategy for sampled-data consensus of multi-agent systems,” *Automatica*, Vol. 50, No. 5, 2014, pp. 1489 – 1496.
- [78] Fan, Y., Feng, G., Wang, Y., and Song, C., “Distributed event-triggered control of multi-agent systems with combinational measurements,” *Automatica*, Vol. 49, No. 2, 2013, pp. 671 – 675.
- [79] Dimarogonas, D. V., Frazzoli, E., and Johansson, K. H., “Distributed Event-Triggered Control for Multi-Agent Systems,” *IEEE Transactions on Automatic Control*, Vol. 57, No. 5, 2012, pp. 1291 – 1297.
- [80] Mu, X., Xiao, X., Liu, K., and Zhang, J., “Leader-following consensus of multi-agent systems with jointly connected topology using distributed adaptive protocols,” *Journal of The Franklin Institute*, Vol. 351, No. 12, 2014, pp. 5399 – 5410.
- [81] Khalil, H., *Nonlinear Systems*, Prentice Hall, 3rd ed., 2002.

- [82] Lin, Z., Francis, B., and Maggiore, M., “State Agreement for Continuous-Time Coupled Nonlinear Systems,” *SIAM Journal on Control and Optimization*, Vol. 46, No. 1, 2007, pp. 288 – 307.
- [83] Isidori, A., *Nonlinear control system*, Springer-Verlag, 3rd ed., 1995.
- [84] Ren, W. and Beard, R. W., “Consensus seeking in multiagent systems under dynamically changing interaction topologies,” *IEEE Transactions on Automatic Control*, Vol. 50, No. 5, 2005, pp. 655 – 661.
- [85] Wang, H., “Passivity based synchronization for networked robotic systems with uncertain kinematics and dynamics,” *Automatica*, Vol. 49, No. 3, 2013, pp. 755 – 761.
- [86] Wang, H., “Flocking of networked uncertain EulerLagrange systems on directed graphs,” *Automatica*, Vol. 49, No. 9, 2013, pp. 2774 – 2779.
- [87] Shi, G. and Johansson, K. H., “Robust Consensus for Continuous-Time Multiagent Dynamics,” *SIAM Journal on Control and Optimization*, Vol. 51, No. 5, 2013, pp. 3673 – 3691.
- [88] Zhou, K., *Essentials of Robust Control*, Prentice Hall, 1st ed., 1998.
- [89] Gahinet, P., Nemirovski, A., Laub, A., and Chilali, M., *LMI Control Toolbox User’s Guide*, The MathWorks, Inc, 1st ed., 1995.

- [90] Gahinet, P. and Apkarian, P., “A Linear Matrix Inequality Approach to H_∞ Control,” *International Journal of Robust and Nonlinear Control*, Vol. 4, No. 4, 1994, pp. 421 – 448.
- [91] Kingston, D. B., Ren, W., and Beard, R. W., “Consensus Algorithms are Input-to-State Stable,” *Proceedings of American Control Conference*, Portland, OR, USA, 2005, pp. 1686 – 1690.
- [92] Lin, W. and Shen, T., “Robust passivity and feedback design for minimum-phase nonlinear systems with structural uncertainty,” *Automatica*, Vol. 35, No. 1, 1999, pp. 35 – 47.
- [93] Marquez, H. J., *Nonlinear control systems : analysis and design*, (John Wiley, 1st ed., 2003).
- [94] Shan, J. and Liu, H. H., “Development of an Experimental Testbed for Multiple Vehicles Formation Flight Control,” *Proceedings of the 2005 IEEE Conference on Control Applications*, 2005, pp. 160 – 164.
- [95] *3-DOF Helicopter Reference Manual*, Quanser Inc, 1st ed., 2010.
- [96] Shan, J., Liu, H., and Nowotny, S., “Synchronised trajectory-tracking control of multiple 3-DOF experimental helicopters,” *IEE Proceedings - Control Theory and Applications*, Vol. 152, No. 6, 2005, pp. 683 – 692.

- [97] Sun, D., Shao, X., and Feng, G., “Position synchronization of multiple motion axes with adaptive coupling control,” *Automatica*, Vol. 39, No. 6, 2003, pp. 997 – 1005.
- [98] Sun, D., Shao, X., and Feng, G., “A Model-Free Cross-Coupled Control for Position Synchronization of Multi-Axis Motions: Theory and Experiments,” *IEEE Transactions on Control Systems Technology*, Vol. 15, No. 2, 2007, pp. 306 – 314.
- [99] Ma, L., Min, H., Wang, S., and Liu, Y., “Consensus of nonlinear multi-agent systems with self and communication time delays: A unified framework,” *Journal of The Franklin Institute*, Vol. 352, No. 3, 2015, pp. 745 – 760.
- [100] Peng, J. and Ye, X., “Distributed adaptive controller for the output-synchronization of networked systems in semi-strict feedback form,” *Journal of The Franklin Institute*, Vol. 351, No. 1, 2014, pp. 412 – 428.
- [101] Li, Z., Ren, W., Liu, X., and Fu, M., “Consensus of Multi-Agent Systems With General Linear and Lipschitz Nonlinear Dynamics Using Distributed Adaptive Protocols,” *IEEE Transactions on Automatic Control*, Vol. 58, No. 7, 2013, pp. 1786 – 1791.
- [102] Mu, X., Xiao, X., Liu, K., and Zhang, J., “Leader-following consensus of multi-agent systems with jointly connected topology using distributed adap-

- tive protocols,” *Journal of The Franklin Institute*, Vol. 351, No. 12, 2014, pp. 5399 – 5410.
- [103] Atrianfar, H. and Haeri, M., “Adaptive flocking control of nonlinear multi-agent systems with directed switching topologies and saturation constraints,” *Journal of The Franklin Institute*, Vol. 350, No. 6, 2013, pp. 1545 – 1561.
- [104] Ma, Q., Wang, Z., and Miao, G., “Second-order group consensus for multi-agent systems via pinning leader-following approach,” *Journal of The Franklin Institute*, Vol. 351, No. 3, 2014, pp. 1288 – 1300.
- [105] Wan, X., Xu, L., Fang, H., Yang, F., and Li, X., “Exponential synchronization of switched genetic oscillators with time-varying delays,” *Journal of The Franklin Institute*, Vol. 351, No. 8, 2014, pp. 4395 – 4414.
- [106] Li, H., Ming, C., Shen, S., and Wong, W., “Event-triggered control for multi-agent systems with randomly occurring nonlinear dynamics and time-varying delay,” *Journal of The Franklin Institute*, Vol. 351, No. 5, 2014, pp. 2582 – 2599.
- [107] Liu, Y., Min, H., Wang, S., Ma, L., and Liu, Z., “Consensus for multiple heterogeneous EulerLagrange systems with time-delay and jointly connected topologies,” *Journal of The Franklin Institute*, Vol. 351, No. 6, 2014, pp. 3351 – 3363.

- [108] Liu, Y., Min, H., Wang, S., Liu, Z., and Liao, S., “Distributed consensus of a class of networked heterogeneous multi-agent systems,” *Journal of The Franklin Institute*, Vol. 351, No. 3, 2014, pp. 1700 – 1716.
- [109] Cortes, J., “Discontinuous dynamical systems - a tutorial on solutions, non-smooth analysis, and stability,” *IEEE Control Systems Magazine*, Vol. 28, No. 3, 2008, pp. 36 – 73.
- [110] Filippov, A. F. and Arscott, F. M., *Differential Equations with Discontinuous Righthand Sides*, Kluwer Academic, 1st ed., 1988.
- [111] Dieci, L. and Lopez, L., “Sliding Motion in Filippov Differential Systems: Theoretical Results and a Computational Approach,” *SIAM Journal on Numerical Analysis*, Vol. 47, No. 3, 2009, pp. 2023 – 2051.
- [112] Shevitz, D. and Paden, B., “Lyapunov stability theory of nonsmooth systems,” *IEEE Transactions on Automatic Control*, Vol. 39, No. 9, 1994, pp. 1910 – 1914.
- [113] Paden, B. and Sastry, S., “A calculus for computing Filippov’s differential inclusion with application to the variable structure control of robot manipulators,” *IEEE Transactions on Circuits and Systems*, Vol. 34, No. 1, 1987, pp. 73 – 82.

- [114] Loria, A., Panteley, E., and Nijmeijer, H., “A remark on passivity-based and discontinuous control of uncertain nonlinear systems,” *Automatica*, Vol. 37, No. 9, 2001, pp. 1481 – 1487.
- [115] Chen, J. and Patton, R. J., *Robust Model-Based Fault Diagnosis for Dynamic Systems*, Kluwer Academic Publishers, 1st ed., 1999.
- [116] Ding, S. X., *Model-based Fault Diagnosis Techniques*, Springer-Verlag, 1st ed., 2008.
- [117] Floquet, T. and Barbot, J. P., “Super twisting algorithm-based step-by-step sliding mode observers for nonlinear systems with unknown inputs,” *International Journal of Systems Science*, Vol. 38, No. 10, 2007, pp. 803 – 815.
- [118] Moreno, J. A. and Osorio, M., “A Lyapunov approach to second-order sliding mode controllers and observers,” *Proceedings of the 2008 IEEE International Conference on Decision and Control*, Cancun, Mexico, December 9 - 11 2008, pp. 2856 – 2861.
- [119] Moreno, J. A. and Osorio, M., “Strict Lyapunov Functions for the Super-Twisting Algorithm,” *IEEE Transactions on Automatic Control*, Vol. 57, No. 4, 2012, pp. 1035 – 1040.

- [120] Davila, J., Fridman, L., and Levant, A., “Second-order sliding-mode observer for mechanical systems,” *IEEE Transactions on Automatic Control*, Vol. 50, No. 11, 2005, pp. 1785 – 1789.
- [121] Massoumnia, M.-A., “A geometric approach to the synthesis of failure detection filters,” *IEEE Transactions on Automatic Control*, Vol. 31, No. 9, 1986, pp. 839 – 846.
- [122] Massoumnia, M.-A., Verghese, G. C., and Willsky, A. S., “Failure detection and identification,” *IEEE Transactions on Automatic Control*, Vol. 34, No. 3, 1989, pp. 316 – 321.
- [123] Bokor, J. and Balas, G., “Detection filter design for LPV systems – A geometric approach,” *Automatica*, Vol. 40, No. 3, 2004, pp. 511 – 518.
- [124] Notash, L. and Huang, L., “On the design of fault tolerant parallel manipulators,” *Mechanism and Machine Theory*, Vol. 38, No. 1, 2003, pp. 85 – 101.
- [125] Lewis, C. L. and Maciejewski, A. A., “Fault Tolerant Operation of Kinematically Redundant Manipulators for Locked Joint Failures,” *IEEE Transactions on Robotics and Automation*, Vol. 13, No. 4, 1997, pp. 622 – 629.

- [126] Wu, E. C., Hwang, J. C., and Chladek, J. T., “Fault-Tolerant Joint Development for the Space Shuttle Remote Manipulator System: Analysis and Experiment,” *IEEE Transactions on Robotics and Automation*, Vol. 9, No. 5, 1993, pp. 675 – 684.
- [127] Zhu, X., Meng, F., Zhang, H., and Cui, Y., “Robust driveshaft torque observer design for stepped ratio transmission in electric vehicles,” *Neurocomputing*, Vol. 164, 2015, pp. 262 – 271.
- [128] Shan, J., “Six-degree-of-freedom synchronised adaptive learning control for spacecraft formation flying,” *IET Control Theory & Applications*, Vol. 2, No. 10, 2008, pp. 930 – 949.
- [129] Xiao, X., Zhou, L., and Zhang, Z., “Synchronization of chaotic Lur’e systems with quantized sampled-data controller,” *Communications in Nonlinear Science and Numerical Simulation*, Vol. 19, No. 6, 2014, pp. 2039 – 2047.
- [130] Wu, L., Qi, T., and Feng, Z., “Average dwell time approach to $\mathcal{L}_2 - \mathcal{L}_\infty$ control of switched delay systems via dynamic output feedback,” *IET Control Theory & Applications*, Vol. 3, No. 10, 2009, pp. 1425 – 1436.
- [131] Xie, L., “Output feedback \mathcal{H}_∞ control of systems with parameter uncertainty,” *International Journal of Control*, Vol. 63, No. 4, 1996, pp. 741 – 750.

- [132] Boyd, S. and Vandenberghe, L., *Convex Optimization*, Cambridge University Press, 2004.
- [133] Ghaoui, L. E., Oustry, F., and AitRami, M., “A Cone Complementarity Linearization Algorithm for Static Output-Feedback and Related Problems,” *IEEE Transactions on Automatic Control*, Vol. 42, No. 8, 1997, pp. 1171 – 1176.
- [134] Boccaletti, S., Kurths, J., Osipov, G., Valladares, D. L., and Zhou, C. S., “The synchronization of chaotic systems,” *Physics reports*, Vol. 366, No. 1, 2002, pp. 1 – 101.
- [135] “Chua’s circuit,” https://en.wikipedia.org/wiki/Chua's_circuit, Accessed: 2016-06-19.
- [136] Guo, G., Ding, L., and Han, Q., “A distributed event-triggered transmission strategy for sampled-data consensus of multi-agent systems,” *Automatica*, Vol. 50, 2014, pp. 1489 – 1496.
- [137] Fei, Z., Gao, H., and Shi, P., “New results on stabilization of Markovian Jump systems with time delay,” *Automatica*, Vol. 45, 2009, pp. 2300 – 2306.

- [138] Meyn, S. P. and Tweedie, R. L., “Stability of Markovian Processes III: Foster-Lyapunov Criteria for Continuous-Time Processes,” *Applied Probability Trust*, Vol. 25, No. 3, 1993, pp. 518 – 548.
- [139] Gahinet, P., “Explicit controller formulas for LMI-based H_∞ synthesis,” *Automatica*, Vol. 32, No. 7, 1996, pp. 1007 – 1014.
- [140] Laub, A. J., *Matrix Analysis for Scientists and Engineers*, (SIAM: Society for Industrial and Applied Mathematics, 1st ed., 2004).